Catheter associated urinary tract infections (CAUTIs): laboratory and clinical evaluation of a novel biofilm resistant polymer coating

Kiril Rosenov Kalenderski, BSc., MSc.

Thesis submitted to the University of Nottingham
for the degree of Doctor of Philosophy.

March 2021

Abstract

Biofilm formation on indwelling urinary catheters causes severe complications in catheterized patients and is commonly linked to symptomatic catheter associated urinary tract infections (CAUTI). The presence of urease producing bacteria, such as *Proteus mirabilis* and *Pseudomonas aeruginosa*, within the biofilm increases the urinary pH, resulting in the precipitation of minerals such as struvite and apatite. The resulting crystalline biofilm can encrust the catheter and result in blockage of urine flow. CAUTI prevention measures such as silver impregnation and antimicrobial catheter coatings, have exhibited limitations in terms of effectiveness and development of antimicrobial resistance.

Urinary catheters manufactured by Camstent Ltd., are coated with a novel polyacrylate copolymer of ethylene glycol dicyclopentenyl ether acrylate (EGDPEA) and di(ethyleneglycol) methyl ether methacrylate (DEGMA). The inability of bacteria to irreversibly attach to the weakly amphiphilic polymers such as EGDPEA inhibits biofilm formation. Combining EGDPEA with DEGMA confers the mechanical and lubricious properties desirable for a flexible coating compatible with implanted medical device applications.

The aim of this study was to demonstrate the ability of the EGDPEA/DEGMA coated Camstent catheters to resist biofilm formation, mineral accumulation, and fibrinogen deposition, and thus assess its potential to reduce symptomatic CAUTI episodes. The objectives were to quantify and compare the amount of biofilm and mineralization that accumulate on Camstent and silicone catheters *in vitro* in an intermittent flow bladder model and within

a first-in-man clinical study. Preliminary biofilm and mineral quantification was via confocal fluorescence microscopy and image analysis, after staining with Syto64 and calcein, respectively. Environmental scanning electron microscopy (ESEM) coupled with energy dispersive X-ray spectroscopy (EDS) were carried out to characterize and compare the morphologies and chemistry of biofilm and minerals associated with Camstent and silicone catheters. 16S rRNA analysis was also carried out to determine any differences in the bacterial species colonizing they two types of surface.

Catheterization damages the mucosal lining of the patient's bladder resulting in an immune response, where host proteins such as fibrinogen can cover the catheter surface and promote bacterial attachment. Consequently, the comparative impact of silicone and Camstent catheterization on urine fibrinogen content and catheter deposition was investigated using ELISA and immunohistochemistry.

Within an *in vitro* bladder model, Camstent catheters exhibited an improved resilience to *P. mirabilis* and *Ps. aeruginosa* biofilm formation in comparison with silicone catheters (*Ps. aeruginosa*- $2.55x10^4$ µg cm^{-2} vs $4.46x10^4$ µg cm^{-2}, *P. mirabilis*- $3.37x10^3$ µg cm^{-2} vs $1.14x10^4$ µg cm^{-2}, dual-species inoculation- $3.75x10^4$ µg cm^{-2} vs $6.31x10^4$ µg cm^{-2}, respectively; $P<0.05$). Additionally, Camstent catheters did not become blocked during any of the experiments using the bladder model, whereas silicone devices were blocked after 57 hours on average following *P. mirabilis* infections, and after an average of 38 hours following dual-species infections with *P. mirabilis* and *Ps. aeruginosa*.

Bladder model experiments were also conducted using non-swarming and urease negative *P. mirabilis* transposon mutants. Urease production was shown to be detrimental to silicone catheter blockage, with *ureR* mutants found to be incapable of blocking silicone catheters within the *in vitro* bladder model. Bladder model inoculations with the non-swarming *flgI* mutant resulted in significantly higher biofilm biomass formed on silicone catheters when compared with the wild-type *P. mirabilis* strain. Bladder model experiments inoculating Camstent catheters with the *flgI* mutant however resulted in no blockage, and significantly less biofilm biomass, in comparison with silicone catheters inoculated with the mutant (1.83 $x10^3$ µg cm^{-2} vs. 5.10 $x10^3$ µg cm^{-2}, respectively; $P<0.05$).

Urinary catheters were recovered from hospitalized patients were separated in to three clinical catheter cohorts predominantly defined by indwelling time (Average indwelling time: Cohort 1- 7 days, Cohort 2- 12 days, and Cohort 3- 23 days). A comparison of Camstent catheters (n=65) with silicone catheters (n=60), across the three clinical cohorts, revealed a significantly lower biofilm formation on the Camstent devices (Cohort 1- 0.037 µg cm^{-2} vs 4.425 µg cm^{-2}, Cohort 2- 0.003 µg cm^{-2} vs 0.022 µg cm^{-2}, Cohort 3- 8.634 µg cm^{-2} vs 20.039 µg cm^{-2}, respectively; $P<0.05$) and mineral accumulation (Cohort 1- 0.077 µg cm^{-2} vs 9.001 µg cm^{-2}, Cohort 2- 0.006 µg cm^{-2} vs 0.207 µg cm^{-2}, Cohort 3- 12.394 µg cm^{-2} vs 74.518 µg cm^{-2}, respectively; $P<0.05$). Further characterization of the biofilm and mineral associated with the two surfaces through ESEM imaging and EDS analysis revealed major differences in the morphology and chemistry of the minerals deposited on Camstent catheters compared with silicone devices. Struvite, apatite, and

calcium carbonate were among the biofilm associated minerals found on silicone catheters, whereas a thin layer of calcium oxalate minerals, products of endogenous metabolism, was found on Camstent catheters. 16S rRNA analysis on the two types of surface also revealed marked differences in microbial community composition.

Quantification of fibrinogen within urine samples from hospitalized patients revealed that catheterization with Camstent catheters (n=3; 1.8 μg ml^{-1}) results in a smaller increase in urinary fibrinogen compared with silicone (n=8; 3.5 μg ml^{-1}). Analysis of the catheters associated with the urine samples also showed that Camstent catheter surfaces (n=3; 14.0 μg cm^{-2}) accumulated less fibrinogen in comparison with silicone surfaces (n=4; 155.4 μg cm^{-2}), despite comparable average post-catheterisation urinary fibrinogen concentrations (3.7 μg ml^{-1} vs. 5.3 μg ml^{-1}, respectively).

The *in vitro* and first-in-man data presented within this study provide evidence that the Camstent coated catheter effectively reduced biofilm formation and mineralization. Additionally, preliminary clinical data suggested that catheterization with Camstent catheters in lower urine fibrinogen and less fibrinogen deposition on the catheter than on silicone. This highlights the potential of the Camstent coating to reduce biofilm formation by Gram positive pathogens such as *Enterococcus faecalis* and *Staphylococcus aureus* that express fibrinogen receptors. Further clinical studies will be required to fully establish the potential of Camstent catheters to prevent CAUTIs.

Declaration

Unless otherwise formally indicated within the text, the research contained within this thesis is the original work of the author. The thesis has not been previously submitted to this or any other university for a degree, and does not include any material already submitted for a degree.

Kiril Rosenov Kalenderski

March 2021

Acknowledgements

Firstly, I would like to acknowledge my supervisors, Professor Paul Williams, Professor Stephan Heeb, and Professor Morgan Alexander, for their continuous guidance, support, and patience throughout my PhD. It has been a real privilege for me to learn from your expertise and experience.

I would also like to express my gratitude to all the past and present members of the labs I have conducted my PhD research within, in particular Dr. Jean-Frederic Dubern, Dr. Jeni Luckett, Nigel Halliday, and Dr. Manuel Romero. I am also very grateful to the technical team within the Nanoscale and Microscale Research Centre, and in particular Nicola Weston and Denise McLean for all their help throughout my project.

The work within this thesis would also not have been possible without our collaborators within Queen's Medical Centre, Nottingham, our industrial collaborators, Camstent Ltd., and in particular the help of Dr. Dave Hampton, Dr. David Humes, and Dr. Christopher Lewis-Lloyd.

Lastly I would like to thank all my friends and family for supporting me throughout my research work over the past 4 years..

Table of Contents

Abstract.....i

Declaration.....v

Acknowledgements.....vi

Table of Contents.....1

List of Tables and Figures.....11

Abbreviations.....16

Chapter 1: Introduction.....17

1.1 Implantable medical devices.....17

1.2 Indwelling urinary catheters.....17

1.3 CAUTIs, uropathogens, and complications.....23

1.3.1 CAUTI infection routes.....24

1.3.2 Uropathogens.....27

1.3.3 CAUTI complications.....28

1.4 Biofilms and mineralization.....29

1.4.1 Urine composition and the immune response to catheterization-Fibrinogen and Tamm-Horsfall Protein (THP).....32

1.4.2 Bacterial attachment.....34

1.4.3 Biofilm formation.....37

1.4.4 Biofilm associated mineralization.....40

1.5 *Proteus mirabilis*.....41

1.5.1 *P. mirabilis* motility- twitch, swim, and swarm 42

1.5.2 *P. mirabilis* - Urease enzyme production 47

1.5.3 Catheter blockage 49

1.6 CAUTI prevention and treatment 52

1.6.1 New antibacterial urinary catheter coating 53

1.7 Hypothesis and aims 54

Chapter 2: Materials and Methods 58

2.1. General microbiological methods 58

2.1.1. Bacterial growth and cultivation 58

2.1.2. Bacterial storage 61

2.1.3 Bacterial enumeration 61

2.1.4 Statistical analysis 61

2.1.5 Bacterial strains and plasmids 62

2.2 General molecular biology methods 63

2.2.1 Polymerase chain reaction (PCR) 63

2.2.2 Gel electrophoresis 64

2.2.3 DNA restriction enzyme digestion 64

2.2.4 Plasmid preparation 64

2.2.5 Chromosomal DNA extraction 65

2.2.6 Gel extraction 65

2.2.7 DNA purification 65

2.2.8 DNA ligation reactions 66

2.2.9 Plasmid transformations of *E. coli* 66

2.2.10 Bacterial conjugation 67

2.3 Transposon mutagenesis methods 70

2.3.1 Transposon mutagenesis of *P. mirabilis* 70

2.3.2 Screening *P. mirabilis* mini-Tn*5* transposon mutants for swarming and urease mutant phenotypes 72

2.3.3 Confirmatory swarming motility and urease production assays 72

2.3.4 *P. mirabilis* transposon mutant growth curves 73

2.3.5 *P. mirabilis* transposon mutant preliminary biofilm assays 73

2.3.6 *P. mirabilis* transposon mutant preliminary biomineralization assays 74

2.3.7 Confirmation of loss of mini-Tn*5* delivery vector in *P. mirabilis* transposon mutants 74

2.3.8 Sequencing of the genes disrupted in *P. mirabilis* transposon mutants 75

2.3.9 Transposon mutant sequencing data analysis 78

2.3.10 *P. mirabilis* transposon mutant swimming motility assays 78

2.3.11 *P. mirabilis* transposon mutant AU biofilm and mineralization assays 79

2.4 *In vitro* bladder model 80

2.4.1 Setting up the *in vitro* bladder model 83

2.4.2 Operating the *in vitro* bladder model.....83

2.4.3 Processing and quantification of biofilm and mineral accumulation on infected catheter samples from *in vitro* bladder model 84

2.4.4 Biofilm and mineral quantification of *in vitro* bladder model recovered catheter samples.....84

2.4.5 Biofilm and mineral characterisation.....87

2.5 Patient catheter sample processing methods.....87

2.5.1 Clinical catheter sourcing, sectioning, and storage 87

2.5.2 Confocal laser scanning microscopy performed on clinical catheters 88

2.5.3 Fibrinogen quantification- Urine sample sourcing, storage, processing, and analysis.....88

2.5.4 Fibrinogen and biofilm quantification- Clinical catheter sourcing, storage, processing, and analysis.....89

2.6 Patient catheter sample further characterisation methods 90

2.6.1 Characterisation of patient catheter biofilm and mineralization via environmental scanning electron microscopy (ESEM) coupled with energy dispersive X-ray spectroscopy (EDS) and scanning electron microscopy (SEM) imaging 90

2.6.2 Calcium oxalate re-suspension and quantification 91

2.6.3 Genomic DNA extraction and 16S rRNA gene sequencing for microbiome comparison of clinical catheter samples.....92

Chapter 3- Construction of a swarming and urease deficient *P. mirabilis* mutant transposon library 96

3.1 Introduction.....96

3.1.1 Bacterial mutagenesis approaches 97

3.1.2 Transposon mutagenesis.....99

3.1.3 Genetic characterisation of transposon mutants 107

3.1.4 Hypothesis and aims.....110

3.2 Results 110

3.2.1 Confirmatory swarming motility and urease production assays....111

3.2.2 *P. mirabilis* transposon mutant growth curves 116

3.2.3 *P. mirabilis* transposon mutant preliminary biofilm assays 118

3.2.4 *P. mirabilis* transposon mutant preliminary mineralization assays 120

3.2.5 Confirmation of loss of mini-Tn*5* delivery vector in *P. mirabilis* transposon mutants 121

3.2.6 Determining the interrupted genes in *P. mirabilis* transposon mutants 124

3.2.7 *P. mirabilis* transposon mutant swimming assays.....128

3.2.8 *P. mirabilis* transposon mutant AU biofilm and mineralization ...130

3.3 Discussion.....133

3.3.1 *P. mirabilis* transposon mutant library screening for phenotypic alterations.....134

3.3.2 Sequencing and genetic characterisation of *P. mirabilis* mini-Tn*5* mutants.....137

3.3.3 The relevance of *ureR* to *P. mirabilis* pathogenicity.....139

3.3.4 The relevance of *flgI* to *P. mirabilis* pathogenicity.....142

3.4 Conclusions.....145

Chapter 4- Modelling biofilm formation and mineralization on catheter devices using an *in vitro* bladder model.....147

4.1 Introduction.....147

4.1.1 Hypothesis and aims.....151

4.2 Results.....154

4.2.1 The susceptibility of Camstent compared with uncoated silicone catheters to blockage by *P. mirabilis* and *P. aeruginosa* as single- and dual-species inoculants.....154

4.2.2 Quantification of biofilm formation on silicone and Camstent catheter devices following single- and dual-species experiments within the *in vitro* bladder model.....156

4.2.3 ESEM imaging and EDS analysis of biofilm formation on silicone and Camstent catheters following single- and dual-species experiments with *P. mirabilis* and *Ps. aeruginosa* within the *in vitro* bladder model 159

4.2.4 The impact of *ureR* and *flgI* deficiencies in *P. mirabilis* transposon mutants upon their ability to cause catheter blockage.....164

4.2.6 Environmental scanning electron microscopy (ESEM) imaging and energy dispersive X-ray spectroscopy (EDS) analysis of catheter associated

biofilm and mineral formation following *in vitro* bladder model experiments with *flgI* and *ureR* mutants in comparison to the *P. mirabilis* WT strain 169

4.2.7 The susceptibility of Camstent compared with uncoated silicone catheters to blockage and biofilm formation by the *P. mirabilis flgI* mutant 172

4.3 Discussion 175

4.4 Conclusions 181

Chapter 5- A novel catheter coating to reduce bacterial biofilm formation and mineralization – A first-in-man pilot study 182

5.1 Introduction 182

5.1.1 Hypothesis and aims 184

5.2 Results 186

5.2.1 Clinical catheter cohorts 186

5.2.2 Biofilm and mineral accumulation on clinical catheter samples 191

5.2.3 Urinary fibrinogen quantification following catheterization with Camstent and silicone catheters 201

5.2.4 Quantification of fibrinogen and biofilm associated with Camstent and silicone catheters 205

5.3 Discussion 210

5.4 Conclusions 214

Chapter 6- Characterisation of biofilm formation and mineral accumulation on clinical catheter samples 215

6.1 Introduction.....215

6.1.1 Hypothesis and aims.....222

6.2 Results.....223

6.2.1 Biofilms and mineralization on catheters recovered from hospitalized patients.....223

6.2.2 Calcium oxalate deposition on silicone and Camstent catheters recovered from hospitalized patients.....228

6.2.3 Microbial communities on silicone and Camstent catheter samples recovered from hospitalized patients.....230

6.3 Discussion.....234

6.4 Conclusions.....238

Chapter 7- General conclusions and future work.....239

References.....244

Appendices.....284

Appendix A- Overview ESEM images of biofilms and mineralization associated with silicone catheters recovered from the *in vitro* bladder model following single- and dual-species experiments with *Ps. aeruginosa* and *P. mirabilis*.....284

Appendix B- Overview ESEM images of biofilms and mineralization associated with Camstent catheters recovered from the *in vitro* bladder model following single- and dual-species experiments with *Ps. aeruginosa* and *P. mirabilis*.....285

Appendix C: Raw EDS spectra of biofilm and mineralization associated with silicone catheters recovered from the *in vitro* bladder model following single-species experiments with *Ps. aeruginosa* and *P. mirabilis*.....286

Appendix D: Raw EDS spectra of biofilm and mineralization associated with a silicone catheter recovered from the *in vitro* bladder model following a dual-species experiment with *Ps. aeruginosa* and *P. mirabilis*.....287

Appendix E: Raw EDS spectra of biofilm and mineralization associated with a Camstent catheter recovered from the *in vitro* bladder model following a single-species experiment with *Ps. aeruginosa* 288

Appendix F: Raw EDS spectra of biofilm and mineralization associated with a Camstent catheter recovered from the *in vitro* bladder model following a single-species experiment with *P. mirabilis*.....289

Appendix G: Raw EDS spectra of biofilm and mineralization associated with a Camstent catheter recovered from the *in vitro* bladder model following a dual-species experiment with *P. mirabilis* and *Ps. aeruginosa* 290

Appendix H- Overview ESEM images of biofilms and mineralization associated with silicone catheters recovered from the *in vitro* bladder model following experiments with *P. mirabilis* WT, and the *flgI* and *ureR* mutants 291

Appendix I: Raw EDS spectra of biofilm and mineralization associated with a silicone catheter recovered from the *in vitro* bladder model following an experiment with *P. mirabilis* WT 292

Appendix J: Raw EDS spectra of biofilm and mineralization associated with a silicone catheter recovered from the *in vitro* bladder model following an experiment with the *flgI* mutant.....293

Appendix K: Raw EDS spectra of biofilm and mineralization associated with silicone catheter devices recovered from the *in vitro* bladder model following experiments with the *flgI* mutant.....294

Appendix L: Protocol PRO033CSP Preventing biofilm on urinary catheters 295

Appendix M: Participant information sheet for the "Preventing biofilm formation on urinary catheters" study 326

Appendix N: Consent form: Preventing biofilm on urinary catheters....332

Appendix O: Biofilm and mineral quantification per section of Camstent and silicone clinical catheter samples.....333

Appendix P: Standard curve used for quantification of urinary fibrinogen 334

Appendix Q: Raw EDS spectra of biofilm and mineralization associated with silicone clinical catheter sample 20.....335

Appendix R: Raw EDS spectra of biofilm and mineralization associated with silicone clinical catheter sample 15.....336

Appendix S: Raw EDS spectra of biofilm and mineralization associated with Camstent clinical catheter sample 18 337

List of Tables and Figures

Figure 1.1 A Foley Urinary Catheter Device.....20

Figure 1.2 The closed urinary catheter drainage system 21

Figure 1.3 The catheter drainage bag 26

Figure 1.4 Biofilm formation and mineralization.....36

Figure 1.5 The swarming cycle of *P. mirabilis* 45

Figure 1.6 Urinary catheter encrustation and blockage 51

Table 2.1 Composition of AU 60

Table 2.2 Bacterial strains and plasmids 62

Table 2.3: Standard PCR thermal cycler protocol for a *Taq* polymerase reaction 63

Table 2.4 Primers used during this study.....69

Figure 2.1 Plasmid map of the pUT mini-Tn*5* GFP *luxABCDE* Km1 vector ..71

Figure 2.2 Sequencing *P. mirabilis* genes disrupted by mini-*Tn*5- A PCR based approach.....77

Figure 2.3 *In vitro* bladder model 81

Figure 2.4 Full laboratory set-up of the *in vitro* bladder model 82

Figure 2.5 Catheter sample sectioning.....86

Figure 2.6 16 rRNA sequencing and data analysis workflow (Novogene) 95

Figure 3.1 *Tn*5 transposon structure 103

Figure 3.2 Cut and paste *Tn*5 transposition mechanism.....104

Figure 3.3 Confirmatory swarming assay examples of mini-Tn*5 P. mirabilis* mutants.....112

Figure 3.4 Confirmatory urease assay examples of mini-Tn*5* *P. mirabilis* mutants....113
Table 3.1 Swarming and urease assays for swarming negative mini-Tn*5* *P. mirabilis* mutants....114
Table 3.2 Swarming and urease assays for urease negative mini-Tn*5* *P. mirabilis* mutants....115
Figure 3.5 Growth curves of mini-Tn*5* *P. mirabilis* mutants....117
Figure 3.6 Preliminary biofilm assays of mini-Tn*5* *P. mirabilis* mutants....119
Figure 3.7 Preliminary mineral assays of mini-Tn*5* *P. mirabilis* mutants....121
Figure 3.8 Confirmation of delivery vector loss in *P. mirabilis* mini-Tn*5* transposon mutants....123
Table 3.3 Urease negative *P. mirabilis* mini-Tn*5* transposon mutant interrupted gene identification....126
Table 3.4 Swarming negative *P. mirabilis* mini-Tn*5* transposon mutant interrupted gene identification....127
Figure 3.9 *P. mirabilis* mini-Tn*5* transposon mutant swimming assays....129
Figure 3.10 Comparing the biofilm formation and mineralization of transposon mutants in AU to *P. mirabilis* WT....131
Figure 3.11 Quantification of transposon mutant AU biofilm formation and mineralization....132
Figure 3.12 *P. mirabilis* urease gene cluster organization....140
Figure 3.13 Schematic of the *P. mirabilis* flagellar assembly....144
Figure 4.1 Catheter blockage time following single- and dual-species *in vitro* bladder model experiments with *P. mirabilis* and *Ps. aeruginosa* using Camstent and silicone devices....155

Figure 4.2 Biofilm formation on Camstent and silicone catheters following single- and dual-species *in vitro* bladder model experiments with *P. mirabilis* and *Ps. aeruginosa*.....157

Figure 4.3 Quantification of biofilm formation on Camstent and silicone catheters following single- and dual-species *in vitro* bladder model experiments with *P. mirabilis* and *Ps. aeruginosa* 158

Figure 4.4 Raw ESEM imaging and EDS spectra data processing 161

Figure 4.5 ESEM imaging and EDS analysis of silicone catheter samples recovered from the *in vitro* bladder model following single- and dual-species experiments with *P. mirabilis* and *Ps. aeruginosa* 162

Figure 4.6 ESEM imaging and EDS analysis of Camstent catheter samples recovered from the *in vitro* bladder model following single- and dual-species experiments with *P. mirabilis* and *Ps. aeruginosa* 163

Figure 4.7 Time taken to block silicone catheters within the *in vitro* bladder model following inoculation with *P. mirabilis* WT, and the *flgI* and *ureR* transposon mutants 165

Figure 4.8 Biofilms and mineralization associated with silicone catheters recovered from the *in vitro* bladder model following inoculation with *P. mirabilis* WT, and the *flgI* and *ureR* mutants.....167

Figure 4.9 Quantification of biofilm and mineralization associated with catheter samples recovered from the *in vitro* bladder model following experiments with *P. mirabilis* WT, and the *flgI and ureR* mutants.....168

Figure 4.10 ESEM imaging and EDS analysis of biofilm and mineralization formed following *in vitro* bladder model experiments with *P. mirabilis* WT, and the *flgI* and *ureR* mutants.....171

Figure 4.11 Camstent and silicone catheter blockage time, biofilm, and mineral biomass accumulation following *in vitro* bladder model experiments using the *flgI* mutant.....173

Figure 4.12 Representative confocal microscope images of biofilm and mineral associated with Camstent and silicone catheters recovered from the *in vitro* bladder model following inoculation with the *flgI* mutant.....174

Table 5.1: Clinical information on pre-op antibiotics administered to patients and bacterial species identified within pre-op urine cultures 187

Table 5.2: Clinical information on catheter samples forming the 3 cohorts of this study.....189

Figure 5.1: Catheter indwelling time histograms 190

Figure 5.2: Confocal microscope images of the biofilm accumulation on Camstent and silicone clinical catheter samples.....193

Figure 5.3: Confocal microscope images of the mineral accumulation on Camstent and silicone clinical catheter samples.....194

Figure 5.4: Biofilm and mineral accumulation on Camstent and silicone clinical catheters 195

Figure 5.5: Correlation of indwelling time with biofilm and mineral accumulation on Camstent and silicone catheters 198

Figure 5.6: Correlation of indwelling time with biofilm accumulation on Camstent and silicone catheters.....199

Figure 5.7: Correlation of indwelling time with mineral accumulation on Camstent and silicone catheters.....200

Figure 5.8: Mean urinary fibrinogen concentration pre- and post-catheterization 203

Figure 5.9: Urinary fibrinogen concentration change following catheterization with Camstent and silicone catheters.....204
Figure 5.10: Fibrinogen and biofilm associated with Camstent and silicone clinical catheters 206
Figure 5.11: Fibrinogen and biofilm biomass associated with Camstent and silicone catheters recovered from hospitalized patients 207
Figure 5.12: Correlating catheter associated fibrinogen with urinary fibrinogen post-catheterization.....209
Figure 6.1: Different types of mineralization associated with the surfaces of clinical urinary catheter devices 220
Figure 6.2: ESEM imaging and EDS analysis of the luminal surfaces of silicone and Camstent clinical catheter samples 224
Figure 6.3: Single-cell SEM images of silicone catheter lumens.....226
Figure 6.4: SEM images of Camstent catheter sample 18.....227
Figure 6.5: Calcium oxalate concentration vs. mineral accumulation on Camstent and silicone catheter samples 229
Figure 6.6: Relative abundance of the top 10 microbial phyla present on silicone and Camstent catheters from hospitalized patients.....232
Figure 6.7: The number of observed microbial species and the microbial community dissimilarity coefficient between silicone and Camstent catheters 233

Abbreviations

CAUTI:	Catheter associated urinary tract infection
IUC:	Indwelling urinary catheter
Amp:	Ampicillin
Km:	Kanamycin
O/N:	Over-night
SEM:	Scanning electron microscope
ESEM:	Environmental scanning electron microscope
LSM:	Laser scanning microscope
UTI:	Urinary tract infection
EGDPEA:	Ethylene glycol dicyclopentenyl ether acrylate
DEGMA:	Di(ethyleneglycol) methyl ether methacrylate
SWN:	Swarming negative
URN:	Urease negative
Rif:	Rifamipicin
Tc:	Tetracycline
WT:	Wild-type

Chapter 1: Introduction

1.1 Implantable medical devices

A medical device which has been surgically or medically introduced within the human body (partly or completely) with the intent of being kept in place following the procedure, can be defined as implantable (Joung, 2013). The purpose of implantable medical devices can be to regain body function, to improve quality of life, or to maintain life. In 2013 it was estimated that 5-6% of people in industrialized countries had at some point in their lives experienced an implantable device (Joung, 2013). Different implantable medical devices employed for the improvement of quality of life of patients include cardiac defibrillators, cochlear implants, bladder stimulators, and wireless pressure sensors (Greatbatch and Holmes, 1991). The major issue to the functionality of implantable medical devices is their susceptibility to bacterial colonization, which can often lead to infections (Khatoon *et al.*, 2018). Infections associated with implantable devices are a major cause of morbidity and mortality in hospitalized patients, while also increasing medical costs and nursing hours (Kazan *et al.*, 2006).

1.2 Indwelling urinary catheters

Patients within hospital and community care facilities often require urinary tract catheterization. The process involves the introduction of a urinary catheter device into the patient's bladder via the urethra, enabling urine drainage and collection. Requirement for catheterization can be brought about by various causes, such as obstruction in the urethra following scarring or prostate

enlargement, but can also be used to measure urine output and manage incontinence (Stickler and Mclean, 1995; Kunin, 2006).

There are three main types of catheter which can be used to collect and contain urine in people with impaired bladder function: intermittent catheters, external catheters, and indwelling catheters (Feneley, Hopley and Wells, 2015). Intermittent urinary catheters consist of a flexible plastic tube with drainage eyes at the tip end, these devices are inserted into the bladder several times a day draining urine in to a suitable container for disposal. Intermittent catheterization is the recommended procedure to manage urinary retention due to its simplicity, effectiveness, and low infection rates (Lapides *et al.*, 1972; Webb, Lawson and Neal, 1990). Physical disabilities, psychological barriers, small bladder capacity, and inadequate urethral pressure are among the reasons why intermittent catheterization may not be possible, in which case external or condom catheters provide an alternative. External catheters consist of a sheath applied over the penis, with a tube at the tip to enable urine drainage (Mastrigt *et al.*, 2009). This type of catheter offers the advantage of being non-invasive and connected to a transportable collection bag which can be attached to the leg. The main setbacks of this approach are associated with high urinary tract infection rates, which can reach up to 40%, the high chance of catheter detachment and leakage, and the nursing time required for condom catheter care (Ouslander, Greengold and Chen, 1987; Smoger, Felice and Kloecker, 2000). Indwelling balloon-retained catheters address many of the issues associated with the alternative devices employed for urinary drainage, in providing security from leakage, as well as a reduction in nursing time required for management, and a

lower number of associated complications in comparison with the external catheters.

The most commonly used indwelling urethral catheter (IUC) is the Foley catheter (Carr, 2000). Silicone, latex, and polyurethane are among the materials commonly used in the manufacturing of these medical devices (Singha, Locklin and Handa, 2017). The Foley catheter is a tubular device with a retention balloon at its tip, which ensures part of the catheter remains in the bladder, allowing drainage at the opposite end of the tube, where the drainage funnel is linked to the catheter bag (Figure 1.1). To enable the retention of the device, the balloon section is inflated using saline solution, and urine from the bladder drains through an opening above the balloon called the catheter eyehole. Once the catheter balloon is inflated within the bladder and a sterile bag attached to the external end of the device, a closed catheter drainage system is assembled (Figure 1.2). The introduction of the closed drainage system has vastly reduced the number of infections associated with urinary catheterization by limiting the exposure of the catheter to the external environment, thus mitigating the opportunity for bacteria to reach the bladder via the device (Thornton and Andriole, 1970; Burke, Larsen and Stevens, 1986; DeGroot-Kosolcharoen, Guse and Jones, 1988; Jordan and Nicolle, 2014).

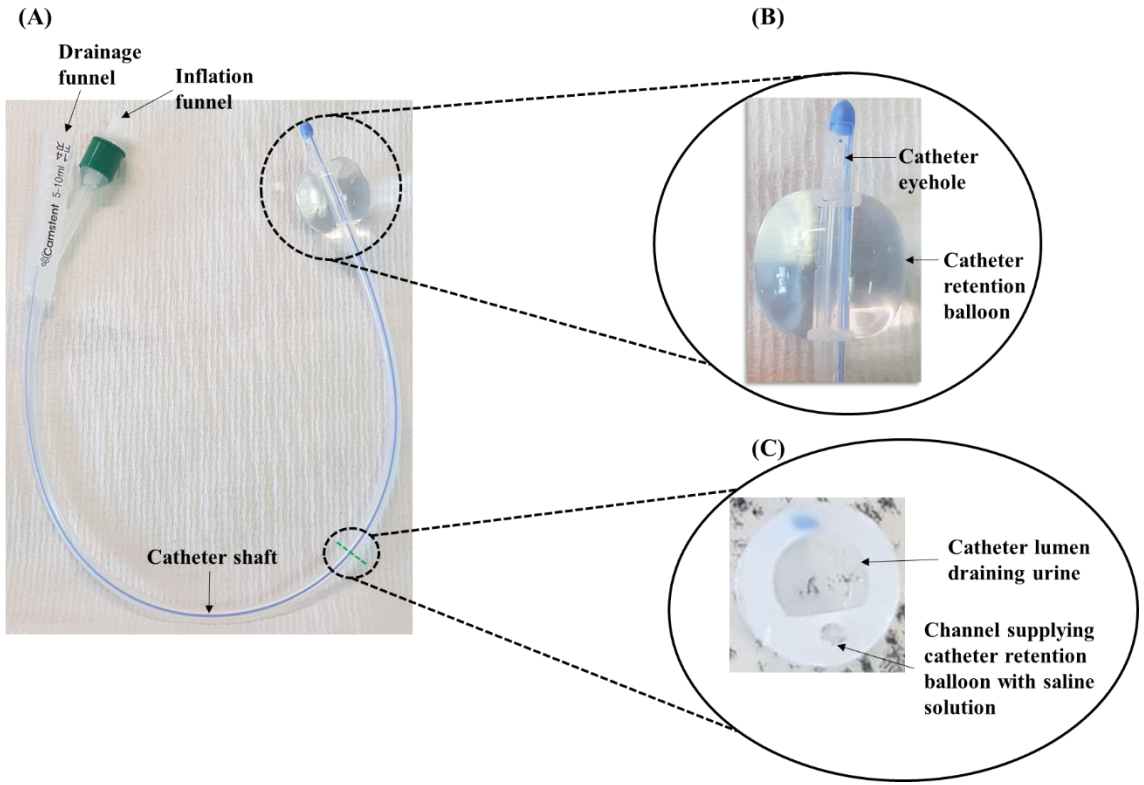

Figure 1.1 A Foley Urinary Catheter Device

(A) A Foley (Camstent) urinary catheter device, with an inflated retention balloon. (B) Catheter retention balloon and catheter eyehole. (C) Cross section of catheter shaft (indicated by green striated line), depicting the channels for urine drainage and balloon inflation.

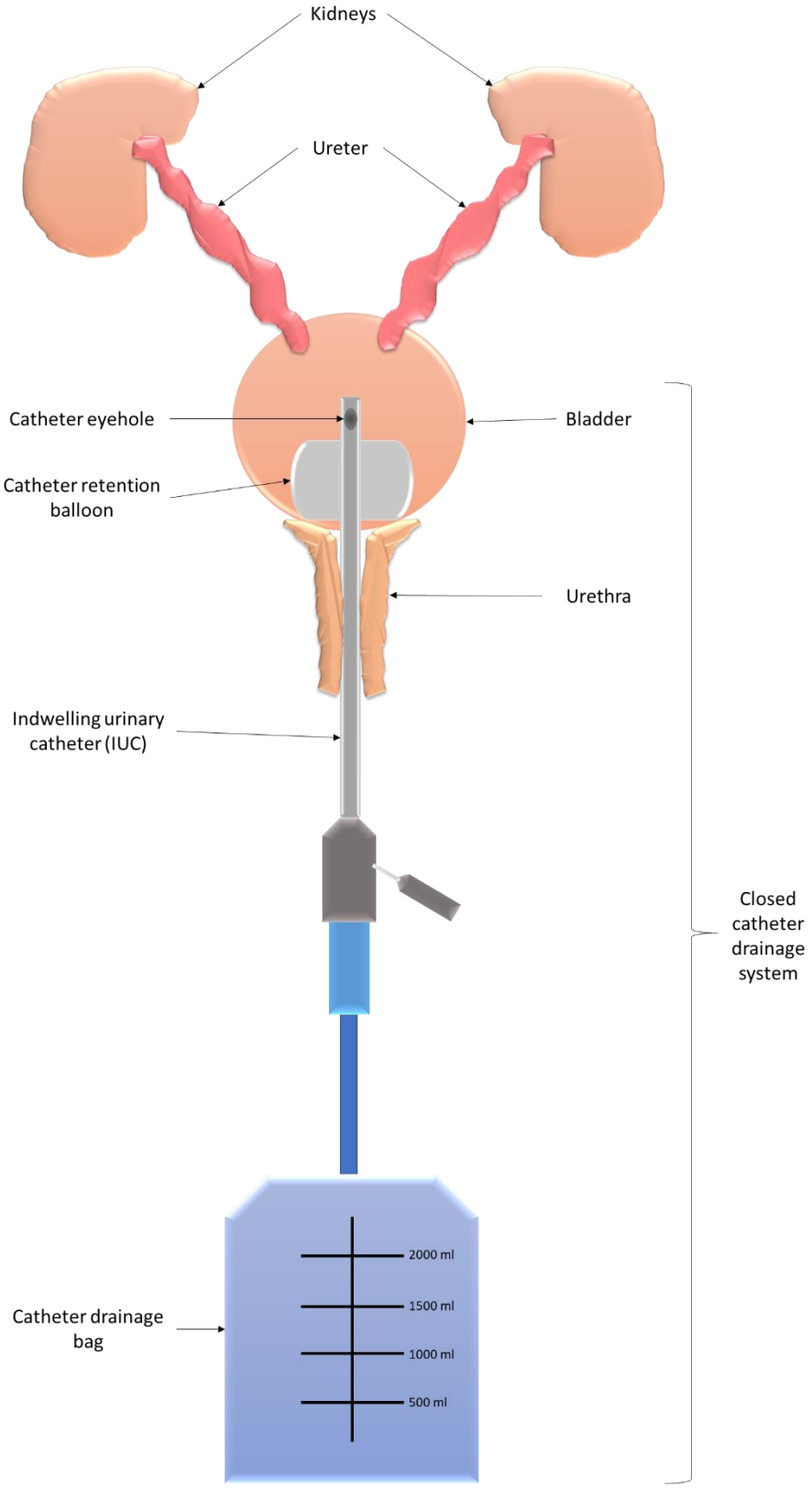

Figure 1.2 The closed urinary catheter drainage system

A diagrammatic overview of the closed urinary catheter drainage system.

IUCs contribute to up to 80% of hospital acquired infections, as well as being the most commonly used indwelling medical device, with 17.5% of patients in 66 European hospitals and 23.6% of patients in 183 US hospitals being catheterized (Zarb *et al.*, 2012; Magill *et al.*, 2014). The risk of infections associated with IUCs arises from the exposure of the bladder environment to bacteria outside the urethra, with the catheter device often acting as the route of access (Stickler, Morris and Williams, 1996). Catheter associated urinary tract infections (CAUTIs) are the most common type of healthcare-associated infection, comprising over 30% of acute care hospital infections (Gardner *et al.*, 2014). The length of time for which patient is catheterized affects the chance of developing a CAUTI, with infection risk increasing by approximately 5% for every extra day of catheterization (Nicolle, 2005).

Long term patient catheterization is generally considered more than 30 days, whereas short term catheterization lasts less than 30 days (Nicolle, 2014). The risk of infection in patients undergoing short term catheterization risk is higher if the urethral meatus is colonized by bacteria defined as potential uropathogens (Garibaldi *et al.*, 1974). It is common practice for catheterized individuals to receive antimicrobial therapy, reducing the rate of infection during the first 4 days of catheterization, however resulting in similar infection rates to patients without antimicrobial intake after the 4 days (Hustinx *et al.*, 1991; Tambyah and Maki, 2000). Patients undergoing long term catheterization are estimated to acquire 3-10 % new infectious organisms per day, which can often add to a developing polymicrobial infection (Warren *et al.*, 1982). The increased risk to patient welfare associated with prolonged catheterization has led to CAUTIs being the source of 50 % of episodes of health-care acquired

bacteraemia in long term care facilities (Nicolle, 2014). Individuals undergoing long term catheterization and cared for within a community setting, are often affected by additional risk factors such as decreased mobility and weaker immune system associated with age, but also co-morbid diseases such as diabetes mellitus, increasing the risk of CAUTI development (Kunin *et al.*, 1992; Meddings *et al.*, 2010).

Complications associated with IUCs can range from fever to urolithiasis, urosepsis, and squamous bladder cancers in patients with chronic CAUTIs (Locke, Hill and Walzer, 1985; Cope *et al.*, 2009; Cameron *et al.*, 2010). Autopsy studies of nursing home patients aged 75 or over indicate 40 % of the individuals undergoing long term catheterization exhibited evidence for acute renal inflammation, as opposed to only 5 % of the individuals without catheters (Warren, Muncie and Hall-Craggs, 1988). Complications associated to CAUTIs such as urinary tract related bacteraemia can cost up to $2,800 per episode (Saint *et al.*, 2000). Taking in to account the additional costs attributed to patients admitted into intensive care units (ICUs), CAUTIs carry an annual economic burden estimated at US$1.7 billion in the US alone (Hollenbeak and Schilling, 2018).

1.3 CAUTIs, uropathogens, and complications

In accordance with the US Centres of Disease Control and Prevention (CDC), a CAUTI can be identified when: a) a patient has had an indwelling urinary catheter for more than 2 days; b) the patient is exhibiting one sign or symptom characteristic of CAUTIs such as fever; and c) the urine culture taken contains over 10^5 CFU/mL of one bacterial species, excluding non-bacterial pathogens (Letica-Kriegel *et al.*, 2019). The prevalence of these infections, as

well as the economic burden and complication risk they carry to the patients' health, make them a healthcare issue of high priority (Nicolle, 2005; Trautner, 2010; Gardner *et al.*, 2014; Letica-Kriegel *et al.*, 2019).

While the adoption of the closed catheter drainage system has proved a successful way to lower the incidence of CAUTIs, the risk of infection, particularly within patients undergoing long-term catheterization, remains high as a result of a number of risk factors such as a regular change of urine collection bags, which would temporarily disturb the closed drainage system (Shbeeb *et al.*, 2014). It has been suggested that the use of the correct catheterization technique, the optimal maintenance of a closed drainage system, and reduction of unnecessary urinary catheter use can lower the incidence of CAUTIs, with up to 69 % of these infections deemed preventable (Gardner *et al.*, 2014).

1.3.1 CAUTI infection routes

IUCs can be exploited by bacteria to bypass host defence and enter the bladder via the lumen of the device (intraluminal route), or by ascending from the perineum to the external catheter surface and eventually the bladder (extraluminal route) (Tambyah, Halvorson and Maki, 1999). The more common mechanism of CAUTI development is via the extraluminal entry of bacteria (66 %), as opposed to the intraluminal route (34 %), whereby the bacteria enter as a result of a contamination in the drainage bag or tubing (Tambyah, Halvorson and Maki, 1999; Warren, 2001). The patient gender can also impact the route of CAUTI development, with the extraluminal route more prevalent in women, and the intraluminal route in men (Tambyah, Halvorson and Maki, 1999). The gender bias exhibited in CAUTI infection routes can result from a number of factors, such as the longer length of male catheters (longer distance for bacteria

to ascend extraluminally) but also the different microbial communities present in male and female urinary tracts (Garibaldi *et al.*, 1974; Nicolle, 2005; Magliano *et al.*, 2012; Feneley, Hopley and Wells, 2015).

Different types of bacteria are also found to prefer a different type of infection route during CAUTI incidence, with Gram positive cocci and yeast pathogens more likely to ascend extraluminally (Tambyah, Halvorson and Maki, 1999). Gram-negative bacilli on the other hand are equally likely to cause CAUTIs via either the extra- or intra-luminal route (MacVane, 2017).

Infections can also arise from the catheter bag used to store the urine flowing down the medical device, with contamination commonly associated with the taps of the bags used to drain the urine (Figure 1.3) (Daifuku and Stamm, 1984; Nickel, Grant and Costerton, 1985; Stamm, 1991). The urine within the bag can serve as a reservoir for the rising bacterial populations, subsequently migrating to the catheter drainage funnel, catheter device itself, and even the bladder, depending on the bacterial motility (Garibaldi *et al.*, 1974; Stickler *et al.*, 2006).

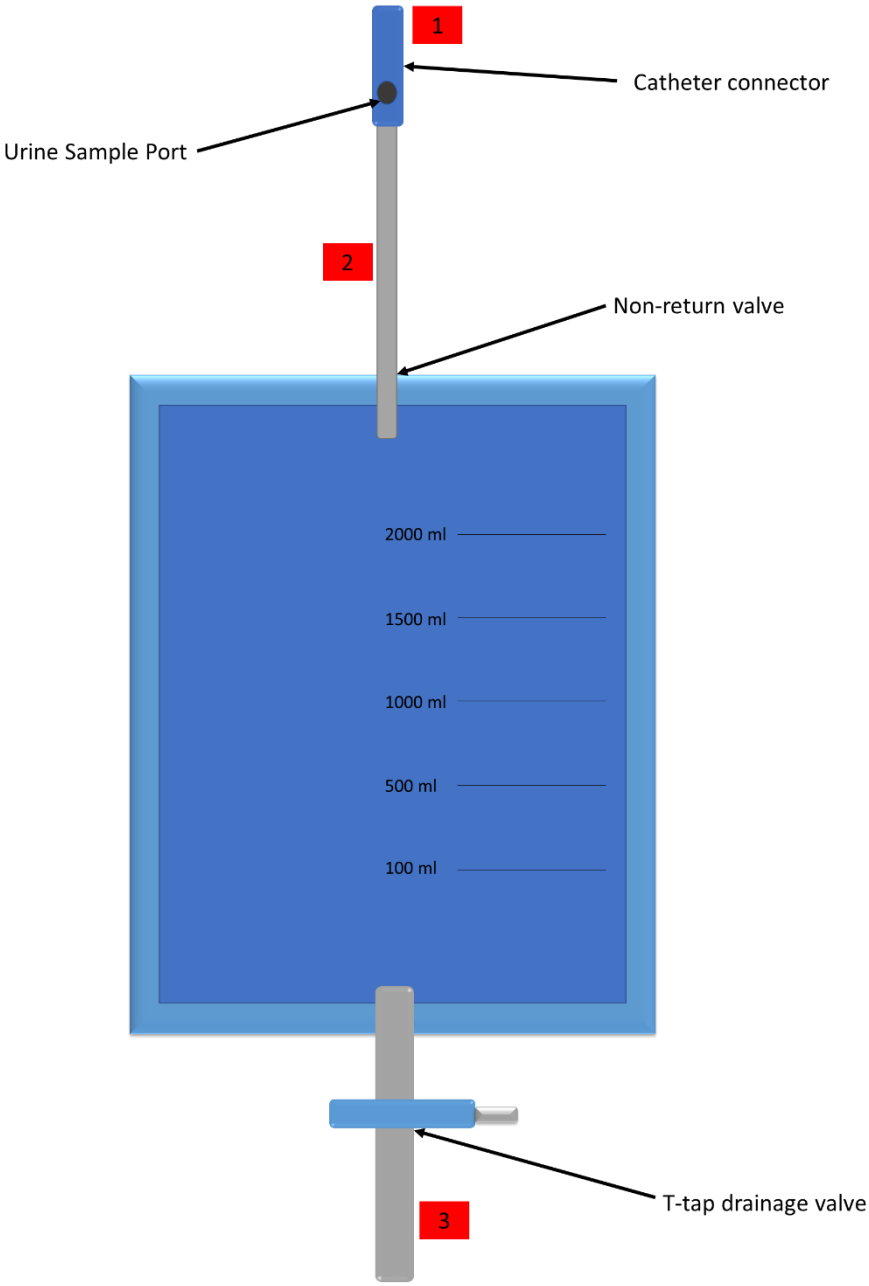

Figure 1.3 The catheter drainage bag

1. A compromised connection of the catheter bag to the catheter device provides an entry port for bacteria into the patient's bladder
2. A urine overfilled bag can serve as a reservoir for infection, there presence of a non-return valve in some bags attempts to address this problem
3. The frequency of use of the drainage valve provides windows of opportunity for bacterial infection

1.3.2 Uropathogens

Urinary pathogens commonly associated with CAUTIs possess several key features which enable them to instigate a persistent infection, such as being potent biofilm formers, urease producers, and having high motility (Xu *et al.*, 2012; Schaffer and Pearson, 2015; Fusco *et al.*, 2017). Bacterial species which meet one or more of these criteria and are regularly identified in CAUTIs include *Proteus mirabilis*, *Pseudomonas aeruginosa*, *Staphylococcus epidermidis*, *Enterococcus faecalis*, *Escherichia coli*, *Klebsiella pneumoniae*, and *Providencia stuartii* (Flores-Mireles *et al.*, 2015). CAUTIs often comprise polymicrobial infections with several uropathogenic bacteria commonly isolated from patient samples, seemingly coexisting and even cooperating (Mach *et al.*, 2009; Terlizzi, Gribaudo and Maffei, 2017; Armbruster, Mobley and Pearson, 2018).

Polymicrobial communities identified in patients diagnosed with CAUTIs are regularly composed of hospital acquired bacteria, commensal bacteria, and common urinary pathogens (Nicolle, 2014; Tien *et al.*, 2017). The diversity of bacteria associated with CAUTIs enables the development of a wide range of antimicrobial resistance, making these infections especially challenging to treat (Alling, Seeberg and Svanborg, 1975; Warren *et al.*, 1982). The general practice of prophylactic antibiotic treatment courses during urinary catheterization within medical facilities, even in cases where a CAUTI is asymptomatic, further intensifies the antibiotic resistance problem associated with these infections (Garibaldi *et al.*, 1974; Bjork, Pelletier and Tight, 1984; Köves, Magyar and Tenke, 2017; Peng *et al.*, 2018). The administration of antibiotics in cases of asymptomatic bacteriuria (ABU) with the intent of UTI

prevention has in fact been outlined as a particularly ineffective measure in tackling infection development, additionally causing adverse patient side-effects and stimulating the emergence of antibiotic resistance (Harding *et al.*, 2002; Trautner and Darouiche, 2004). The only beneficial effect of antibiotic administration to asymptomatic catheterized individuals has been shown to be upon physicians themselves, with studies showing that patients taking chronic urinary anti-microbials received less non-protocol antibiotics from their assigned physicians in comparison to the untreated group of patients (Warren *et al.*, 1982).

1.3.3 CAUTI complications

Symptomatic CAUTIs are linked to complications ranging from mild fever to severe pyelonephritis, and even urosepsis and death if untreated (Warren, 2001; Niël-Weise and Van Den Broek, 2009). The recurrence of complicated CAUTIs results in long term morbidity linked to the catheter device encrustation or blockage with mineralized biofilms, increasing the resistance of pathogenic bacteria to host immune responses and antibiotic treatments (Stickler and Zimakoff, 1994).

The prolonged patient hospitalization associated with CAUTI complications increases the risk of nosocomial infections, infection by multiple drug resistant microorganisms, and the economic burden (Al-Hazmi, 2015). Patients who have acquired a catheter associated nosocomial bacteraemia have their hospital stay increased by up to 19 days on average and their hospital costs tripled, in comparison to similar patients without this complication (Rose *et al.*, 1977). CAUTI complications also increase the risk of patient death, with

catheterization associated bacteriuria increasing the chance of mortality some 2.8-fold (Platt *et al.*, 1982, 1983).

1.4 Biofilms and mineralization

Single-celled organisms such as bacteria are capable of adopting multicellular behaviours such as biofilm formation, enhancing their potential for survival in challenging environments. The formation of a biofilm, where a community of microorganisms is attached to a surface, can be described as a dynamic developmental process encompassing multiple regulatory networks, impacting gene expression, and thus mediating the organization of bacterial cells in a spatial and temporal sense (Figure 1.4) (Ramsay *et al.*, 1989; Parsek and Singh, 2003; Monds and O'Toole, 2009; Kostakioti, Hadjifrangiskou and Hultgren, 2013). The biofilm formation process re-programs the bacterial cells in terms of the most favourable mechanism of nutrient uptake, the surface molecules expressed and the virulence factors engaged, building up the capabilities of the microbial community to sustain itself within the prevailing environment (Cincarova *et al.*, 2016; Dzianach *et al.*, 2019; Graeber *et al.*, 2019; Vyas *et al.*, 2019). The extracellular polymeric substance (EPS) comprises the self-generated extracellular matrix of biofilms (~90 % of biofilm biomass), within which bacterial cells are enmeshed (Flemming and Wingender, 2010). The composition of the EPS includes various components such as polysaccharides, proteins, nucleic acids, and lipids, stabilising the biofilm community, mediating surface adhesion, and acting as a 3D polymer network interconnecting the bacterial cells (Flemming and Wingender, 2010; Kostakioti, Hadjifrangiskou and Hultgren, 2013).

Biofilm formation affects most physiological processes within a wide range of ecosystems, with an estimated 99.9 % of bacteria growing as biofilms on a broad range of surfaces (Costerton, Geesey and Cheng, 1978; Costerton *et al.*, 1995; Donlan and Costerton, 2002). Medical devices such as IUCs are particularly prone to biofilm formation as they can disrupt the commensal bacterial communities of the urinary tract, in the case of indwelling devices, allowing the abundance of biofilm forming bacteria to rise (Hashmi *et al.*, 2003; Horwitz *et al.*, 2015). IUCs damage the mucosal lining of the patient's bladder and introduce pathogenic biofilm forming bacteria, resulting in an immune response where host proteins such as fibrinogen can cover the device surface, further promoting bacterial attachment and biofilm formation (Glahn, 1988; Flores-Mireles *et al.*, 2014; Colomer-Winter, Lemos and Flores-Mireles, 2019).

Resilient infections resulting from bacterial biofilm formation on IUCs are at the centre of the persistence, recurrence, and relapse of UTI diagnosed patients. The increased resistance to environmental cues, antimicrobial agents, and simple shear stress (such as urine flow), that biofilm formation provides for pathogenic bacteria colonizing medical devices makes these infections particularly difficult to treat (Trautner and Darouiche, 2004; Singh *et al.*, 2017; Khatoon *et al.*, 2018). Animal infection models have been used to demonstrate the increased resistance of infectious microorganisms to antimicrobial treatments conveyed by biofilm formation, with one example being planktonic *P. mirabilis* cells eradicated rapidly and efficiently by ciprofloxacin in UTIs induced in mice, however upon the establishment of a biofilm the pathogen was able to induce a persistent and recurrent infection despite antibiotic administration (Kadurugamuwa *et al.*, 2005).

There are a number of characteristics which biofilms confer to microbial cells to improve their resilience and enable the establishment of a recurrent infection including poor antibiotic penetration, nutrient limitation, slow growth as an adaptive stress response, the formation of persister cells, and protection from the host-immune response (Delcaru *et al.*, 2016). Some of the mechanisms through which biofilms confer resistance include a physical barrier, where anionic and cationic molecules within the EPS bind charged compounds including antibiotics, physiological limitation (e.g. age, starvation, growth-rate reduction), which would reduce the biofilm susceptibility, multi-drug efflux pumps, and microbial genetic diversification (Yin *et al.*, 2019). The MexAB-OprM and MexCD-OprJ multi-drug efflux pumps examples of *Ps. aeruginosa* biofilm confer resistance to antimicrobials such as tobramycin, gentamicin, and tetracycline (Soto, 2013).

In addition to the implications which biofilms have upon the resilience and recurrence of CAUTIs as a result of their multiple defence mechanisms against environmental pressures, they also have practical consequences from a clinical perspective impacting the results of microbiological studies (Trautner and Darouiche, 2004). In the presence of biofilms within CAUTIs both bacterial species identification and antibiotic susceptibility have commonly been shown to be misleading, as results are focused on the planktonic cells present within urine culture at the time of collection, neglecting the biofilm community formed on the indwelling catheter device (Nickel *et al.*, 1994). This could in turn affect the treating physician's judgement of the infection severity, as well as having implications for the choice of antibiotic treatment.

Biofilms are considered to follow a general model of development where initial reversible attachment is followed by a transition to irreversible attachment, maturation, and eventually dispersion (Donlan, 2002; Sauer *et al.*, 2004; Toutain *et al.*, 2007; Beloin, Roux and Ghigo, 2008; Kostakioti, Hadjifrangiskou and Hultgren, 2013). Depending on the bacteria which compose the biofilm however, specific bacterial communities such as those consisting of urease enzyme producers can develop characteristics such as mineralization, altering the biofilm structure, composition, and enhancing its resistance to antimicrobials (Oki *et al.*, 2010; Li *et al.*, 2015; Wilks, Fader and Keevil, 2015; Bisht and Ann Wakeman, 2019).

1.4.1 Urine composition and the immune response to catheterization-Fibrinogen and Tamm-Horsfall Protein (THP)

The urine of healthy individuals is nutrient limited, making it unsuitable for bacterial growth (Aubron *et al.*, 2012). The daily protein excretion in the urine of a healthy individual is less than 150 mg/day (Barratt and Topham, 2007). Two main sources contribute 97% of urinary proteins: glomerular filtration of plasma proteins and sloughed epithelial cells. 3% of protein excreted in urine originates from epithelia lining the urinary tract, which include exosomes secreted by B cells, T cells, platelets, and enterocytes (Barratt and Topham, 2007). Trauma in patients, such as the placement of a urinary catheter, alters urinary composition, with components promoting bacterial growth such as catecholamines increasing in abundance (Lyte and Ernst, 1992). It has been demonstrated that the urine of trauma patients supports the growth of *E. coli* much better than the urine of healthy patients, with change in urinary glucose,

amino acid, and iron levels likely contributing to the improved bacterial proliferation (Aubron *et al.*, 2012).

Fibrinogen is a protein found in blood plasma and produced by the liver as a coagulation factor, forming part of the normal blood clotting mechanism (Lowe, Rumley and Mackie, 2004). The protein is released in response to injury with the purpose of developing a clot and preventing extensive bleeding (Mosesson, 2005). The mechanical stress and tissue damage resulting from IUC placement results in an increase in circulating fibrinogen, entry in to the bladder, and deposition on the medical device in a time dependent manner (Parsons, 1986; Goble, Clarke and Hammonds, 1989; Peychl and Zalud, 2008). Fibrinogen deposition on the catheter surface facilitates uropathogen colonization and persistence on the medical device and bladder (Flores-Mireles *et al.*, 2016). Specific examples of pathogenic bacteria shown to exploit the fibrinogen coverage of medical devices include *E. faecalis*, *Staphylococcus aureus*, and *Candida albicans* (Nallapareddy *et al.*, 2006; Flores-Mireles *et al.*, 2014; Walker *et al.*, 2017). All of these uropathogens encode surface proteins and adhesins, such as *Ebp* in *E. faecalis* and *Mp*58 in *C. albicans*, which enable the bacteria, normally poorly binding to bladder mucosa, to attach to the fibrinogen covered IUC and persist in the bladder environment increasing the risk of CAUTIs (Sepúlveda *et al.*, 1998; Flores-Mireles *et al.*, 2014).

Tamm-Horsfall protein (THP) is a versatile glycoprotein capable of binding to a range of different surfaces (Serafini-Cessi, Malagolini and Cavallone, 2003). It is the most abundant protein in normal urine, with its presumed function being to bind and help clear uropathogens from the urinary tract (Kumar and Muchmore, 1990; Rampoldi *et al.*, 2011). In the presence of

an IUC however, this protein can cover the medical device surface forming a conditioning layer which enhances bacterial attachment and subsequent biofilm formation. *In vitro* murine models have previously demonstrated the enhanced binding of *E. coli* in the presence of elevated THP levels via type 1 fimbrae (Mobley *et al.*, 1987; Pak *et al.*, 2001; Raffi *et al.*, 2012). Clinical catheter studies have also demonstrated that the presence of a THP coating on latex and silicone devices can facilitate the binding of *E. coli* and *Ps. aeruginosa*, with the amount of adsorbed THP higher on culture positive catheters (Raffi *et al.*, 2012).

1.4.2 Bacterial attachment

Bacterial attachment to surfaces is mediated by cell organelles, namely any pili or flagella the cells may possess, but also by the type of surface encountered (Tuson and Weibel, 2013; Berne *et al.*, 2015). The presence of a conditioning film on surfaces, defined as the adsorption of (macro)molecules onto the substrate, can alter the physicochemical properties of the material and influence bacterial attachment (Lorite *et al.*, 2011). The roughness of medical device material surfaces, such as latex of IUCs, has been found to promote bacterial cell attachment and biofilm formation (Allion, Baron and Boulange-Petermann, 2006; Siddiq and Darouiche, 2012). Alternatives to latex such as silicone and polyurethane (PUR) are therefore now the more popular choices as base catheter materials, overcoming some of the problems associated with latex catheter devices (Singha, Locklin and Handa, 2017). Silicone and PUR based catheters are also associated with issues however, with the engineering techniques employed in the manufacturing of catheters producing rough catheter eyehole rim surfaces, increasing susceptibility of this part of the devices to bacterial attachment (Stickler *et al.*, 2003; Jacobsen *et al.*, 2008).

When free-swimming planktonic bacteria interact with a surface, such as that of a medical device, they can sense and determine how favourable that surface is for biofilm formation depending on environmental factors such as spatial gradients, chemical gradients, osmolality, presence of soluble compounds, and the chemical and physical properties of the surface (Palmer, Flint and Brooks, 2007; Tuson and Weibel, 2013). In general, every surface is advantageous for bacteria in comparison to a liquid, as all surfaces adsorb macromolecules (conditioning layer) (Palmer, Flint and Brooks, 2007; Petrova and Sauer, 2012). The conditioning layer is a favourable environment for the metabolic activity of bacteria, providing nutritional cues in the form of proteins and polysaccharides, which can serve as triggers for biofilm formation (Donlan, 2002). Altering the chemical and physical properties of a surface however can have a detrimental effect on the strength of bacterial adhesion and the biofilm formation. For example, PEG-based and zwitterionic polymers have been shown to effectively exclude biomolecules from surfaces, as a result of their high hydrophilicity (Kingshott *et al.*, 2003; Cheng *et al.*, 2007).

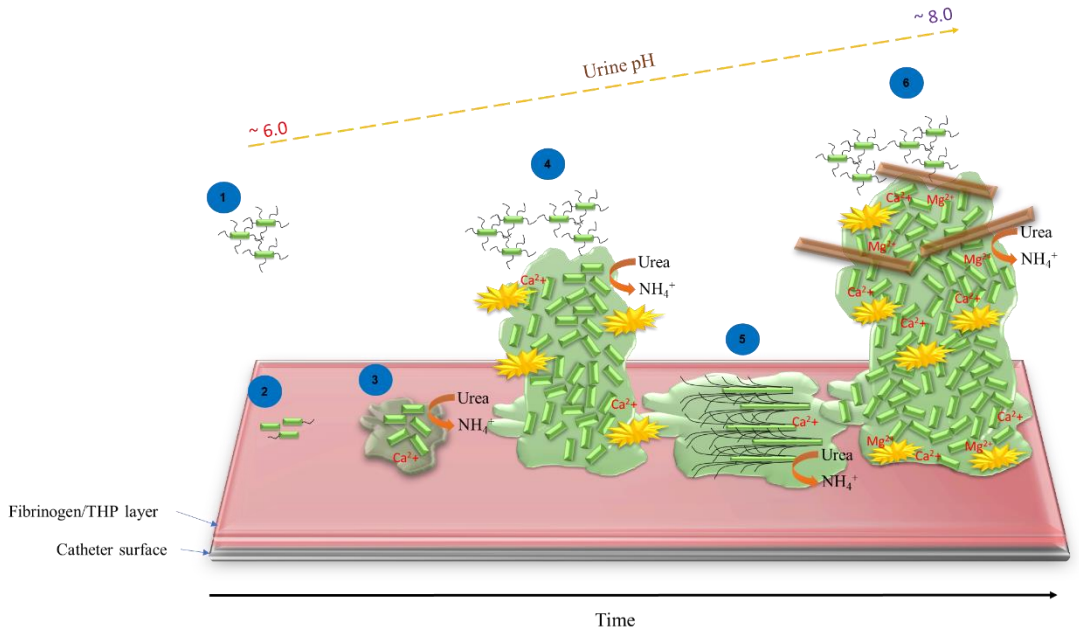

Figure 1.4 Biofilm formation and mineralization

1. Planktonic swimming bacterial cells enter urine of the catheterized urinary tract
2. The planktonic bacteria attach to the catheter surface coated in conditioning film (THP/fibrinogen layer may form as film over surface or in patches), forming microcolonies
3. Microcolonies produce EPS and urease adsorbing calcium cations, resulting in mineral precipitation
4. The biofilm reaches a mature stage, releasing individual bacterial cells for further colonization, the consistent activity of the urease enzyme has caused urinary pH to rise to approximately 8.0, instigating the mineralization of the biofilm matrix
5. A biofilm composed of *P. mirabilis* can also initiate further colonization via swarming motility
6. The appearance of struvite and apatite mineralization within the biofilm matrix stabilizes its structure and increase its resistance to environmental cues

1.4.3 Biofilm formation

The occurrence of the transition from reversible attachment of bacterial cells to a surface, to irreversible attachment is detrimental to the commencement of the biofilm formation process (Sauer *et al.,* 2002; Agladze, Jackson and Romeo, 2003). When bacteria attach reversibly they exhibit a low binding strength enabling them to readily detach and return to planktonic state, but also spinning, vibrating or moving motions associated with the presence of flagella (Toutain *et al.*, 2007; Petrova and Sauer, 2012). The irreversible attachment of bacterial cells to a surface can often be identified by contact along their long axis, reduced flagellar rotation, and increased polysaccharide production (Belas, 1996; Petrova and Sauer, 2012).

Following the irreversible attachment of bacterial cells to a surface, the expression of various different genes is altered, motility related genes such as the flagellar genes are generally downregulated, while genes important for synthesis of exopolysaccharides part of the biofilm matrix, such as *pslACDEFGHIJKL* in *P. aeruginosa,* undergo upregulation (Jansen *et al.*, 2004; Overhage *et al.*, 2005; Mika and Hengge, 2013). The alterations in gene expression enable the irreversibly attached bacteria to transition into the next stage of biofilm formation where cells are able form microcolonies (Figure 1.4). Microcolonies form as the bacterial cell population grows via clonal expansion, resulting in aggregation (Aparna and Yadav, 2008). Inter-communication between bacteria in the form of quorum sensing enables the organisms to control the aggregation progress, and therefore the development of the 3D structure of the biofilm (Camilli and Bassler, 2006).

A crucial component of the biofilm's 3D structure is the extracellular matrix (EM), providing protection to the bacterial cells from desiccation and immune responses, but also acting as a diffusion barrier (Martínez and Vadyvaloo, 2014). Part of the EM is the extracellular polymeric substance (EPS), increasingly produced by bacteria as the biofilm matures, associated with improved cell adherence, quorum sensing, and genetic material exchange such as conjugation (Donlan, 2002; Bogino *et al.*, 2013).

Quorum sensing communication between bacterial cells is of crucial importance to biofilm development as it facilitates the controlled spatial distribution of aggregating cells (Nadell *et al.*, 2008; Li and Tian, 2012; Gao *et al.*, 2016). Bacteria conduct quorum sensing via extracellular signalling molecules called autoinducers (AIs), which accumulate as bacterial population density rises, enabling bacteria to adjust gene expression in accordance with the increase or decrease in their cell numbers (Rutherford and Bassler, 2012). Quorum sensing systems differ among bacteria, with Gram-positive bacteria using autoinducing peptides (AIPs) as signalling molecules, while Gram-negative bacteria incorporate AIs such as acyl-homoserine lactones (AHLs) or other molecules which are capable of diffusing through the bacterial membrane, such as 2-heptyl-3-hydroxy-4-quinolone (PQS) in *Ps. aeruginosa* (Papenfort and Bassler, 2016). *S. aureus* and *Ps. aeruginosa* are just two examples of clinically relevant bacteria which use quorum sensing for virulence factor regulation (Williams and Cámara, 2009; Thoendel *et al.*, 2011). The EPS surrounding the bacterial cells ensures the efficiency of quorum sensing communication during this stage of biofilm development by limiting the leaching of quorum sensing molecules in to the surrounding media (Nadell *et*

al., 2008). Efficient quorum sensing communication enables the biofilm to develop by facilitating the necessary gene expression for maturation (Miller and Bassler, 2001; Khmel and Metlitskaya, 2006).

According to the generally accepted model of biofilm formation planktonic bacterial cells initially colonise materials, the cells subsequently form microcolonies, which eventually mature into what we refer to as a biofilm (Figure 1.4) (Donlan, 2002). The mature biofilms of certain bacterial species such as *Ps. aeruginosa* take up characteristic shapes such as "mushrooms", within particular growth models such as flow cells, with the distribution of the bacterial cells within these structures depending on their function within the biofilm (Klausen *et al.*, 2003; Mann and Wozniak, 2012; Ghanbari *et al.*, 2016). For example, it has been demonstrated that immobile *Ps. aeruginosa* bacterial cells are part of the lower part of the mushroom structures of the biofilm (stalks), whereas motile cells of this bacterial species colonise the top part of the mushrooms (Klausen *et al.*, 2003).

While the "mushroom" shaped mature biofilm has been a distinguishing feature of *Ps. aeruginosa*, the general model of biofilm formation has been widely accepted for most biofilm forming bacterial species (Donlan, 2002; López, Vlamakis and Kolter, 2010). There are however bacterial species who differ in their biofilm formation from the generally accepted model, such as urease producing bacteria. Urease producing bacteria are particularly prominent pathogens within the urinary tract, as they are able to incorporate minerals within their biofilms, altering the biofilm organisation and becoming yet more resilient and stable as a community (Shu *et al.*, 2003; Oki *et al.*, 2010; Li *et al.*, 2015; Vandecandelaere *et al.*, 2017).

1.4.4 Biofilm associated mineralization

Mineralization associated with urease producing bacteria such as *P. mirabilis* often consist of two components, large struvite [$NH_4MgPO.\ 6H_2O$] and smaller apatite [$Ca_{10}(PO_4)_6(OH)_2$] minerals (Figure 1.4) (Torzewska and Rozalski, 2014; Prywer, Sadowski and Torzewska, 2015). The urease enzymes produced by bacterial cells hydrolyse urea in to ammonia, increasing the pH of the urine, resulting in the precipitation of minerals and their incorporation into the biofilm (Colin *et al.*, 2016; Cortese *et al.*, 2018). As the bacterial biofilm and its associated mineralization develop, medical devices such as catheters become encrusted. The mineral encrustation can restrict the urine flow and eventually cause blockage of the device (Nicola Sian Morris and Stickler, 1998; Stickler and Feneley, 2010; Milo *et al.*, 2017). Studies investigating the incidence of morbidity linked to patient catheterization indicate that up to 48 % of patients with long-term catheter devices experienced blockage, with 37 % reporting the flow of urine by-passing the medical device (Kohler-Ockmore, 1996).

Urease producing bacteria also incorporate the anionic nature of their EM to attract and bind precipitates from urine, such as calcium and magnesium cations (Rodriguez-Navarro *et al.*, 2012; Anbu *et al.*, 2016). As the pH of the urine increases, the abundance of cationic precipitates also rises, and their incorporation in to the biofilm is believed to be important for mineralization (Broomfield *et al.*, 2009; Cortese *et al.*, 2018). The alkalinity of the biofilm is crucial to the stability and growth of crystallization and the EM plays an important role in maintaining the alkaline environment by scavenging ammonium ions, a by-product of urea hydrolysis carried out by the urease enzyme (Carter *et al.*, 2009; Oki *et al.*, 2010; Zhou *et al.*, 2019). The anionic

capsule polymers (CPSs) possessed by certain uropathogens such as *P. mirabilis* further enhance their ability to bind and retain magnesium ions subsequently incorporated within struvite mineral formation (Dumanski *et al.*, 1994; Rózalski, Sidorczyk and Kotełko, 1997). As well as impacting medical devices, the process of biofilm mineralization is linked to the formation of kidney and bladder stones within patients (Delcaru *et al.*, 2016). It is estimated that approximately 10 % of people will be diagnosed with urinary stone formation in their lifetime, with bacteria isolated from 15-70 % of stones (Thompson and Stamey, 1973; Pak, 1998; Tavichakorntrakool *et al.*, 2012).

1.5 *Proteus mirabilis*

Proteus mirabilis is the most potent urease producer among uropathogens, with the enzyme produced known to be particularly reactive, making this bacterial species a prominent cause of CAUTIs (Broomfield *et al.*, 2009; Flores-Mireles *et al.*, 2015; Armbruster *et al.*, 2017). The opportunistic nature of this Gram-negative pathogen enables it to infect compromised individuals with ongoing urinary tract issues, as well as patients undergoing prolonged catheterization (Jacobsen *et al.*, 2008).

While *P. mirabilis* infections are often counteracted via the administration of antibiotics such as ceftriaxone or gentamicin, there is an increase in the number of multi-antibiotic resistant clinical strains isolated (Stock, 2003; Wang *et al.*, 2014). Studies suggest that over the last 10 years there has been a significant increase in resistance of *P. mirabilis* to 3rd-generation cephalosporins and ciprofloxacin, linked to an increase in prevalence of strains producing antibiotic resistance enzymes including AmpC β-lactamases, extended-spectrum β-lactamases (ESBL), and carbapenemases (Jacoby, 2009;

Datta *et al.*, 2014; Wang *et al.*, 2014). The trend of increase in antibiotic resistance has led to a rise in mortality and morbidity rates in *P. mirabilis* associated CAUTIs (Giamarellos-Bourboulis *et al.*, 2006; Chen *et al.*, 2012).

1.5.1 *P. mirabilis* motility- twitch, swim, and swarm

P. mirabilis normally inhabits the intestinal tract of humans, however it is able to express various virulence factors making it a particularly harmful pathogen should it find itself within a part of the human body where it can cause an infection, such as the urinary tract (Hamilton *et al.*, 2018). The invasiveness of *P. mirabilis* as a pathogen is related to its ability to spread throughout the host's body or medical device via its three modes of motility- twitching, swimming, and swarming (Hola, Peroutkova and Ruzicka, 2012). When bacteria of this species are found on solid surfaces, they tend to twitch, a type of motility independent of flagella, instead involving the extension and retraction of type IV pili, which can be conducted by individual cells or cell communities (Mattick, 2002). When the bacterial cells are within a liquid medium, such as urine, they manifest swimming motility, characterised by the presence of 6 to 10 rotating peritrichous flagella on the bacterium surface, driven by a specific cue such as a chemical gradient (Macnab, 2003; Schaffer and Pearson, 2015).

While swimming and twitching are widely encountered modes of motility among various bacteria, swarming motility is characteristic of only three bacterial families; *Firmicutes* (e.g. *Bacillus cereus*), *Alphaproteobacteria* (e.g. *Rhodospirillum rubrum*), and *Gammaproteobacteria* (e.g. *P. mirabilis* and *Ps. aeruginosa*) (Mattick, 2002; Kerchove and Elimelech, 2008; Bottone, 2010; Kearns, 2010). *P. mirabilis* is one of the widely-recognised swarming species of bacteria, with this mode of motility being a crucial component of its ability to

colonise medical devices, as it enables the bacterial cells to move across solid surfaces (Figure 1.4) (Jones *et al.*, 2004; Pearson *et al.*, 2010; Schaffer and Pearson, 2015; Armbruster, Mobley and Pearson, 2018).

The mechanism of swarming motility in *P. mirabilis* requires communication between the single bacterial cells, as well as gene expression alterations (Girgis *et al.*, 2007; Saak and Gibbs, 2016). As the number of flagella are particularly important in *P. mirabilis* swarming motility, the genes responsible for the development of these organelles on the surface of cells have been found to be particularly upregulated (Morgenstein, Szostek and Rather, 2010). Signalling by protein exchange through contact dependent secretion systems, between the *P. mirabilis* cells during swarming is very important to this type of motility as the bacteria cannot swarm alone, but must instead implement an orderly and organised swarming front coordinated by multicellular cooperation (Wenren *et al.*, 2013; Tipping and Gibbs, 2019).

The swarmer cell differentiation, migration and behaviour, associated with the capability of *P. mirabilis* to colonize IUCs, can be described by 4 distinguished phases. These include the induction of differentiation in to swarming cells, the lag period prior to swarming behaviour establishment, active migration by swarming motility, and a consolidation phase (Belas, Schneider and Melch, 1998).

1.4.1.1 Cell Differentiation

The process of *P. mirabilis* cell differentiation occurs in response to contact with a surface or medium of sufficient viscosity to affect the flagellar rotation of the swimming bacteria (Figure 1.5) (Allison *et al.*, 1993). Flagellar

rotation within *P. mirabilis* is coordinated by the master operon *flhDC*, this operon is upregulated via *umoD* when the flagella can no longer rotate freely following interactions with a solid or viscous medium (Dufour, Furness and Hughes, 1998). The inhibition of flagellar rotation subsequently triggers events resulting in the upregulation of flagellar biosynthesis genes, such as *flaA*, as well as genes linked to the elongation of the cells, such as *mtgA* (Pearson *et al.*, 2010). The result of the cell differentiation process is the hyperflagellated, multinucleate, elongated morphology of *P. mirabilis* cells necessary for swarming (Allison *et al.*, 1994).

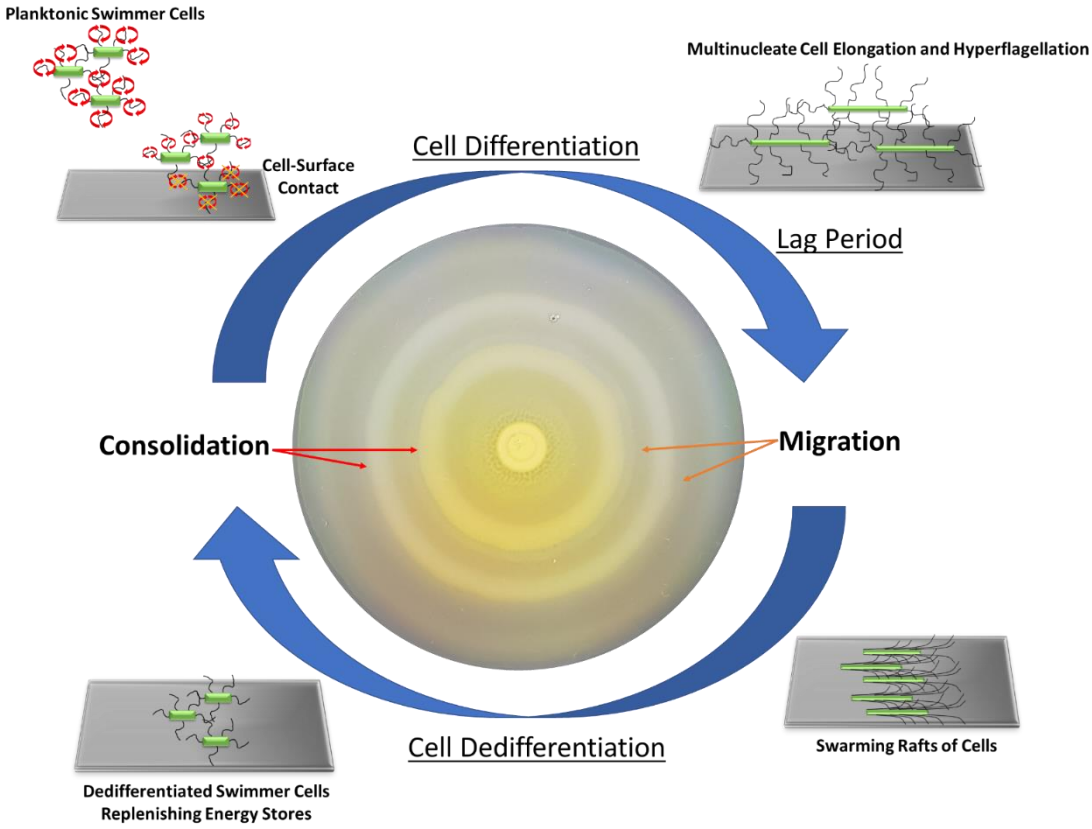

Figure 1.5 The swarming cycle of *P. mirabilis*

The characteristic bulls-eye pattern exhibited by *P. mirabilis* swarming on agar. The bacterial cells swarm from the central colony before dedifferentiating and entering a consolidation state. Once they have generated enough energy the cells differentiate once more and begin migrating, proceeding through the cycle of swarming motility. The image was obtained during the present study (Figure adapted from Belas, 1996).

1.4.1.2 Lag Period and Migration

Multiple bacterial cells must experience the effect of the medium change (increase in viscosity which prevents swimming motility), as swarming is a multicellular mode of motility dependent upon cell-cell interactions (Williams and Schwarzhoff, 1978). Differentiated *P. mirabilis* cells exhibit a 3 h lag period at 37^{o}C prior to migrating, associated to the required communication between a number of bacterial cells before engaging in swarming (Belas, Schneider and Melch, 1998). The swarming motility of *P. mirabilis* is a highly organised endeavour where differentiated individual cells are connected by flagella and arranged to form characteristic rafts, allowing them to swarm over solid or viscous surfaces (Stickler and Hughes, 1999; Jones *et al.*, 2004).

1.4.1.3 Consolidation

The swarming front of *P. mirabilis* cells eventually slows down, at this point the bacteria dedifferentiate taking up a shorter rod shaped morphology, in a process known as consolidation (Pearson *et al.*, 2010). It has been proposed that the reason for the cessation of swarming could be the depletion of energy stores by the cells, as they are believed to be dependent on internal energy storage during the motility process rather than active energy production (Williams and Schwarzhoff, 1978). It is likely that during the consolidation phase, the *P. mirabilis* cells generate fresh stores of energy for a subsequent swarming cycle. This has been supported by findings indicating an upregulation of nutrient uptake genes in bacterial cells during consolidation (Pearson *et al.*, 2010; Long, 2018).

The cyclical nature of the swarming and consolidation intervals results in the characteristic bull's eye pattern that *P. mirabilis* is commonly associated

with (Figure 1.5) (Pearson *et al.*, 2010; Schaffer and Pearson, 2015). While the link between swarming and CAUTIs is still up for debate in literature due to the lack of swarmer cells isolated from the catheterized urinary tract, this type of motility would enable *P. mirabilis* to access tissues following colonization of medical devices such as catheters (Jones *et al.*, 2005; Jacobsen *et al.*, 2008; Hola, Peroutkova and Ruzicka, 2012; Armbruster, Mobley and Pearson, 2018). Furthermore, it has been demonstrated that cues specific to the urinary tract and urine initiate a swarming response in *P. mirabilis* cells (Armbruster, Hodges and Mobley, 2013).

The swarming behaviour of *P. mirabilis* has been shown to be key to the colonization of urinary silicone and latex catheters (Sabbuba, Hughes and Stickler, 2002; Jones *et al.*, 2004). This mode of motility is thought to be crucial to both infection routes on to the catheter from the patient perineum and catheter drainage bag (Hamamci *et al.*, 1998; Peters *et al.*, 2011; Gorbachinsky *et al.*, 2014). The up-regulation of a number of virulence genes during swarming supports the idea that *P. mirabilis* swarms up the catheter devices to cause CAUTIs (Schaffer and Pearson, 2015).

1.5.2 *P. mirabilis* - Urease enzyme production

P. mirabilis urease is a crucial virulence factor in medical device infections caused by this pathogen (Armbruster, Mobley and Pearson, 2018). Urease is a nickel metalloenzyme located in the cell cytoplasm and encoded by the *ureDABCEFG* operon (Island and Mobley, 1995; Boer, Mulrooney and Hausinger, 2014). The production of urease is upregulated in *P. mirabilis* infections *in vivo*, with the UreR regulator inducing expression of the urease operon in the abundance of urea within the infection site, such as the urinary

tract (D'Orazio, Thomas and Collins, 1996; Poore and Mobley, 2003). The potency and activity of the urease enzyme produced by *P. mirabilis* is much higher than that of other prominent urease producing pathogens such as *Ps.* aeruginosa and *K. pneumoniae* (Broomfield *et al.*, 2009; Armbruster, Smith, *et al.*, 2017). The urease enzyme hydrolyses urea in to ammonia and carbon dioxide, with the ammonia acting as a nitrogen source assimilated in to biomolecules via glutamine synthetase (GlnA) or glutamate dehydrogenase (GdhA) (Pearson *et al.*, 2011).

The ammonia released following urease activity also raises the pH of urine. The increase in pH results in precipitation of polyvalent cations and anions from urine, triggering urolithiasis (Armbruster, Mobley and Pearson, 2018). The process of urolithiasis involves the formation of large struvite and smaller apatite minerals, involved in the biofilm mineralization (Figure 1.4). Depending on the severity of the urolithiasis and the time for which the biofilm is allowed to develop i.e. catheter indwelling time, the urine flow through the medical device may become blocked rendering the device useless (Stickler, 2014). The mineralized biofilms of *P. mirabilis* and other urease producing pathogens also contribute to antibiotic resistance, as the crystals incorporated can protect bacteria and reduce treatment efficiency (Schaffer and Pearson, 2015).

Pathogens such as *Ps. aeruginosa*, *S. aureus*, and *Morganella morganii* can produce urease and raise urinary pH to 6.9-7.4, however more potent urease producers such as *P. mirabilis*, *P. vulgaris*, and *Providencia rettgeri* are able to generate a higher pH (8.3-8.4) and cause more rapid blockage of urinary catheters (Broomfield *et al.*, 2009). While *P. mirabilis* is the predominant microorganism in up to 44 % of CAUTIs, up to 25 % of bacteraemia cases

involving the pathogen have been polymicrobial, indicating a possible synergistic relationship (John W. Warren, Tenney, *et al.*, 1982; Watanakunakorn and Perni, 1994; Armbruster, Prenovost, *et al.*, 2017). Co-colonization with *P. mirabilis* and common urease producing urinary pathogens such as *Prov. stuartii*, *K. pneumoniae*, and *Ps. aeruginosa* results in increased urease activity and higher infection severity, increasing the number of patients diagnosed with bacteraemia and urolithiasis (Li, Lu, Hannah R Brady, *et al.*, 2016; Armbruster, Smith, *et al.*, 2017).

1.5.3 Catheter blockage

Stone formation following urease enzyme production by *P. mirabilis* is the most frequent cause of urinary catheter blockage (Figure 1.6) (Mobley and Warren, 1987; Kunin, 1989; Stickler, 2008, 2014; Cortese *et al.*, 2018). Once the catheter becomes blocked, the catheterized patient is effectively incontinent. The leakage from the device as a result of lack of drainage can cause skin irritation and bed sores in bedridden patients. The reflux of urine in to the upper urinary tract resulting from the blocked catheter device is one cause for symptomatic CAUTI episodes including pyelonephritis, septicaemia, and endotoxic shock (Jacobsen *et al.*, 2008; Stickler and Feneley, 2010; Hsiao *et al.*, 2015).

Catheter blockage is also a recurring phenomenon in specific patients, and often catheter replacement and antibiotic therapy cannot prevent the occurrence of another blockage event (Kunin, Chin and Chambers, 1987; Stickler and Feneley, 2010; Fisher *et al.*, 2018). Patients with a history of recurring catheter blockage are commonly referred to as “blockers” and are characterised by alkalinized urine and high ammonium urinary concentrations,

both linked to an infection caused by a urease producing pathogen (Getliffe, 1994). The impact of the recurrence of catheter blockage in patients is the eventual development of renal calculi within the bladder and urinary tract (Nicolle, 2012). Since renal calculi are a direct result of infection by a urease producing pathogen, such as *P. mirabilis*, they are also predominantly composed of struvite and apatite (Feneley, Hopley and Wells, 2015).

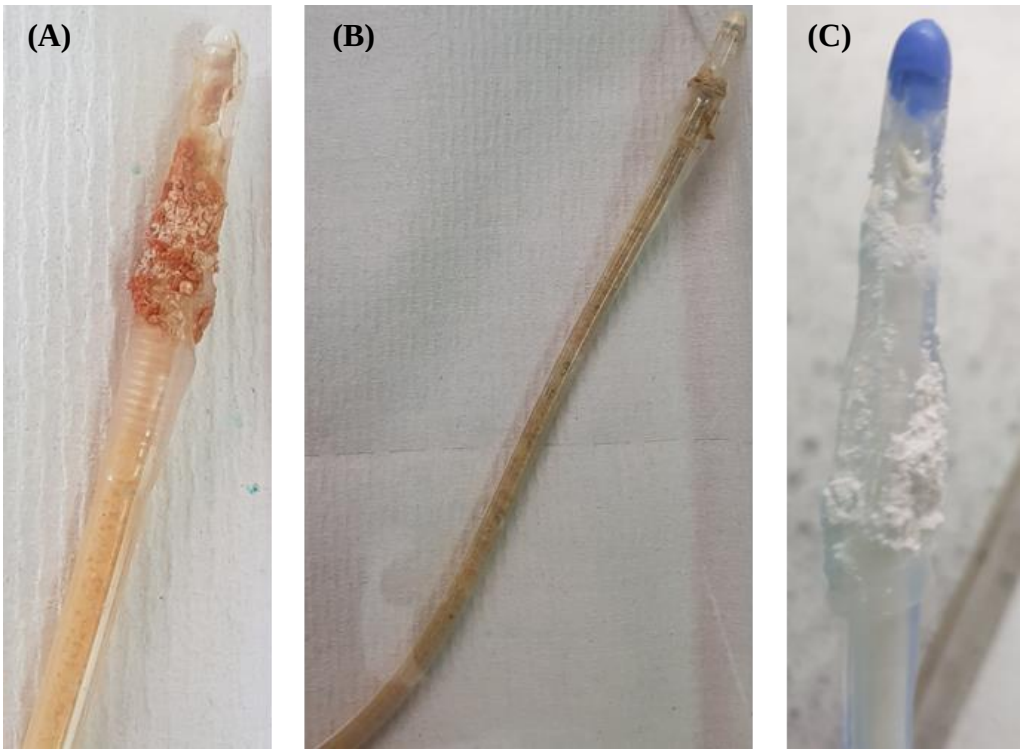

Figure 1.6 Urinary catheter encrustation and blockage

Photographs of encrustation and blockage of clinical urinary catheter devices (A and B), and a urinary catheter blocked as a result of colonization by an *in vitro* grown biofilm (C).

1.6 CAUTI prevention and treatment

CAUTI prevention options predominantly revolve around antimicrobials, aiming to kill pathogenic bacteria capable of causing an infection. Silver has been extensively explored due to it being one of the few FDA approved antimicrobial agents for urinary catheter coating (Singha, Locklin and Handa, 2017). Only low concentrations of silver are required to kill bacteria by disrupting membrane function of the cells, causing protein dysfunction, or oxidative stress resulting from antioxidant depletion (Kumar and Münstedt, 2005; Lemire, Harrison and Turner, 2013). A silver catheter coating is however expensive and has been shown to be limited in infection prevention (Singha, Locklin and Handa, 2017).

Another popular catheter coating focuses on the incorporation of antibiotics such as rifampicin and nitrofurantoin, often shown to be more efficient than silver alloys against CAUTIs (R. Pickard *et al.*, 2012; Robert Pickard *et al.*, 2012a; Salvarci, Koroglu and Gurpinar, 2015). The efficacy of antibiotic coatings however diminishes over time due to leaching from the catheter as well as a result of the increase in prevalence of bacterial antibiotic resistance (Hoffman, 2001; Stewart and Costerton, 2001; Köves, Magyar and Tenke, 2017). Other CAUTI treatment and prevention methods include the use of liposomes to release antimicrobials such as ciprofloxacin and triclosan, as well as the incorporation of enzymes of hydrolytic, oxidative, or quorum quenching nature (Pearson, Van Delden and Iglewski, 1999; Pugach *et al.*, 1999; Hedstrom, 2002; Gaonkar, Caraos and Modak, 2007; Finnegan *et al.*, 2010). The efficacy of all these methods however has been limited by their susceptibility to

the development of bacterial resistance to the antimicrobials incorporated (Lasic and Papahadjopoulos, 1998; Tenovuo, 2002; Fuchs and Tiller, 2006).

1.6.1 New antibacterial urinary catheter coating

A more recent approach to alleviating the burden of CAUTIs employs the coating of indwelling urinary catheters using biomaterials with biocidal or anti-bacterial attachment properties (Francolini *et al.*, 2017; Singha, Locklin and Handa, 2017). While the efficiency of biocidal biomaterials such as poly(2-(dimethylamino)ethyl methacrylate) (PDMAEMA) has been shown to vary significantly between different pathogens, such as Gram-negative bacteria, anti-bacterial attachment polymers have shown potential in preventing the formation of biofilms, thus presenting the possibility of reducing the incidence of symptomatic CAUTIs, without contributing to the spread of resistance to antimicrobials (Franklin and Snow, 2005; Cheng *et al.*, 2009; Banerjee, Pangule and Kane, 2011; Timofeeva and Kleshcheva, 2011; Hook *et al.*, 2012). The three types of synthetic polymer materials that have been shown to prevent biofilm formation without killing the bacterial cells include poly(ethylene glycol) (PEG)- based polymers, zwitterionic polymers, and weakly amphiphilic poly(meth)acrylates (Cheng et al., 2009; Banerjee, Pangule and Kane, 2011; Hook et al., 2012).

The high hydrophilicity of PEG-based and zwitterionic polymers enables them to prevent bacterial attachment via exclusion of biomolecules from the surface due to their water association (Li *et al.*, 2005; Barbey *et al.*, 2009; Diaz Blanco *et al.*, 2014). The development of a high-throughput method of screening to investigate bacterial attachment and biofilm formation via polymer microarrays has been instrumental to the discovery of novel materials suitable

for medical device applications, with the aim of reducing infections (Hook *et al.*, 2012, 2013; Dundas *et al.*, 2019). The highest resistance to bacterial biofilm formation has been exhibited by poly(meth)acrylate polymers with cyclic and hydrocarbon pendant groups (Hook *et al.*, 2012). The mechanism of biofilm prevention of these types of polymers is associated to their hydrophilicity and molecular rigidity, incorporating a weak hydrophilic ester and a large hydrophobic pendant group (Dundas *et al.*, 2019). High-throughput screening of a library of poly(meth)acrylate polymers printed as microarrays, resulted in the identification of ethylene glycol dicyclopentenyl ether acrylate (EGDPEA) as particularly effective in the prevention of biofilm formation (Hook *et al.*, 2012). The poor mechanical properties of EGDPEA can be improved by co-polymerization with di(ethyleneglycol) methyl ether methacrylate (DEGMA), at a 25:75 v:v% ratio, which provides a flexible coating necessary for medical device applications that retains the antibiofilm properties (Hook *et al.*, 2012; Adlington *et al.*, 2016). Following the success of the EGDPEA/DEGMA co-polymer coating in preventing biofilm formation in *in vitro* and *in vivo* studies, it has been applied to silicone urinary catheter devices manufactured by Camstent Ltd.

1.7 Hypothesis and aims

The EGDPEA/DEGMA coating of Camstent catheters was hypothesised to improve resistance to biofilm formation in comparison with silicone catheters, within *in vitro* and clinical settings.

The overall aim of this project was to demonstrate the impact of biofilm resistant biomaterial coatings for medical devices on catheter associated biofilms. The efficacy of the biomaterial co-polymer EGDPEA/DEGMA

catheter coating applied to Camstent catheters was evaluated based on biofilm formation, mineral accumulation, propensity for blockage, and fibrinogen deposition and release following catheterization, in comparison with uncoated silicone catheter devices.

The project seeks to obtain an overview of the bacterial communities observed within catheter associated biofilms, as well as characterize the biofilm and mineralization composition accumulating *in vivo* following device-associated infections, reproducing and supporting the observations via *in vitro* experimentation.

The project also explores the impact of urease production and swarming motility upon the ability of *P. mirabilis* to cause catheter-associated crystalline biofilms within an *in vitro* bladder model.

The investigations below were performed in an effort to achieve these aims:

1. **Transposon mutagenesis library generation**

   A screen of mini-Tn*5* *P. mirabilis* lacking the ability to produce urease or to exhibit swarming motility was performed and resulted in the isolation of a number of mutants defective for each virulence factor of interest. The mutants were characterised in order to confirm that there are no secondary mutations arising following the mini-Tn*5* insertion affecting their ability to cause infection, other than urease production or swarming. The most appropriate mutants were selected for evaluation in an *in vitro* bladder model.

2. **Catheter associated biofilms and mineralization within an *in vitro* bladder model**

Selected mini-Tn*5 P. mirabilis* mutants lacking the ability to produce the urease enzyme or swarm, were used to inoculate silicone catheter devices within an *in vitro* bladder model, comparing their performance to wild-type *P. mirabilis* based on catheter blockage time, biofilm formation, and mineral accumulation.

EGDPEA/DEGMA coated catheters and uncoated silicone devices were be exposed to single- and multi-species inoculations with *P. mirabilis* and *Ps. aeruginosa*, within an *in vitro* bladder model, monitoring blockage time and quantifying biofilm formation.

3. **Quantification of biofilm formation, mineral accumulation, and fibrinogen deposition on catheters and urinary fibrinogen concentration following catheterisation of hospitalized patients**

Biofilm formation, mineralization, and fibrinogen accumulation on Camstent and silicone catheters recovered from hospitalized patients was quantified and compared, following staining, using confocal microscopy. Additionally, urinary fibrinogen concentration in patients catheterised with Camstent and silicone catheters was quantified and compared, pre- and post-catheterisation.

4. **Clinical catheter associated biofilm and mineral characterisation**

Biofilms and minerals associated with clinical catheter samples were imaged using an environmental scanning electron microscope (ESEM) and a scanning electron microscope (SEM), as well as analysed using energy

dispersive X-ray spectroscopy (EDS). This enabled the characterisation and comparison of the morphology and chemistry of any biofilm formation, as well as the elemental composition of mineralization, on uncoated silicone catheters and EGDPEA/DEGMA coated Camstent catheters. 16S rRNA gene sequencing was also conducted, comparing the microbial communities associated with the two surface types.

Chapter 2: Materials and Methods

2.1. General microbiological methods

2.1.1. Bacterial growth and cultivation

General bacterial cultures were grown in Luria-Bertani (LB) broth (Sigma Aldrich, Gillingham, UK) in a shaking incubator at 200 rpm, or LB agar (Liquid LB medium supplemented with 1.5 % w/v technical grade agar (Oxoid Basingstoke, UK)). Both LB liquid and agar bacterial growth experiments were carried out at 37^{o}C. Inhibition of swarming of bacterial cultures such as *P. mirabilis* for the purpose of generating single colonies was attained via growth on LSW- agar (10 g L^{-1} tryptone (Oxoid Basingstoke, UK), 5g L^{-1} yeast extract (Oxoid Basingstoke, UK), 5 mL of 20 % v/v glycerol (VWR Lutterworth, UK), 0.4 g of NaCl (Fisher Scientific), and 20 g of technical grade agar (Oxoid Basingstoke, UK) (Belas, Erskine and Flaherty, 1991). For motility assays, the composition of the agar used was modified as appropriate, swimming motility agar was composed of 1 % w/v tryptone, 0.5 % w/v NaCl, and 0.3 % w/v technical grade agar and swarming motility plates consisted of liquid LB broth supplemented with 1.5 % w/v technical grade agar (Kearns, 2010; O'May and Tufenkji, 2011; Fusco *et al.*, 2017). Artificial urine (AU) was routinely used for biofilm growth experiments (Table 2.1) (Brooks and Keevil, 1997). All of the medium components were dissolved in pre-heated dH_2O (maximum 40 ^{o}C), with the exception of lactic acid, calcium chloride, potassium dihydrogen phosphate, and di-potassium hydrogen phosphate, which were individually dissolved in dH_2O and subsequently added to the main solution (Lehman and Donlan, 2015). Sterilization of the AU medium was carried out via membrane filtration (0.22 µm, Corning), and the pH was adjusted to 6.5 using hydrochloric acid

(HCl) and sodium hydroxide (NaOH). Bacterial growth was routinely carried out in 50 mL sterile falcon tubes (Greiner Bio-One) or sterile glass 100 mL conical flasks. 5-10 mL of growth medium was routinely used, with the addition of appropriate antibiotic.

Table 2.1 Composition of AU

The table below outlines the constituents of 1 L of AU made up in dH_2O.

Constituent	**Quantity (g)**	**Supplier**
Peptone L37	1	Oxoid Basingstoke, UK
Yeast extract	0.005	Oxoid Basingstoke, UK
Lactic acid	0.1	Sigma Aldrich, Gillingham, UK
Citric acid	0.4	Sigma Aldrich, Gillingham, UK
Sodium bicarbonate	2.1	Scientific Laboratory Supplies, Nottingham, UK
Urea	10	Fisher Scientific, Loughborough, UK
Uric acid	0.07	Alfa Aesar, Heysham, UK
Creatinine	0.8	Sigma Aldrich, Gillingham, UK
Calcium chloride dihydrate	0.37	Honeywell Fluka, Charlotte, US
Sodium chloride	5.2	Fisher Scientific, Loughborough, UK
Iron II sulphate heptahydrate	0.0012	Sigma Aldrich, Gillingham, UK
Magnesium sulphate heptahydrate	0.49	Sigma Aldrich, Gillingham, UK
Sodium sulphate decahydrate	3.2	Sigma Aldrich, Gillingham, UK
Potassium dihydrogen phosphate	0.95	Sigma Aldrich, Gillingham, UK
Di-potassium hydrogen phosphate	1.2	Sigma Aldrich, Gillingham, UK
Ammonium chloride	1.3	Sigma Aldrich, Gillingham, UK

2.1.2. Bacterial storage

5 mL bacterial cultures were grown overnight (O/N) at 37^{o}C in a 200 rpm shaking incubator. 0.5 mL of this bacterial culture was mixed with 0.5 mL 50% w/v glycerol in a cryotube (Sarstedt AG) and stored at -80 ^{o}C. Bacteria were plated on LB agar from glycerol freezer stocks when required. Working stocks of bacteria plated on agar were stored at 4 ^{o}C for up to 5 days.

2.1.3 Bacterial enumeration

The Miles and Misra method was used to generate viable bacterial counts on LB agar (Miles, Misra and Irwin, 1938). Serial dilutions of bacterial cultures from 10^{-1} up to 10^{-7} mL were plated in 10 µL aliquots on to the appropriately spaced, marked zones on the agar plates. Triplicates of each viable count were carried out, using the mean to determine the colony forming units per mL of bacterial culture (CFU mL^{-1}).

2.1.4 Statistical analysis

All experiments were carried out in triplicate, unless otherwise stated, indicating the generated mean or median values with standard error or 95% confidence intervals, respectively. Statistical analysis was undertaken using IBM SPSS 24, Microsoft Office Excel, and GraphPad Prism 7 (GraphPad Inc, CA, USA). Routine data analysis performed included Linear Regressions, T-tests, and Mann-Whitney U tests.

2.1.5 Bacterial strains and plasmids

Table 2.2 Bacterial strains and plasmids

The table below lists all the bacterial strains and plasmids used during the presented study.

Species/Strain/Plasmid	Antibiotic Selection	Source/Reference
Escherichia coli		
S17-1 λ*pir* pUT mini-Tn*5* GFP *luxABCDE* Km1	Km 50 µg mL^{-1}	A gift from Dr Philip Hill. Winson *et al*., 1998.
Proteus mirabilis		
Hauser, 1885	Rif 50 µg mL^{-1}	This laboratory. Hauser, 1885.
Hauser, 1885- *dsRed*	Gm 10 µg mL^{-1}	This laboratory. Hauser, 1885.
Hauser, 1885- transposon mutants	Rif 50 µg mL^{-1} and Km 50 µg mL^{-1}	This laboratory. Hauser, 1885.
Pseudomonas aeruginosa		
PAO1-UW- *mTurquoise*	Tc 25 µg mL^{-1}	This laboratory. Jacobs *et al*., 2003.

2.2 General molecular biology methods

2.2.1 Polymerase chain reaction (PCR)

PCR reaction mixtures were prepared in 0.2 mL PCR tubes (Greiner Bio-One). The thermal cycler utilised was a Biometra T3000. GoTaq G2 Green Master Mix (Promega), containing G2 *Taq* DNA polymerase, 400 µM dATP, 400 µM dGTP 400 µM dCTP 400 µM dTTP, and 3 mM $MgCl_2$, was routinely used in PCR reactions.

A 25 µL PCR reaction mixture contained 9.5 µL of nuclease free water, 12.5 µL of GoTaq G2 Green Master Mix, 2 µL primer mix (10 [pmol] forward and 10 [pmol] reverse primer), and 2 µL of DNA template.

Table 2.3: Standard PCR thermal cycler protocol for a *Taq* polymerase reaction

Phases	Temperature	Time	Cycles
Initial Denaturation	95ºC	5 mins	1x
Denaturation	95ºC	30 secs	35x
Annealing	45ºC	30 secs	35x
Elongation	72ºC	1 min	35x
Final elongation	72ºC	10 mins	1x
Cooling	4ºC	∞	-

The standard DNA concentration resulting from PCR amplification routinely ranged between 10-250 ng μL^{-1}. The annealing temperature used during a PCR cycle varied depending on the primers incorporated within the reaction (Tables 2.3 and 2.4).

2.2.2 Gel electrophoresis

Agarose gel electrophoresis was carried out for the purpose of DNA size separation. Biorad sub-cell GT mini electrophoresis tanks powered by a Biorad powerpack 300 were incorporated for the procedure. The agarose gels were composed of 1% w/v agarose (Sigma Aldrich) in 1x tris-acetate ethylenediaminetetraacetic acid (EDTA) buffer (TAE) (50 x TAE Solution, Fisher Scientific). 0.5 µL SYBR Safe DNA Gel Stain (Invitrogen, Thermo Fisher Scientific) was mixed into the agarose gel, before drying the gel for 20 min. Voltage of 100 V in 1x TAE buffer was run during the procedure to separate the fragmented DNA. Fragments were visualised using UV transluminescence on a Gel Doc XR+ Gel Documentation System (Biorad).

2.2.3 DNA restriction enzyme digestion

DNA was routinely digested using restriction enzymes purchase from Promega and New England Biolabs (Southampton and Ipswich, UK). Each digestion reaction contained up to 29 µL DNA (depending on the concentration), 1 µL of each restriction endonuclease (10 U μL^{-1}), 3.5 µL 10 x buffer, and nuclease free water to make up the final 35 µL volume. The digestion reaction mixtures were incubated for 18 h at 37 ^{o}C. The reactions were subsequently heated to the appropriate temperature for endonuclease inactivation, according to the manufacturer's instructions. The products of restriction enzyme digestion reactions were visualised using gel electrophoresis (2.2.2).

2.2.4 Plasmid preparation

Plasmid DNA from *E. coli* was routinely isolated using GenElute Plasmid Miniprep (Sigma-Aldrich). To obtain a bacterial cell pellet, 1 mL of an O/N bacterial culture was centrifuged (Eppendorf Centrifuge 5418) at 14,000 g

for 2 min at room temperature. The supernatant was discarded, and the pellet of bacterial cells was used to extract the plasmid following the manufacturer's instructions. All centrifugation steps during the protocol were performed at 14,000 g. Final elution volume of plasmids was 30 µL, unless otherwise stated. Plasmid concentrations were quantified using a nanodrop spectrophotometer (Nanodrop 1000, Thermo Scientific), and stored at -20^{o}C.

2.2.5 Chromosomal DNA extraction

1 mL of an O/N bacterial culture was centrifuged at 14,000 g for 2 min at room temperature. The supernatant was discarded, harvesting the bacterial cell pellet. Wizard Genomic DNA Purification Kit (Promega) was used to extract the chromosomal DNA from the bacterial cells, following the manufacturer's instructions for gram-negative bacteria. The chromosomal DNA extracted was quantified spectrophotometrically using the Nanodrop and stored at -20^{o}C.

2.2.6 Gel extraction

Bands of interest from agarose gels containing DNA fragments separated via gel electrophoresis (2.2.2) were cut using a sterile scalpel and transferred in to 1.5 mL sterile microcentrifuge tubes. DNA from the agarose fragments was purified using the Monarch DNA Gel Extraction Kit (New England Biolabs). All centrifugation steps were performed at 14,000 x g. Extracts were eluted in 6 µL volumes, and quantified using the Nanodrop, prior to storage at -20 ^{o}C.

2.2.7 DNA purification

Purification of DNA from PCR reactions was carried out using a QIAquick PCR Purification Kit (Qiagen). All centrifugation steps were

performed at 14,000 g. Extracts were eluted in 30 µL volumes, and quantified using the Nanodrop, prior to storage at -20^{o}C.

2.2.8 DNA ligation reactions

Ligation reactions containing 1 µL T4 ligase (1U µL^{-1}), 1.8 µL of 10x ligation buffer, vector and insert DNA, making up an 18 µL final volume, were carried out in PCR tubes. The concentration (200-500 ng µL^{-1}) of vector and insert DNA determined the volume added to the ligation reactions. The ligation reactions were incubated at 16 ^{o}C for 2 h, and subsequently 4 ^{o}C overnight (approximately 16 h) in a thermocycler (Biometra T3000).

2.2.9 Plasmid transformations of *E. coli*

Electrocompetent *E. coli* S17 λ*pir* cells were prepared and thawed on ice. 50 µL of competent cells and a maximum of 2 µL of DNA (unless dialysed) at a concentration of 20-200 ng µL^{-1} were mixed in a 1.5 mL Eppendorf safe-lock tube. The mixture was transferred into a 2mm electroporation cuvette (Flowgen) and electroporated using a MicroPulser electroporator (Bio-Rad). 950 µL of LB broth was added to the electroporated cells, mixed, and transferred to a clean 1.5 mL Eppendorf safe-lock tube. The mixture was incubated at 37^{o}C, shaking at 200 rpm, for 1 h. Following incubation 100 µL of the mixture was spread plated on an LB agar plate containing the appropriate antibiotic selective pressure. The remaining 900 µL of cell mixture was centrifuged at 5000 x g for 3 min. The cell pellet was re-suspended in 100 µL of LB broth and plated onto an LB agar plate containing the appropriate antibiotic. LB agar plates were incubated at 37 ^{o}C O/N.

2.2.10 Bacterial conjugation

Conjugational plasmid transfer from *E. coli* S17 λ*pir* to *P. mirabilis* was routinely carried out. Both donor and recipient bacterial strains were grown O/N at 37^{o}C shaking at 200 rpm, with appropriate antibiotic selection. The bacterial strains were subsequently harvested from the cultures via centrifugation at 3000 x g for 5 min. The supernatants were discarded, and the remaining pellets were re-suspended in 1 mL phosphate buffered saline (PBS), within 1.5 mL microfuge tubes. Bacterial suspensions were subsequently centrifuged at 5000 x g for 3 min, before discarding the supernatants and re-suspending the pellets in PBS for a second time. The PBS wash step of the bacterial cultures was repeated once more for a total of 3 times, before the pellets were resuspended in 0.5 mL LB each and mixed within the same 1.5 mL microfuge tube. The mixed bacterial suspension in LB was centrifuged at 5000 x g for 3 min and the pellet resuspended in 100 µL of LB. The 100 µl mixed bacterial suspension in LB liquid medium was spotted in the centre of an LSW- agar plate and dried, before incubating the plate at 37^{o}C O/N.

After approximately 16 h incubation, the bacteria were harvested from the plate by scraping the conjugation spot using a sterile 10 µL plastic loop and resuspending in 1 mL of LB in a 1.5 mL microfuge tube. 100 µL of the bacterial suspension was spread plated on an LSW- agar plate containing the appropriate antibiotic. The remaining 900 µL of bacterial suspension were centrifuged at 5000 x g for 3 min, discarding the supernatant and resuspending the resulting pellet in 100 µL of LB medium. The concentrated bacterial suspension was also spread plated on an LSW- agar plate with the appropriate antibiotic. The two

LSW- agar plates were incubated at 37ºC O/N and used to select for transconjugant colonies.

Table 2.4 Primers used during this study

*products are variable due to the degenerate nature of the primers used, this was necessary as the location of the mini-Tn*5* transposon insertion is unknown, and the products varied in size.

Primer Name	**Sequence 5'-3'**	**Annealing Temperature (ºC)**	**Product and reference**
Transposon Mutant Sequencing:			
1	TTTTTACACTGATGAATGTTCCC	30, 43	variable*, (Jones *et al.*, 2004)
2a	GGCCACGGGTCGACTAGTANNNNNNNNNNAGAG	30, 43	variable*, (Manoil, 2000)
2b	GGCCACGGGTCGACTAGTANNNNNNNNNNACGCC	30, 43	variable*, (Manoil, 2000)
2c	GGCCACGGGTCGACTAGTANNNNNNNNNNGATAT	30, 43	variable*, (Manoil, 2000)
3	CGGATTACAGCCGGATCCCCG	43	variable*, (Jones *et al.*, 2004)
4	GGCCACGCGTCGACTAGTAC	43	variable*, (Manoil, 2000)

2.3 Transposon mutagenesis methods

2.3.1 Transposon mutagenesis of *P. mirabilis*

The experimental method of transposon mutagenesis incorporated in this study has been previously undertaken using a range of bacterial species (Jones *et al.*, 2004; Holling *et al.*, 2014). The pUT mini-Tn*5* GFP *luxABCDE* Km1 vector (Figure 2.1) carrying the transposon was transferred into *P. mirabilis* via conjugation (2.2.10) from *E. coli* S17.1λpir. Multiple conjugations were carried out simultaneously to improve the throughput of mutant generation. Using antibiotic selection (50 µg mL^{-1} kanamycin and 50 µg mL^{-1} rifampicin) to confirm transposon transfer into *P. mirabilis*, transconjugants were selected and picked on to the appropriate phenotype selection plates.

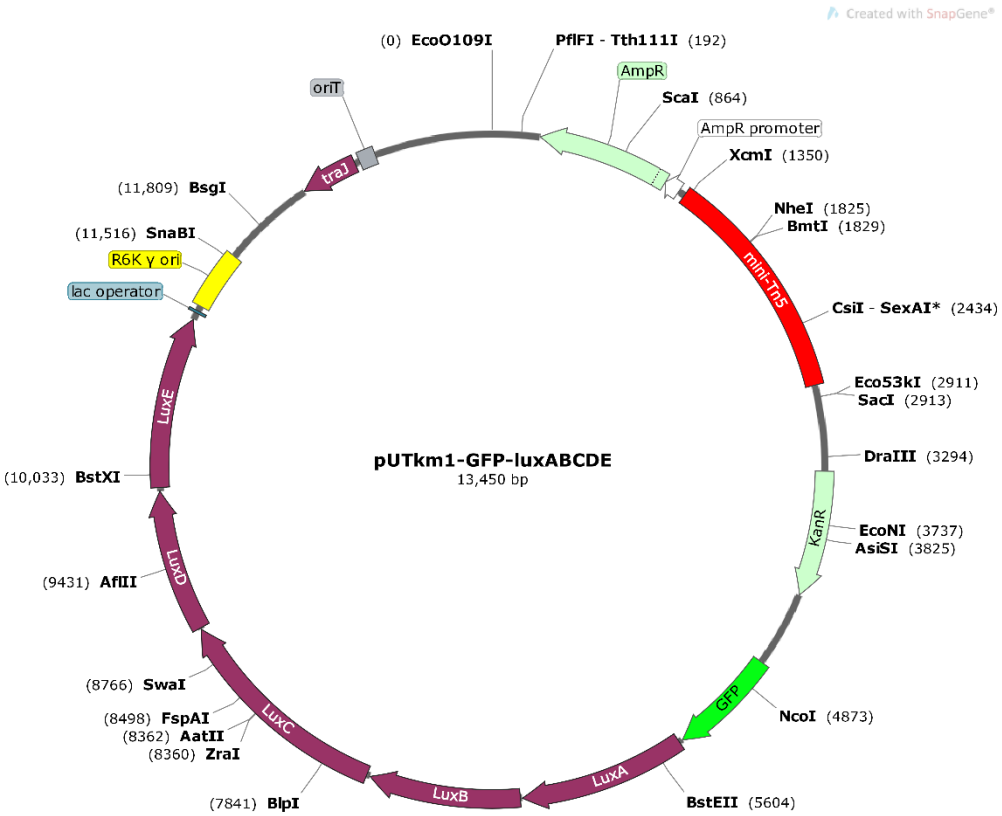

Figure 2.1 Plasmid map of the pUT mini-Tn*5* GFP *luxABCDE* Km1 vector

The plasmid construct was made by de Lorenzo and Timmis (1994). The plasmid was modified to carry the GFP gene and *luxABCDE* operon. The plasmid also carries kanamycin (KanR) and ampicillin (AmpR) genes. The complete plasmid construct was a kind gift from Dr Philip Hill.

2.3.2 Screening *P. mirabilis* mini-Tn*5* transposon mutants for swarming and urease mutant phenotypes

P. mirabilis transposon mutants were spotted on gridded square culture bio-assay dishes (Thermo-Scientific), with selection consisting of 1.5 % LB agar for swarming phenotype screening, and 2.5% Christensen agar containing 2 % urea (Sigma-Aldrich), prepared following the manufacturer's instructions, for urease production (Christensen, 1946; Armbruster, Hodges and Mobley, 2013). 556 transposon mutants were screened per phenotype per experiment until 11283 mutants were screened for swarming and urease production, achieving 95% genome coverage (Clarke and Carbon, 1976). Each suspected swarming or urease transposon mutant was sub-cultured on an individual LB agar plate supplemented with 50 µg mL^{-1} rifampicin and 40 µg mL^{-1} kanamycin.

2.3.3 Confirmatory swarming motility and urease production assays

Following the initial sub-culture of mini-Tn*5* mutants with suspected defects in swarming motility or urease enzyme production, the bacteria were subjected to confirmatory assays. Both types of mutants were tested for both urease production and swarming motility. Urease production assays consisted of spread plating the mini-Tn*5* mutants on individual 2.5% Christensen agar plates containing 2% v/v urea, followed by incubation for 16 h at 37 ^{o}C. Swarming assays were conducted by spotting 5 µL of late exponential growth phase cultures, adjusted to OD_{600}- 1.0, in the centre of individual 1.5 % LB agar plates and incubated for 16 h at 30 ^{o}C (Pearson *et al.*, 2010).

2.3.4 *P. mirabilis* transposon mutant growth curves

Growth curve assays were carried out using each *P. mirabilis* mutant and compared with the wild-type bacterium. O/N cultures of the bacteria were set up in 5 mL of LB broth within 50 mL falcon tubes and grown at 37 ^{o}C with shaking at 200 rpm. After approximately 16 h of growth, the O/N cultures were used to inoculate 30 ml of LB broth in 100 mL conical flasks. The flasks were incubated in a 37 ^{o}C incubator shaking at 200 rpm for 24 h. The starting OD_{600} of the cultures was adjusted using at 0.01. For the first 6 h, the OD_{600} of the cultures was recorded every 2 h, with a final reading taken at the 24 h time point.

2.3.5 *P. mirabilis* transposon mutant preliminary biofilm assays

The biofilm assays were conducted in 96-well cell culture plates (Black, Flat-Bottom, Greiner Bio-One), filled with 100 µL LB broth, and inoculated with 2 µL of exponentially growing bacterial culture (OD_{600}- 0.5). To prevent evaporation, the plates were loosely sealed in re-sealable plastic bags and incubated at 37 ^{o}C in static conditions for 48 h. Following incubation, the LB broth medium was removed, and the wells washed twice with deionised water (dH_2O), to remove any loosely attached material. After air drying the plates for 10 min, the wells were stained with 100 µL of 2 µM Syto64 DNA dye and incubated for 15 min at room temperature. The dye was subsequently removed and the wells were washed twice using dH_2O, and air dried for 10 min. The fluorescence intensity of the wells was measured using a TECAN (Infinite, M200Pro) (Excitation/Emission λ - 510/670 nm). The fluorescence intensity readings of the mini-Tn*5* mutants were compared with wild type *P. mirabilis*.

2.3.6 *P. mirabilis* transposon mutant preliminary biomineralization assays

For the biomineralization assay of *P. mirabilis* transposon mutants, 24-well plates were filled with 1 mL of AU. The wells of the 24-well plate were inoculated with 200 µL of exponentially growing (OD_{600}- 0.5) bacterial culture. Plates were loosely sealed within a re-sealable plastic bag and incubated at 37 ^{o}C in static conditions for 1 h, followed by incubation at 37 ^{o}C for 24 h, shaking at 100 rpm. The medium within the wells was aspirated following incubation, and two wash steps were performed in each well using dH_2O, before air drying for 10 min. 400 µL of a 1 µM calcein solution was applied to each well, staining any minerals produced as a result of *P. mirabilis* urease enzyme production (Tambutté *et al.*, 2011). The wells were incubated with the dye at room temperature for 15 min, before aspirating the dye and performing 2 more wash steps using dH_2O and drying for a further 10 min. The fluorescence intensity within the wells of mini-Tn*5* mutants was quantified using a TECAN (Infinite, M200Pro) (Excitation/Emission λ – 495/515 nm) and compared statistically to values obtained for the *P. mirabilis* wild-type.

2.3.7 Confirmation of loss of mini-Tn*5* delivery vector in *P. mirabilis* transposon mutants

Due to the nature of the PCR sequencing strategy employed within this study, for the purpose of identifying the mini-Tn*5* transposition site, it is necessary to confirm that the entire pUT mini-Tn*5* GFP *luxABCDE* Km1 vector did not co-integrate into the bacterial chromosome. As the PCR sequencing strategy relies on the tags of known sequence provided by the mini-Tn*5* transposon for the amplification and identification of the mutated genes, the presence of the delivery vector would result in PCR amplification of its own

sequence rather than the gene of interest. The presence of the *bla* gene on the delivery vector confers resistance to ampicillin to mutants carrying the co-insertion (Figure 2.1). To test and exclude mutants with the pUT delivery vector co-insertion from further genotypic analysis, all transposon mutants tested on solid media containing ampicillin. LB agar plates were supplemented with 100 µg mL^{-1} ampicillin and inoculated with a late exponential growth phase culture (OD_{600}- 1.0). *P. mirabilis* wild type (Hauser, 1885) was used as a negative control, and the *E. coli* S17.1λpir carrying the pUT delivery vector was used as a positive control.

2.3.8 Sequencing of the genes disrupted in *P. mirabilis* transposon mutants

A PCR based approach was used to sequence the interrupted genes within the transposon mutants (Figure 2.2) (Manoil, 2000; Holling *et al.*, 2014). PCR reactions were performed following the procedure, and using the reagents, described in section 2.2.1. The sequencing method requires two separate PCR reactions, with the initial reaction performed using genomic DNA extracted from the transposon mutants (2.2.5). The following PCR protocol was adopted for the first reaction:

Stage 1 (1x): 95°C for 5 min

Stage 2 (8x): 94°C for 30 sec

30°C for 35 sec

72°C for 45 sec

Stage 3 (30x): 94°C for 30 sec

43°C for 35 sec

72°C for 45 sec

Stage 3 (1x): 4°C

Following the first PCR reaction, the amplified DNA product was cleaned up as indicated in section 2.2.7. The clean DNA was subsequently used as a template in a second PCR reaction:

Stage 1 (1x): 95°C for 2 min

Stage 2 (30x): 94°C for 30 sec

43°C for 35 sec

72°C for 45 sec

Stage 3 (1x): 75°C for 5 min

Stage 3 (1x): 4°C

Gel electrophoresis (2.2.2) was used to visualise the products of the second PCR reaction. Extraction of the DNA bands from the gels was performed as described in section 2.2.6, before sequencing the samples. Products from this experiment were sequenced at Source Bioscience, Nottingham (UK) using primer 3, as described in the cloning-free approach for sequencing (Manoil, 2000; Holling *et al.*, 2014).

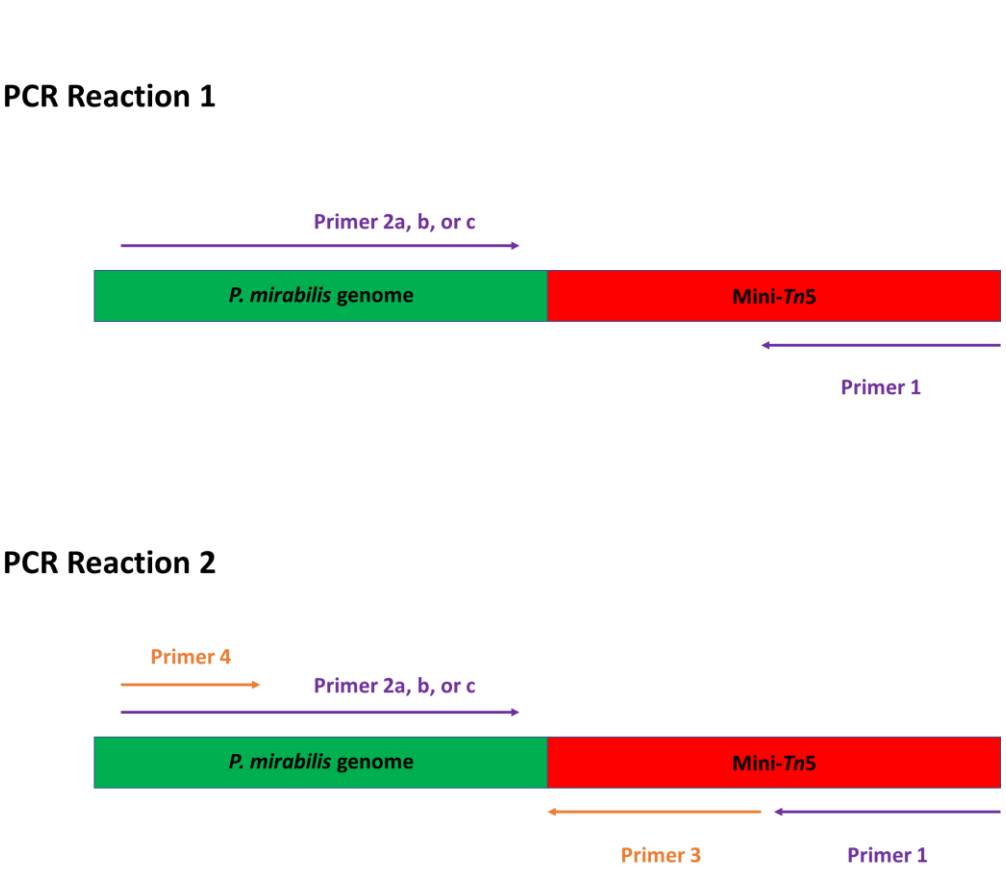

Figure 2.2 Sequencing *P. mirabilis* genes disrupted by mini-*Tn*5- A PCR based approach

The diagram shown in this figure depicts the PCR method undertaken to sequence the genes interrupted in transposon mutants (Figure adapted from Manoil, 2000 and Holling, 2014). PCR reaction 1 was carried out using primer 1 in combination with primer 2a, b, or c. Using the product of the first PCR reaction, reaction 2 was carried adding primers 3 and 4. Primers 1 and 3 anneal to a specific sequence on the mini-*Tn*5 transposon, whereas primers 2a, b, and c bind to several sites on the bacterial genome upstream of the transposon, due to their semi-degenerate nature. Primer 4 hybridized to a specific sequence at the 5' end of primers 2a, b, and c. This method allowed the identification of the flanking sequences of the Tn5 insertion, and subsequently the interrupted genes within the transposon mutants via sequencing.

2.3.9 Transposon mutant sequencing data analysis

Whole genome sequencing of the *P. mirabilis* wild-type strain used in this study was performed by MicrobesNG (Birmingham). The whole genome data was used as a reference for correlating sequences obtained from the transposon mutants via the PCR method described in section 2.3.8 (Figure 2.2), and thus the identification of the transposon interrupted genes. Sequences obtained from the transposon mutants were correlated with the *P. mirabilis* whole genome sequence using the PATRIC and BLAST genome alignment tools (Wattam *et al.*, 2016). All BLAST matched searches were manually inspected to confirm the interruption of the indicated gene.

2.3.10 *P. mirabilis* transposon mutant swimming motility assays

Swimming assays were conducted on selected transposon mutants for further analysis using swim agar described in section 2.1.1. The swimming agar plates were dried for approximately 40 min within a fume hood. 5 µL of O/N bacterial culture was pipetted at the interface between the agar and petri dish, by stabbing the plates with the pipette tip in centre through the agar layer. The plates were wrapped in parafilm and placed in a plastic box in the presence of a moist tissue, to prevent moisture level variability, and incubated at 37 ^{o}C for 16 h. The swimming capabilities of each mutant were expressed as percentages of the swimming ability of *P. mirabilis* WT, producing swimming indices for each strain.

The swimming assay protocol was adapted to enable confocal microscope (LSM 700, Zeiss) imaging by placing 1-1.2 mm thick, interleaved, glass microscope slides (Dixon Science, UK) within petri dishes prior to pouring the swimming agar. The plates were inoculated with 5 µL of O/N bacterial

culture at the interface between the agar and the glass slide. The plates were wrapped in parafilm and incubated at 37 ^{o}C within a plastic box in the presence of a moist tissue for 4 h. The glass slide was recovered alongside the slab of agar immediately above it by carefully cutting the agar around the slide and using tweezers to remove it from the petri dish. Lens cleaning tissues (Fisher Scientific, UK) were used to clean the bottom surface of the glass slide, before positioning the sample comprising the slide and agar slab on the top surface for imaging using a confocal microscope (LSM 700, Zeiss). A green fluorescence channel (EGFP- Excitation/Emission λ - 488/509 nm) was applied during imaging enabling the detection of any signal associated with the expression of the mutated genes, as a result of the presence of the *gfp* reporter sequence part of the mini-Tn*5* construct used for transposon mutant generation (Figure 2.1). 30 cycle time series were generated using the confocal microscope to display the swimming motility of the cells.

2.3.11 *P. mirabilis* transposon mutant AU biofilm and mineralization assays

P. mirabilis transposon mutants deficient in swarming motility and urease production that exhibited no other phenotypic deficiencies and were successfully sequenced, were selected for biofilm and mineralization assays in AU. The biofilm and mineralization assays were conducted in 24-well plates, with each well supplemented with a 1 cm silicone catheter cross section. Each well was filled with 980 µL AU medium and inoculated with 20 µL of exponentially growing bacterial culture (OD_{600}- 0.5). To prevent evaporation, the plates were loosely sealed in re-sealable plastic bags and incubated at 37 ^{o}C, shaking at 40 rpm, for 48 h. Following incubation, the AU medium was disposed of, and the catheter sections were washed twice using dH_2O, to remove any

material unattached to the surface such as planktonic bacterial cells. 20 µL of 1 µM calcein dye was applied to each sample, subsequently incubating the samples for 15 min in the dark. Two wash steps using dH_2O were carried out to rinse off the calcein stain, before applying 20 µL of 2 µM Syto64 DNA dye to each sample and incubating for 15 min at room temperature. The dye was removed and the wells were washed twice using dH_2O, and air dried for 10 min. Catheter sections were imaged with a confocal scanning laser microscope (CSLM), LSM 700 Zeiss.

2.4 *In vitro* bladder model

The *in vitro* bladder model illustrated in Figures 2.3 and 2.4 was used to investigate the impact of transposon mutations upon the ability of *P. mirabilis* to form biofilms, mineralization, and block catheter devices. The model was also used to assess the performance of the EGDPEA/DEGMA coated catheter devices in comparison to uncoated silicone catheters, in response to single- and multi-species bacterial inoculations.

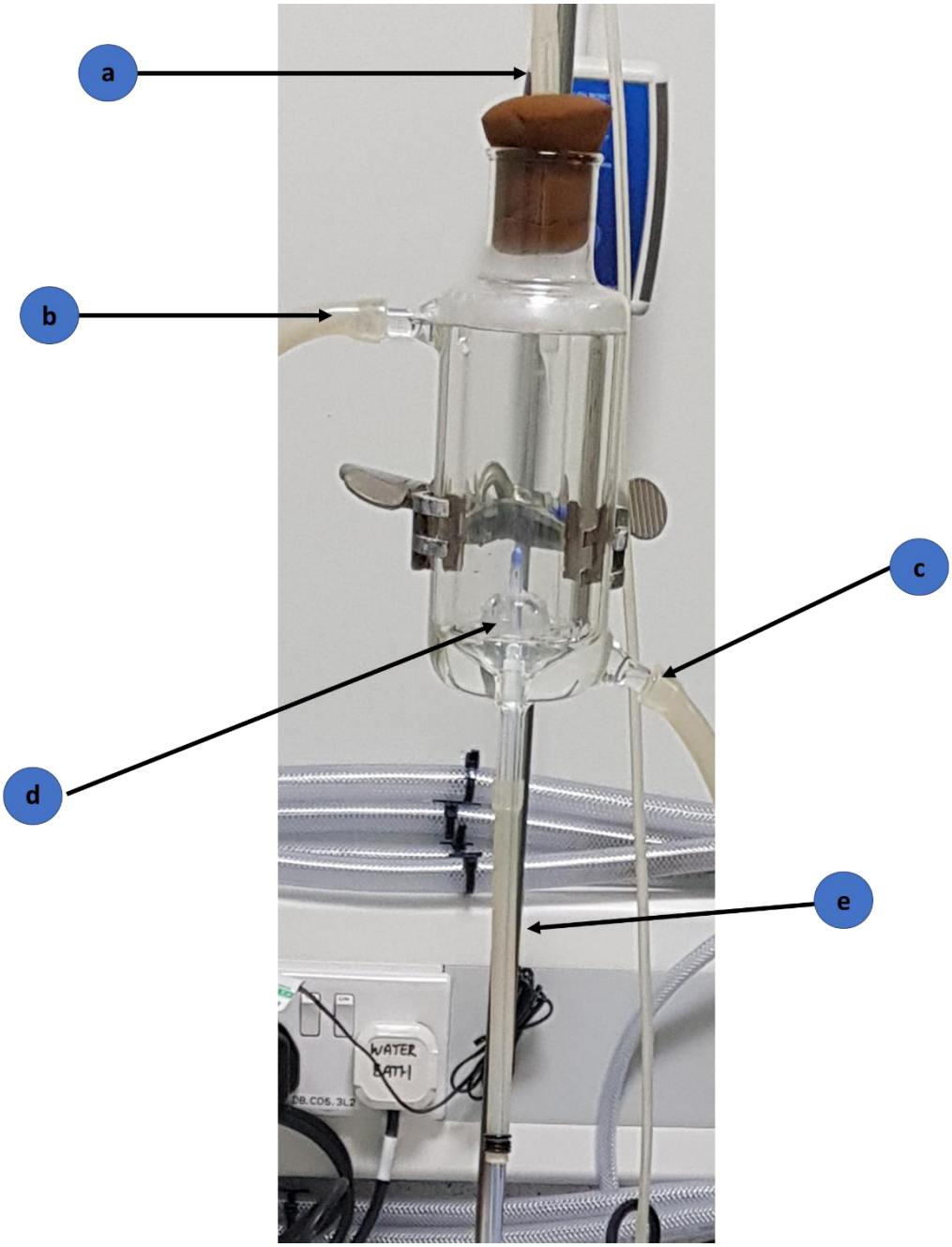

Figure 2.3 *In vitro* bladder model

The glass vessel which represents the bladder chamber is double walled, allowing for urine to flow into the inner chamber (a), as well as water from a heated water bath to circulate within the outer chamber, surrounding the inner chamber, thus maintaining its temperature at 37 ^{o}C (b and c). A peristaltic pump was connected to a Pasteur pipette (Fisher Scientific) delivering artificial urine into the bladder at a rate of 0.75 mL min^{-1}. The catheter devices were introduced into the bladder through an opening at the bottom of the vessel and retained inside via the inflation of its balloon (d). An artificial urethra (e) was attached at the opening through which the catheter was inserted, to maintain the device position and prevent media leakage.

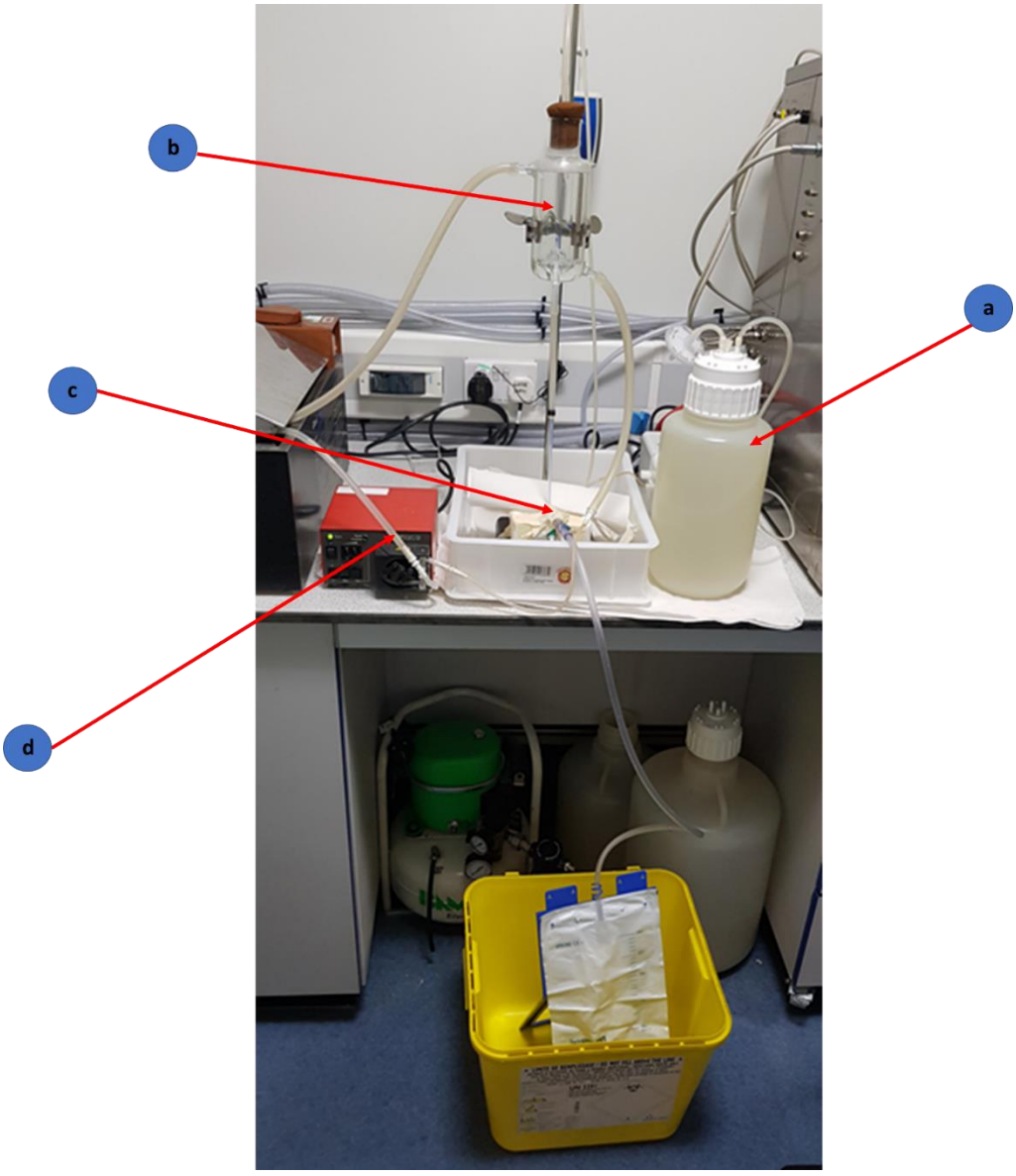

Figure 2.4 Full laboratory set-up of the *in vitro* bladder model

The bottle of artificial urine (a) was connected to the peristaltic pump supplying the bladder chamber (b) with growth medium. Once the medium in the bladder chamber had reached a volume which submerges the catheter eyehole, artificial urine flowed down the catheter device (c) and was collected in a catheter bag (T-tap Ugo 13). The water jacket around the glass vessel was supplied by a second pump which circulated water from the heated water bath (d), maintaining the bladder at 37 ^{o}C.

2.4.1 Setting up the *in vitro* bladder model

All components of the bladder model were autoclaved before assembly. The closed drainage system from the medium reservoir (4 L capacity) to the catheter bag was assembled first in aseptic conditions. All the catheters used in the bladder model experiments were size 14 French (Fr). The balloon of the catheters was inflated with 10 mL of saline solution to retain the device in the bladder. AU medium was supplied to the bladder chamber via a peristaltic pump (Ismatec, ISM931) at a flow rate of 0.75 mL min^{-1} connected to a Pasteur pipette (Fisher Scientific) through silicone tubing. Once the closed drainage system was complete the water jacket was attached bringing the temperature of the bladder chamber to 37 ^{o}C before the inoculation of bacteria.

2.4.2 Operating the *in vitro* bladder model

The bacterial inoculum was prepared by initially growing an O/N culture in 5 mL of LB with the appropriate antibiotic when required. Subsequently using this culture, the OD_{600} of 5 mL of AU was adjusted to 0.05 and grown at 37 ^{o}C in an incubator with shaking at 200 rpm, for approximately 4 h. When the OD_{600} of the bacterial culture in AU reached 0.5, it was used to adjust the OD_{600} of 10 mL of fresh AU medium to 0.05 ($1x10^{8}$ CFU mL^{-1}). For dual-species inoculations, the starting OD_{600} was adjusted to 0.05 at a ratio of 1:1 ($1x10^{4}$ CFU mL^{-1} of each bacterium). Exponentially growing cells in AU medium were used to inoculate the bladder chamber. The bacteria were grown for 1 h following inoculation, enabling them to establish within the vessel, before commencing the continuous supply of artificial urine via the peristaltic pump. With the maximum capacity of the medium reservoir set at 4 L, at a flow rate of 0.75 mL min^{-1}, the longest possible bladder model experimental run time,

assuming no disruption of the closed drainage system to refill the reservoir, was roughly 89 h. Experiments within the *in vitro* bladder model were timed and device blockage prior to the maximum experimental run time of 89 h was recorded.

2.4.3 Processing and quantification of biofilm and mineral accumulation on infected catheter samples from *in vitro* bladder model

Catheters recovered from the bladder model were sectioned as to expose the luminal surface for analysis (Figure 2.5). The sections of catheter were subsequently assigned for different methods of biofilm and mineral characterisation including CSLM imaging, ESEM imaging, and EDS analysis (Sections 2.4.5 and 2.4.6).

2.4.4 Biofilm and mineral quantification of *in vitro* bladder model recovered catheter samples

Following sectioning of the catheter samples recovered from the bladder model, the lumens of the respective sections were washed by gentle agitation in PBS (100 µL). Two 100 µL dH_2O wash steps were subsequently carried out for each catheter section. Catheters recovered following experiments conducted as part of the investigation into the impact of transposon mutations upon infection development, were stained using the DNA dye Syto64 and the mineralization dye calcein. Each 5 cm cross section was initially stained via the application of 100 µL Syto64 at a concentration of 2 µM. Samples were incubated for 15 min in the dark. Following incubation two 100 µL dH_2O steps were carried out, prior to the application of 100 µL of 1 µM calcein dye. The samples were again incubated for 15 min in the dark and washed twice with dH_2O. The incorporation of fluorescently tagged bacterial strains, *P. mirabilis*- dsRed

(Excitation/Emission λ - 558/584 nm) and *Ps. aeruginosa*- mTurquoise (Excitation/Emission λ - 434/474 nm), throughout the bladder model experiments comparing the EGDPEA/DEGMA coated catheters to the control silicone devices allowed the quantification of the biofilm biomass accumulated on catheter sections by measuring fluorescence in the absence of staining (Hauser, 1885; Jacobs *et al.*, 2003). Fluorescence associated with biofilm and mineral formation for stained samples, and biofilm formation for samples infected with fluorescently tagged bacteria, were quantified using a CSLM (LSM 700, Zeiss), taking 5 Z-stacked images (2.5mm x 2.5mm) of the lumens of each 5 cm catheter section. The biofilm and mineral biomass associated with the catheter samples was determined by quantifying the fluorescence associated with each image using comstat2/ImageJ (Heydorn *et al.*, 2000).

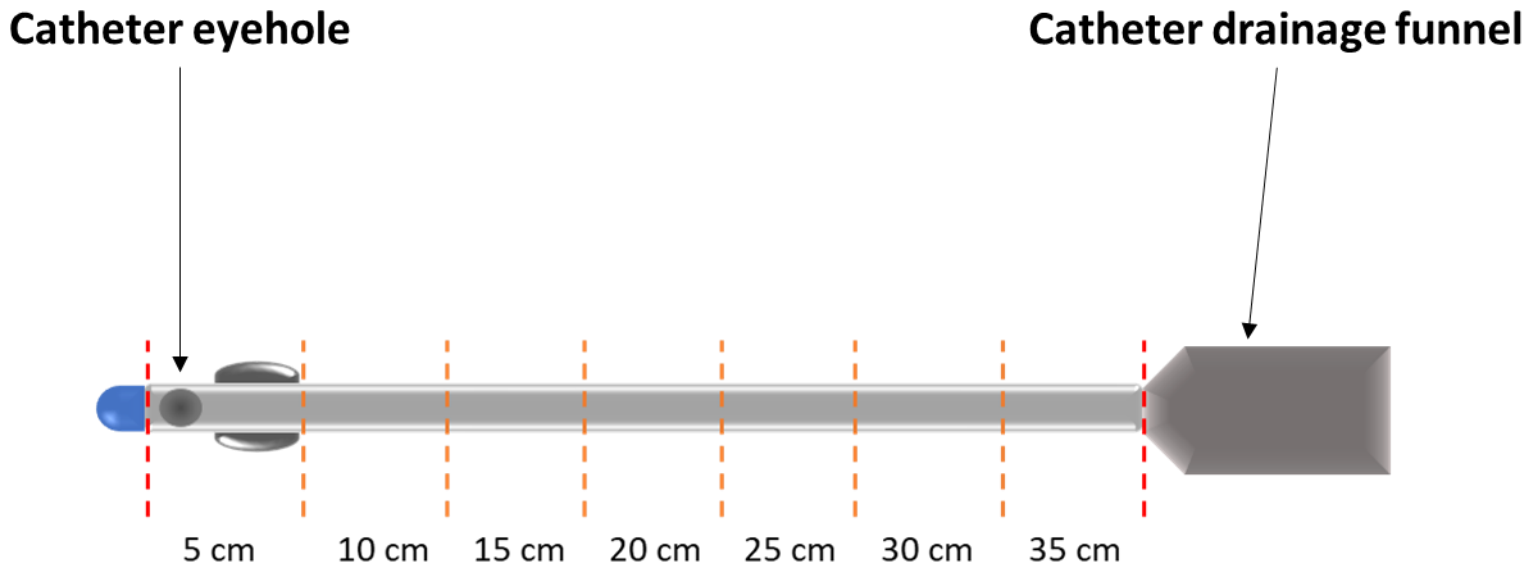

Figure 2.5 Catheter sample sectioning

Catheter devices were cut in cross section to expose the lumen, discarding the catheter tip and drainage funnel. The cross section of the catheter shaft was cut in to seven 5 cm pieces from the proximal end (catheter eyehole side) to the distal end (catheter drainage funnel side). The lumens of the 5 cm cross-sections were analysed in experiments throughout this study.

2.4.5 Biofilm and mineral characterisation

Sections of catheter devices recovered from the *in vitro* bladder model selected for further characterisation via ESEM imaging and EDS analysis, were vapour fixed in a fume hood O/N using 4% (v/v) formaldehyde solution (Chao and Zhang, 2011). The fixed samples were imaged using an ESEM (FEI Quanta 650), coupled with EDS analysis quantifying the elemental composition of biofilm and mineral structures associated with the catheter surface.

2.5 Patient catheter sample processing methods

2.5.1 Clinical catheter sourcing, sectioning, and storage

Indwelling urinary catheters were recovered from hospitalized patients undergoing urological and gastro-intestinal surgery. Catheters were routinely recovered after a range of indwelling times and placed in sterile containers. The samples were stored for up to 7 days at 4 ^{o}C prior to processing. Catheters were cut into 5 cm cross-sections exposing their luminal surfaces (Figure 2.5). Sections designated for confocal microscopy were immediately processed and imaged using a CSLM (LSM 700, Zeiss). Only sections at 5 cm, 20 cm, and 35 cm of clinical catheters forming cohorts 1 and 2 were analysed using confocal microscopy (Table 5.2). All seven 5 cm sections were analysed for catheter samples part of cohort 3. 3 cm sections of the catheters designated for genomic DNA (gDNA) extraction and subsequent 16S rRNA gene sequencing were stored in 1.5 mL of PBS within 2 mL cryotubes at -80 ^{o}C. 1 cm sections of the catheter samples designated for ESEM imaging and EDS analysis were fixed as described in section 2.4.6 and stored within 2 mL cryotubes at 4 ^{o}C. Catheter sections of 1 cm in length allocated for SEM imaging were perfusion-fixed using

2.5 % (v/v) glutaraldehyde in 0.05 M sodium cacodylate buffer overnight at room temperature and stored at 4 ^{o}C within 2 mL cryotubes prior to imaging.

2.5.2 Confocal laser scanning microscopy performed on clinical catheters

Following sectioning of the clinical catheter samples, the staining and imaging procedure described in section 2.4.5 was carried out. Following imaging with a CSLM (LSM 700, Zeiss), the biofilm biomass and mineralization accumulated on the clinical catheter samples was determined by quantification of Syto64 (Excitation/Emission λ - 599/619 nm) and calcein (Excitation/Emission λ - 488/515 nm) fluorescence associated with the images, respectively, using comstat2/ImageJ software (Heydorn *et al.*, 2000).

2.5.3 Fibrinogen quantification- Urine sample sourcing, storage, processing, and analysis

Urine samples were sourced from hospitalized patients pre- and post-catheterization. The samples were aliquoted in 1.5 ml cryo-tubes and stored at -20 ^{o}C. A high sensitivity human fibrinogen ELISA kit (Abcam) was used to quantify the fibrinogen present within the urine samples. The urine samples were diluted at a 1 in 3 ratio in Sample Diluent NS and centrifuged at 2000 x g for 10 minutes. Fibrinogen quantification was conducted following the manufacturer's instructions. The OD of samples at 450 nm was recorded using a TECAN (Infinite, M200Pro). The urinary fibrinogen concentrations were measured in duplicates and interpolated from a fibrinogen standard curve (see Appendix P), correcting the values for the sample dilution.

2.5.4 Fibrinogen and biofilm quantification- Clinical catheter sourcing, storage, processing, and analysis

Indwelling urinary catheters corresponding to the urine samples used for fibrinogen quantification were recovered from hospitalized patients. The catheters were processed as described in section 2.5.1. Only the first 5 cm of the catheters, closest to the eyehole (Figure 2.5), were used for fibrinogen and biofilm quantification. For fibrinogen quantification 100 µL of 10 % (v/v) fetal bovine serum (Sigma-Aldrich) diluted in dH_2O was applied to the lumens of the 5 cm catheter eyehole end sections (Figure 2.5) for 1 hour. 30 µL of 40 µg mL^{-1} (v/v) primary fibrinogen antibody (Fibrinogen alpha chain Polyclonal Antibody, ThermoFisher), diluted in dH_2O, was subsequently added to the cow serum on the catheter sections. The samples were incubated at 4 ^oC O/N. Following incubation, the samples were washed three times in dH_2O. 100 µL of 0.02 µM (v/v) secondary antibody (Qdot 705 goat F(ab')2 anti-rabbit IgG conjugate (H+L), ThermoFisher), diluted in dH_2O, was applied to the catheter sections and they were incubated in the dark at room temperature for 1 h. The samples were subsequently washed three times in dH_2O. For biofilm staining, 100 µL of 1 µg mL^{-1} (v/v) FM 1-43FX dye (ThermoFisher), diluted in DMSO, was applied to the catheter sections, and they were incubated in the dark for 30 min at room temperature. The samples were subsequently washed with dH_2O, and imaged using a confocal microscope (LSM 700, Zeiss). The biofilm and fibrinogen biomass accumulated on the clinical catheter samples was determined by quantification of FM 1-43 (Excitation/Emission λ - 472/580 nm) and secondary antibody (Qdot 705) (Excitation/Emission λ – 405/705 nm) fluorescence associated with the images, respectively, using comstat2/ImageJ

software (Heydorn *et al.*, 2000). Co-localization analysis of the images and Pearson correlation coefficient calculations were conducted using the Coloc2 plugin of the Fiji software (Manders *et al.*, 1992; Schindelin *et al.*, 2012).

2.6 Patient catheter sample further characterisation methods

2.6.1 Characterisation of patient catheter biofilm and mineralization via environmental scanning electron microscopy (ESEM) coupled with energy dispersive X-ray spectroscopy (EDS) and scanning electron microscopy (SEM) imaging

Patient catheter associated biofilm and mineral morphology, as well as elemental composition, were characterised via ESEM imaging coupled with EDS analysis, as well as SEM imaging. 1 cm samples set aside during the sectioning of the clinical catheters for CLSM imaging as described in section 2.5.1, were prepared for ESEM imaging and EDS analysis as described in section 2.4.6. SEM imaging was conducted using a scanning electron microscope (SEM, FEI Quanta200 3D DualBeam) to image 1 cm catheter samples at various points down the length of the medical devices. Prior to imaging the catheter sections were perfusion-fixed using 2.5% (v/v) glutaraldehyde in 0.05 M sodium cacodylate buffer overnight at room temperature. Subsequently the catheter sections were washed in the buffer for 15 min prior to post-fixation using a 1:1 solution of 0.05 M buffer and 1 % osmium tetroxide for 1 h. Following post fixation procedures, the samples were washed using dH_2O twice for 5 min. Ascending series of 50 %, 60 %, 70 %, 80 %, 90 %, and 100 % ethanol solutions were used to dehydrate the samples, submerging the sections for 15 min at each step. Critical point drying of the samples was carried out using a Leica EM CPD300 critical point dryer, before

gold-sputter coating the samples and visualising within the SEM at an accelerating voltage of 15 kV.

2.6.2 Calcium oxalate re-suspension and quantification

Calcium oxalate re-solubilization and extraction was carried out on 10 Camstent and 10 silicone catheters with the highest confocal microscopy estimated mineral accumulation. For each catheter sample selected for this experiment 3 x 4 cm cross-sectional pieces were used. The catheter sections were submerged in 2 mL of 5 M hydrochloric acid (HCl) and incubated at room temperature for 16 h (Hodgkinson, 1981). An oxalate assay kit (Sigma-Aldrich) was used to quantify the calcium oxalate within the sample solutions following the manufacturer's instructions. As a positive re-suspension control, 20 mg of calcium oxalate powder (Sigma-Aldrich) was re-solubilized in 2 mL of 5 M HCl, while a 5M HCl solution was used as a negative resuspension control. 10 µL of each sample were transferred in to three separate wells of a 96-well plate. 10 µL of dH_2O was used as a blank, and 10 µL of standard solution (500 µM) was added to an internal standard well. 5 µL of Reagent A provided was diluted in 20 mL of dH_2O. 30 µL of diluted reagent A were was subsequently added to each well and incubated at room temperature for 2 minutes, tapping the lightly on the sides. Blank reagent for sample blank wells was prepared by mixing 155 µL of Reagent B and 1 µL horseradish peroxidase (HRP) enzyme for each well. Working reagent for sample, control and internal standard wells was prepared by mixing 155 µL Reagent B, 1 µL oxidase (OX) enzyme, and 1 µL HRP enzyme for each well. 150 µL of blank reagent was added to each sample blank well, and 150 µL of working reagent was added to each sample, control, and internal standard well. The 96-well plate was incubated for 10 minutes at room

temperature. The OD at 595 nm was read for each well using a TECAN (Infinite, M200Pro). The resuspension procedure was confirmed to be successful following quantification of the control wells producing concentrations of 10 mg ml^{-1} and 0 mg ml^{-1} for the positive and negative controls respectively.

2.6.3 Genomic DNA extraction and 16S rRNA gene sequencing for microbiome comparison of clinical catheter samples

Genomic DNA (gDNA) extraction was carried out using the PureLink Microbiome DNA Purification Kit (Invitrogen). Catheter sections of 3 cm in length were cut in to three 1 cm pieces using a sterile scalpel. Each sample was added to a bead tube pre-loaded with 800 µL of S1 lysis buffer. 100 µL of S2 lysis enhancer was added to each reaction tube and vortexed for 30 s. The tubes were subsequently incubated at 65 ^{o}C for 10 min. To bead beat the samples, the FastPrep-24 5G instrument (MP Biomedicals) was used, spinning the bead tubes containing the samples at 6 metres/second for 1 min. The PureLink Microbiome DNA Purification Kit protocol for environmental swab samples was subsequently followed to obtain the final DNA elution. DNA was eluted in 40 µL of nuclease-free water (Millipore) and the DNA concentration was quantified using the QuBit 2.0 fluorimeter (Invitrogen). Genomic DNA extractions were conducted on 2 silicone and 3 Camstent patient catheters with the highest confocal microscopy estimated biofilm biomass. The extractions for each type of catheter sample were combined in general silicone and Camstent pools, to obtain the necessary quantity of DNA for sequencing ($\geq$12 ng μL^{-1}), and were subsequently split into triplicates. The two sets of pooled triplicates of gDNA samples, corresponding to Camstent and silicone catheters, were submitted for analysis by Novogene.

DNA quality validation, 16S rRNA gene sequencing, and bioinformatic analysis were performed by Novogene (Figure 2.6). The company extracted the total genomic DNA from the submitted samples using the CTAB/SDS method (Figure 2.6A) (Xia *et al.*, 2019). Monitoring of DNA concentration and purity was conducted on 1 % agarose gels. DNA was diluted to 1 ng μL^{-1}. The 16S rRNA genes of the V3-V4 region were amplified using specific primers- 341F and 806R (Muyzer, De Waal and Uitterlinden, 1993; Caporaso *et al.*, 2011; Takahashi *et al.*, 2014). All PCR reactions were carried out with Phusion® High-Fidelity PCR Master Mix (New England Biolabs). PCR product quantification and qualification was carried out by mixing 1X loading buffer (containing SYB green) with PCR products and carrying out detection via electrophoresis on 2 % agarose gel. The samples with a bright main band in the region of 400-450 bp were selected for further experimentation. The PCR products were mixed in equidensity ratios and mixtures were purified using a Qiagen Gel Extraction Kit (Qiagen, Germany). The NEBNext Ultra DNA Library Pre ® Kit for Illumina was used to generate sequencing libraries. Quality of libraries was assessed on the QuBit 2.0 fluorimeter (Thermo Scientifict) and Agilent Bioanalyzer 2100 system. An Illumina MiSeq platform was used for library sequencing, generating 250 bp paired-end reads.

Data analysis was conducted by firstly assigning paired-end reads to samples based on their unique barcode (Figure 2.6B). The reads were then truncated by cutting off the barcode and primer sequence. The FLASH software was used to merge the paired-end reads, generating raw tags (Magoc and Salzberg, 2011). Specific filtering conditions were applied to generate high-quality clean tags in accordance with the QIIME quality control process

(Caporaso *et al.*, 2010; Bokulich *et al.*, 2013). To obtain effective tags, chimeras were first identified by comparing tags with the refence database (Gold Database) using the UCHIME algorithm, and subsequently removed (Edgar *et al.*, 2011; Haas *et al.*, 2011). Uparse software was used to analyse and assign sequences with ≥97 % similarity to the same operational taxonomic unit (OTU) (Edgar, 2013). The GreenGenes database was used based on the RDP classifier algorithm, to annotate taxonomic information relevant to the sequences analysed (DeSantis *et al.*, 2006; Wang *et al.*, 2007). Phylogenetic relationships of different OTUs were determined via multiple sequence alignments using the MUSCLE software (Edgar, 2004). Normalization of OTU abundance was conducted using a sequence number standard based on the sample with the least sequences. Alpha and beta diversity analyses were subsequently all performed on the normalized data output. Alpha diversity was applied to analyse the complexity of microbial diversity through indices such as Observed-species. All sample indices were calculated with QIIME (Version 1.7.0) and displayed with R software (Version 2.15.3) (Caporaso *et al.*, 2010). The QIIME software (Version 1.7.0) was also used to evaluate microbial community complexity in the form of beta diversity, with calculations conducted in terms of both weighted and unweighted unifrac distance (Caporaso *et al.*, 2010).

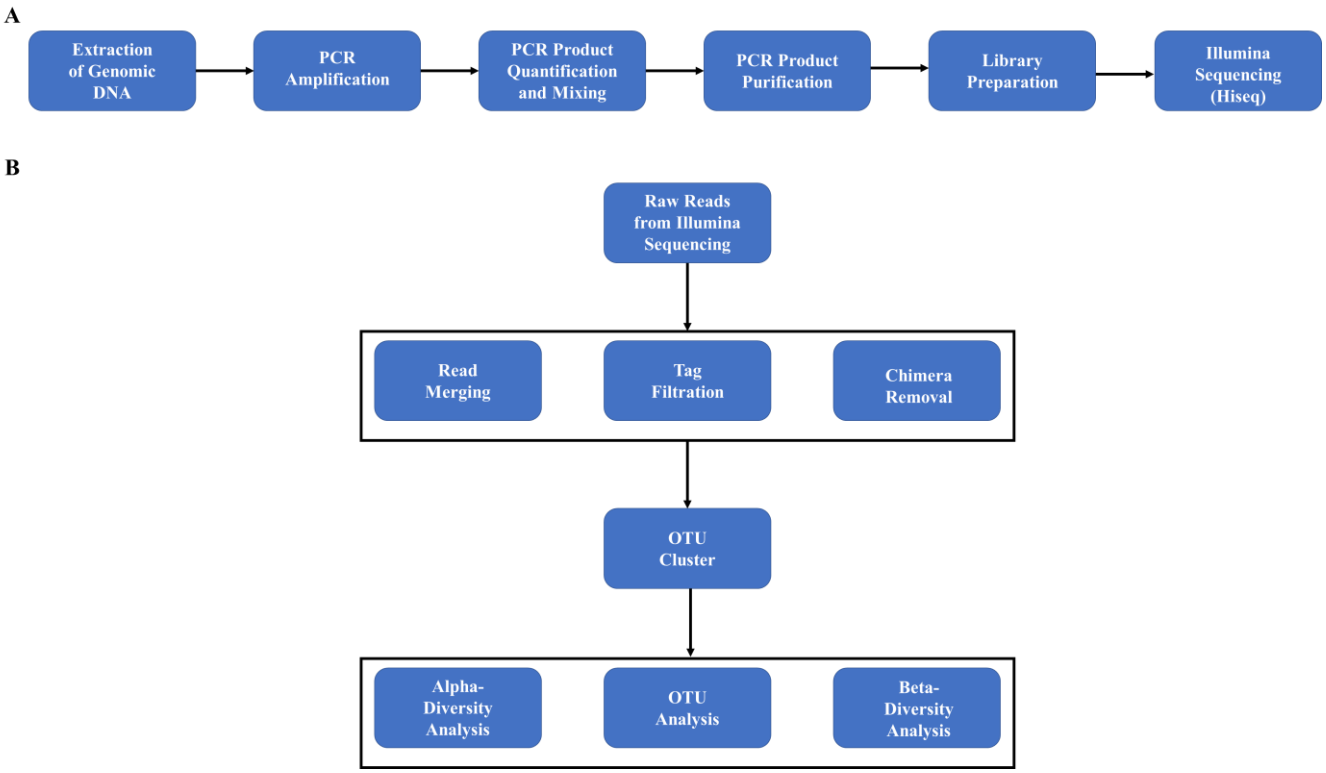

Figure 2.6 16 rRNA sequencing and data analysis workflow (Novogene)

Sequencing (A) and data analysis (B) work flow diagrams adapted from Novogene 16S analysis report.

Chapter 3- Construction of a swarming and urease deficient *P. mirabilis* mutant transposon library

3.1 Introduction

Developing an understanding of the pathogenesis of bacteria is largely dependent upon the elucidation of the impact of specific gene products upon the onset and establishment of infection. Genetics and molecular approaches have largely been adopted for this purpose, the reason for this is that host-pathogen interactions can be highly complex, making experiments of a physiological and biochemical nature particularly challenging to conduct (Hensel and Holden, 1996). Molecular genetic approaches used to study microorganisms can be differentiated in to three main sub-categories: gene expression based techniques (such as reverse genetics and gene transfer), mutation based techniques (such as transposon mutagenesis), and comparative genomics (adopting bioinformatics to compare pathogenic and non-pathogenic related strains identifying genes responsible for virulence) (Lewenza *et al.*, 2005; Tettelin *et al.*, 2008; Maddamsetti and Lenski, 2018; Fels, Gevaert and Van Damme, 2020). The continuous optimization of molecular genetic approaches and their application to study bacterial pathogenicity factors have resulted in the ability to pinpoint crucial genes responsible for ensuring an effective onset of infection, by controlling processes such as biofilm formation, urease enzyme production, and swarming (Morgenstein, Szostek and Rather, 2010; Holling *et al.*, 2014; Schaffer *et al.*, 2016).

The growing capabilities of sequencing bacterial genomes contribute largely to the success of implementing molecular genetic approaches in studying

bacterial virulence factors (Imelfort *et al.*, 2009). In the past, high costs and time constraints meant that only single strains per species would have been sequenced and designated as "reference genomes", which have been used as blueprints for further sequencing approaches (Smits, 2019). In recent years however emerging sequencing platforms such as next generation sequencing (NGS) have enabled a process called whole genome sequencing (WGS), allowing the sequencing of larger genomes in a more time and cost efficient manner (Giani *et al.*, 2020). This has paved the way for wide scale sequencing of bacterial strains of interest powering molecular genetics approaches investigating the genes crucial to specific phenotypes in pathogenic bacteria (Smits, 2019; Giani *et al.*, 2020). The incorporation of NGS to sequence a *P. mirabilis* SCDR1 strain, isolated from a diabetic ulcer patient, and identifying multiple genes encoding antibiotic and metal resistance mechanisms is just one example of the impact of the advent of whole genome sequencing technologies (Saeb *et al.*, 2017).

3.1.1 Bacterial mutagenesis approaches

Advances in sequencing technologies have enabled a range of studies into bacterial pathogenesis based on mutagenesis approaches, which can be sub-divided in to two main categories; directed and random. Site-directed mutagenesis (SDM) allows us to introduce mutations within specific DNA regions of bacterial chromosomes and plasmids via polymerase chain reactions (PCR) or restriction endonuclease reactions (RER), and is most commonly applied with the aim of disrupting protein interactions, blocking post-translational modifications, or silencing enzymatic activity (Bachman, 2013; Xu and Zhang, 2016). SDM itself can be further sub-divided into single site-directed mutagenesis and multiple site directed mutagenesis (Multi-SDM), with Multi-

SDM allowing researchers to introduce multiple mutations at a time, further enhancing the time efficiency and simplifying the protocol steps (Liang *et al.*, 2012). Directed mutagenesis has been incorporated in the study of the pathogenicity of bacteria commonly colonising the urinary tract during infections such as *P. mirabilis*. One example of this was the generation of an *mrpA* mutant via the insertion of a kanamycin resistance gene within the *P. mirabilis* gene, and testing the virulence of the mutant generated in a mouse urinary tract infection model (Schaffer *et al.*, 2016). This enabled the authors to elucidate the importance of the mannose-resistant fimbrae coded by the *mrpA* gene to cluster development and retention of the bacterium within the bladder lumen, a process crucial to the survival and virulence of *P. mirabilis* within this environment (Schaffer *et al.*, 2016).

One of the main issues with using SDM for the study of bacterial pathogenesis is that the method requires the researcher to know the sequence or location of the gene to be cloned. Random mutagenesis on the other hand is a method for the generation mutants via random chromosomal disruption through the incorporation of mutagens or transposons (Kulasekara, 2014). Unlike SDM, this method offers researchers the opportunity to identify novel genes important to bacterial virulence, without any prior knowledge or assumptions about the gene sequence. Random mutagenesis does however carry its own issues in that large mutant libraries need to be generated via screening to achieve the appropriate genome coverage for the bacterium of interest, as well as subsequently having to characterise the library and selecting mutants relevant to the virulence trait being studied (Bratulic and Badran, 2017). This procedure can

be particularly time consuming especially if the bacterium incorporated in the study is one with a relatively large genome.

Common mutagens incorporated for the purpose of random mutagenesis of bacterial chromosomal DNA include chemicals such as sodium bisulphate, hydrazine, and methoxylamine (Shortle and Nathans, 1978; Kadonaga and Knowles, 1985; Deshler, 1992). This type of mutagenesis is an efficient way to generate enzymes, proteins, metabolic pathways, and genomes with desired properties (Labrou, 2010). The main advantages of incorporating this type of methodology include its applicability to various systems and studies, the generation of large mutant libraries, and comparable cost efficiency. There are however also numerous disadvantages associated with this method of random mutagenesis, including it is laborious in nature, the use of harmful chemicals and radiation, the possibility of multiple mutations within the bacterial chromosome, as well as difficulty in the identification of the sites of DNA damage (Bose, 2016).

3.1.2 Transposon mutagenesis

While random mutagenesis via the incorporation of chemical mutagens and radiation was a common method for the generation of mutant libraries in the past, the large number of issues associated with it has resulted in the adoption of alternative methodologies such as transposon mutagenesis (Bose, 2016; Freed, 2017). Transposons are naturally occurring genetic elements characterised by their mobility, enabling them to integrate at various sites within DNA sequences. There are two main groups of transposons: Class I which are retrotransposons found in eukaryotic cells and Class II which are DNA transposons found in both eukaryotic and prokaryotic cells (Babakhani and Oloomi, 2018). The DNA

transposons category includes bacterial transposon families which harbour antibiotic resistance genes making them problematic as it enables resistance transmission resulting from conjugative transfer (Bennett, 2008). On the other hand, for the purpose of research the antibiotic resistance genes carried by DNA transposons provide a way to screen transposon mutant libraries and confirm the integration of the mobile element within the chromosome of the target organism.

DNA transposons in bacteria can be further sub-categorized into transposable phage Mu, insertion sequences (ISs), non-composite Tns, and composite Tns. The transposable phage Mu can carry out two transposition mechanisms: lytic and lysogenic. It also differs from the other DNA transposons in that it incorporates proteins MuA, MuB, IHF, and HU, for the purpose of transposition and replication (Harshey, 2012). ISs are defined by their small size (700-2500bp) and the fact that they only encode transposase proteins necessary for transposition activity (Siguier, Gourbeyre and Chandler, 2014). Unlike ISs, non-composite transposons such as Tn*3* also carry drug resistance genes, they also do not contain ISs within their DNA sequence (Kostriken, Morita and Heffron, 1981). Drug resistance genes are also carried by composite transposons, however unlike the non-composite elements, composite transposons are flanked by ISs (Tansirichaiya, Mullany and Roberts, 2016).

Due to the known sequences that transposons carry, researchers are able to identify the interrupted genes within the bacterial chromosome via DNA sequencing, making them an important tool for the purpose of random mutagenesis and in molecular biology as a whole (Kristich *et al.*, 2008). Transposons enable the generation of large mutant libraries in a quick and cost-efficient way, in the absence of harmful substances which are incorporated in

random mutagenesis protocols using mutagens. The ability of transposons to self-regulate and integrate within DNA independent of homology, has resulted in their incorporation in numerous studies of virulence factors with previously unknown origins (Autret *et al.*, 2001; Sakata *et al.*, 2019). The main set-back of using this method for the purpose of random mutagenesis is the presence of transposon "hot-spots" within bacterial DNA sequences, these are locations within the sequence at which transposon will integrate more readily, thus preventing generation of libraries spanning the entire genome of interest (Levy, Schwartz and Ast, 2009).

For the purpose of random mutagenesis within Gram-negative bacteria the Tn*5* transposon has been one of the most widely used mobile elements (Cebolla and Arévalo-Rodríguez, 2010; Naorem *et al.*, 2018; Nazareno, Acharya and Dumenyo, 2020). Tn*5* is a 5.8 kbp naturally occurring prokaryotic transposon, consisting of two ISs (IS*50*R and IS*50*L), with the transposase gene (Tnp) carried by IS*50*R (Figure 3.1) (Bhasin *et al.*, 2000). The IS*50* elements are flanked by 19-bp end sequence (ES) repeats, important for the recognition of the site by Tnp during the transposition. The Tnp protein subsequently brings together the two ESs thus creating the synaptic complex formed of the transposon DNA sequence and the Tnp transposase (Figure 3.2) (Bhasin, Goryshin and Reznikoff, 1999; Bhasin *et al.*, 2000). Following the process of synaptic complex formation, the DNA adjacent to the ESs is cleaved in the presence of magnesium ions, releasing the ES-donor backbone (DBB), forming what is referred to as a DEB complex. The DEB complex subsequently proceeds to catalyse the Tn*5* transposition, integrating the transposon within the target host DNA, in what is defined as a "cut and paste"

transposition mechanism (Figure 3.2) (Curcio and Derbyshire, 2003; Vaezeslami, Sterling and Reznikoff, 2007). The presence of activated 3'-OH groups at the ends of the transposon result in the occurrence of a nucleophilic reaction during the transposon binding to a random target DNA site (Reznikoff *et al.*, 1999). The result of this reaction is a 9-bp spacing following the transposon insertion into the host chromosome, these gaps are repaired once the Tnps are released from the target DNA, resulting in the presence of 9-bp duplications (Reznikoff, 2003).

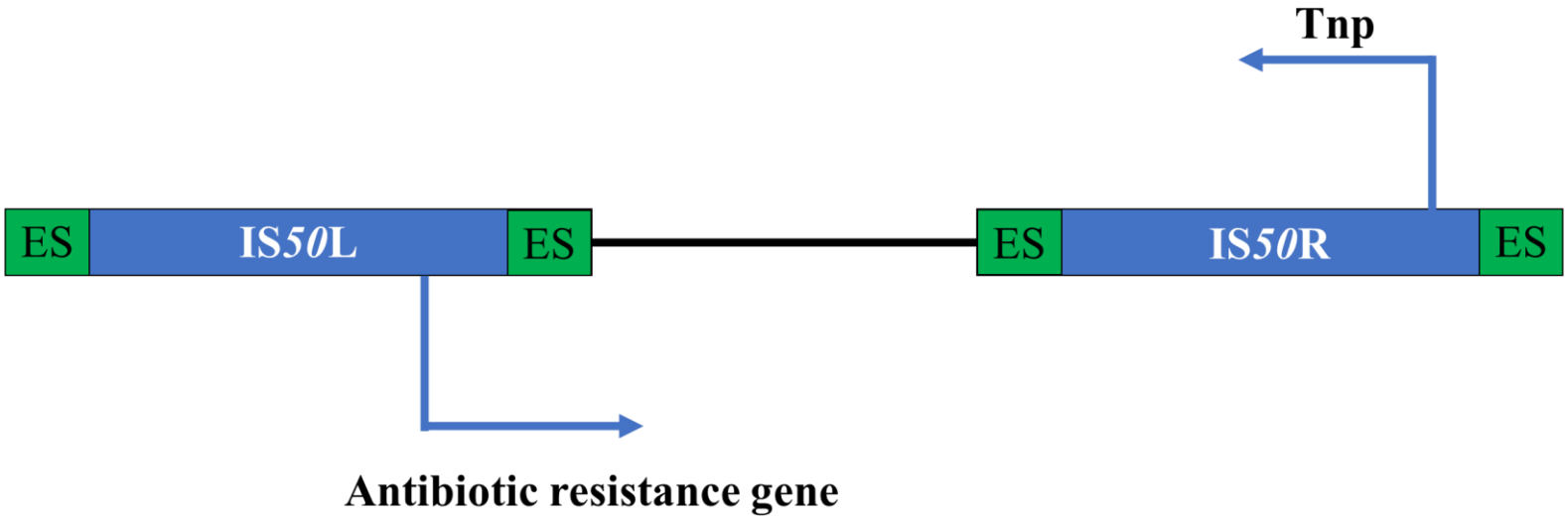

Figure 3.1 *Tn*5 transposon structure

A schematic representation of the *Tn*5 transposon structure consisting of two ISs (IS*50*L and IS*50*R). IS*50*L carries the transposase gene (Tnp), with both ISs flanked by 19-bp ESs. Figure adapted from Bhasin *et al*., 2000.

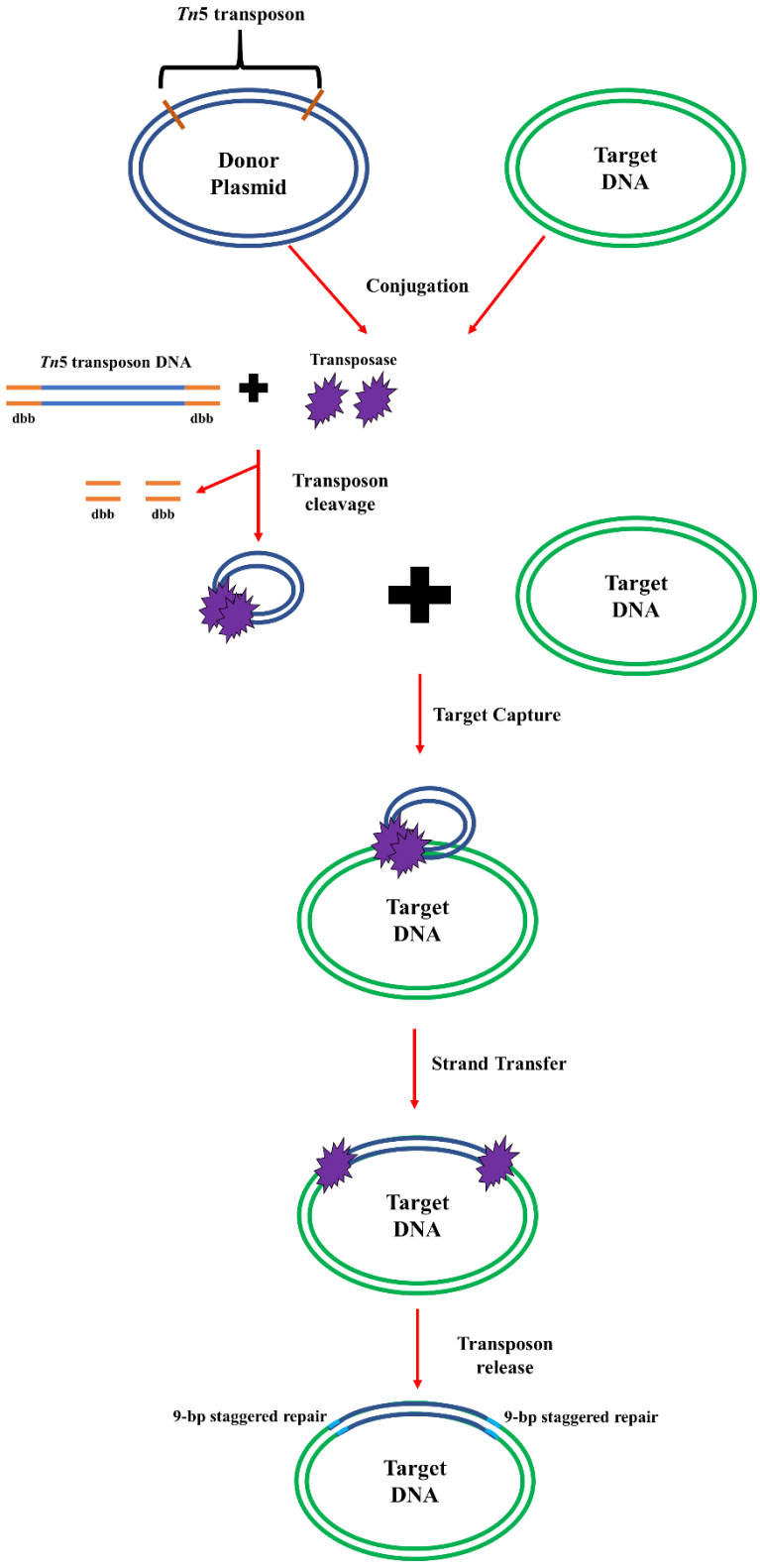

Figure 3.2 Cut and paste *Tn*5 transposition mechanism

A schematic representation of the *Tn*5 transposition mechanism, through which the mobile element interrupts DNA sequences within genomes of interest. Figure adapted from Vaezeslami *et al*., 2007.

The mini-Tn*5* derivative of the Tn*5* transposon has been adapted for molecular biology purposes by constructing plasmids carrying the mobile element, reducing the wild type transposon size, adding antibiotic selection markers, as well as introducing multiple cloning sites to enable alterations of the vectors (De Lorenzo *et al.*, 1990; Weitz *et al.*, 2001). The R6K-based pUT suicide delivery vectors carrying the mini-Tn*5* mobile elements constructed by De Lorenzo *et al.*, in 1990 have become a particularly popular tool for molecular biology as well as base plasmids for further modifications tailoring the constructs to experimental protocols (Winson *et al.*, 1998; Cebolla and Arévalo-Rodríguez, 2010; Martínez-García *et al.*, 2014). The origin of transfer, *oriT*, carried by these mini-Tn*5* vectors enable conjugation in the bacterial strains of interest, while the R6K origin of replication prevents replication in bacteria lacking the π protein (Lee and Grossman, 2007; Rakowski and Filutowicz, 2013). For example, *E. coli* produces the π protein and is therefore commonly used as the host of the mini-Tn*5* vectors, as the binding of this protein to the iterons of the R6K origin of replication enables the plasmid to replicate and not integrate within the bacterium's chromosome (Ratnakar *et al.*, 1996). This is particularly important as once the plasmid is conjugated into a bacterial strain designated for transposon mutagenesis, which cannot produce the π protein, the transposon would integrate at a random site within the genome while the vector and transposition mechanism will be lost. This makes the mini-Tn*5* constructs an efficient tool for the generation of stable transpositions in Gram-negative hosts, while mitigating the chance of multiple transposon insertions.

A mini-Tn*5* construct has been used to generate random transposon mutant libraries in a wide range of bacteria such as *Ps. aeruginosa*, *Ps.*

fluorescens, *Vibrio fischeri*, *Halomonas eurihalina*, and *Sinorhizobium meliloti* (Rajendran *et al.*, 1994; Llamas *et al.*, 2000; Pobigaylo *et al.*, 2006; Overhage *et al.*, 2007; Lyell *et al.*, 2008). These experiments were conducted with various objectives including the identification of antibiotic resistance genes, elucidating genes involved in motility, and exopolysaccharide deficiencies. In *P. mirabilis*, mini-Tn*5* transposon mutagenesis has in the past been incorporated for the generation of a large mutant library investigating genes important for the ability of the bacterium to cause CAUTIs (Armbruster *et al.*, 2017). Additionally, the authors focused their research on polymicrobial interactions during CAUTIs, identifying the necessity for genes involved in branched-chain amino acid biosynthesis by *P. mirabilis* in cases of co-infection with *P. stuartii* due to the high-affinity import of leucine by the latter bacterium (Armbruster *et al.*, 2017).

Further modifications to the mini-Tn*5* system via the addition of genes such as *gfp* and *lux*, extend the functionality of the construct allowing researchers to incorporate the mutants generated in gene expression studies. A mini-Tn*5*-*luxCDABE* has been incorporated for the generation of a random mutant library in *Ps. aeruginosa*, screening the mutants under magnesium and phosphate limitation (Lewenza *et al.*, 2005). The action of *luxCDABE* as a real time reporter of gene expression enabled the authors to identify numerous genes crucial for the adaptation to the environmental conditions investigated. By creating a mini-Tn*5*-*gfp* derivative of the mini-Tn*5* construct, researchers were able to mutagenize *Agrobacterium tumefaciens* and isolate mutants expressing the GFP protein, allowing them to use these as reporters to follow the expression of the mutated genes under various growth conditions such as acidic pH (Tang, Lu and Pan, 1999).

3.1.3 Genetic characterisation of transposon mutants

To make use of transposon mutant libraries it is important to conduct an accurate and high-throughput method of sequencing for the determination of the interrupted genes. Methods such as transposon directed insertion site sequencing (TraDIS) enable the sequencing of large mutant libraries reaching 1.1 million transposon mutants via Illumina nucleotide sequencing. TraDIS relies on the PCR amplification of transposon containing DNA sequences following the fragmentation of genomic DNA extracted from the transposon mutants, selectively enriching for transposon-flanking sequences, and thus mapping a large number of transposon insertions simultaneously (Langridge *et al.*, 2009; Barquist *et al.*, 2016). The system is adaptable to different types of transposons and has been widely used in various different bacterial species including *Salmonella typhimurium*, *Clostridium difficile*, *Mycobacterium marinum*, and *E. coli* (Eckert *et al.*, 2011; Chaudhuri *et al.*, 2013; Dembek *et al.*, 2015; Weerdenburg *et al.*, 2015). While TraDIS offers a very high throughput method of transposon mutant library generation and sequencing, it relies upon advanced sequencing instrumentation such as paired end Illumina flow cells and an Illumina sequencer, which may not be widely available and can be relatively expensive.

Cloning based transposon mutant library sequencing approaches offer one alternative, where individual transposon mutant genomic DNA is extracted and digested using a restriction enzyme with numerous restriction sites within the host genome such as EcoRI, EcoRV and HindIII (Smith and Enquist, 1999; Chen *et al.*, 2000; Kiljunen *et al.*, 2014). A self-ligation procedure is subsequently undertaken using the digested genomic DNA, followed by

transformation of the ligation into *E. coli* and selection based on the antibiotic resistance marker carried by the transposon. Using a primer based on the known transposon sequence, the interrupted gene can then be identified by sequencing the cloned DNA fragment. While this method is an accurate way for the characterisation of mutations during transposon mutagenesis, the procedure can be laborious when sequencing large mutant libraries.

Another way of sequencing the interrupted genes within transposon mutant libraries is by incorporating a PCR-based technique amplifying the sequences flanking the mobile element (Manoil, 2000; Jacobs *et al.*, 2003). The two step PCR procedure incorporates primers based on the known transposon sequence, as well as semi-degenerate primers which bind to multiple sites within the bacterial chromosome. As the transposon-based primers read outwards from the known sequence and the semi-degenerate primers read towards to the transposon, the PCR reactions produce a DNA segment of the gene or genes flanking the transposition (Figure 2.2). The primers specific to the transposon sequence can subsequently be used to sequence the product of the PCR reactions.

Once the DNA sequence flanking the transposon insertions is identified it must be associated with a gene within the bacterial chromosome in order to elucidate the disrupted function within the mutants. The sequenced regions flanking the transposition site are therefore compared to previously sequenced genomes of the bacterial host via the Basic Local Alignment Search Tool (BLAST) of the National Centre for Biotechnology Information (NCBI) (Altschul *et al.*, 1990). BLAST is the most commonly incorporated tool to identify sequence similarities, providing various options for alignment including

nucleotide and protein, as well as statistically quantifying the alignment match identified (Pertsemlidis and Fondon, 2001; Kerfeld and Scott, 2011). The protein database associated with the previously sequenced bacterial genomes and genes provided by the BLAST tool enables researchers to assign a function to the transposon interrupted DNA sequences.

Much of the most recent work focusing on *P. mirabilis* has incorporated the full sequence of the clinical isolate *P. mirabilis* HI4320 as a reference genome (Pearson *et al.*, 2008). The availability of reference genomes has enabled researchers to compare the genetic composition of clinically isolated strains at different points in time and map them back to the available sequence using BLAST or similar alignment tools, thus monitoring trends in important virulence factors such as the presence of β-lactamase genes associated multi-drug resistance (Mac Aogáin, Rogers and Crowley, 2016; Hu *et al.*, 2020). The complete *P. mirabilis* HI4320 reference genome also enables researchers to use the BLAST tool to map and identify gene sequences present within other strains of the bacterium, such as the O-polysaccharide encoding *waaL* gene homologues identified within *P. mirabilis* R110, 51/57, and HI4320 (Aquilini *et al.*, 2010). The whole genome reference sequence can be beneficial for the discovery of genetic differences between *P. mirabilis* strains too, such as the absence of the cationic antimicrobial resistance gene *mig-14* within HI4320, identified within the 51/57 strain, with the BLAST tool revealing its functionality based on comparison to the *Salmonella enterica* reference genome (Brodsky *et al.*, 2002; Aquilini *et al.*, 2010).

3.1.4 Hypothesis and aims

Mini-Tn*5* transposon mutagenesis of *P. mirabilis* was hypothesised to generated random mutants, some of which following screening, would be identified as deficient in one of the two main virulence factors of the bacterium: swarming motility and urease production. The aim of this chapter was to isolate mutants from the library generated, impacted solely within the identified virulence factor of interest, with limited secondary phenotypic effects, and thus selected for further experiments comparing their behaviour to *P. mirabilis* WT on silicone and Camstent-coated catheters within an *in vitro* bladder model.

The objectives to address the aims of this work were:

- To generate a *P. mirabilis* mini-Tn*5* transposon mutant library
- To screen the transposon mutant library for urease production and swarming motility
- To select transposon mutants with compromised swarming motility or urease production and limited secondary phenotypic effects
- To identify the mini-Tn*5* disrupted genes via bioinformatic analysis of the transposon flanking regions

3.2 Results

Following the screening of 11283 *P. mirabilis* transposon mutants for swarming and urease deficiencies, a library of mutants deficient in each trait was generated. A total of 18 *P. mirabilis* mutants unable to produce the urease enzyme and mutants incapable of swarming were isolated following transposon mutagenesis. Further characterisation studies were carried out for all 18 urease

negative transposon mutants, whereas a sub-set of the first 20 non-swarming transposon mutants was selected for further analysis.

3.2.1 Confirmatory swarming motility and urease production assays

Sub-cultured *P. mirabilis* transposon mutants from preliminary swarming and urease screens were incorporated in confirmatory assays to establish the aberrations in the phenotypic traits of interest (Figures 3.3 and 3.4). These assays were also used to confirm that urease production was not impacted within swarming negative mutants, and swarming motility was not impacted within urease negative mutants. (Tables 3.1 and 3.2). All swarming negative mini-Tn*5 P. mirabilis* mutants within the selected sample set exhibited urease production. All urease negative *P. mirabilis* isolates exhibited swarming motility, with the exception of transposon mutant URN2.

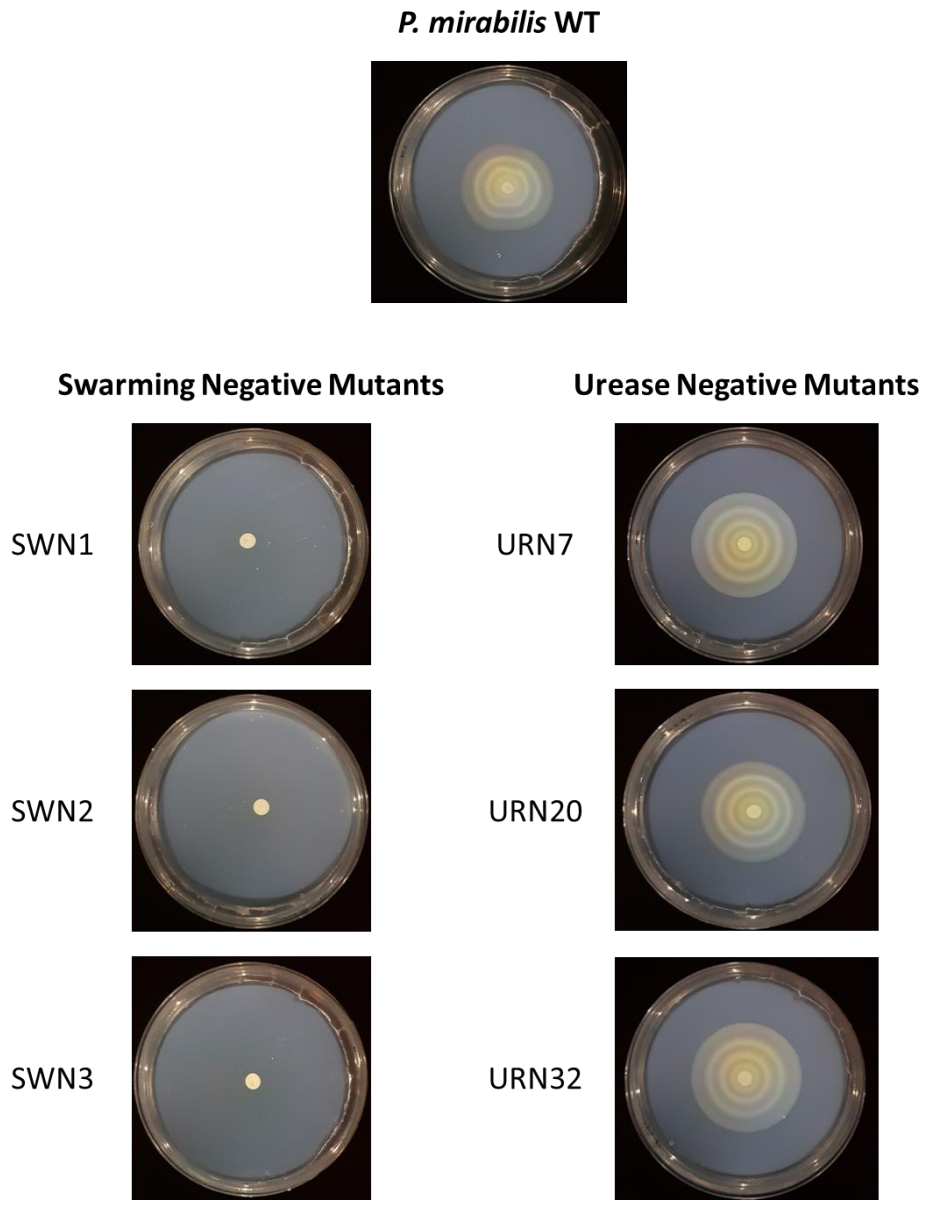

Figure 3.3 Confirmatory swarming assay examples of mini-Tn*5* *P. mirabilis* mutants

Swarming assays conducted by inoculating 1.5 % LB agar plates with *P. mirabilis* wild type (WT) and swarming (SWN) and urease (URN) negative mini-*Tn*5 *P. mirabilis* mutants.

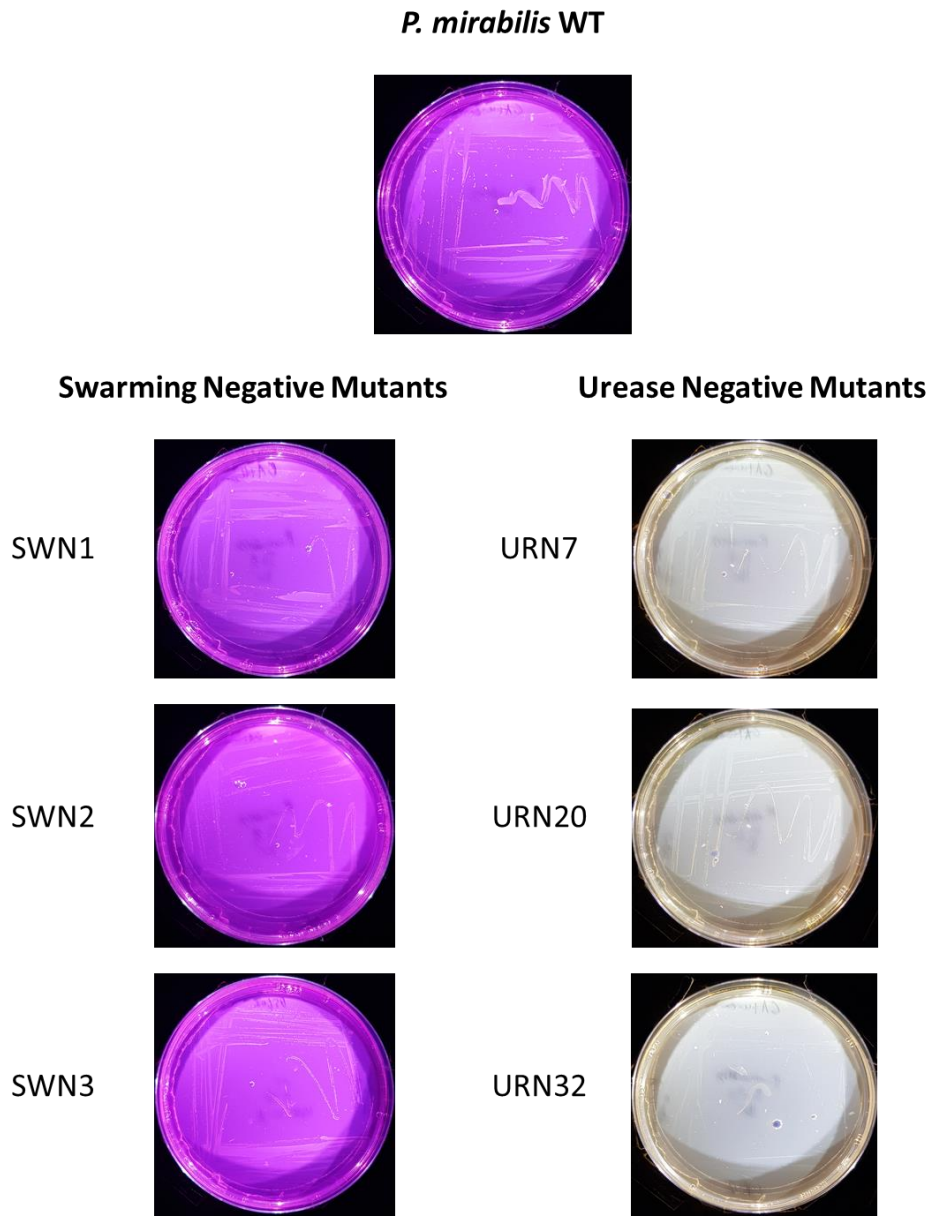

Figure 3.4 Confirmatory urease assay examples of mini-Tn*5* *P. mirabilis* mutants

Urease production assays conducted by inoculating Christensen agar plates supplemented with urea, with *P. mirabilis* WT and swarming (SWN) and urease (URN) negative mini-Tn*5* *P. mirabilis* mutants. The colour of the agar changes from yellow (pH 6.8) to purple/pink (pH 8.2) as a result of the presence of the pH indicator phenol red. The reaction occurs in response to the degradation of urea by urease producing bacteria, increasing the levels of ammonia and raising the pH of the growth medium.

Table 3.1 Swarming and urease assays for swarming negative mini-Tn*5* *P. mirabilis* mutants

Strain	Swarming	Urease Production
P. mirabilis WT	✓	✓
SWN1	X	✓
SWN2	X	✓
SWN3	X	✓
SWN4	X	✓
SWN5	X	✓
SWN6	X	✓
SWN7.1	X	✓
SWN7.3	X	✓
SWN9	X	✓
SWN11	X	✓
SWN14	X	✓
SWN15	X	✓
SWN16.1	X	✓
SWN16.2	X	✓
SWN18	X	✓
SWN20	X	✓
SWN21	X	✓
SWN22	X	✓
SWN23	X	✓
SWN24	X	✓

Complete results from swarming and urease assays conducted for a sample set of swarming negative mini-Tn*5* *P. mirabilis* mutants isolated from the initial screening. *P. mirabilis* WT strain was used as a positive control.

Table 3.2 Swarming and urease assays for urease negative mini-Tn*5* *P. mirabilis* mutants

Strain	Swarming	Urease Production
P. mirabilis WT	✓	✓
URN2	X	X
URN7	✓	X
URN17	✓	X
URN20	✓	X
URN32	✓	X
URN34	✓	X
URN35	✓	X
URN36	✓	X
URN37	✓	X
URN40.1	✓	X
URN40.2	✓	X
URN52	✓	X
URN55	✓	X
URN68	✓	X
URN88	✓	X
URN97	✓	X
URN98	✓	X
URN107	✓	X

Complete results from swarming and urease assays conducted for all of the urease negative mini-Tn*5* *P. mirabilis* mutants isolated from the initial screening. *P. mirabilis* WT strain was used as a positive control.

3.2.2 *P. mirabilis* transposon mutant growth curves

All 18 of the urease negative mini-Tn*5* *P. mirabilis* mutants were screened for growth defects (Figure 3.5). The transposon insertion affected the growth of only one of the mutants screened (URN2), resulting in slower exponential phase of growth when compared to the wild-type *P. mirabilis* strain (Figure 3.5A). None of the 20 non-swarming mini-Tn*5* mutants exhibited significant deviation from the growth pattern of the wild-type *P. mirabilis* strain (Figure 3.5B).

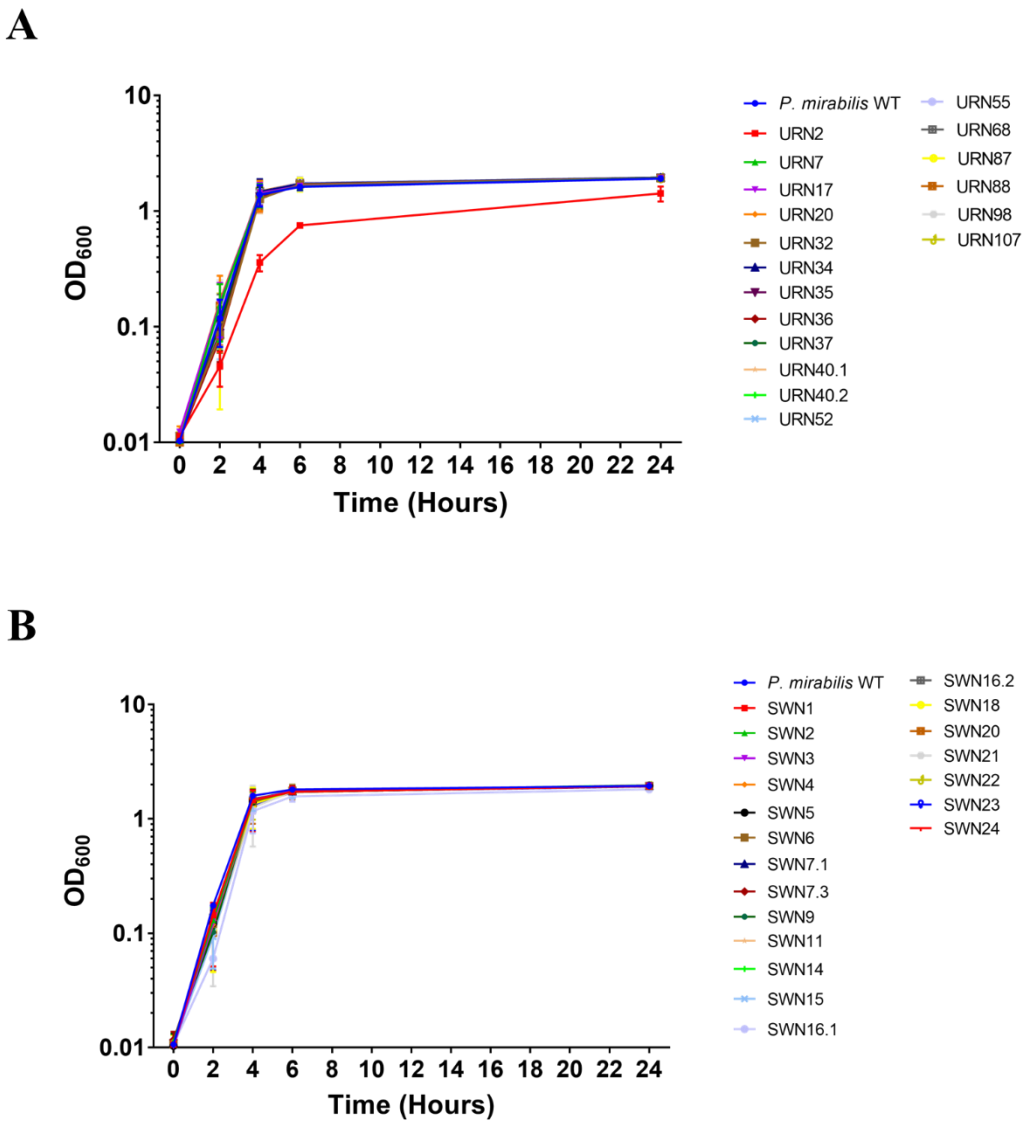

Figure 3.5 Growth curves of mini-Tn*5* *P. mirabilis* mutants

Growth curves generated for urease negative (A) and swarming negative (B) mini-Tn*5* *P. mirabilis* mutants. Values represent the mean optical density (OD) at a wavelength of 600 nm for each mutant analysed following three experimental replicates. Error bars represent the standard deviation of the mean values.

3.2.3 *P. mirabilis* transposon mutant preliminary biofilm assays

The preliminary biofilm assays for the urease negative *P. mirabilis* mini-Tn*5* transposon mutants indicated comparable biofilm formation for all isolates, except URN2, to the *P. mirabilis* WT strain (Figure 3.6A). The swarming negative *P. mirabilis* transposon mutants exhibited more variable biofilm activity relative to the WT strain (Figure 3.6B). 10 of the swarming negative isolates exhibited reduced biofilm activity (RBFA), on the other hand the 10 remaining isolates exhibited comparable biofilm activity (CBFA) to wild-type *P. mirabilis*. This is indicative of the greater apparent impact of swarming upon the *P. mirabilis* biofilm formation capabilities, in comparison with urease production.

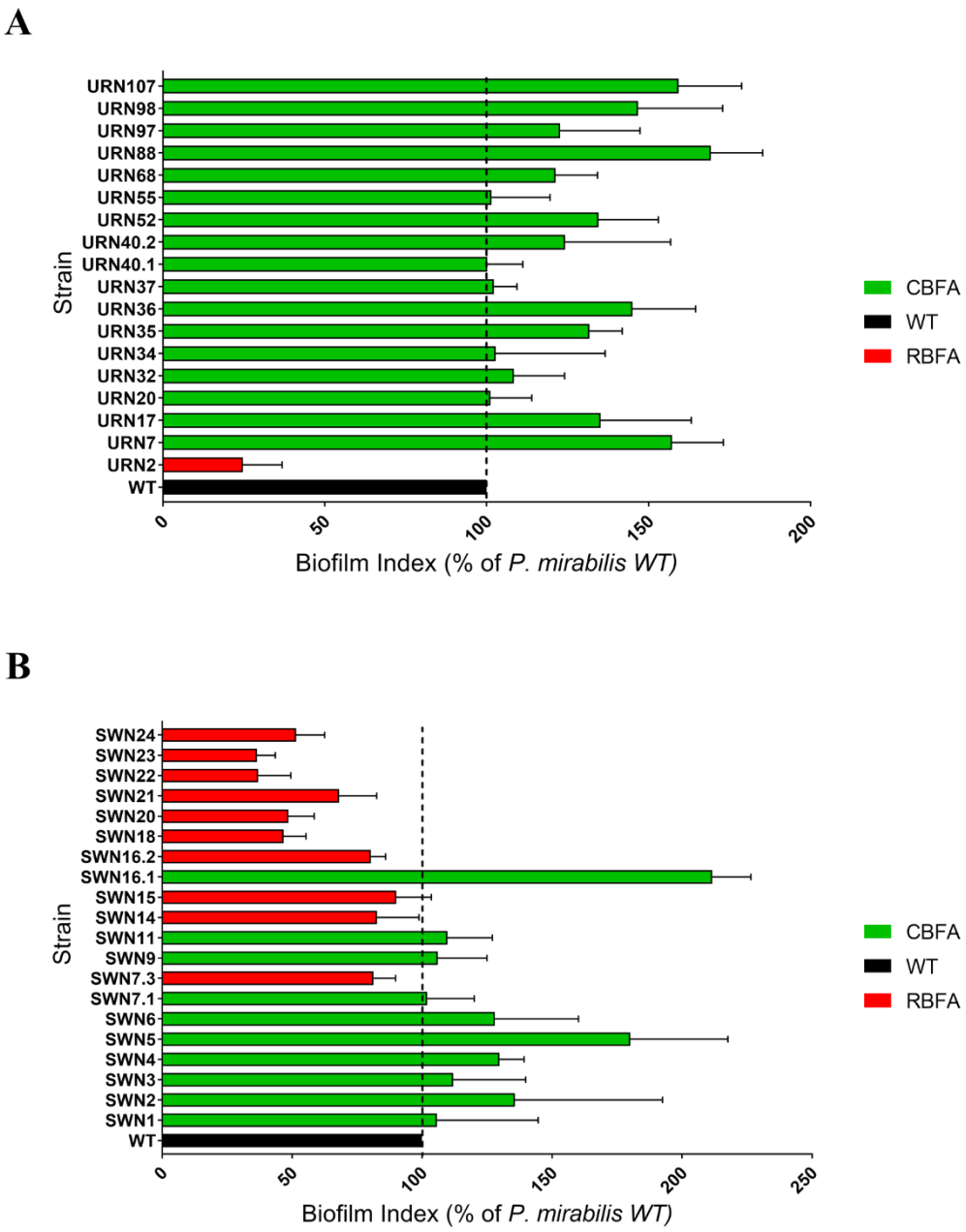

Figure 3.6 Preliminary biofilm assays of mini-Tn*5* *P. mirabilis* mutants

Biofilm assays conducted for urease negative (URN) and swarming negative (SWN) *P. mirabilis* mini-Tn*5* transposon mutants. The biofilm activity of the strains was determined based on TECAN readings following growth and staining (Syto64 DNA dye) of the biofilm formed on the bottom of 96-well microtiter plates (See Section 2.3.5). Biofilm index values are a measure of the transposon mutant activity, expressed as a percentage of the *P. mirabilis* WT strain's activity. -CBFA- Comparable biofilm activity to the WT strain (≥100%). -WT- *P. mirabilis* wild-type strain biofilm activity (100%). -RBFA- Reduced biofilm activity relative to the WT strain (<100%). Error bars represent the standard error of the mean values.

3.2.4 *P. mirabilis* transposon mutant preliminary mineralization assays

Mineral assays conducted for the *P. mirabilis* mini-Tn*5* urease negative transposon mutants indicated a deficiency in their ability to initiate mineralization in artificial urine (Figure 3.7A). The inability of these mutants to produce the urease enzyme, responsible for the hydrolysis of urea, means they cannot efficiently increase the pH of the medium and are thus unable to cause mineral precipitation. Swarming negative *P. mirabilis* mini-Tn*5* transposon mutants exhibited variable mineralization activity, similar to the data obtained on the biofilm activity of these mutants (Figure 3.7B). From the 20 swarming negative transposon mutants tested for mineralization, 7 exhibited a mineral activity comparable with that of the *P. mirabilis* WT strain.

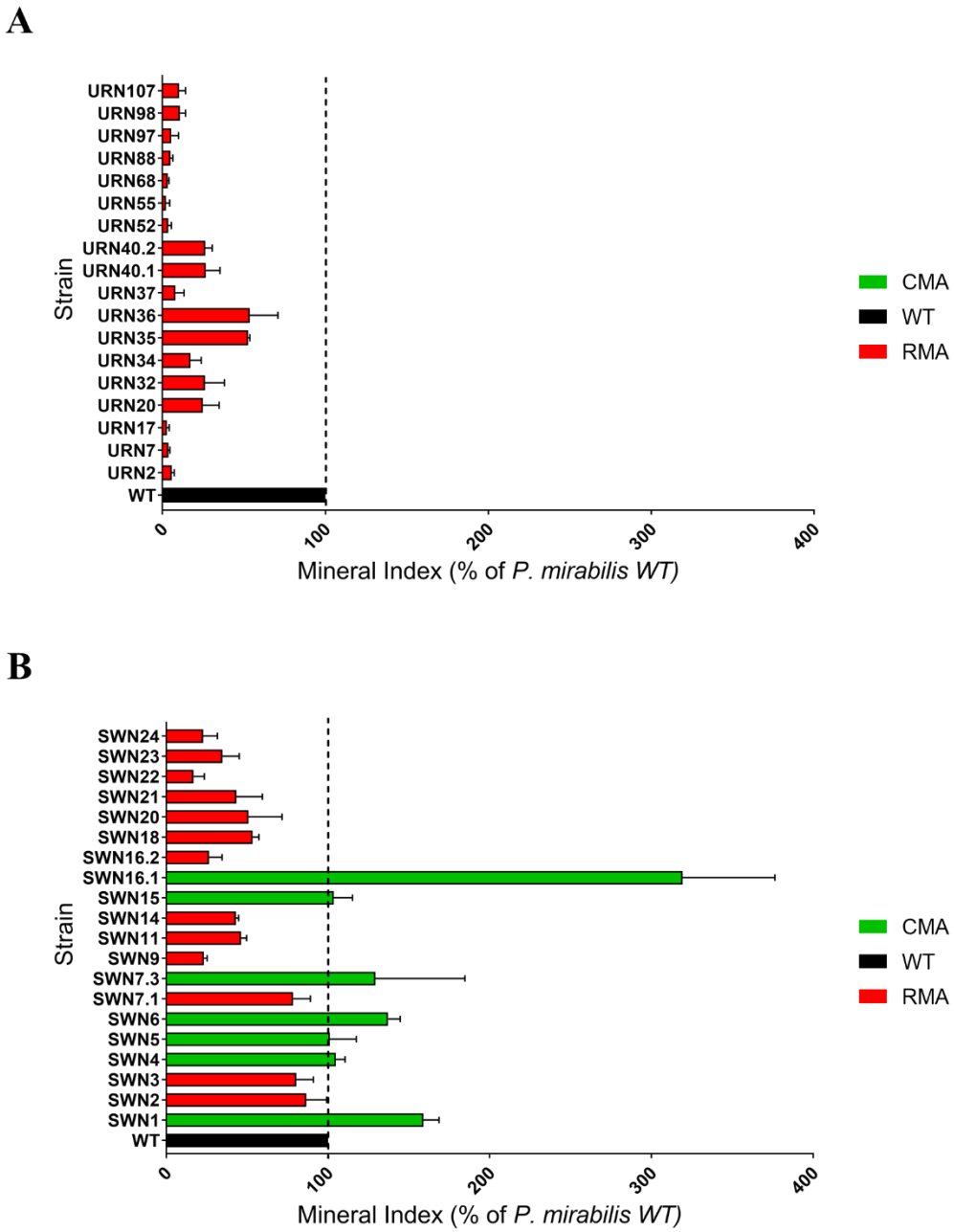

Figure 3.7 Preliminary mineral assays of mini-Tn*5* *P. mirabilis* mutants

Mineral assays conducted for urease negative (URN) and swarming negative (SWN) *P. mirabilis* mini-Tn*5* transposon mutants. Mineral index values are a measure of the transposon mutant activity, expressed as a percentage of the *P. mirabilis* WT strain's activity. -CMA- Comparable mineral activity to the WT strain (≥100%). -WT- *P. mirabilis* wild-type strain mineral activity (100%). -RMA- Reduced mineral activity relative to the WT strain (<100%). Error bars represent the standard error of the mean values.

3.2.5 Confirmation of loss of mini-Tn*5* delivery vector in *P. mirabilis* transposon mutants

P. mirabilis mini-Tn*5* transposon mutants were plated on LB agar plates supplemented with ampicillin to screen for the co-insertion of the pUT mini-Tn*5* GFP *luxABCDE* Km1 vector. The *P. mirabilis* WT strain was used as a negative control in the experiment, while the *E. coli* strain carrying the pUT mini-Tn*5* GFP *luxABCDE* Km1 vector was used as the positive control (Figure 3.8A). All swarming negative transposon mutants exhibited ampicillin susceptibility indicating that they did not carry the vector co-insertion and could therefore be sequenced using the PCR sequencing method (Figure 3.8B) (Section 2.3.7). 4 of the 18 urease negative *P. mirabilis* transposon mutants exhibited resistance to ampicillin, indicating that the plasmid had co-inserted within them and they would therefore not be suitable for sequencing using the PCR based sequencing approach (Figure 3.8C).

The pUT plasmid vector integrated within roughly 10 % of the transposon mutant strains characterised within this study. By comparison, similar studies reported between 16 % and 35 % of transposon mutant strains carrying a proportion of the suicide delivery vector used during the transposon mutagenesis protocols incorporated (Belas, Erskine and Flaherty, 1991; Holling *et al.*, 2014). One explanation for the lower rate of delivery vector co-integration reported here could be that the screening was only reliant on ampicillin resistance of the strains, whereas it is possible that parts of the vector other than the *bla* gene conferring this antibiotic resistance may have been retained. There is therefore a possibility that the 10 % vector co-integration rate could be an underestimate.

A

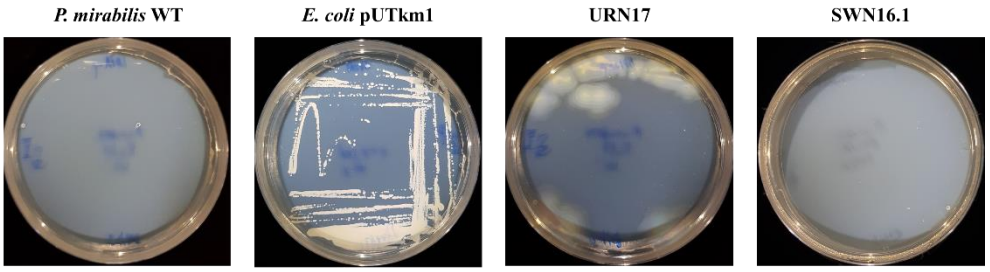

B

Strain	Ampicillin Susceptibility
***P. mirabilis* WT**	✓
***E. coli* pUTkm1**	X
SWN1	✓
SWN2	✓
SWN3	✓
SWN4	✓
SWN5	✓
SWN6	✓
SWN7.1	✓
SWN7.3	✓
SWN9	✓
SWN11	✓
SWN14	✓
SWN15	✓
SWN16.1	✓
SWN16.2	✓
SWN18	✓
SWN20	✓
SWN21	✓
SWN22	✓
SWN23	✓
SWN24	✓

C

Strain	Ampicillin Susceptibility
***P. mirabilis* WT**	✓
***E. coli* pUTkm1**	X
URN2	X
URN7	✓
URN17	X
URN20	✓
URN32	✓
URN34	✓
URN35	✓
URN36	✓
URN37	✓
URN40.1	✓
URN40.2	X
URN52	X
URN55	✓
URN68	✓
URN88	✓
URN97	✓
URN98	✓
URN107	✓

Figure 3.8 Confirmation of delivery vector loss in *P. mirabilis* mini-Tn*5* transposon mutants

LB agar plates supplemented with Ampicillin (A) were used to screen swarming negative (B) and urease negative (C) *P. mirabilis* transposon mutants for the co-insertion of the pUT mini-Tn*5* GFP *luxABCDE* Km1 vector. (✓)- ampicillin susceptible. (X)- ampicillin resistant. This step of the protocol is conducted at the final stage of the experiment in the interest of keeping any isolated mutants deemed un-identifiable by the selected sequencing strategy within this piece of work, but may be of value and therefore used in future experiments (identifying the interrupted gene by an alternative sequencing method).

3.2.6 Determining the interrupted genes in *P. mirabilis* transposon mutants

The *P. mirabilis* mini-Tn*5* transposon mutant sequencing was conducted following a well-documented PCR based approach from previous studies, with primer 2b providing the optimum amplification of the DNA sequences flanking the mini-Tn*5* insertions during the first PCR step (Figure 2.2) (Manoil, 2000; Jacobs *et al.*, 2003; Gallagher *et al.*, 2007, 2013). Adopting the PCR based sequencing method outlined in section 2.3.8, the disrupted genes within the 14 urease negative transposon mutants, confirmed to not be carrying vector co-insertion, were identified by amplifying the mini-Tn*5* flanking regions (Table 3.3). Of the subset, 20 swarming negative mutants selected for characterisation, the 5 transposon mutants with comparable biofilm and mineralization capabilities to the *P. mirabilis* WT strain were also sequenced (Table 3.4). All DNA sequences flanking the mini-Tn*5* insertion were initially mapped on the *P. mirabilis* WT strain sequence, obtained following whole genome sequencing (section 2.3.8), and subsequently cross-checked with the *P. mirabilis* HI4320 reference genome (Pearson *et al.*, 2008).

The *ureR* gene was interrupted within all sequenced *P. mirabilis* mini-Tn*5* urease negative isolates (Table 3.3). This gene encodes a transcriptional activator for the entire urease operon and therefore the interruption of this gene prevented the up-regulation of genes necessary for the production of urease (Dattelbaum *et al.*, 2003). The sequenced swarming negative mutants on the other hand carried the transposon insertion within the *flgI* gene, the expression of which is necessary for the formation of the flagellar P-ring protein (Table 3.4) (Hizukuri *et al.*, 2008). The P-ring protein is a crucial structural component of the basal body, necessary for flagella assembly within *P. mirabilis*. In the

absence of the P-ring protein the process of flagellar assembly seizes, rendering the transposon mutants incapable of swarming. The high frequency of transposon insertions within the *ureR* and *flgI* genes of *P. mirabilis* observed here, suggests transposon hotspots within these parts of the bacterial genome.

Table 3.3 Urease negative *P. mirabilis* mini-Tn*5* transposon mutant interrupted gene identification

Mutant ID	Locus Tag	Interrupted Gene	Gene Function
URN7	PMI3681	*ureR*	Urease operon transcriptional activator
URN20	PMI3681	*ureR*	Urease operon transcriptional activator
URN32	PMI3681	*ureR*	Urease operon transcriptional activator
URN34	PMI3681	*ureR*	Urease operon transcriptional activator
URN35	PMI3681	*ureR*	Urease operon transcriptional activator
URN36	PMI3681	*ureR*	Urease operon transcriptional activator
URN37	PMI3681	*ureR*	Urease operon transcriptional activator
URN40.1	PMI3681	*ureR*	Urease operon transcriptional activator
URN55	PMI3681	*ureR*	Urease operon transcriptional activator
URN68	PMI3681	*ureR*	Urease operon transcriptional activator
URN88	PMI3681	*ureR*	Urease operon transcriptional activator
URN97	PMI3681	*ureR*	Urease operon transcriptional activator
URN98	PMI3681	*ureR*	Urease operon transcriptional activator
URN107	PMI3681	*ureR*	Urease operon transcriptional activator

A summary of the interrupted genes within the urease negative *P. mirabilis* mini-Tn*5* transposon mutants. The locus identifier was derived by mapping the flanking sequences to the reference genome *P. mirabilis* HI4320 (Pearson *et al*., 2008).

Table 3.4 Swarming negative *P. mirabilis* mini-Tn*5* transposon mutant interrupted gene identification

Mutant ID	Locus Tag	Interrupted Gene	Gene Function
SWN1	PMI1647	*flgI*	Flagellar P-ring protein precursor (basal body P-ring protein)
SWN4	PMI1647	*flgI*	Flagellar P-ring protein precursor (basal body P-ring protein)
SWN5	PMI1647	*flgI*	Flagellar P-ring protein precursor (basal body P-ring protein)
SWN6	PMI1647	*flgI*	Flagellar P-ring protein precursor (basal body P-ring protein)
SWN16.1	PMI1647	*flgI*	Flagellar P-ring protein precursor (basal body P-ring protein)

A summary of the interrupted genes within the swarming negative *P. mirabilis* mini-Tn*5* transposon mutants. The locus identifier was derived by mapping the flanking sequences to the reference genome *P. mirabilis* HI4320 (Pearson *et al*., 2008).

3.2.7 *P. mirabilis* transposon mutant swimming assays

Following the identification of *flgI* as the mutated gene, crucial to flagella biosynthesis, within the non-swarming *P. mirabilis* mutants sequenced, assays were conducted to evaluate any impact of the mutation upon the strain's swimming motility (Figure 3.9). Standard swimming plate assays, confocal microscopy data comparing the *flgI* mutant, SWN1, with *P. mirabilis* WT revealed that the swarming negative mutant is incapable of carrying out swimming motility as well. The urease negative mutant (URN7) on the other hand exhibited no difference in swimming motility when compared with the wild-type strain.

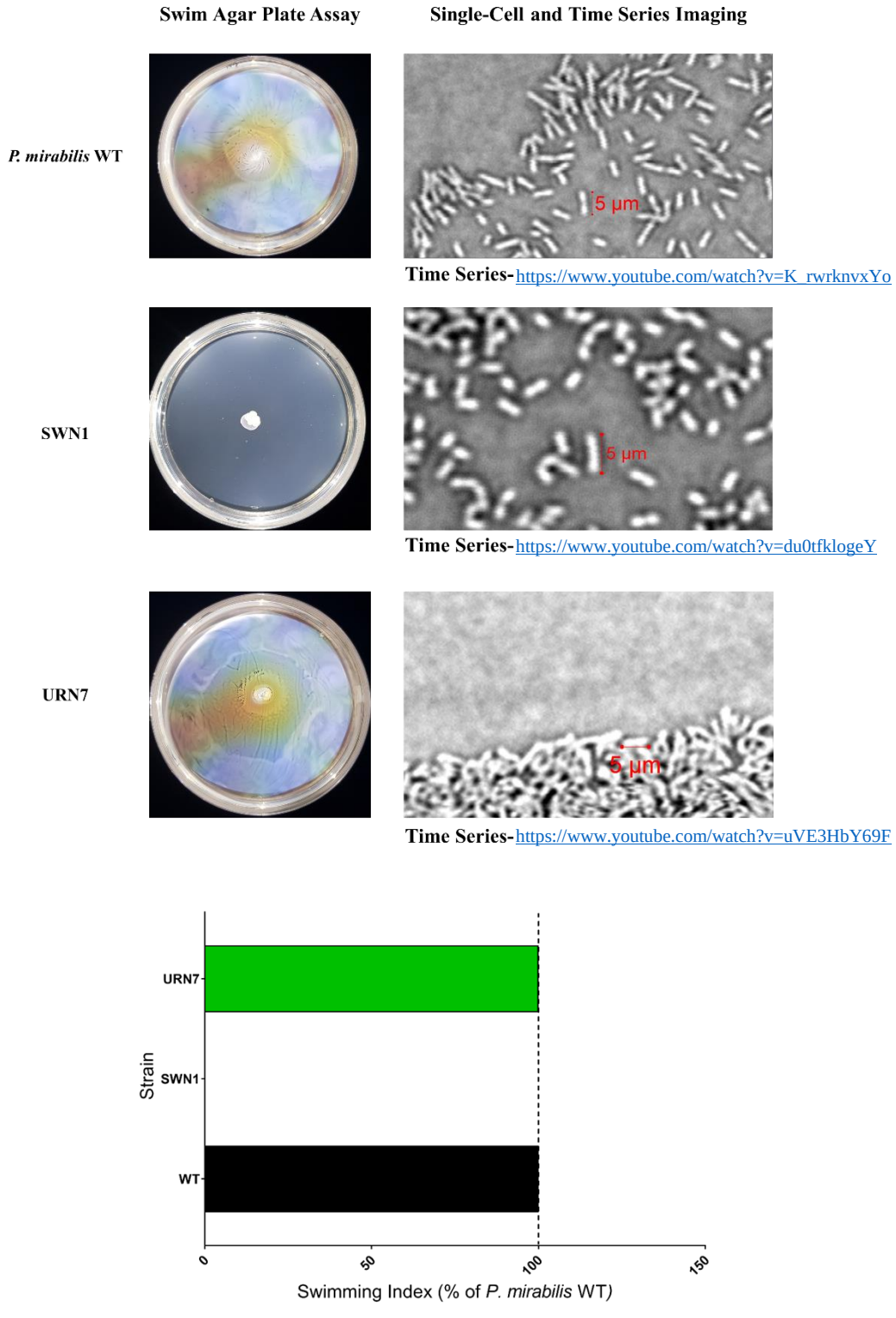

Figure 3.9 *P. mirabilis* mini-Tn*5* transposon mutant swimming assays

P. mirabilis WT, SWN1 (*flgI*-), and URN7 (*ureR*-) swimming motility assays presented as swim agar plate images and confocal microscopy single-cell images and time-series videos. Single-cell images and time-series were generated using confocal microscope LSM 700, Zeiss.

3.2.8 *P. mirabilis* transposon mutant AU biofilm and mineralization

SWN1 (*flgI*-) and URN7 (*ureR*-) were the swarming negative and urease negative transposon mutants, respectively, selected for evaluation of biofilm formation and mineral production during growth in AU for comparison with the wild-type. While AU contains urea at levels which in the past have been shown to inhibit swarming in *P. mirabilis*, the strains capable of producing urease will hydrolyse the substance via the action of the enzyme, depleting the urea concentration over the 48 h incubation time below the swarming inhibitory level (Van Asten and Gaastra, 1999; Armbruster, Hodges and Mobley, 2013). The urease negative mutant on the other hand would be incapable of hydrolysing the urea, which would likely impact its ability to swarm, highlighting any impact of the mutation upon the strain's ability to form a biofilm within a medium replicating the urinary tract environment.

Both transposon mutants exhibited comparable biofilm morphology to wild-type *P. mirabilis* (Figure 3.10). Mineralization morphology associated with SWN1 was also comparable with the wild-type *P. mirabilis* strain, however the URN7 transposon mutant produced markedly less mineral as a result of the lack of urease enzyme production (Figure 3.10). The comstat2/ImageJ quantification of the biofilm and mineral associated with each confocal microscope image supported the preliminary observations in that there was no significant difference in biofilm formation between the two mutants and wild-type *P. mirabilis*, whereas the URN7 mutant produced significantly less mineral in comparison to SWN1 and the wild-type strain (Figure 3.11).

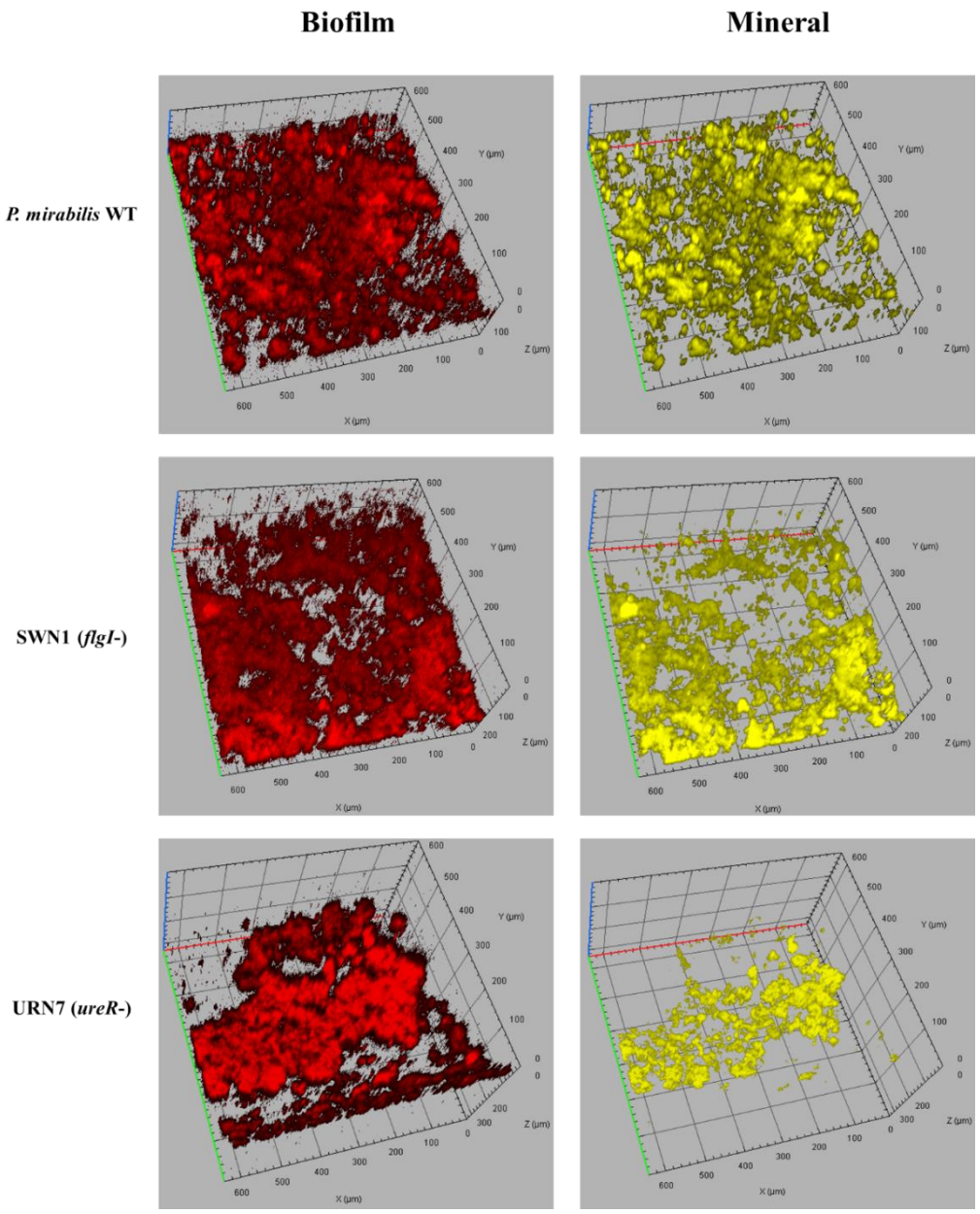

Figure 3.10 Comparing the biofilm formation and mineralization of transposon mutants in AU to *P. mirabilis* WT

Representative confocal microscope images of *P. mirabilis* WT, SWN1 (*flgI*-) and URN7 (*ureR*-) biofilm and mineral formation formed in AU.

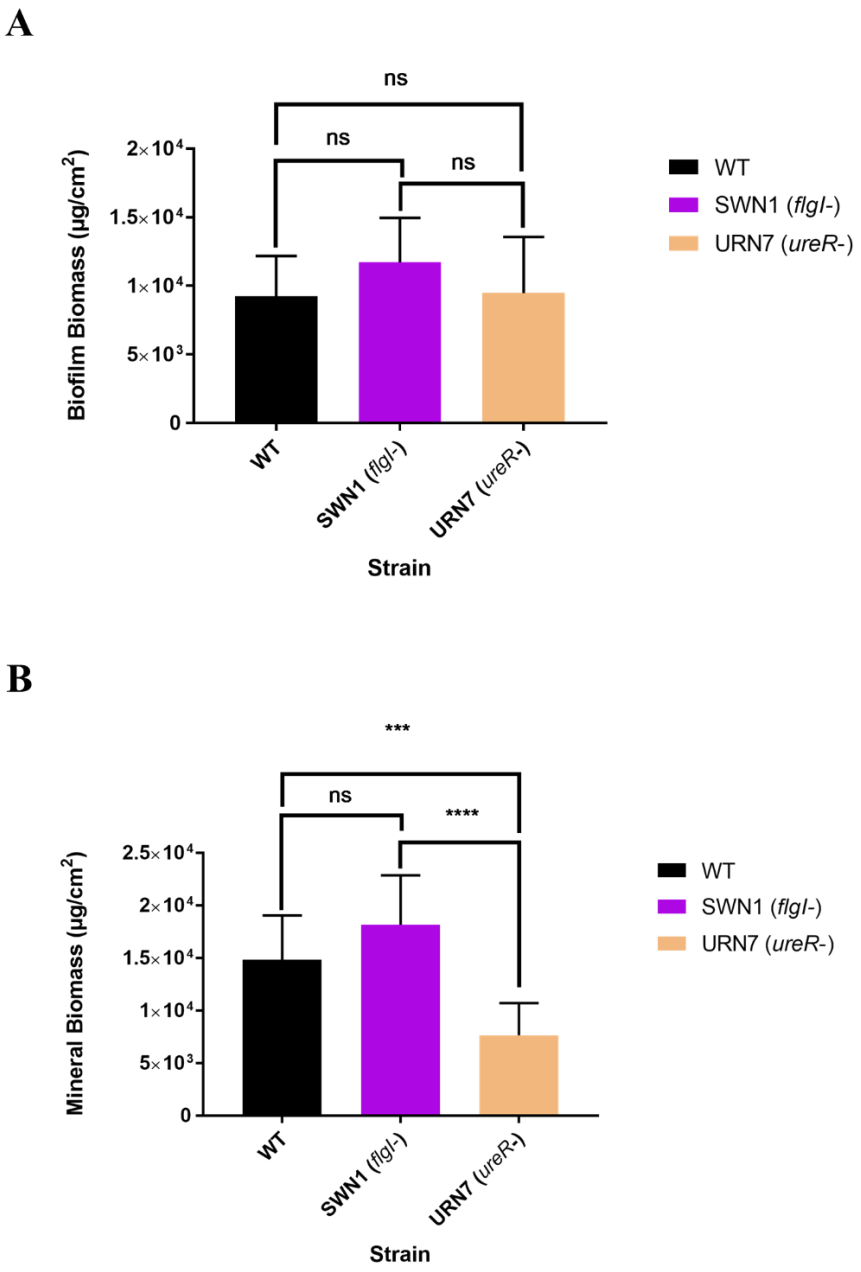

Figure 3.11 Quantification of transposon mutant AU biofilm formation and mineralization

The median biofilm (A) and mineral (B) biomass quantified from confocal microscope images of *P. mirabilis* WT, SWN1 (*flgI*-) and URN7 (*ureR*-), via comstat2/ImageJ. Error bars represent the 95% confidence intervals of the median values. (not significant (ns) ≥ 0.05, *$p \leq 0.05$, **$p \leq 0.01$, ***$p \leq 0.001$, ****$p \leq 0.0001$) A Mann-Whitney-U statistical test was conducted as opposed to a student's t-test due to the lack of normal distribution and unequal variances of the data.

3.3 Discussion

The random nature of the genetic interruptions associated with transposon mutagenesis has made it an invaluable method for the discovery of previously unknown genes crucial to the pathogenicity of *P. mirabilis* as well as other bacterial strains of clinical relevance (Belas, Erskine and Flaherty, 1991; Himpsl *et al.*, 2008; Holling *et al.*, 2014; Armbruster *et al.*, 2017; Rather, 2019). The regulated and efficient manner of stable transposon insertions make this method of mutagenesis highly advantageous when compared to approaches incorporating cloning vectors, which can be associated with stability issues, problems linked to multiple plasmid copies, plasmid supercoiling, and the formation of secondary structures (Cunningham, Montelaro and Rushlow, 1993; Malagón and Aguilera, 1998; Godiska *et al.*, 2009; Ivics and Izsvák, 2010). Selecting the appropriate screening methods for the isolation of the mutants of interest is as important as the generation of the transposon mutant library itself. As the mini-Tn*5* construct can integrate at any location within the target bacterium's chromosome, interrupting any possible gene, researchers must design an effective way to isolate the mutants expressing phenotypic differences of interest when compared to the wild-type strain. One of the most common pathogenicity factors screened for following the generation of transposon mutant libraries is biofilm formation (Rollefson, Levar and Bond, 2009; Puttamreddy, Cornick and Minion, 2010; Hadjifrangiskou *et al.*, 2012; Holling *et al.*, 2014). Due to the complexity of the process of biofilm formation and it being associated with multiple bacterial genes, it is particularly important to develop a comprehensive and often multi-stage screen to fully evaluate the performance of the transposon mutants as well as the morphology and characteristics that the

biofilms exhibit (Holling *et al.*, 2014). Transposon mutagenesis studies using *P. mirabilis* in the past have also commonly looked to investigate genes involved in the mineralization of biofilms, the onset of CAUTIs, and the formation of Dienes lines (demarcation of the interaction between two different swarming strains of *P. mirabilis*) (Gibbs, Urbanowski and Greenberg, 2008; Holling *et al.*, 2014; Armbruster *et al.*, 2017).

3.3.1 *P. mirabilis* transposon mutant library screening for phenotypic alterations

Within this study a comprehensive approach to screening the transposon mutant libraries generated has been undertaken, with the aim of developing a detailed overview of the impact of the mutations identified. While the primary interest of the study was swarming and urease deficiencies in the *P. mirabilis* mutants, potential impact upon secondary factors such as growth patterns were investigated to select the most appropriate strains for further experimentation.

There were a number of phenotypic trends of interest observed throughout the screening experiments conducted, such as the fact that none of the swarming deficient mutants characterised within the study exhibited deficiencies in urease production or growth, and all but one urease mutants exhibited swarming and growth comparable to the wild-type *P. mirabilis* strain. These data trends suggest that the mutations within the transposon mutants screened were specifically impacting either swarming or urease production, with a limited effect upon other bacterial phenotypic traits accounted for within this study. Previous studies incorporating transposon mutagenesis in *P. mirabilis* presented data concurrent with findings within this study, with most isolated and characterised mutants indicating no growth deficiencies within rich LB medium,

additionally urease activity was not found to be affected in any of the non-swarming mutants identified by the authors, and vice versa (Jones *et al.*, 2004, 2005; Armbruster *et al.*, 2017).

The inability to produce the urease enzyme and the deficiency in swarming motility had profoundly different effects upon the ability of the transposon mutants to produce biofilms. The comparable biofilm activity of all but one urease negative mutants to the wild-type *P. mirabilis* strain indicated that the urease enzyme is not required by the bacterium to produce a biofilm under the conditions investigated. LB medium was used for the preliminary biofilm assays within this study, as growing the *P. mirabilis* biofilms within AU would have resulted in mineralization which would have interfered with the spectrophotometric method of analysis incorporated (Holling *et al.*, 2014). Additionally, AU unlike LB notably contains urea, which the urease negative mutants would not be able to hydrolyse, this in turn may result in a difference in growth and biofilm forming capabilities in comparison to wild-type *P. mirabilis* within this medium (Estiu and Merz, 2004; Wasfi *et al.*, 2020). For this reason, any urease negative mutants selected from the preliminary biofilm assays for further characterisation, subsequently underwent confirmatory biofilm assays within AU.

The impact of swarming upon the ability of *P. mirabilis* to form biofilms and cause infection has been largely debated in literature, with hyperflagellated swarmer cells shown to produce more urease in the presence of urine in comparison to small swimming cells, as well as enabling the colonization of catheter surfaces, thus playing an important role in infection onset (Falkinham and Hoffman, 1984; Allison, Lai and Hughes, 1992; Jones *et al.*, 2004). On the

other hand, investigations into the impact of swarming motility upon crystalline biofilm formation have shown no significant differences in bacterial adhesion or biofilm forming capabilities associated with the ability of *P. mirabilis* to swarm (Jones *et al.*, 2005). Within the preliminary biofilm screens conducted as part of this study, we observed swarming negative mutants exhibiting significant variability in biofilm activity, suggesting that different mutations impacting the swarming phenotype of the bacterium affect its biofilm forming capabilities in different ways. As the aim of study is to isolate swarming and urease negative transposon mutants with limited secondary phenotypic aberrations, only mutants with comparable biofilm activity to the wild-type *P. mirabilis* strain were selected for further characterisation. While non-swarming mutants with compromised biofilm activity do not warrant further investigation due to the scope of this study, they may however be useful to characterise within future work due to the potential of the interrupted genes as drug targets.

While mineral assays screening urease negative *P. mirabilis* transposon mutants expectedly revealed a reduced amount of mineralization produced by the mutants in comparison to the wild-type strain, mineral production was still apparent despite the absence of the urease enzyme within the mutant isolates. The secondary virulence factor associated with *P. mirabilis* crystalline biofilm formation, namely CPSs, may offer an explanation for this phenomenon (Jacobsen and Shirtliff, 2011). CPSs comprise the outermost structural components of bacterial surfaces and have commonly been found to be crucial to virulence by enhancing surface adhesion and providing protection for the bacterial cells from environmental cues, such as antibiotics (Hoyle, Alcantara and Costerton, 1992). The structure and chemical composition of CPSs is

bacterial strain-specific, with variability commonly shown at species level (McLean and Brown, 2020). In *P. mirabilis*, the capsule polymer is always present during infection and biomineralization and enables the weak binding and concentration of mineral ions available within the growth medium (Dumanski *et al.*, 1994; Wasfi *et al.*, 2020). This results in the presence of a reduced level of mineralization associated with urease-deficient *P. mirabilis* strain growth and biofilm formation.

Even though all swarming negative mutants were confirmed as positive for urease enzyme production, mineralization screening revealed that the majority of the mutants exhibited a reduced activity in comparison to the wild-type *P. mirabilis* strain. Past studies investigating the phenotypic characteristics of *P. mirabilis* during swarming have revealed an approximately 30-fold increase in urease production in the elongated multi-nucleate swarmer cells, in comparison to the planktonic swimmer cells of the bacterium (Falkinham and Hoffman, 1984; Allison, Lai and Hughes, 1992). In line with these findings, the inability of mutants to swarm may have impacted the ability of some of the isolates to efficiently raise the pH of the artificial urine medium and produce minerals, as a result of their inability to increase urease enzyme expression unlike the *P. mirabilis* wild-type strain. For the purpose of the aims and scope of this study however, only the non-swarming mutants exhibiting no deficiencies in mineralization were selected for further characterization.

3.3.2 Sequencing and genetic characterisation of *P. mirabilis* mini-Tn*5* mutants

Following the phenotypic screening, a total of 19 *P. mirabilis* mini-Tn*5* mutants (5 swarming negative and 14 urease negative) were selected as potential

candidates for further study. The 19 transposon mutants were sequenced via a PCR based approach deriving the sequences flanking the transposon insertions within the bacterial genome via the incorporation of specific and semi-degenerate primers. BLAST searches resulted in the identification of the same gene interruption within all 5 swarming negative mutants, *flgI*, as well as the same gene interruption within all 14 urease negative mutants, *ureR*. These findings point to the presence mini-Tn*5* hot-spots within the parts of the *P. mirabilis* genome which encode the *flgI* and *ureR* genes. While previous studies incorporating the mini-Tn*5* construct for transposon mutagenesis within *P. mirabilis* have reported no significant hot-spots present, within this study we have conducted screening specifically focused on the pathogenicity factors of swarming and urease production, rather than a more general mechanism such as biofilm formation affected by multiple bacterial genes and operons (Belas, Erskine and Flaherty, 1991; Jones *et al.*, 2004, 2005). The more focused approach adopted within this study in turn increases the chances of identifying sites within the bacterial genome where the transposon integrates preferentially. The presence of hot-spots associated with the Tn*5* transposon have been well documented in previous research, with this phenomena commonly associated with a bias towards guanine (G) and cytidine (C) base pair containing sequences (Lodge, Weston-Hafer and Berg, 1988; Green *et al.*, 2012). In line with these findings, the 10 bp sequences of *flgI* and *ureR* immediately following the transposon insertions identified within this study also contain a high G/C base pair content of 70-80 %.

3.3.3 The relevance of *ureR* to *P. mirabilis* pathogenicity

Urease enzyme production is a virulence factor crucial to *P. mirabilis* pathogenicity as it is required for the formation of its characteristic crystalline biofilm, which is part of what makes this bacterium a prominent pathogen. The cluster of genes encoding the urease enzyme in *P. mirabilis* has been identified in previous studies, consisting of a total of eight contiguous genes (Figure 3.12) (Jones and Mobley, 1989; Sriwanthana, Island and Mobley, 1993; Mobley, Island and Hausinger, 1995). The urease gene cluster can be sub-divided in to regulatory, accessory, and structural genes. The structural genes within the cluster are 3: *ureA, ureB,* and *ureC*. These genes are responsible for the structural sub-units of the apoenzyme. This enzyme however is catalytically inactive in the absence of the nickel metallocentre, encoded by the accessory genes of the urease cluster (Mobley, Island and Hausinger, 1995). There are 4 accessory genes within the cluster: *ureD, ureE, ureF,* and *ureG*. The expression of these genes results in the production of an active urease enzyme by *P. mirabilis*. The *ureR* gene on the other hand is the only regulatory gene within the urease cluster. It is transcribed in the opposite direction to the rest of the genes within the cluster and is responsible for the positive activation of expression of the urease operon (Dattelbaum *et al.*, 2003).

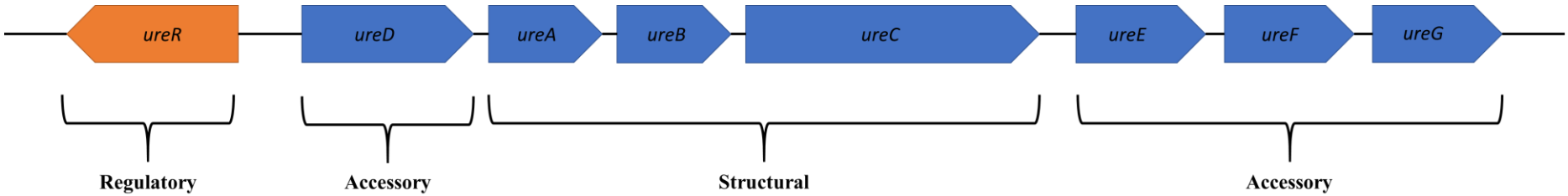

Figure 3.12 *P. mirabilis* urease gene cluster organization

The organization of the gene cluster responsible for urease enzyme production within *P. mirabilis*. The genes within the cluster are sub-divided in three categories based on their function: regulatory, accessory, and structural. Figure adapted from Mobley, Island, and Hausinger, 1995.

The product of the *ureR* regulatory gene is a dimeric transcriptional regulator composed of 293-amino-acid-polypeptides identical in nature, UreR (Poore *et al.,* 2001). The presence of the characteristic AraC signature sequence in addition to a putative helix-turn-helix means that the UreR falls within the AraC/XylS family of transcriptional regulators (D'Orazio and Collins, 1993; Nicholson *et al.,* 1993). Available urea within the surrounding medium of *P. mirabilis* cells acts as an effector molecule and is bound by UreR. The transcriptional regulator subsequently binds within a 491-bp *ureR-ureD* intergenic region, recruiting RNA polymerases and activating the transcription of the urease cluster (Thomas and Collins, 1999; Dattelbaum *et al.*, 2003).

Studies investigating the impact of *ureR* mutations in *P. mirabilis* have found no aberrations in the bacterium's ability to swarm or grow, while urease activity on the other hand was undetectable, confirming the findings from data presented here (Dattelbaum *et al.,* 2003). Additionally, while wild-type *P. mirabilis* exhibits a basal level of urease activity, which increases approximately 5.7 fold in presence of urea, as a result of the *ureR,* transcriptional regulator action, *ureR* mutants haven been found to neither increase their production of the urease enzyme in response to urea nor exhibit the basal urease activity characteristic to the wild-type strain (Jones and Mobley, 1988; Dattelbaum *et al.,* 2003). The impact of the *ureR* mutation upon *P. mirabilis* pathogenicity has also been investigated within mouse models, revealing the inability of the mutant to effectively colonize the bladder or kidneys of mice without being able to produce the urease enzyme (Dattelbaum *et al.,* 2003). Within the current study, the *P. mirabilis ureR* transposon mutant exhibited biofilm formation which was not significantly different to the wild-type

P. mirabilis strain despite producing significantly less mineral within the urea containing artificial urine medium. For a complete evaluation of the impact of the *ureR* mutation upon the ability of the strain to cause catheter infections, the mutant is to be introduced within an *in vitro* bladder model and its performance compared to the wild-type *P. mirabilis* strain.

3.3.4 The relevance of *flgI* to *P. mirabilis* pathogenicity

The structure of the bacterial flagellum is made up of three main components: the filament, the hook, and the basal body (Figure 3.13). The filament is linked to the hook structure outside the cell, the hook structure enters the cell wall which is composed of the outer membrane and peptidoglycan (PG) layer in Gram-negative bacteria. Within the cell wall the hook is attached to the basal body structure of the flagellum. The process of flagellar assembly within Gram-negative bacteria is conducted in a highly ordered manner. Flagellar formation begins with the assembly of the motor components including the MS ring and the C ring (Morimoto and Minamino, 2014; Barker *et al.,* 2017). The transport apparatus and the distal rod structure are subsequently formed upon the base provided by the motor components. The P- and L-ring structures form around the distal rod, enabling the assembly of the flagellar hook and filament (Hizukuri *et al.,* 2008). Disruption of the formation of any of the flagellar components during the process of morphogenesis leads to an inactive flagellar structure and motility deficiency in the associated bacterium (Hizukuri *et al.,* 2006). The P ring of the flagellar structure, which acts to hold the distal rod in place during flagellar rotation, is formed of 26 copies of the FlgI protein, encoded by the *flgI* gene (Hizukuri *et al.,* 2006, 2008). Since this gene is interrupted within all the non-swarming *P. mirabilis* mutants isolated during this

study, the isolates are incapable of constructing the flagellar structure beyond the distal rod.

While the function of the FlgI protein, and the impact of the *flgI* gene mutation have been well established in *E. coli* and other Gram-negative bacteria, information on the importance of this gene within *P. mirabilis* is limited (Jones *et al.*, 1990; Hizukuri *et al.*, 2006, 2008; Apel and Surette, 2008). One study investigating the induction of genes during swarming within wild-type *P. mirabilis* BB2000 and *fliL* mutants of the bacterium, reported that both variants up-regulated the *flgI* gene during the manifestation of swarming motility (Cusick *et al.*, 2012). Mutations in the *fliL* gene within *P. mirabilis* result in inadequate differentiation into swarmer or "pseudoswarmer cells of the bacterium under conditions which would not promote swarming motility, suggesting the importance of the gene to surface sensing. The authors hypothesize that the increase in *flgI* expression may be a way for pseudoswarmer cells to compensate the lack of FliL flagellar structural protein, thus enabling the cells to swarm regardless of the mutation. Other studies investigating the transcriptome of *P. mirabilis* during swarming have also found significant up-regulation of *flgI*, emphasising the importance of FlgI to *P. mirabilis* swarming motility (Pearson *et al.*, 2010). Preliminary screens of the *flgI P. mirabilis* mutant within this study have shown an increase in biofilm formation within AU in comparison to the wild-type strain of the bacterium. While this increase is not significant within the initial screens, it hints at possible differences in infection manifestation of the mutant when compared to the wild-type bacterium, which are to be investigated further within an *in vitro* bladder model.

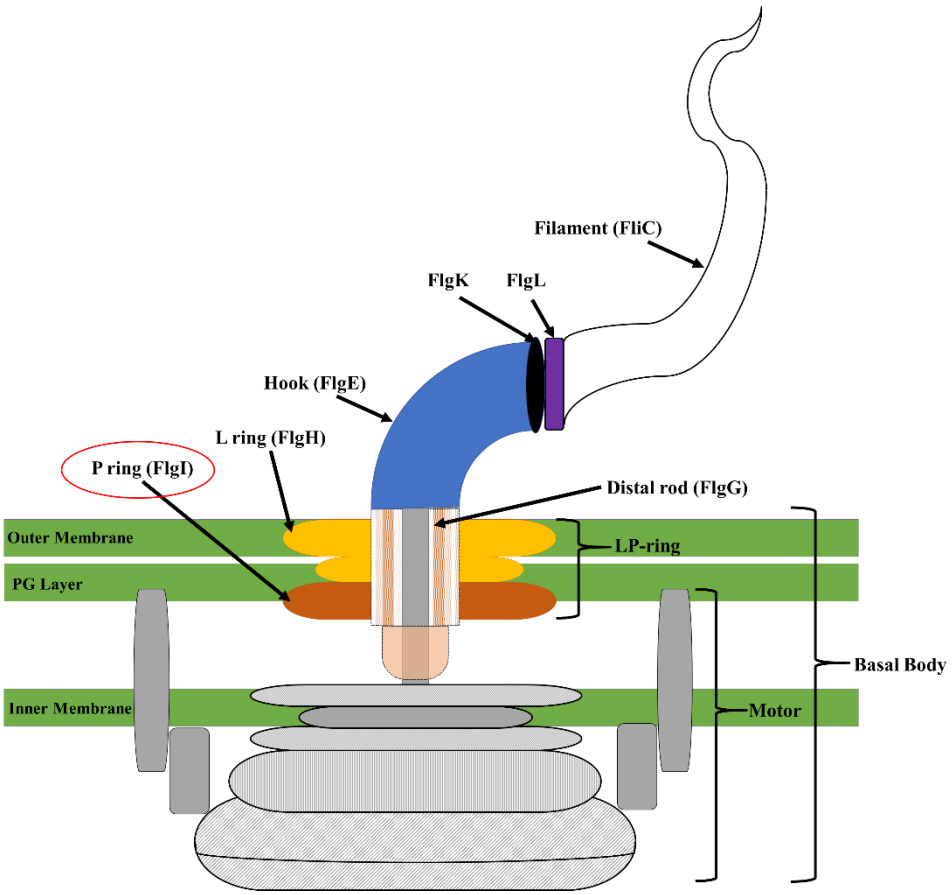

Figure 3.13 Schematic of the *P. mirabilis* flagellar assembly

The figure shows a diagrammatic representation of a characteristic flagellar assembly of Gram-negative bacteria such as *P. mirabilis*. The motor of the assembly produces torque, which is transmitted to the hook by the distal rod, enabling the rotation of the flagellum. The LP-ring holds the rod in place during flagella rotation. Figure adapted from Morimoto and Minamino, 2014 and Barker *et al*., 2017.

3.4 Conclusions

- Following the generation of a random transposon mutant bank, screening focused on swarming motility and urease production of the *P. mirabilis* mutants was conducted, resulting in the successful isolation of swarming and urease deficient mutants for further study.
- The process of comprehensive phenotypic screening resulted in the production of subsets of swarming and urease deficient mutants, which were selected for further investigation and sequencing.
- All non-swarming mutants were found to carry the mini-Tn*5* transposon insertion within the *flgI* gene, while all urease deficient mutants isolated within this study were interrupted in the *ureR* gene, indicating the presence of Tn*5* hot-spots within these regions of the *P. mirabilis* genome.
- The screening conducted within this chapter indicated differences in AU biofilm formation and mineralization brought about by the mutations within the *flgI* and *ureR* genes of *P. mirabilis* in comparison to the wild-type strain, prompting further investigation into the ability of these mutants to form crystalline biofilms on catheters within an *in vitro* bladder model.
- URN2 was the only mutant identified as incapable of swarming and producing the urease enzyme. Additionally, growth curves suggested that the mutation reduced the strains growth rate when compared with the *P. mirabilis* WT strain. It would therefore be of interest to future experiments to implement an alternative sequencing strategy and

determine the interrupted gene, as it may be a possible drug-target candidate.

Chapter 4- Modelling biofilm formation and mineralization on catheter devices using an *in vitro* bladder model

4.1 Introduction

Models for the investigation of biofilm formation relevant to clinical infections span a wide range in the way they can be set up depending on their purpose. *In vitro* and *ex vivo* biofilm development models can be split into 4 categories, including static systems such as microtiter plate models, open systems such as microfermentors, microcosms such as airway epithelial cell models, and *ex vivo* such as cardiac valve models (Genevaux, Muller and Bauda, 1996; Ghigo, 2001; Woodworth *et al.*, 2008; Chuang-Smith *et al.*, 2010; Lebeaux *et al.*, 2013). Each of these models provides distinct advantages, with the strengths of static biofilm models for example including speed, reproducibility, and simplicity, while microcosm models allow for more host-bacterial and bacterial-bacterial interactions to be accounted for. For the purpose of studying CAUTIs, one of the most important features of the biofilm model is the inclusion of intermittent flow to model the dynamics of urine production. Flow cell systems can be categorized as part of an open system biofilm model, allowing the observation of biofilm formation over time, as well as extensive analysis of the biofilm morphology as it develops (Stickler, Morris and Winters, 1999; Sternberg and Tolker-Nielsen, 2006).

Growth models have been developed to represent the urinary tract, the urethral meatus, a CAUTI, and the bladder (Stickler, Morris and Winters, 1999; Gaonkar, Sampath and Modak, 2003; Rosenblatt *et al.*, 2017; Cortese *et al.*,

2018). The *in vitro* urinary tract model was designed to study the migration of microbial pathogens along the surface of urinary catheters from the meatus to the bladder (Gaonkar, Sampath and Modak, 2003). While this model enabled researchers to investigate infection development on catheter devices, it did not allow for the effective monitoring of biofilm development. The meatus model on the other hand offers a way of testing the susceptibility of intermittent catheter devices to bacterial colonisation (Holland and Fish, 2012). The model relies on the protrusion of the catheter tip through an inoculated agar plate, which would represent the meatus surrounding the medical device during catheterization (Cortese *et al.*, 2018). The colonization of the catheter was quantified by cutting off the portion of the catheter which was passed through the agar plate, and enumerating the bacteria recovered from the section following sonication (Holland and Fish, 2012). This model enables researchers to track the impact of the initial process of catheterization, however it does not allow for the monitoring of continuous infection development. The *in vitro* CAUTI model offers another alternative to studying catheter associated bacterial colonization, incorporating an agar urethra to represent the meatus, as well as a bladder representing chamber where catheter devices are introduced (Rosenblatt *et al.*, 2017). The model does not however allow for medium drainage down the catheter device and is therefore inapplicable to the study of biofilm and mineralization development within the lumen over time. The *in vitro* bladder model on the other hand does not offer the advantage of a representative meatus for inoculation in the form of agar surrounding a catheter, however it does enable researchers to track biofilm and mineral development over a number of days, as medium drains intermittently down the medical device incorporated (Stickler,

Morris and Winters, 1999). The model design also provides a water jacket to maintain the bladder chamber at 37^{o}C, as well as enabling the researchers to easily recover colonized catheters following a set period of time, or as a result of device blockage preventing drainage. This in turn allows researchers to monitor susceptibility of catheter devices to an adverse consequence of CAUTIs in the form of blockage, as well as studying the biofilm developed within the device.

Different versions of bladder flow cell models have been adopted over time to accurately represent CAUTI development (Barford *et al.*, 2008; Maierl *et al.*, 2015; Azevedo *et al.*, 2017; Zhang *et al.*, 2020). While the bladder chamber design remains overly consistent across the publications, with small variations surrounding the water jacket, the artificial urine medium used has been variable. The two main types of artificial urine used for the study of biofilm development within bladder flow cell models have been the formulations by Griffith *et al.*, in 1976 and Brooks and Keevil in 1997 (Rogers *et al.*, 1996; Wilks, Fader and Keevil, 2015; Milo *et al.*, 2016, 2017, 2021; Nzakizwanayo *et al.*, 2019). One of the key differences between the two formulations was the content of oxalate within the earlier artificial urine medium composition (Griffith, Musher and Itin, 1976). This difference can be quite important as calcium oxalate has been shown be an important factor to consider when monitoring the mineralization of catheter devices (Grases *et al.*, 2001). The artificial urine described by Brooks and Keevil however offered the advantages of simplicity of preparation and reproducibility between batches, which is imperative during the operation of a user-intensive biofilm formation model such as the *in vitro* bladder model (Brooks and Keevil, 1997).

The catheterized *in vitro* bladder model set up within this study was used to test the performance of the EGDPEA/DEGMA coated Camstent urinary catheter against a standard silicone catheter with respect to biofilm formation caused by two of the most common CAUTI pathogens: *P. mirabilis* and *Ps. aeruginosa* (Jacobsen *et al.*, 2008; Mittal *et al.*, 2009; Schaffer and Pearson, 2015; Ferreiro *et al.*, 2017; Armbruster, Mobley and Pearson, 2018). The two catheter types were assessed for biofilm formation and time taken to block. These infection parameters were selected as they are strongly linked to symptomatic CAUTIs. Environmental scanning electron microscopy (ESEM) coupled with energy dispersive X-ray spectroscopy (EDS) was conducted on samples recovered from the *in vitro* bladder model to determine the biofilm and mineral morphologies associated with the catheters, as well as speculate on the impact these may have had upon blockage time.

Adopting the bladder model set-up also allowed for investigations into the interactions of *P. mirabilis* and *Ps. aeruginosa* during biofilm formation and the effect this has upon any subsequent catheter device blockage. Previous literature has suggested a cooperative interaction between *P. mirabilis* and various bacterial species capable of producing the urease enzyme including *Ps. aeruginosa*, increasing overall urease activity, resulting in a more resilient mineralized biofilm, providing the basis for a more persistent CAUTI (Armbruster *et al.*, 2014; Armbruster *et al.*, 2017). Investigations into the specific interactions of *P. mirabilis* and *Ps. aeruginosa* during biofilm formation in flow cell models revealed the detrimental impact of biomineralization to the survival and distribution of *P. mirabilis* in the multi-species biofilm (Li, Lu, Hannah R Brady, *et al.*, 2016). However, similar bladder model set-ups to that

used within this study have shown that co-inoculation of *P. mirabilis* and *Ps. aeruginosa* may actually result in a delayed catheter blockage when compared with *P. mirabilis* alone (Macleod and Stickler, 2007). Experiments carried out within this study aimed to build on the pre-existing knowledge of *P. mirabilis* and *Ps. aeruginosa* interactions within a catheterized *in vitro* bladder model, and how these interactions impact symptomatic CAUTI manifestations in the form of biofilm formation and catheter device blockage on catheters coated with the Camstent biofilm inhibitory polymer.

Swarming and urease negative *P. mirabilis* mutants were incorporated within the *in vitro* bladder model with the aim of investigating the impact of deficiencies in these pathogenicity factors upon biofilm formation, mineralization, and catheter blockage. Infection development following inoculation of the mutants within the model was monitored and compared to experiments where the bladder was inoculated with the wild-type *P. mirabilis* strain.

4.1.1 Hypothesis and aims

P. mirabilis inoculation of the bladder model was hypothesised to result in silicone catheter blockage. While inoculation with *Ps. aeruginosa* was hypothesised to result in a higher amount of biofilm production when compared to *P. mirabilis*, no blockage was expected due to the reduced potency of the urease enzyme, and thus lower level of biomineralization produced by the bacterium. Co-inoculation of the bladder model with *P. mirabilis* and *Ps. aeruginosa* was hypothesised to reduce the time taken to block a silicone catheter, as a result of an increase in overall urease activity and thus biomineralization, as well as result in a higher amount of biofilm formation

when compared to single-species inoculations. It was hypothesised that through the action of the EGDPEA/DEGMA biofilm preventative coating, Camstent catheters would be able to resist catheter blockage and exhibit a lower amount of biofilm formation following inoculations with *P. mirabilis* and *Ps. aeruginosa* in single- and dual-species experiments. The inoculation of the bladder model with the swarming negative *flgI P. mirabilis* mutant was hypothesised to result in no significant difference in silicone catheter biofilm formation and blockage time when compared to the wild-type strain. The urease negative *ureR P. mirabilis* mutant was hypothesised to be incapable of causing catheter blockage due to its inability to effectively cause biomineralization, while producing a comparable amount of biofilm to the wild-type strain.

The first aim of this chapter was to compare the susceptibility to blockage and biofilm formation of silicone with Camstent coated catheters, following single- and dual-species inoculations within an *in vitro* bladder model with *P. mirabilis* and *Ps. aeruginosa*. The chapter also aimed to determine the impact of swarming motility and urease production upon the ability *P. mirabilis* to cause catheter blockage, biofilm formation, mineralization, within an *in vitro* bladder model.

The objectives to address the aims of this work were to:

1. Determine and compare the blockage time and biofilm formation associated with silicone catheters within the *in vitro* bladder model following single- and dual-species inoculations with *P. mirabilis* and *Ps. aeruginosa*.

2. Determine and compare blockage time and biofilm formation on EGDPEA/DEGMA coated Camstent catheters with uncoated silicone devices, following exposure to single- and dual-species inoculations with *P. mirabilis* and *Ps. aeruginosa*.
3. Determine and compare the blockage time, biofilm formation, and mineralization associated with silicone catheter devices following inoculations of the *in vitro* bladder model with the *P. mirabilis* non-swarming *flgI* mutant, and non-urease producing *ureR* mutant.

4.2 Results

4.2.1 The susceptibility of Camstent compared with uncoated silicone catheters to blockage by *P. mirabilis* and *P. aeruginosa* as single- and dual-species inoculants

Single-species inoculations of silicone catheters within the bladder model with *P. mirabilis* resulted in blockage after an average of 57 h (Figure 4.1). Experiments inoculating the silicone catheters with *Ps. aeruginosa* on the other hand did not result in blockage. While dual-species experiments with *P. mirabilis* and *Ps. aeruginosa* blocked silicone catheter devices after an average of only 38 h. Camstent catheter devices coated with the anti-biofilm formation co-polymer, EGDPEA/DEGMA, on the other hand were resistant to blockage within the *in vitro* bladder model following single- and dual-species inoculations with *P. mirabilis* and *Ps. aeruginosa* (Figure 4.1).

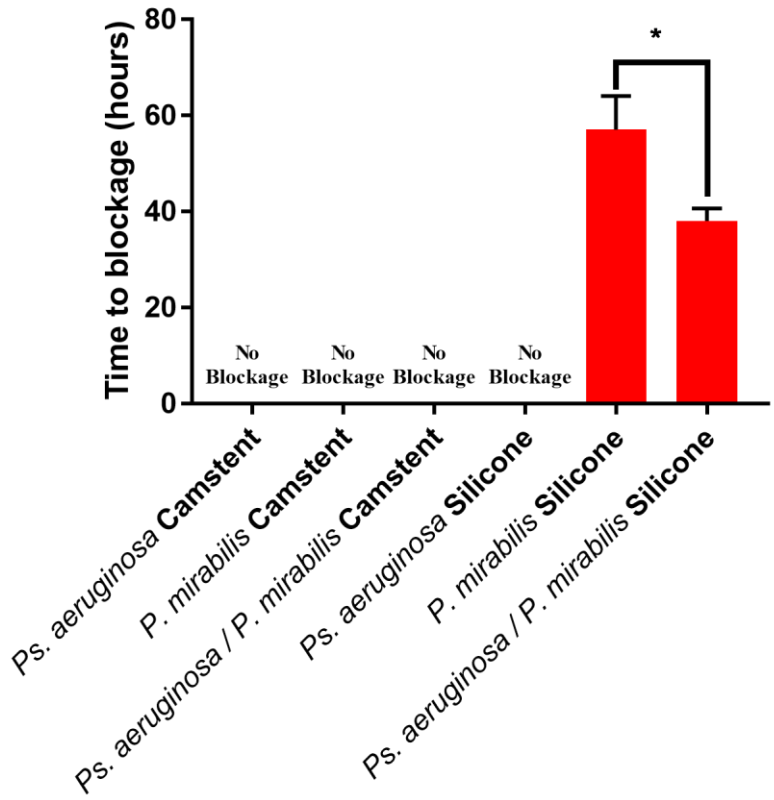

Figure 4.1 Catheter blockage time following single- and dual-species *in vitro* bladder model experiments with *P. mirabilis* and *Ps. aeruginosa* using Camstent and silicone devices

The mean time taken for Camstent and silicone urinary catheter devices to become blocked within the *in vitro* bladder model following single- and dual-species inoculation with *P. mirabilis* WT (*dsRed*) and *Ps. aeruginosa* PAO1-UW (*mTurquoise*). The maximum run time of this experimental set-up allowed for was 89 hours. The data presented within the figure is the result of 3 experimental replicates for each strain/catheter condition. Error bars represent the standard deviation of the mean values. A student's t-test was conducted to determine the significant of the difference in blockage time. (not significant (ns) ≥ 0.05, *$p \leq 0.05$, **$p \leq 0.01$, ***$p \leq 0.001$, ****$p \leq 0.0001$)

4.2.2 Quantification of biofilm formation on silicone and Camstent catheter devices following single- and dual-species experiments within the *in vitro* bladder model

Imaging of biofilm formation accumulated on Camstent and silicone catheters revealed distinct differences (Figures 4.2 and 4.3). *Ps. aeruginosa* formed characteristic biofilms on silicone samples with distinctive mushroom-like microcolonies present, while biofilm formation on Camstent catheters was a markedly reduced differing in morphology and biofilm biomass (Figure 4.2). On silicone catheters, *P. mirabilis* formed a biofilm with morphology different from that of *Ps. aeruginosa*, lacking any obvious mushroom-like microcolonies, and presenting a more uneven surface likely resulting from increased mineralization (Figure 4.2). Camstent catheters colonized by *P. mirabilis* only exhibited a patchy pattern of bacterial growth associated with the luminal surfaces. Co-inoculating *P. mirabilis* and *Ps. aeruginosa* in dual-species experiments using silicone catheters produced mixed biofilms containing both mushroom-like microcolonies, as well as large gaps likely corresponding to the presence of struvite mineralization (Figure 4.2). The mixed biofilms were dominated by *Ps. aeruginosa*, with *P. mirabilis* cells predominantly focused round the gaps in the biofilms formed by minerals. Camstent catheters again exhibited a more patchy variant of the pattern of biofilm growth observed on silicone samples following co-inoculation experiments with *P. mirabilis* and *Ps. aeruginosa*. Quantification of the confocal microscope images revealed a significantly higher amount of biofilm formed on silicone compared with Camstent devices following single- and dual-species inoculations of the *in vitro* bladder model with *P. mirabilis* and *Ps. aeruginosa* (Figure 4.3).

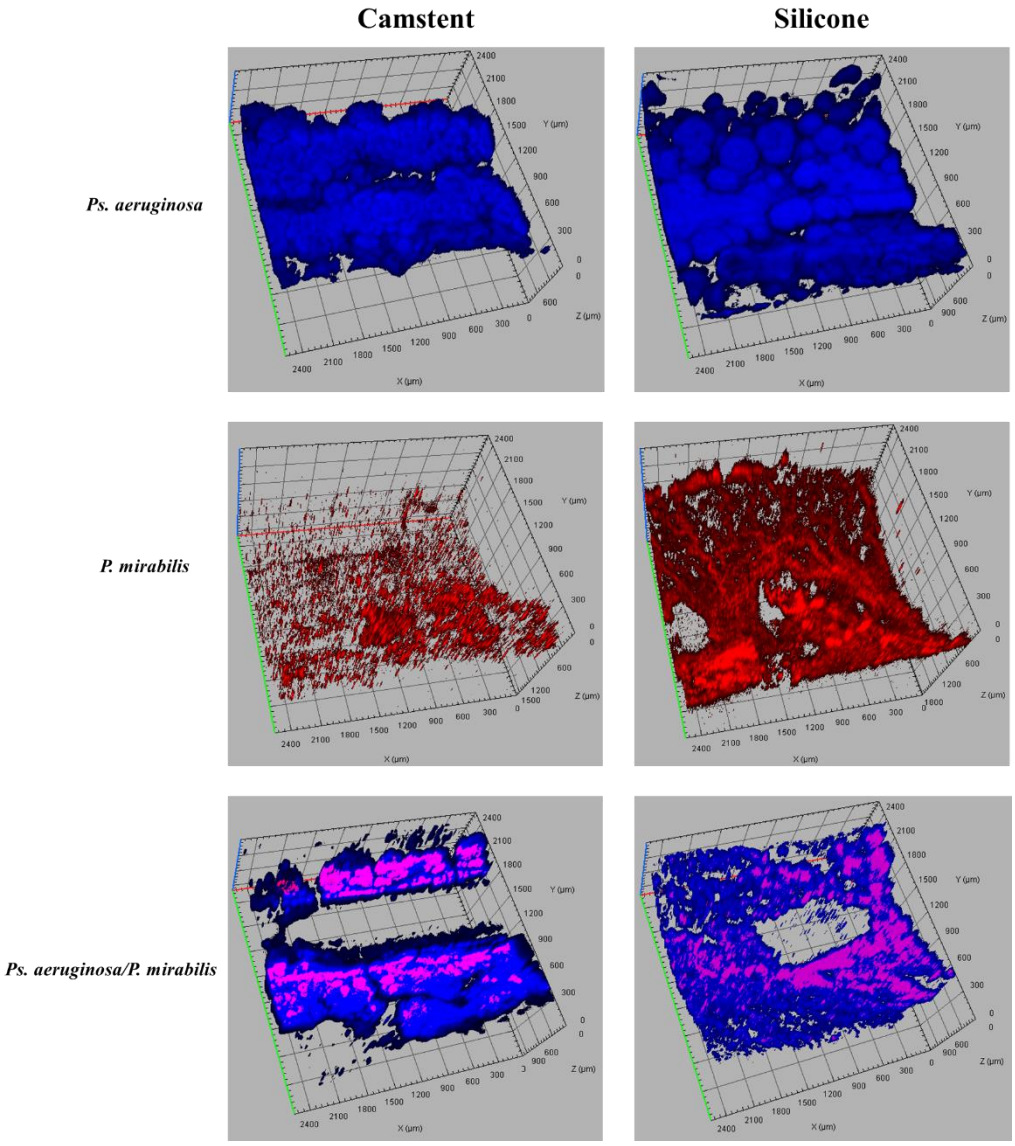

Figure 4.2 Biofilm formation on Camstent and silicone catheters following single- and dual-species *in vitro* bladder model experiments with *P. mirabilis* and *Ps. aeruginosa*

Representative confocal microscope images of biofilm formation on EGDPEA/DEGMA coated Camstent catheters and silicone samples following single- and dual-species experiments with *P. mirabilis* WT (*dsRed*) and *Ps. aeruginosa* PAO1-UW (*mTurquoise*) within the *in vitro* bladder model. Red colour corresponds to *P. mirabilis* WT, blue colour corresponds to *Ps. aeruginosa* PAO1-UW, and pink/purple colour represents a mixture of the two bacterial species. The biofilms were formed within artificial urine over a maximum of 89 hours. The fields of view were selected to represent the median values of quantified biofilm associated with each experiment.

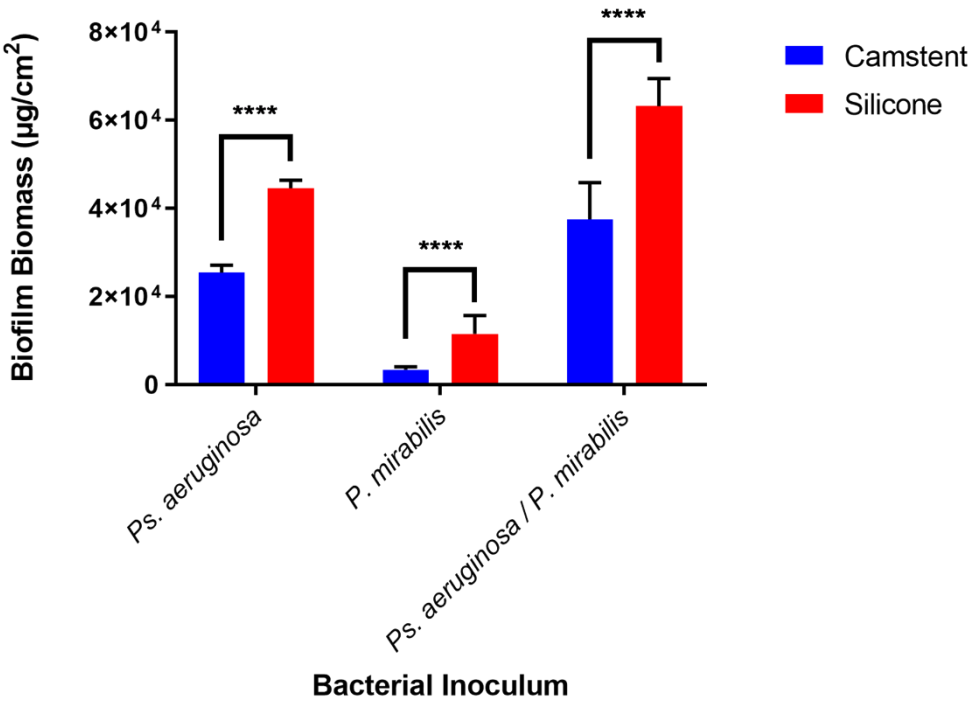

Figure 4.3 Quantification of biofilm formation on Camstent and silicone catheters following single- and dual-species *in vitro* bladder model experiments with *P. mirabilis* and *Ps. aeruginosa*

The median confocal microscopy estimated biofilm biomass accumulated within the lumen of Camstent and silicone catheter devices following single- and dual-species *in vitro* bladder model experiments with *P. mirabilis* WT (*dsRed*) and *Ps. aeruginosa* PAO1-UW (*mTurquoise*). The fluorescence emitted from the biofilms formed by the fluorescently tagged bacterial strains was quantified from confocal microscope images using Comstant2/ImageJ. The results presented within the figure were generate over three experimental replicates for each strain/catheter type. Error bars represent the 95% confidence intervals of the median values. Mann-Whitney-U statistical tests were performed to compare the amount of biofilm accumulated on the two types of catheters. (not significant (ns) ≥ 0.05, *p ≤ 0.05, **p ≤ 0.01, ***p ≤ 0.001, ****p ≤ 0.0001)

4.2.3 ESEM imaging and EDS analysis of biofilm formation on silicone and Camstent catheters following single- and dual-species experiments with *P. mirabilis* and *Ps. aeruginosa* within the *in vitro* bladder model

ESEM imaging of the lumens of silicone and Camstent catheters enabled further characterisation of the biofilms and minerals formed following experiments within the *in vitro* bladder model, providing insights into the mechanism driving the differing device blockage times (Figures 4.4, 4.5, and 4.6). EDS analysis raw data was processed by applying a higher resolution ESEM image, as well as removing trace elements from the data and focusing on the nitrogen, magnesium, phosphorus, and calcium contents within the samples. The quantification of these elements enables the identification of biofilm and different types of mineralization associated with the surfaces of catheters (Figure 4.4). EDS settings such as the power of the electron beam were adjusted based on the presence of a silicone peak within the spectrum, which would be indicative of penetration beyond the biofilm/mineral structure.

On silicone *Ps. aeruginosa* formed a thick biofilm, defined by the high nitrogen content, with a widespread distribution of smaller apatite crystals, defined by an elevated calcium and phosphorus composition (Figure 4.5A). In contrast, on Camstent catheters *Ps. aeruginosa* formed a thinner biofilm layer encompassing apatite minerals (Figure 4.6A).

P. mirabilis produced a thin and patchy layer of biofilm formation on Camstent catheters covered only in small apatite minerals, reflected in the low nitrogen and high calcium and phosphorus contents associated with the device surface, that was revealed by EDS analysis (Figure 4.6B). On silicone catheters on the other hand *P. mirabilis* colonization resulted in the formation of large

struvite crystals (Figure 4.5B). These crystals are defined by an elemental composition comprising high amounts of magnesium and phosphorus as well as their distinct morphology. Mineral formations of this type are also associated with a high nitrogen content indicating the presence of biofilm structure throughout and beneath the porous nature of these minerals.

On silicone catheters, co-inoculation with *P. mirabilis* and *Ps. aeruginosa* produced a mixed biofilm morphology made up of components observed in single-species experiments with each bacterium (Figure 4.5C). The samples were covered in large struvite and smaller apatite minerals, both of which were associated with a high nitrogen content indicative of the biofilm structure surrounding them. In contrast, on Camstent catheters co-inoculation with *P. mirabilis* and *Ps. aeruginosa* resulted in the production of a nitrogenous structure which could be defined as a biofilm monolayer, as well as a prevalence of apatite mineralization, however clearly absent were the large struvite crystals found to be associated with silicone samples (Figure 4.6C). Overview ESEM images of biofilms and mineralization associated with the silicone and Camstent catheters following single- and dual-species inoculations with *P. mirabilis* WT (*dsRed*) and *Ps. aeruginosa* PAO1-UW (*mTurquoise*) within the *in vitro* bladder model were also generated (see Appendices A and B).

Raw Dataset

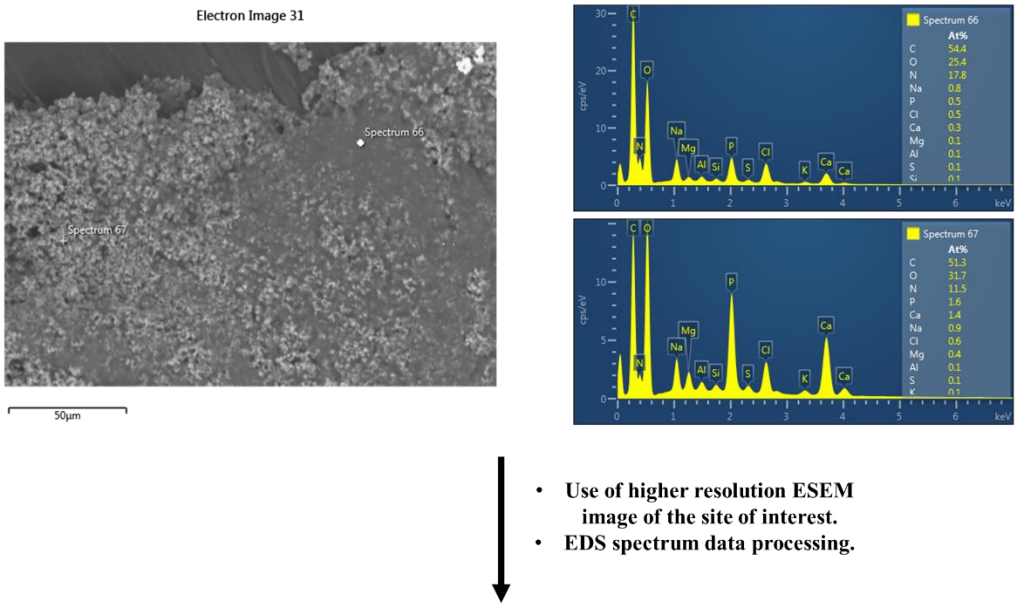

- **Use of higher resolution ESEM image of the site of interest.**
- **EDS spectrum data processing.**

Presented Figure

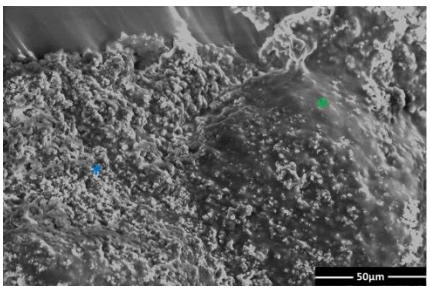

Symbol	Structure	Relative elemental composition (At %)			
		Nitrogen	Magnesium	Calcium	Phosphorus
*	Biofilm	17.8	0.1	0.3	0.5
*	Apatite	11.5	0.4	1.4	1.6

Figure 4.4 Raw ESEM imaging and EDS spectra data processing

Raw data generated via ESEM imaging and EDS analysis of samples was processed and adapted for figure presentation. A higher resolution ESEM image of the site of interest was incorporated and the trace elements of the EDS spectra were not included in the final figures. Nitrogen content was selected as a representative element of biofilm formation as it can be associated with organic proteinaceous structures. Magnesium, calcium, and phosphorus contents were selected for incorporation into figures as they are the main constituents of mineralization associated with catheter devices recovered from the *in vitro* bladder model as well as those of clinical origin. Carbon and oxygen contents were not included within the final figure as they could comprise either biofilm structure or mineralization.

A

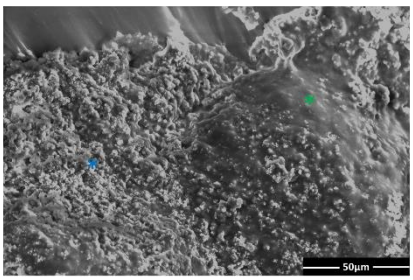

***Ps. aeruginosa* PAO1-UW (*mTurquoise*)**

Symbol	Structure	Relative elemental composition (At %)			
		Nitrogen	Magnesium	Calcium	Phosphorus
*	Biofilm	17.8	0.1	0.3	0.5
*	Apatite	11.5	0.4	1.4	1.6

B

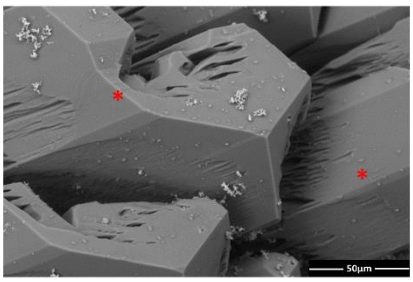

***P. mirabilis* WT (*dsRed*)**

Symbol	Structure	Relative elemental composition (At %)			
		Nitrogen	Magnesium	Calcium	Phosphorus
*	Struvite	8.6	4.3	0.4	5.1
*	Struvite	10.3	3.9	0.4	3.5

C

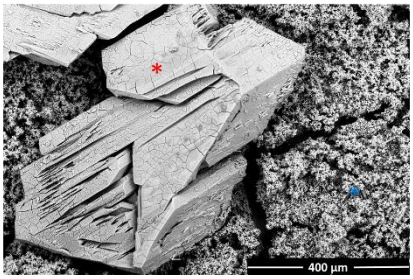

***Ps. aeruginosa* PAO1-UW (*mTurquoise*)/*P. mirabilis* WT (*dsRed*)**

Symbol	Structure	Relative elemental composition (At %)			
		Nitrogen	Magnesium	Calcium	Phosphorus
*	Apatite	3.7	2.2	10.4	8.5
*	Struvite	5.7	6.4	0.7	7.5

Figure 4.5 ESEM imaging and EDS analysis of silicone catheter samples recovered from the *in vitro* bladder model following single- and dual-species experiments with *P. mirabilis* and *Ps. aeruginosa*

ESEM images revealing the differing morphologies of biofilm and mineral formation associated with silicone catheters following inoculations with *Ps. aeruginosa* PAO1-UW (*mTurquoise*) (A) and *P. mirabilis* WT (*dsRed*) (B) and a co-inoculum of the two bacterial species (C). EDS analysis was coupled with ESEM (FEI Quanta 650) imaging enabling the determination of the elemental composition and thus identification of structures within the images. For raw EDS spectra see Appendices C and D.

A

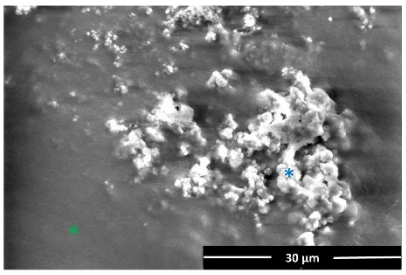

***Ps. aeruginosa* PAO1-UW (*mTurquoise*)-Camstent**

Symbol	Structure	Relative elemental composition (At %)			
		Nitrogen	Magnesium	Calcium	Phosphorus
*	Apatite	8.2	0.6	2.9	3.1
*	Biofilm Monolayer	12.2	0.2	0.3	0.8

B

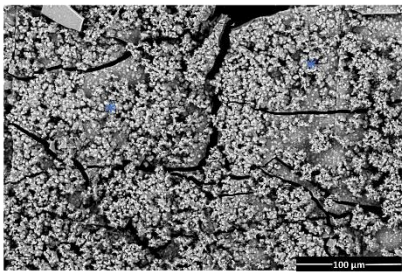

***P. mirabilis* WT (*dsRed*)- Camstent**

Symbol	Structure	Relative elemental composition (At %)			
		Nitrogen	Magnesium	Calcium	Phosphorus
*	Apatite	0.8	2.2	10.3	8.6
*	Apatite	0.4	2.1	10.6	8.3

C

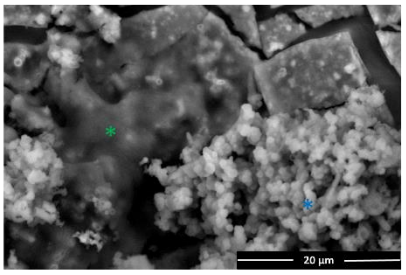

***Ps. aeruginosa* PAO1-UW (*mTurquoise*)/*P. mirabilis* WT (*dsRed*)- Camstent**

Symbol	Structure	Relative elemental composition (At %)			
		Nitrogen	Magnesium	Calcium	Phosphorus
*	Apatite	1.4	1.9	8.3	7.8
*	Biofilm Monolayer	9.9	0.8	2.9	3.2

Figure 4.6 ESEM imaging and EDS analysis of Camstent catheter samples recovered from the *in vitro* bladder model following single- and dual-species experiments with *P. mirabilis* and *Ps. aeruginosa*

ESEM images revealing the differing morphologies of biofilm and mineral formation associated with Camstent catheters inoculated with *Ps. aeruginosa* PAO1-UW (*mTurquoise*) (A) and *P. mirabilis* WT (*dsRed*) (B) and a co-inoculum of the two bacterial species (C). EDS analysis was coupled with ESEM (FEI Quanta 650) imaging enabling the determination of the elemental composition and thus identification of structures within the images. For raw EDS spectra see Appendices E, F, and G.

4.2.4 The impact of *ureR* and *flgI* deficiencies in *P. mirabilis* transposon mutants upon their ability to cause catheter blockage

Two transposon mutants were incorporated within the *in vitro* bladder model, the first carrying a transposon insertion within the *ureR* gene, rendering it incapable of producing the urease enzyme, and the second incapable of swarming as a result of a transposon insertion within the *flgI* gene. The performance of these mutants within the *in vitro* bladder model was initially assessed in terms of the time taken to block a silicone urinary catheter (Figure 4.7). The *P. mirabilis* WT strain required an average of 65 h to completely block artificial urine flow down the medical device. The non-swarming *flgI* mutant exhibited no significant difference in blockage time, taking an average of 63 h to completely stop urine flow down the catheter, while the *ureR* mutant was found to be completely incapable of causing catheter blockage over the 89 h length of the experiment.

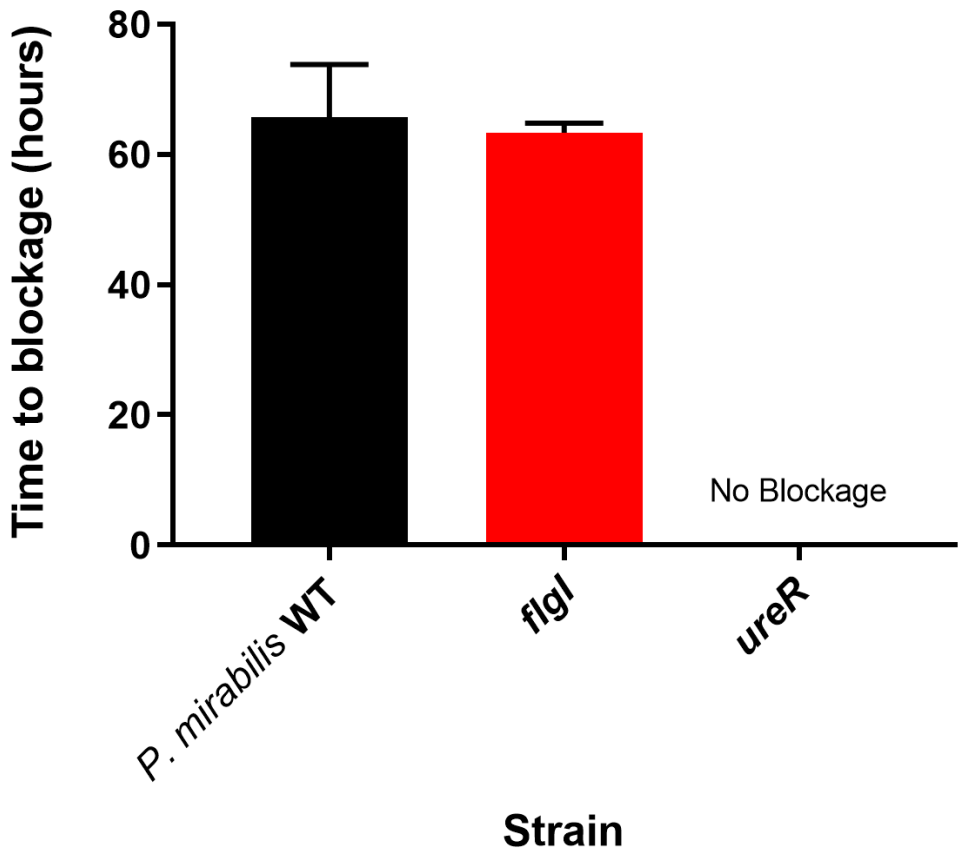

Figure 4.7 Time taken to block silicone catheters within the *in vitro* bladder model following inoculation with *P. mirabilis* WT, and the *flgI* and *ureR* transposon mutants

In vitro bladder model experiments investigating the time taken to block silicone catheters following inoculation with *P. mirabilis* WT, and the *flgI* and *ureR* transposon mutants. The maximum experimental run-time of the bladder model setup was 89 hours, with AU used as the growth medium. Data presented within the figure was the result of 3 experimental replicates. Error bars represent the standard deviation of the mean values.

4.2.5 The impact of *ureR* and *flgI* mutations in *P. mirabilis* transposon mutants upon their ability to form catheter associated biofilms and mineralization

Confocal microscopy performed on silicone catheter devices recovered from the *in vitro* bladder model following colonization by *P. mirabilis* WT, the non-swarming *flgI* mutant, and the urease negative *ureR* mutant revealed distinct differences in the biofilm and minerals formed by the different strains in AU (Figures 4.8 and 4.9). The *flgI* mutant formed significantly more biofilm on the surface of the silicone catheters compared with the *P. mirabilis* WT strain (Figure 4.9A). However, the amount of mineral associated with the *P. mirabilis* WT biofilm was comparable with the level of mineralization presented during inoculation with the *flgI* transposon mutant (Figure 4.9B). The inability of the *ureR* mutant to produce the urease enzyme expectedly resulted in a significantly lower amount of mineralization presented during *in vitro* bladder model experiments when compared with both *P. mirabilis* WT and the *flgI* transposon mutant (Figure 4.9B). While the amount of biofilm produced by the *ureR* mutant was found to be comparable to *P. mirabilis* WT, it was still significantly lower than the biofilm produced by the *flgI* mutant (Figure 4.9A).

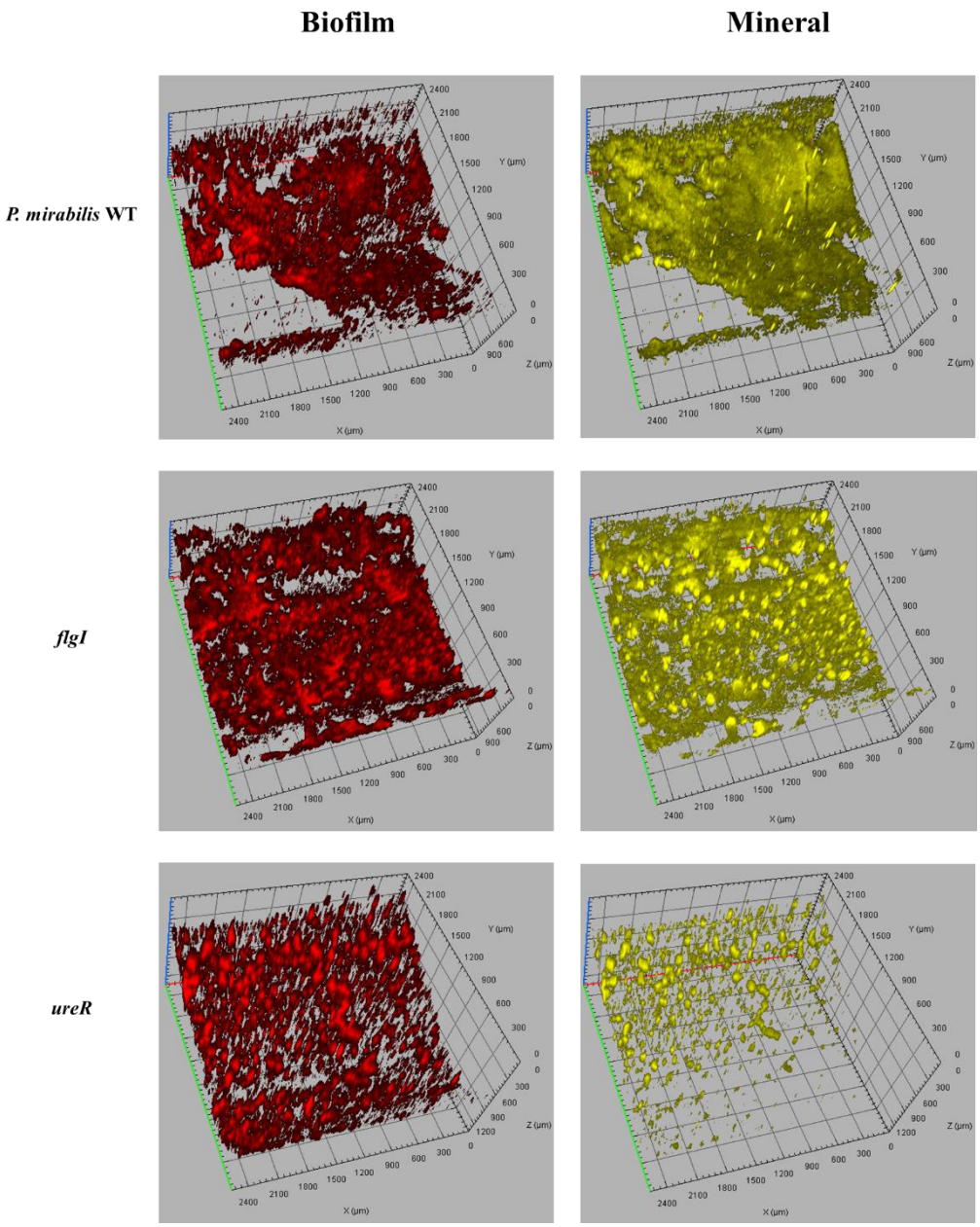

Figure 4.8 Biofilms and mineralization associated with silicone catheters recovered from the *in vitro* bladder model following inoculation with *P. mirabilis* WT, and the *flgI* and *ureR* mutants

Representative confocal microscope images of *P. mirabilis* WT, *flgI*, and *ureR*, biofilm and mineral formation on catheter devices within the *in vitro* bladder model. The biofilms and minerals were formed within artificial urine. Images were generated following staining with Syto64 for biofilm formation and calcein for mineralization.

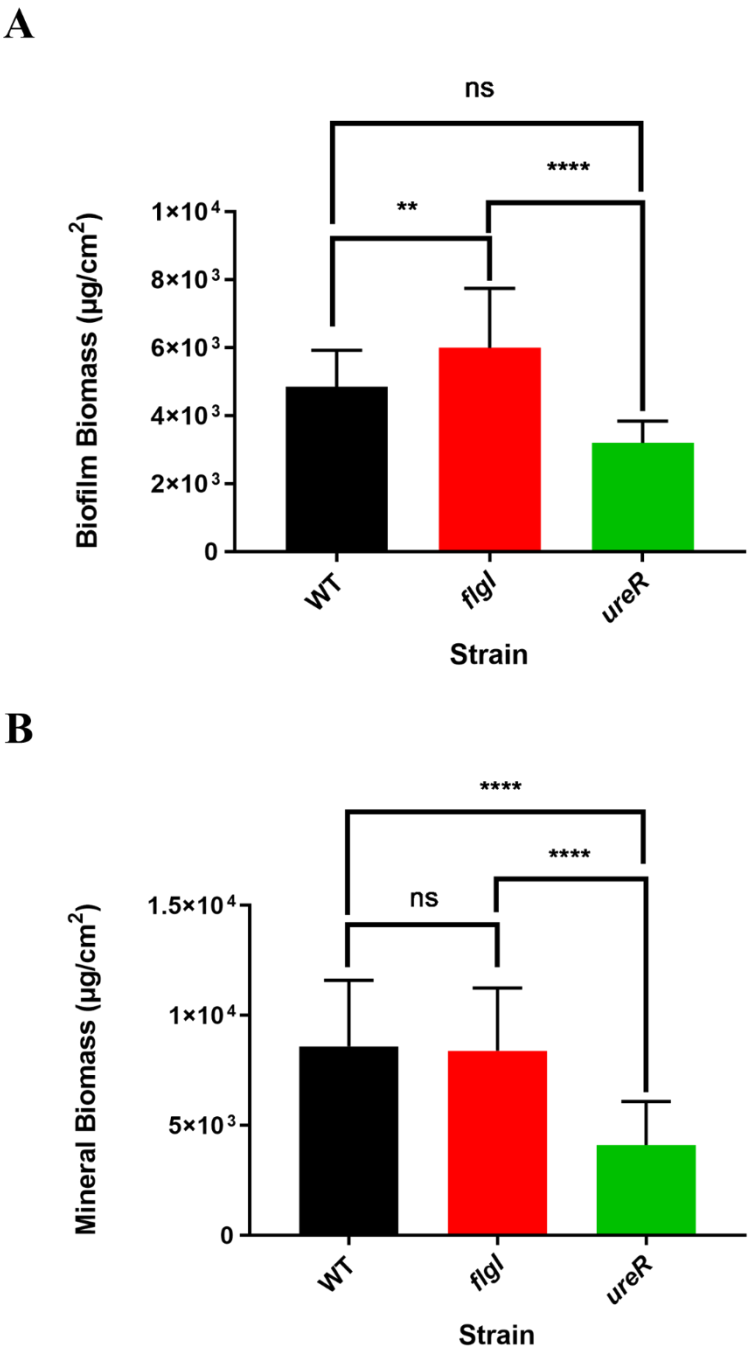

Figure 4.9 Quantification of biofilm and mineralization associated with catheter samples recovered from the *in vitro* bladder model following experiments with *P. mirabilis* WT, and the *flgI and ureR* mutants

The median biofilm (A) and mineral (B) biomass quantified from confocal microscope images of catheters recovered from the *in vitro* bladder model following inoculations with *P. mirabilis* WT, and the *flgI* and *ureR* mutants. Quantification of fluorescence from confocal microscope images corresponding to biofilm and mineralization was done using comstat2/ImageJ. Data presented within the fire was the result of 3 experimental replicates for each strain tested. Error bars represent the 95% confidence intervals of the median values. (not significant (ns) ≥ 0.05, *$p \leq 0.05$, **$p \leq 0.01$, ***$p \leq 0.001$, ****$p \leq 0.0001$)

4.2.6 Environmental scanning electron microscopy (ESEM) imaging and energy dispersive X-ray spectroscopy (EDS) analysis of catheter associated biofilm and mineral formation following *in vitro* bladder model experiments with *flgI* and *ureR* mutants in comparison to the *P. mirabilis* WT strain

ESEM imaging coupled with EDS analysis of the *P. mirabilis* WT biofilm formed on the surface of catheter devices recovered from the *in vitro* bladder model revealed the presence of large struvite minerals characterised by their high magnesium and phosphorus content, and smaller apatite minerals defined by their calcium and phosphorus content (Figure 4.10A). The EDS spectra of the minerals also revealed a high nitrogen content indicating the presence of the *P. mirabilis* biofilm encompassing the apatite crystals and found throughout the porous nature of the struvite structures. The *flgI* mutant revealed a thick pattern of biofilm formation defined by its nitrogenous content, enmeshed together with struvite apatite mineralization as indicated by the elevated magnesium and calcium levels, respectively (Figure 4.10B). The surfaces of catheter devices colonized by the *P. mirabilis ureR* mutant presented a distinct lack of struvite mineralization or a thick mesh of apatite, with the only minerals present likely to be the result of the CPS driven activity of the bacterium, which allows the bacterium to accumulate mineral ions in the absence of the urease enzyme (Figure 4.10C). While these minerals were associated with a similar elemental composition to apatite mineralization, in the form of high calcium and phosphorus content, their morphology was found to be distinctly different. In the absence of the high mineral content characteristically associated with *P. mirabilis* biofilms, the ESEM images were

also able to reveal the single bacterial cells associated with the surface of the urinary catheter colonized by the *ureR* mutant (Figure 4.10C). Overview ESEM images of biofilms and mineralization associated with the silicone catheters following inoculations with *P. mirabilis* WT, and the *flgI* and *ureR* mutants within the *in vitro* bladder model were also generated (see Appendix H).

A

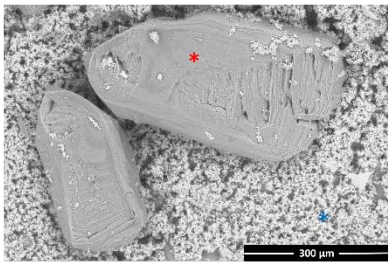

P. mirabilis WT- Silicone

Symbol	Structure	Relative elemental composition (At %)			
		Nitrogen	Magnesium	Calcium	Phosphorus
*	Apatite	5.9	1.6	8.7	7.3
*	Struvite	6.8	6.6	1.2	7.1

B

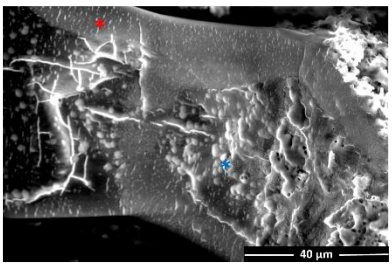

flgI- Silicone

Symbol	Structure	Relative elemental composition (At %)			
		Nitrogen	Magnesium	Calcium	Phosphorus
*	Apatite	3.1	1.3	7.1	5.4
*	Struvite	4.6	6.3	1.4	5.6

C

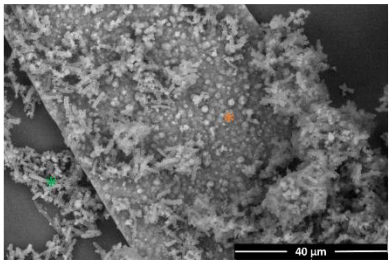

ureR- Silicone

Symbol	Structure	Relative elemental composition (At %)			
		Nitrogen	Magnesium	Calcium	Phosphorus
*	CPS driven mineralization	0.3	1.3	9.9	7.6
*	Bacterial Cells	1.57	0.9	4.8	4.3

Figure 4.10 ESEM imaging and EDS analysis of biofilm and mineralization formed following *in vitro* bladder model experiments with *P. mirabilis* WT, and the *flgI* and *ureR* mutants

ESEM images revealing the differing morphologies of biofilm and mineral formation associated with the *P. mirabilis* WT (A) strain when compared with the *flgI* (B) and *ureR* (C) mutants. The CPS of *P. mirabilis* drives mineralization by accumulating mineral ions from the AU medium in the absence of the urease enzyme. EDS analysis was coupled with ESEM (FEI Quanta, 650) imaging enabling the determination of the elemental composition and thus identification of structures within the images. For raw EDS spectra see Appendices I, J, and K.

4.2.7 The susceptibility of Camstent compared with uncoated silicone catheters to blockage and biofilm formation by the *P. mirabilis flgI* mutant

With the *flgI P. mirabilis* mutant shown to produce a significantly higher amount of biofilm on silicone catheter devices when compared to the wild-type strain, experiments were conducted to determine the ability of the mutant to form biofilms, mineralization, and cause blockage on Camstent catheters as well (Figure 4.11). While the *flgI* mutant caused silicone catheter blockage within the *in vitro* bladder model after an average of 63 hours, the mutant was found to be incapable of causing Camstent catheter blockage over the maximum experimental run-time of 89 hours (Figure 4.11A). Additionally, the *flgI* mutant formed significantly less biofilm ($3.4x10^3$ µg cm^{-2}) and mineral ($4.5x10^3$ µg cm^{-2}) on Camstent catheters on average within the *in vitro* bladder model when compared with the average biofilm ($6.0x10^3$ µg cm^{-2}) and mineral ($8.4x10^3$ µg cm^{-2}) accumulated on silicone devices (Figure 4.11 B and C). Representative confocal microscope images of the biofilm and mineral biomass accumulated on Camstent catheters within the *in vitro* bladder model following *flgI* inoculation revealed a patchy pattern of coverage, which was in sharp contrast with the consistent layer of biofilm and mineral biomass coverage formed on silicone devices (Figure 4.12).

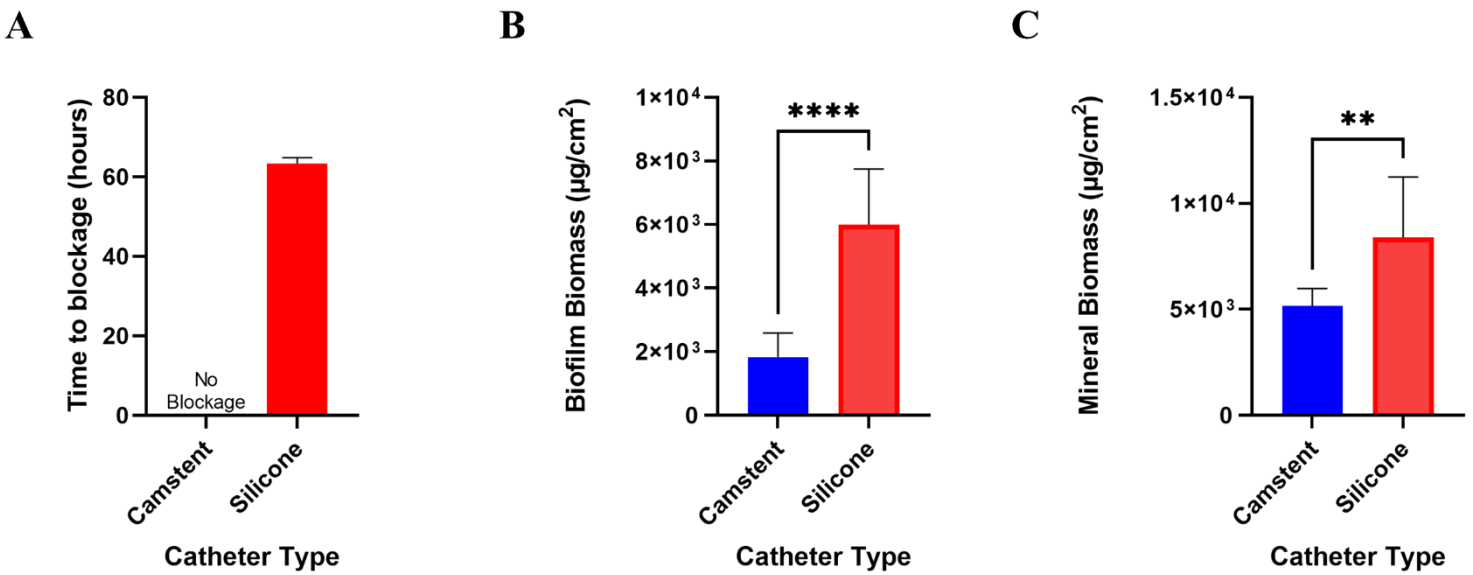

Figure 4.11 Camstent and silicone catheter blockage time, biofilm, and mineral biomass accumulation following *in vitro* bladder model experiments using the *flgI* mutant

The figure shows the mean time taken to block Camstent and silicone catheter devices (A) within the *in vitro* bladder model, recorded following inoculations with the *P. mirabilis flgI* mutant, as well as the median biofilm (B) and mineral (C) biomass associated with the catheter samples. Catheter devices recovered from the *in vitro* bladder model were stained with Syto64 for biofilm, and calcein for mineralization. The biofilm and mineral biomass accumulated on catheter devices recovered from the experiments was quantified based on fluorescence associated with confocal microscopy images, using Comstat2/ImageJ. For the blockage time part of the figure (A) the error bars represent the standard deviation of the mean. For biofilm and mineral biomass the error bars represent the 95% confidence intervals of the median values. (not significant (ns) ≥ 0.05, *$p \leq 0.05$, **$p \leq 0.01$, ***$p \leq 0.001$, ****$p \leq 0.0001$) All data presented within the figure is the result of 3 experimental replicates.

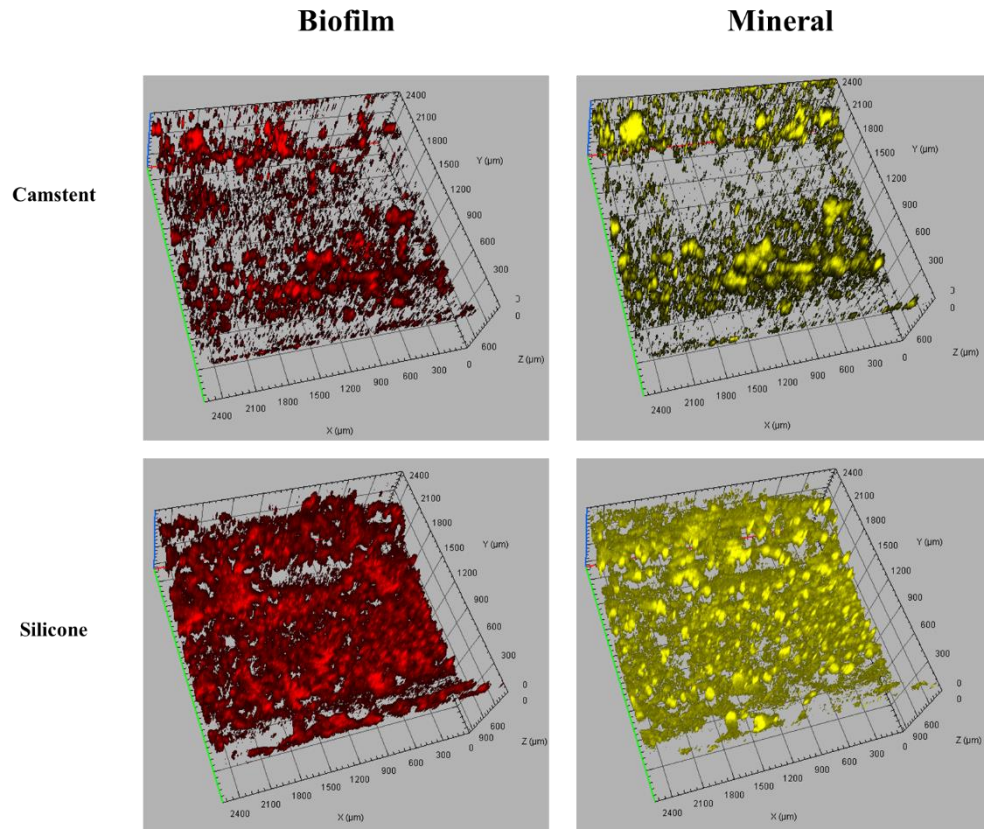

Figure 4.12 Representative confocal microscope images of biofilm and mineral associated with Camstent and silicone catheters recovered from the *in vitro* bladder model following inoculation with the *flgI* mutant

Camstent and silicone catheter associated biofilm and mineralization following *in vitro* bladder model experiments with the *P. mirabilis flgI* mutant. Samples were stained with Syto64 for biofilm, and calcein for mineral, and imaged with the confocal microscope (LSM 700, Zeiss).

4.3 Discussion

Blockage of silicone urinary catheters within *in vitro* bladder model set-ups has been investigated and reported numerous times in literature (Morris and Stickler, 1998; Stickler, Morris and Winters, 1999; Milo *et al.*, 2017; Nzakizwanayo *et al.*, 2019). Investigations into the interactions between common uropathogenic strains have revealed that device blockage time varies depending on the bacterial species (Macleod and Stickler, 2007). Experiments conducted here explored *P. mirabilis* and *Ps. aeruginosa* single- and dual-species catheter associated biofilms. In line with findings previously reported in literature, *P. mirabilis* blocked the silicone catheters, whereas *Ps. aeruginosa* did not, most likely due to the reduced potency of its urease enzyme and therefore insufficient mineral production (Stickler *et al.*, 1998; Milo *et al.*, 2017). Dual-species experiments investigating the interaction between *P. mirabilis* and *Ps. aeruginosa* within the *in vitro* bladder model revealed a decrease in the amount of time taken to block the silicone catheters when compared to single-species inoculations with *P. mirabilis*. While this contradicts some previous observations on the impact of dual-species inoculations, each experimental setup is likely to be impacted by numerous factors such as the formulation of artificial urine medium incorporated, the artificial urine flow rate within the bladder model, and the specific strains of bacterium incorporated for inoculation, which can all lead to differing outcomes in terms of device blockage (Stickler *et al.*, 1998; Macleod and Stickler, 2007). Additionally, urease producing microorganisms such as *Ps. aeruginosa* have been previously found to enhance the urease activity of *P. mirabilis in vitro* as well as effectively form polymicrobial biofilms, which may offer an explanation for the differing

observations from the *in vitro* bladder model dual-species inoculations presented here (Li, Lu, Hannah R Brady, *et al.*, 2016; Armbruster, Smith, *et al.*, 2017).

The first *in vitro* data generated on the complete EGDPEA/DEGMA coated Camstent catheter device revealed a significantly reduced susceptibility to *P. mirabilis* and *Ps. aeruginosa* biofilm formation and device blockage when compared to uncoated silicone devices. The data is indicative of the successful application of the anti-biofilm biomaterial coating to a urinary catheter device, replicating it's efficacy from preliminary studies in reducing the amount of biofilm formation, and thus alleviating the urease producing microbial community associated complications in the form of blockage of urinary drainage (Hook *et al.*, 2012, 2013). The Camstent catheters also showed improved resistance to biofilm formation, mineralization, and blockage when compared with silicone catheters following *in vitro* bladder model experiments with the *flgI* mutant of *P. mirabilis*, which had produced a higher amount of biofilm than the wild-type strain on silicone devices. The significant reduction in the amount of biofilm formed by two of the most prominent CAUTI pathogens on the EGDPEA/DEGMA coated Camstent catheters highlights the potential of these devices in addressing the rising issue of medical device infections and their associated complications. Furthermore, the data highlight the impact which biomaterial coatings can have upon biofilm formation and infection development, and the need for further investigations into the mechanisms through which these surfaces affect bacterial communities.

While *P. mirabilis* and *Ps. aeruginosa* are some of the most prominent CAUTI pathogens in terms of biofilm formation and infection associated complications, it would be important to also assess the efficacy of the

EGDPEA/DEGMA coated Camstent catheters against a wider variety of common urinary tract pathogens such as uropathogenic *E. coli* and Gram-positive staphylococci and enterococci (Johnson, 1991; Kucheria *et al.*, 2005; Raz, Colodner and Kunin, 2005; Jacobsen *et al.*, 2008; Guiton *et al.*, 2013; Walker *et al.*, 2017). Additionally, while the *in vitro* bladder model provides a close replicate of the urinary tract environment enabling the simulation of infection development, the setup presented here does not address the impact of host proteins, such as fibrinogen and THP, to the catheter surfaces which can influence the development of biofilms by certain bacterial pathogens (Raffi et al., 2012; Flores-Mireles et al., 2016). A demonstrated reduction in biofilm formation and colonisation by a wider array of pathogenic bacteria as a result of the EGDPEA/DEGMA coating, within models replicating the human urinary tract environment more accurately, would further highlight the potential impact of Camstent catheters upon the alleviation of CAUTI associated complications.

In vitro bladder model experiments using the non-swarming and non-swimming *P. mirabilis flgI* mutant showed that these genetically inactivated modes of motility are not crucial for crystalline biofilm formation and subsequent blockage of silicone catheters. Previous studies investigating this topic of research have reported similar findings, with *P. mirabilis* B4 transposon mutants incapable of swarming or swimming causing catheter device blockage within a time-frame which did not significantly differ from the wild-type strain (Jones *et al.*, 2005). Additionally, while not significantly different, the study by Jones *et* al., from 2005 reported that experiments with the motility impaired mutants resulted in a faster blockage of the catheter devices by an average of 4 h when compared with *P. mirabilis* B4 (Jones *et al.*, 2005). This was also, to an

extent, reproduced within experiments presented here with the *flgI* mutant blocking the catheter ~2 h faster than the *P. mirabilis* WT strain.

The significantly higher amount of biofilm found to be associated with the *P. mirabilis flgI* mutant when compared with the wild-type strain offers one possible explanation for the increased rate of catheter blockage observed. Motility impaired *flgI* mutants lack flagella in the absence of the P-ring which is composed of the FlgI protein, the flagellar assembly ceases (Hizukuri *et al.*, 2006, 2008). In *Ps. aeruginosa* it has been found that when incapable of instigating flagellar rotation or biosynthesis, exopolysaccharide production is reduced, resulting in an increased amount of biofilm formation (Garrett, Perlegas and Wozniak, 1999; Hickman and Harwood, 2008; Harrison *et al.*, 2020). While link between flagellar rotation/biosynthesis and exopolysaccharide production has not yet been established in *P. mirabilis*, it may offer an explanation for the significantly higher amount of biofilm and thus faster catheter blockage associated with the *flgI* transposon mutant compared with wild-type. Exopolysaccharides within the *P. mirabilis* extracellular matrix have been commonly quantified and have been shown to be of semi-crystalline nature, however the specific exopolysaccharides produced by the bacterium are yet to be fully identified (Stankowska *et al.*, 2012; Czerwonka *et al.*, 2014; Lahaye *et al.*, 2014). One study did however reveal the presence of specific extracellular glycoconjugates within the *P. mirabilis* biofilm matrix, including N-acetylglucosamine, N-acetylgalactosamine, and sialic acids (Moryl *et al.*, 2014). Comparing the production of these sugars and acids within *P. mirabilis* WT biofilms with the *flgI* mutant biofilms may provide evidence for a link between flagellar biosynthesis and exopolysaccharide production .

Urease enzyme driven mineralization is a crucial virulence factor and the mechanism through which *P. mirabilis* is able to cause urinary catheter encrustations and subsequent blockage (Nicola Sian Morris and Stickler, 1998; Stickler, 2008; Schaffer and Pearson, 2015). This has also been demonstrated within experiments conducted here, with *in vitro* bladder model inoculations using the urease-negative *P. mirabilis ureR* mutant shown to result in significantly less mineral formation on the surface of silicone catheters, as well as being unable to cause catheter blockage over the experimental time period. This data provides further evidence that in contrast to flagellar mediated motility, urease production is imperative to the ability of *P. mirabilis* to cause CAUTI complications in the form of mineral encrustation on catheters, associated with patient pain and discomfort, as well as catheter blockage which can lead to distension and reflux of urine to the upper urinary tract.

It is important to note that the *in vitro* bladder model set-up incorporated here only enables the investigation of the impact of *P. mirabilis* flagellar mediated motility and urease production upon descending catheter infections. In order to investigate the impact of these virulence factors upon the more common ascending forms of catheter infections, the bacterial inoculum would have to be introduced on the outer surface of the urethra, or at the connection between the catheter drainage bag and the device's drainage funnel (Wright *et al.*, 2011; Assadi, 2018). It is possible that investigating the impact of *P. mirabilis* flagellar mediated motility upon ascending catheter infections may highlight a role for swarming, as the bacteria would be required to migrate over catheter surfaces and access their lumens to effectively initiate infection. It has been hypothesised that this type of motility may enable the bacterium to overcome some of the

intrinsic urinary tract defence mechanisms such as the viscous layer of mucous known to trap bacterial cells incapable of swarming (Belas, Goldman and Ashliman, 1995; Jones *et al.*, 2005).

4.4 Conclusions

- *P. mirabilis* WT was shown to be capable of blocking silicone catheters throughout *in vitro* bladder model experiments conducted here, whereas *Ps. aeruginosa* was shown to be incapable. Co-inoculating the *in vitro* bladder model with the two bacteria resulted in the quickest blockage time.
- Single- and dual-species *in vitro* bladder model experiments with *P. mirabilis* and *Ps. aeruginosa* with Camstent catheters resulted in no blockage over the maximum experimental run-time of 89 hours, as well as a lower amount of biofilm formation when compared with silicone devices.
- The urease-negative *P. mirabilis ureR* mutant was unable to block silicone catheters within the *in vitro* bladder model, indicating the importance of mineralization to blockage.
- The swarming-negative *P. mirabilis flgI* mutant did not show a significant difference in time taken to block silicone catheters within the *in vitro* bladder model, when compared with *P. mirabilis* WT. The *flgI* mutant did however produce significantly more biofilm on silicone catheters within the *in vitro* bladder model when compared with the wild-type strain.
- The *flgI* mutant was unable to block Camstent catheters within the *in vitro* bladder model, and produced significantly less biofilm and mineralization when compared with silicone devices.

Chapter 5- A novel catheter coating to reduce bacterial biofilm formation and mineralization – A first-in-man pilot study

5.1 Introduction

The EGDPEA/DEGMA coating applied to Camstent catheters has been shown to effectively reduce biofilm formation of common bacterial pathogens including *E. coli*, *Ps. aeruginosa*, and *S. aureus*, within *in vitro* and *in vivo* assays in past studies, as well as *Ps. aeruginosa* and *P. mirabilis* inoculations within *in vitro* bladder model experiments conducted in Chapter 4 (Hook *et al.*, 2012, 2013). Infections within catheterized patients however can be much more complex than the simulated infections carried out within *in vitro* and mouse foreign body implant experiments and are thus likely provide a more stringent test for the biofilm resistant capabilities of the EGDPEA/DEGMA coating.

Many catheter coatings and CAUTI prevention measures have shown potential in resisting bacterial biofilm formation within *in vitro* and *in vivo* studies in the past, however few of them have been able to reproduce these results under clinical conditions (Singha, Locklin and Handa, 2017). Silver alloy coatings of catheter devices are one example of a CAUTI prevention measure which has undergone exhaustive *in vitro* and *in vivo* studies proving its biocidal activity (Stamm, 1991; Saint *et al.*, 1998; Johnson, Kuskowski and Wilt, 2006). However, the effectiveness of silver as a urinary catheter coating within clinical conditions has been shown to be severely limited (Riley *et al.*, 1995; Schierholz *et al.*, 1998; Pickard *et al.*, 2012). Catheter impregnation with antibiotics such as rifampicin and nitrofurantoin is another CAUTI prevention measure which

has been extensively explored *in vitro* (Johnson, Kuskowski and Wilt, 2006; Salvarci, Koroglu and Gurpinar, 2015). While this solution offered a cheaper and more efficient way to manage CAUTIs when compared with silver alloy coatings, the increasing prevalence of multi-antibiotic resistant bacteria diminishes its impact over time (Stewart and Costerton, 2001; Johnson, Kuskowski and Wilt, 2006; Regev-Shoshani *et al.*, 2011; Kilonzo *et al.*, 2014). Additionally, antibiotic impregnated catheters have been associated with numerous side-effect such as tumours in animal subjects and patient discomfort which have cast further doubt over the potency of this type of method CAUTI management (Hiraku *et al.*, 2004; Robert Pickard *et al.*, 2012b). This is indicative of the difficulty in replicating antimicrobial catheter coating efficacy within a clinical environment. One of the main underlying reasons for the reduced effectiveness of CAUTI prevention measures within clinical conditions are the shortcomings of the *in vitro* and *in vivo* studies in terms of replicating the complexity of the urinary tract environment.

The variability of patient urine composition and pH, the attachment of host proteins relevant to biofilm formation such as fibrinogen and THP, as well as the wide bacterial species diversity present within the urinary tract can be particularly challenging to reproduce effectively within laboratory experiments testing CAUTI prevention measures (Mathur *et al.*, 2006a, 2006b; Raffi *et al.*, 2012; Flores-Mireles *et al.*, 2016; Kline and Lewis, 2016). Additionally, other clinically relevant factors such as the length of patient catheterization, antibiotic administration, pre-existing medical conditions such as renal calculi, and the type of surgical procedure which the patient may have undergone, will influence CAUTI development and the efficacy of prevention measures (Grases *et al.*,

2001; Hooton *et al.*, 2010; Djordjevic *et al.*, 2016; Carvalho, 2018; Liu *et al.*, 2018). This emphasises the necessity for detailed clinical studies, that can account for the numerous factors which may affect symptomatic CAUTI development, for assessing the true potential of antimicrobial catheter coatings.

Camstent catheters (*n*=65) coated with the EGDPEA/DEGMA co-polymer were used to catheterize hospitalized patients and their performance compared with uncoated silicone catheters (*n*=60). By determining the amount of biofilm, mineral, and fibrinogen accumulated on these catheters, as well as the change in urinary fibrinogen concentration, following catheterization, preliminary data on the potential clinical impact of the coating could be obtained.

5.1.1 Hypothesis and aims

Camstent coated clinical catheters were hypothesised to exhibit a lower amount of biofilm formation in comparison with uncoated silicone catheters. Camstent catheters were also hypothesised to be associated with a lower amount of mineralization when compared with silicone catheters, due to the inability of urease producing bacteria to form biofilms effectively on the EGDPEA/DEGMA coated devices. Catheterization with Camstent catheters was hypothesised to result in a smaller increase in fibrinogen urinary concentration when compared with silicone devices, following patient reports of smoother insertion of the EGDPEA/DEGMA coated catheter. The aim of this chapter was to demonstrate the efficacy of Camstent catheters in reducing biofilm formation and mineral accumulation within a clinical setting, when compared with silicone devices. A secondary aim of the chapter was to compare any change in the fibrinogen concentration within urine following

catheterization with Camstent and silicone catheters, as well as the fibrinogen attachment to the lumens of the devices.

The objectives to address the aims of this work were to:

1. Quantify and compare biofilm formation on EGDPEA/DEGMA coated Camstent catheters to uncoated silicone devices, recovered from post-surgical catheterized patients
2. Quantify and compare the mineral accumulation on EGDPEA/DEGMA coated Camstent catheters to uncoated control silicone devices, recovered from post-surgical catheterized patients
3. Quantify and compare the urinary fibrinogen concentration pre- and post-catheterization with Camstent and silicone catheters
4. Quantify and compare the fibrinogen attachment to Camstent and silicone catheters, and determine how this correlates with the amount of biofilm formed on the devices

5.2 Results

5.2.1 Clinical catheter cohorts

The Camstent and silicone clinical catheter samples were received from 5 different medical facilities across the UK: University College Hospital at Westmoreland Street, Queen's Medical Centre, Nottingham, University Hospital Southampton, University Hospital of Wales, Cardiff, and the James Cook University Hospital, Middlesbrough. Relevant ethics forms can be found in Appendices L, M, and N. A total of 125 catheters were recovered from 105 male and 20 female patients, with catheter sample sizes ranging from 12 F to 18 F (F- French scale system used to measure catheter size- 1 mm = 3 Fr). 19 different antibiotics administered to patients prior to surgical procedures (pre-op) and catheterization (Table 5.1A). Gentamicin, co-amoxiclav, and metronidazole were among the most commonly used prophylactic antibiotics. Out of the 125 catheterized patients, 21 presented positive pre-op urine cultures, 6 of which exhibited unidentified mixed growth. 10 specific bacterial species were identified within pre-op patient urine cultures, with *E. coli* found to be the most common (Table 5.1B). In patients with positive pre-op urine cultures, antibiotics with a more specific spectrum of activity were administered such as ciprofloxacin in the cases of *E. coli* infection.

Table 5.1: Clinical information on pre-op antibiotics administered to patients and bacterial species identified within pre-op urine cultures

A

Antibiotic	No. of Patients
Gentamicin	50
Co-amoxiclav	45
Metronidazole	35
Augmentin	30
Cefuroxime	24
Nitrofurantoin	14
Ceftriaxone	11
Trimethoprim	7
Ciprofloxacin	6
Amoxicillin	4
Clindamycin	2
Cefuroxime	2
Piperacillin	2
Fosfomycin	1
Co-trimoxazole	1
Clotrimazole	1
Benzylpenicillin	1
Cephalexin	1
Vancomycin	1

B

Bacterial Species	No. of Patients
E. coli	7
Klebsiella pneumoniae	3
Citrobacter freundii	2
Ps. aeruginosa	2
Staphylococcus hominis	2
P. vulgaris	1
Staphylococcus aureus	1
Streptococcus constellatus	1
Enterococcus faecalis	1
Candida parapsilosis	1

(A) Clinical information on the antibiotics administered to catheterized patients before surgical procedures (pre-op). Antibiotics were administered on their own and in combinations in varying dosages. (B) Specific bacterial species identified within pre-op urine cultures of catheterized patients. Single and multiple bacterial species were identified within the patient urine cultures. There were a total of 21 positive pre-op urine cultures, 6 of which presented unidentified mixed growth.

The clinical catheter samples were divided into three separate cohorts primarily defined by their indwelling time, with cohort 1 being composed of samples with the shortest indwelling times, and cohort 3 comprising samples with the longest indwelling times (Table 5.2). The distribution of the indwelling times of all clinical catheter samples analysed in this study is exhibited in Figure 5.1. There was a total number of 3 (1 Camstent and 2 silicone) confirmed urinary tract infections (UTIs) following catheterization (Table 5.2). The total number of blocked catheter devices was also 3 (all silicone samples).

Biofilm and mineral analysis of samples within cohorts 1 and 2 was carried out on three sections of the catheter devices: the proximal section (5 cm), the section in the middle of the catheter shaft (20 cm), and the distal section (35 cm) (Section 2.5.1). Catheter samples from cohort 3 were analysed in more detail, quantifying biofilm and mineral accumulation on all 7 of the 5 cm sections. Samples from this cohort were also selected for further characterisation of biofilm and mineral accumulation using ESEM imaging and EDS analysis, as the longer indwelling time allowed more extensive maturation of any crystalline biofilm forming within the catheter lumens.

Table 5.2: Clinical information on catheter samples forming the 3 cohorts of this study

Cohort Number	Sample Count		Mean Indwelling Time (Days)		Median Indwelling Time (Days)		Nature of Surgical Procedures	Number of Confirmed UTIs (post-catheterization)		Number of Catheter Blockage Events	
	Camstent	Silicone	Camstent	Silicone	Camstent	Silicone		Camstent	Silicone	Camstent	Silicone
1	20	20	6	7	5	4	Gastro-intestinal	0	0	0	1
2	17	17	10	12	11	10	Urinary Tract	0	0	0	0
3	28	23	19	27	18	14	Urinary Tract	1	2	0	3

Clinical information associated with catheter samples from the 3 cohorts, including number of samples analysed, indwelling time, nature of surgical procedure undertaken, and complications (confirmed UTIs and device blockage events) following catheterization. The 3 cohorts were designed based predominantly on the indwelling times of the samples they are composed of, with cohort 1 containing samples with the shortest indwelling times, and cohort 3 containing samples with the longest indwelling times. Additionally, samples within cohorts 1 and 2 were processed by a 3 section protocol, whereas samples part of cohort 3 were processed by a 7 section protocol (Section 2.5.1).

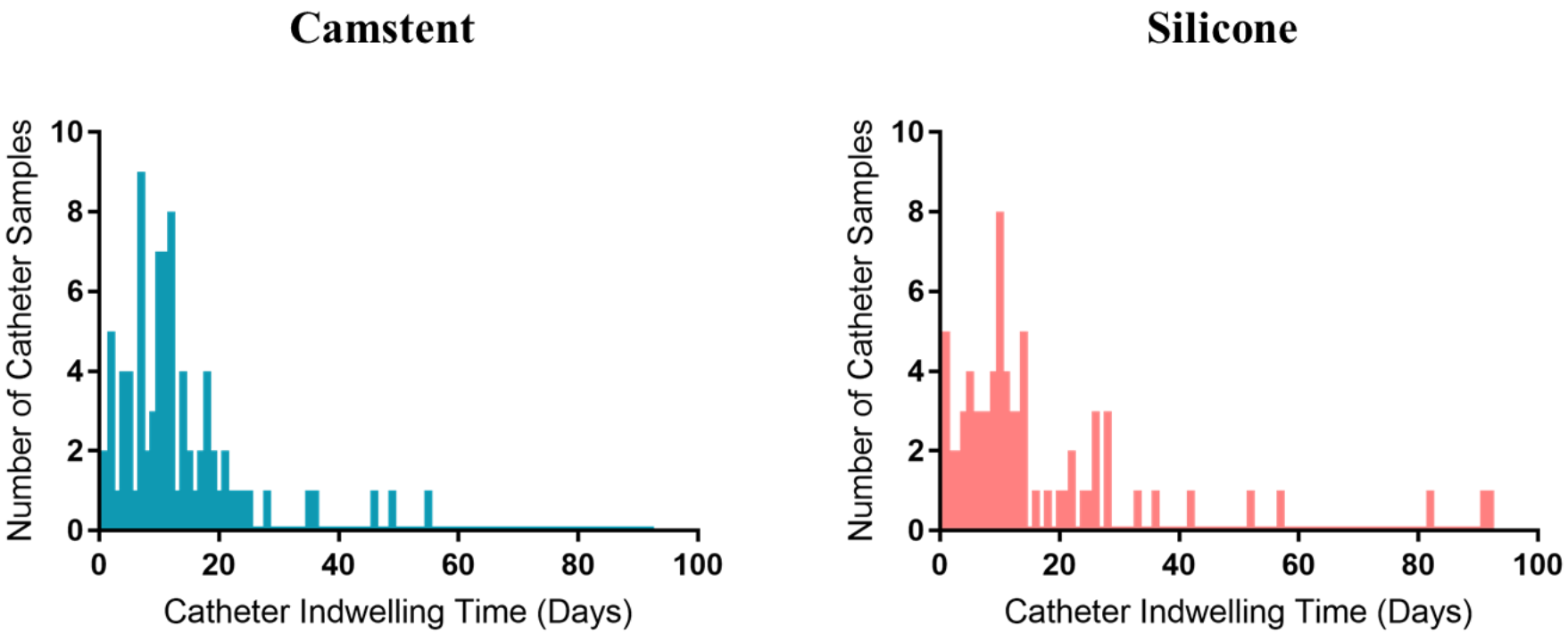

Figure 5.1: Catheter indwelling time histograms

Histograms of the distribution of catheter indwelling times for all Camstent and silicone catheter samples analysed. Total number of catheters analysed- 125.

5.2.2 Biofilm and mineral accumulation on clinical catheter samples

Following confocal microscopy and image analysis, biofilm and mineral deposition on the lumen of each catheter was quantified. Figures 5.2 and 5.3 show examples of the lumens of each catheter section stained with Syto64 for biofilm and calcein from mineral from which the average biofilm and mineral accumulation per clinical catheter sample was calculated. The median biofilm biomass accumulation was shown to be significantly lower on Camstent in comparison with silicone catheters across all three clinical cohorts (Figure 5.4A). Camstent and silicone catheters within cohort 3 were associated with the greatest amount of biofilm, those from cohort 2 exhibited the lowest biofilm values within the 3 cohorts. The accumulation of mineral was also significantly higher on silicone catheters in comparison with Camstent devices (Figure 5.4B). Similar to biofilm formation, Camstent and silicone catheters within cohort 3 exhibited the greatest mineral content, and samples within cohort 2 the lowest within the 3 clinical cohorts.

By considering the confocal microscopy data alongside the clinical data, the blocked silicone catheters accumulated an average biofilm biomass of 353.9 μg cm^{-2} and average mineral biomass of 292.7 μg cm^{-2}. Both the biofilm and mineral values associated with the blocked catheters were significantly higher than the median values for these two variables associated with their respective clinical cohorts (Figure 5.4). The diagnosis of 3 patients with UTIs, 2 of which were catheterized with silicone and one with a Camstent device, allowed for a preliminary comparison of the way the two types of samples responded to infection. The silicone catheter samples recovered from UTI diagnosed patients were associated with an average biofilm biomass of

1608.6 µg cm^{-2} and an average mineral biomass of 869.2 µg cm^{-2}. The Camstent catheter recovered from a UTI diagnosed patient presented with much lower biofilm (9.55 µg cm^{-2}) and mineral (0.03 µg cm^{-2}) biomass values in comparison with the silicone samples recovered from UTI diagnosed patients.

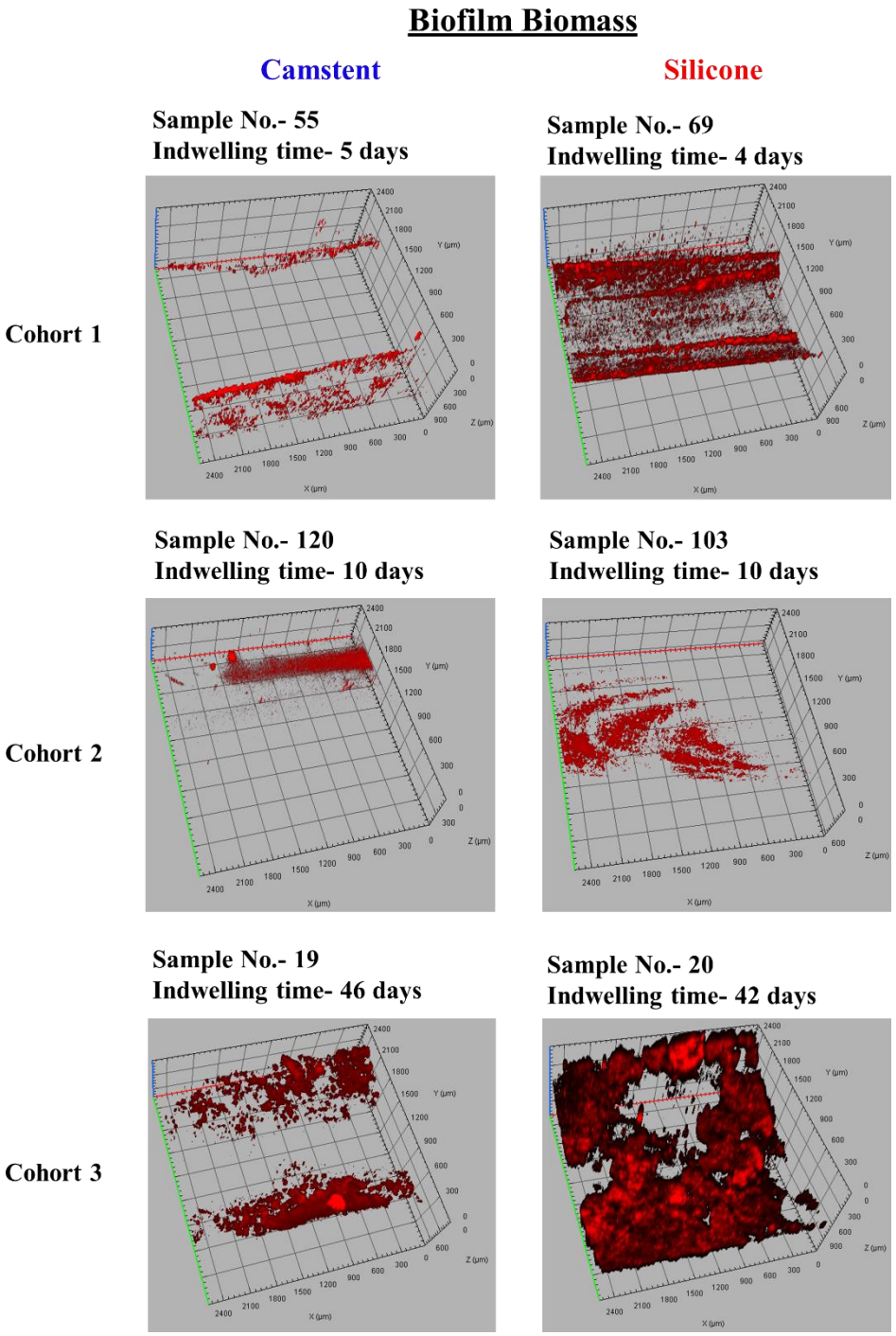

Figure 5.2: Confocal microscope images of the biofilm accumulation on Camstent and silicone clinical catheter samples

Representative confocal microscopy images of biofilm biomass accumulated on Camstent and silicone catheter samples within cohorts 1, 2, and 3. Samples were stained with Syto64 and imaged with a confocal microscope (LSM 700, Zeiss).

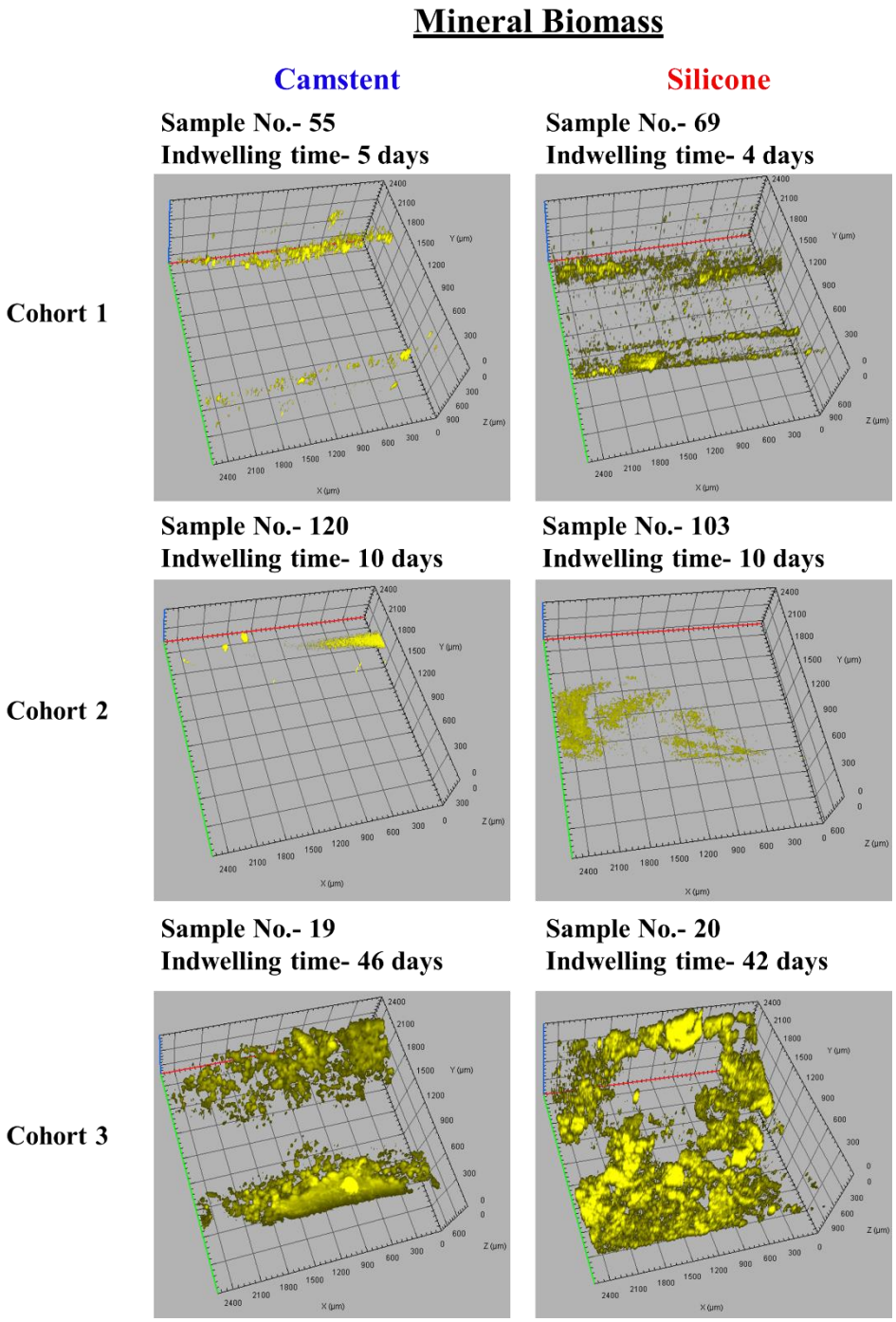

Figure 5.3: Confocal microscope images of the mineral accumulation on Camstent and silicone clinical catheter samples

Representative confocal microscopy images of the mineral biomass accumulated on Camstent and silicone catheter samples within cohorts 1, 2, and 3. Samples were stained with calcein and imaged with a confocal microscope (LSM 700, Zeiss).

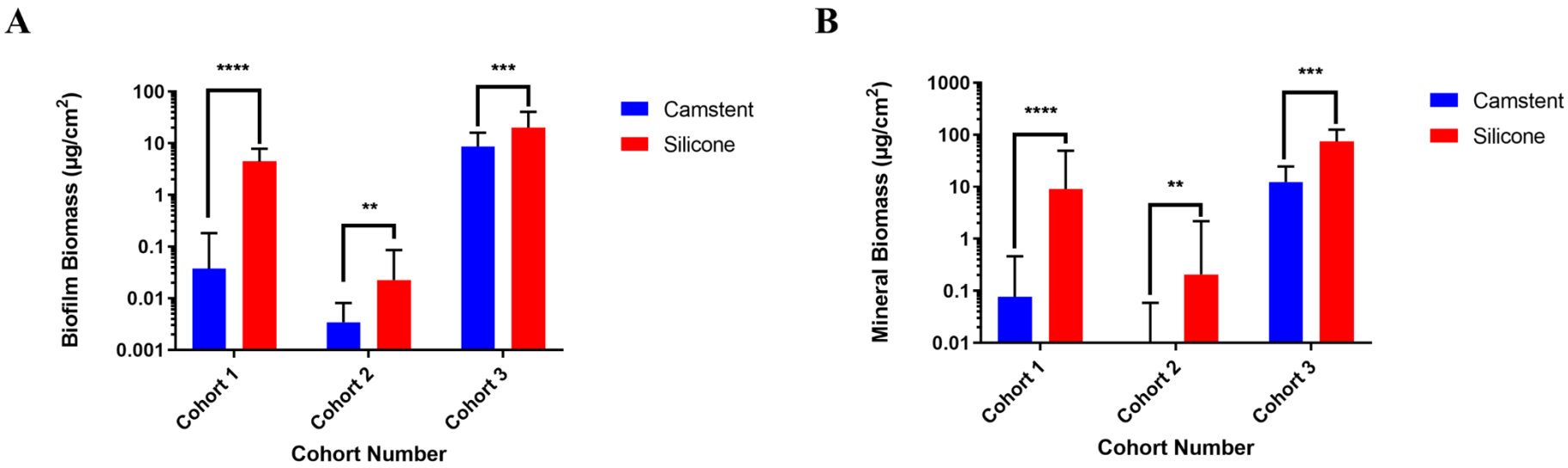

Figure 5.4: Biofilm and mineral accumulation on Camstent and silicone clinical catheters

The median biofilm (A) and mineral (B) biomass accumulated on clinical catheter samples analysed for cohorts 1, 2, and 3. The total number of catheters analysed was 125. Biofilm and mineral accumulation on catheters recovered from hospitalized patients, stained with Syto64 for biofilm and calcein for mineral, was quantified from confocal microscope images using Comstat2/ImageJ. The data have been normalized by dividing biofilm and mineral values for each catheter sample by the square root of their respective indwelling times. Error bars represent the 95% confidence intervals of the median values. (not significant (ns) ≥ 0.05, *$p \leq 0.05$, **$p \leq 0.01$, ***$p \leq 0.001$, ****$p \leq 0.0001$)

The association of both the greatest biofilm and mineral biomass values, with catheter samples within the cohort with the longest average indwelling time (Cohort 3- 23 days), suggested a relationship between the two variables measured within the study and the number of days for which catheter samples were indwelling. A Spearman's rank correlation was generated to explore the relationship between catheter indwelling time and biofilm and mineral biomass accumulation on the samples (Figures 5.5, 5.6, and 5.7). The statistical analysis revealed a significant correlation present between catheter indwelling time and the average biofilm and mineral biomass accumulation on the devices, regardless of whether the catheters were Camstent or silicone (Figure 5.5). The strength and significance of the relationship however is stronger for Camstent catheters, than it is for the silicone samples, in terms of both biofilm (Figure 5.6) and mineral (Figure 5.7) biomass.

The difference in strength of the relationship, between indwelling time and biofilm and mineral biomass, for Camstent and silicone catheters can be explained by the distribution of the data within the scatter plots, indicating a flattening curve as the indwelling time increased beyond 30 days (Figures 5.6 and 5.7). A possible reason behind this is a threshold of biofilm and mineral accumulation being reached on catheter samples indwelling longer than 30 days. The threshold of approximately 10000 $\mu g\ cm^{-2}$ of biofilm/mineral biomass likely signifies the maximum amount of biofilm and mineral biomass capable of occupying the lumen of catheter samples, in the format in which the samples have been analysed within this study. The relationship is therefore stronger and more significant for Camstent catheters, as there were fewer of these samples which were indwelling beyond 30 days, impacting the distribution of the data

and resulting in a more linear correlation (Figures 5.6A and 5.7A). With silicone samples on the other hand the number of catheters which were indwelling for longer than 30 days is higher, however the biofilm and mineral accumulation associated with these samples does not necessarily increase, due to the aforementioned threshold having most likely been reached (Figures 5.6B and 5.7B). This in turn affects the correlation parameters resulting in a lower r-value and significance of the linear correlation explored by the statistical test.

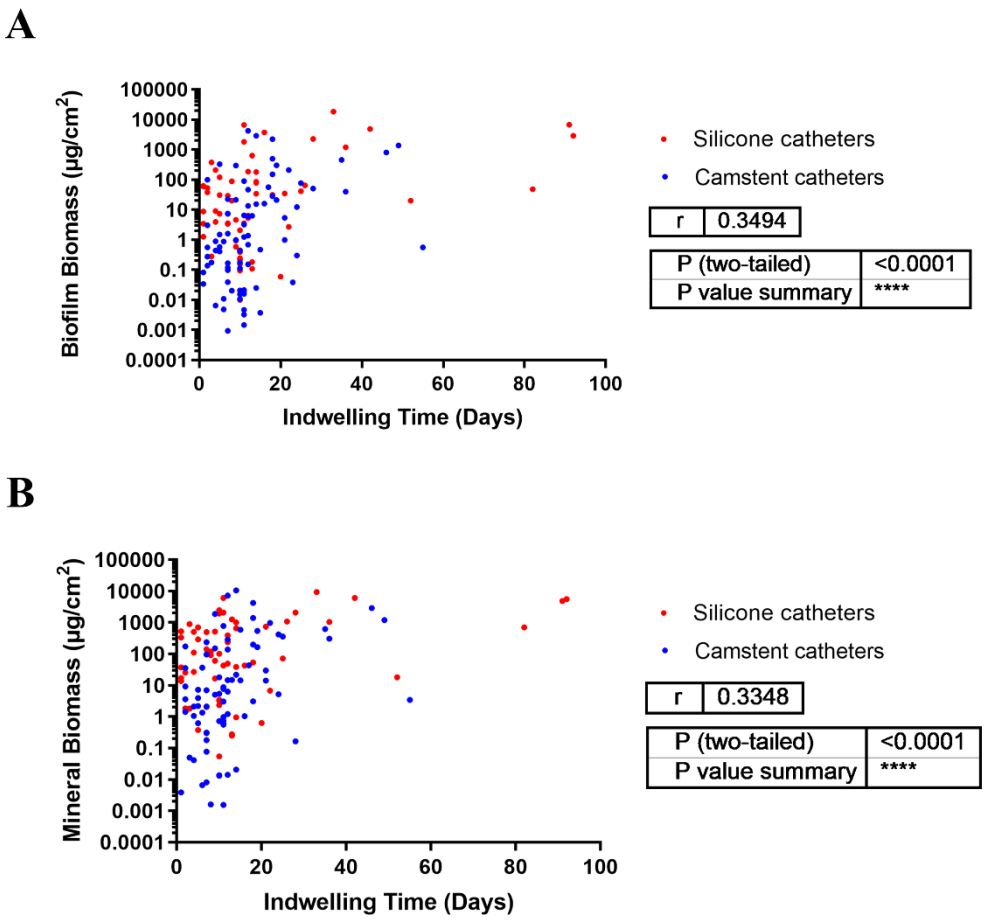

Figure 5.5: Correlation of indwelling time with biofilm and mineral accumulation on Camstent and silicone catheters

Scatter plots of the average biofilm and mineral accumulated on Camstent and silicone clinical catheter samples against the indwelling time associated with the respective samples. Spearman's rank correlation was used to determine the strength of the relationship between catheter indwelling time and the biofilm and mineral biomass accumulated on the samples.

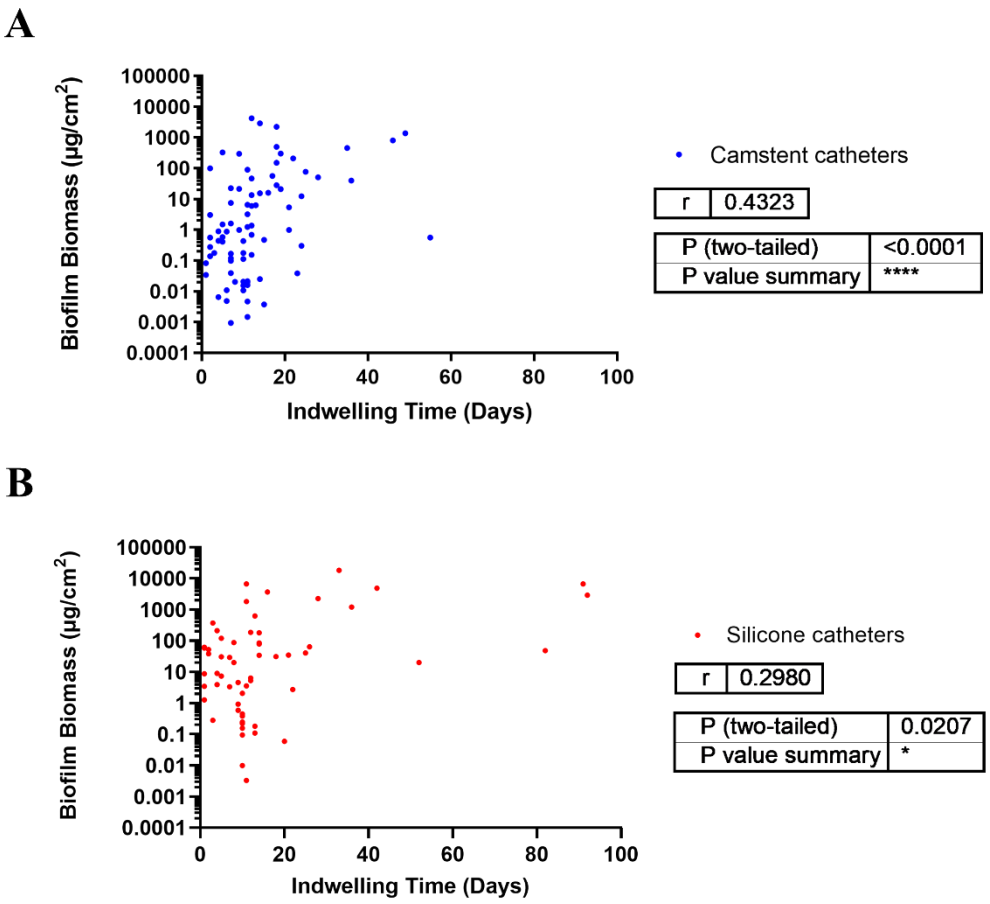

Figure 5.6: Correlation of indwelling time with biofilm accumulation on Camstent and silicone catheters

Scatter plots of the average biofilm accumulated on Camstent (A) and silicone (B) catheter samples against the indwelling time associated with the respective samples. Spearman's rank correlation was used to determine the strength of the relationship between biofilm biomass and catheter indwelling time.

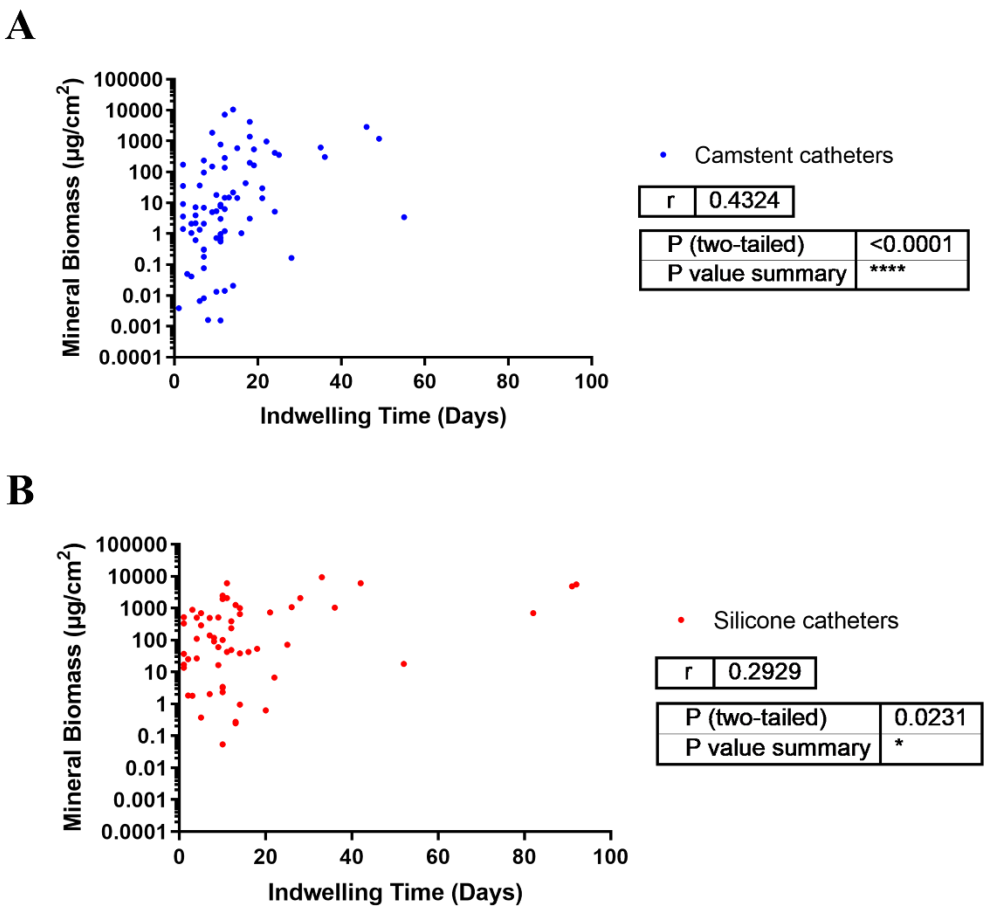

Figure 5.7: Correlation of indwelling time with mineral accumulation on Camstent and silicone catheters

Scatter plots of the average mineral accumulated on Camstent (A) and silicone (B) catheter samples against the indwelling time associated with the respective samples. Spearman's rank correlation was used to determine the strength of the relationship between mineral biomass and catheter indwelling time.

5.2.3 Urinary fibrinogen quantification following catheterization with Camstent and silicone catheters

A total of 11 (3 Camstent and 8 silicone) urine sample sets (pre- and post-catheterization) were sourced from hospitalized patients at Queen's Medical Centre, Nottingham (for ethics forms see Appendices L, M, and N). Catheterization of the patients lasted between 1 and 3 days, with catheter size varying between 10 and 14 Fr. All of the patients catheterized were male. The fibrinogen content within the urine samples pre- and post-catheterization was quantified (Figure 5.8). Across all individual patient urine samples analysed, fibrinogen concentration increased following catheterization, regardless of whether a Camstent or silicone catheter was used (Figure 5.8A). The most apparent increase in fibrinogen concentration was observed within sample K0368614-Silicone, from an average of 34.85 pg mL^{-1} pre-catheterization to an average of 7397.28 pg mL^{-1} post-catheterization. Comparing the mean fibrinogen concentration within patient urine samples prior to catheterization with Camstent and silicone catheters revealed comparable levels of the protein present (Camstent- 1891.09 pg mL^{-1} vs. silicone- 2411.14 pg mL^{-1}) (Figure 5.8B). Post-catheterization urinary fibrinogen content however was much higher in patients catheterized with silicone catheters (5906.78 pg mL^{-1}) when compared with patients catheterized with Camstent catheters (3655.99 pg mL^{-1}). Comparing the urinary fibrinogen concentration change following catheterization revealed further differences between the two types of catheters, with the introduction of Camstent catheters resulting in an increase in fibrinogen by an average of 1764.89 pg mL^{-1}, whereas placement of silicone

catheters increased the fibrinogen concentration by 3495.64 pg mL^{-1} on average (Figure 5.9).

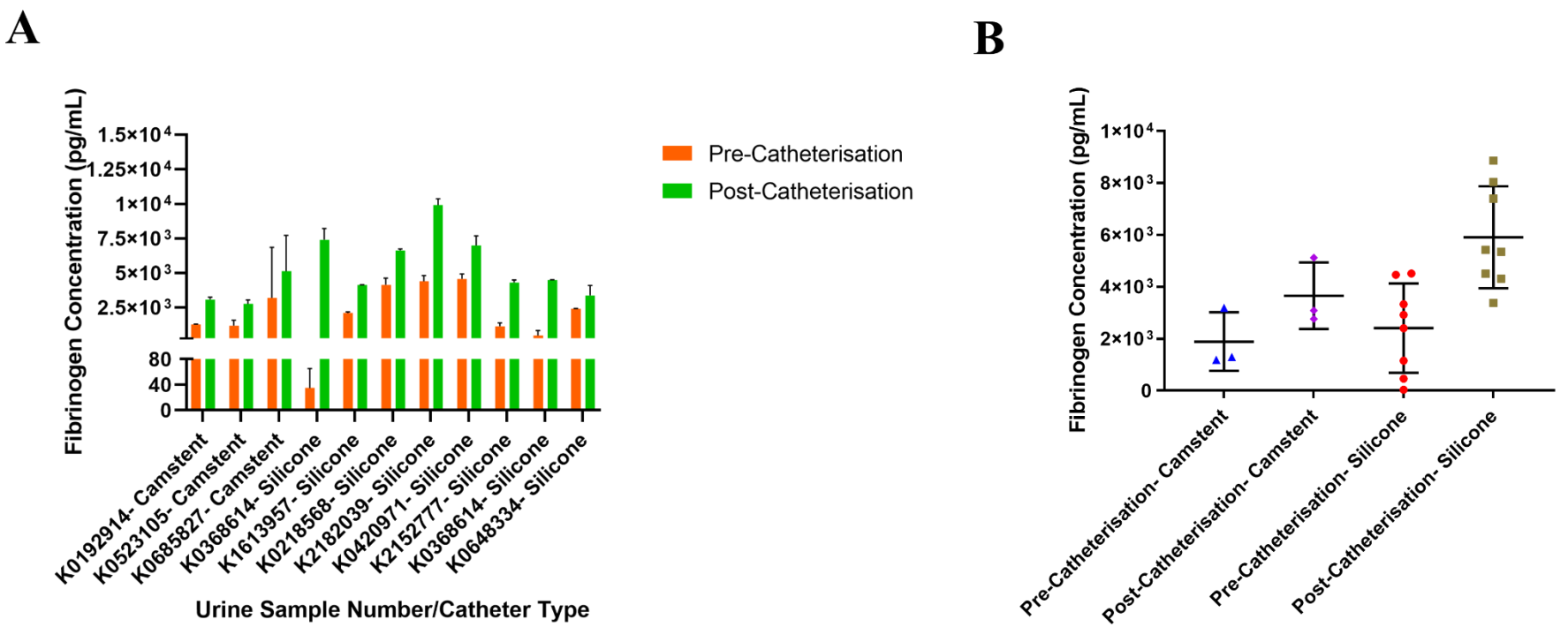

Figure 5.8: Mean urinary fibrinogen concentration pre- and post-catheterization

(A) The fibrinogen concentration within the individual urine samples of hospitalized patients pre- and post-catheterization with silicone and Camstent catheters. (B) The mean fibrinogen concentration within patient urine samples pre- and post-catheterization with Camstent and Silicone catheters. Error bars represent the standard deviation of the mean values. Fibrinogen concentration within urine samples was quantified using a high sensitivity human fibrinogen ELISA kit (Abcam) (Section 2.5.3).

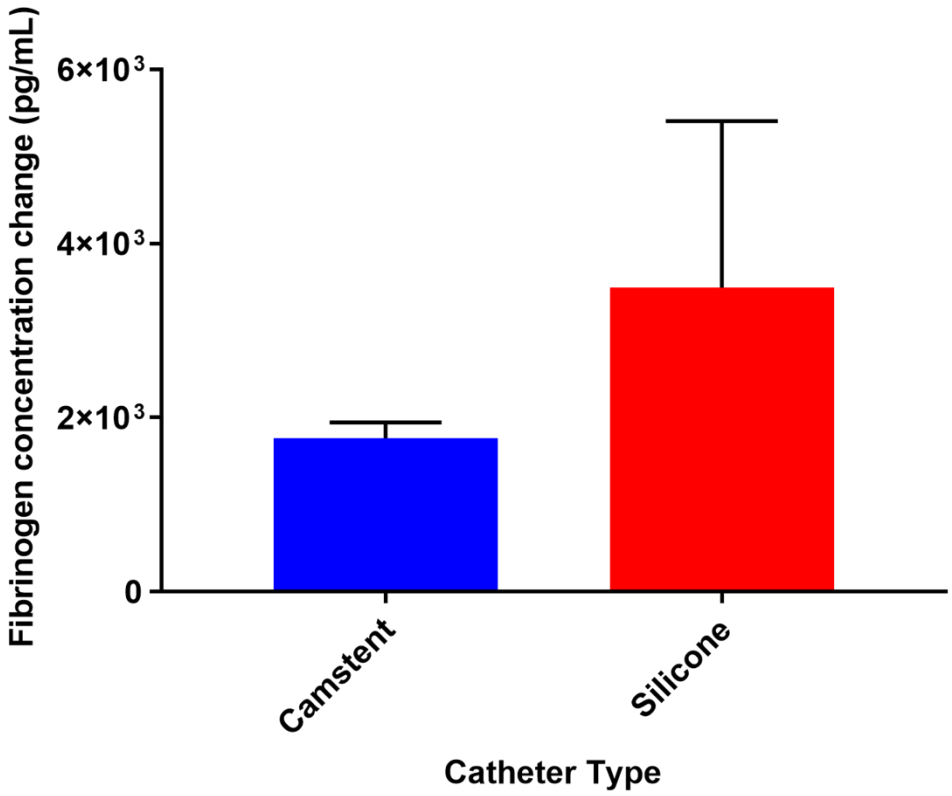

Figure 5.9: Urinary fibrinogen concentration change following catheterization with Camstent and silicone catheters

The mean change in fibrinogen concentration in patient urine following catheterization with Camstent and silicone catheters. The error bars represent the standard deviation of the mean values.

5.2.4 Quantification of fibrinogen and biofilm associated with Camstent and silicone catheters

The catheter samples associated with 7 (3 Camstent and 4 silicone) of the urine sample sets analysed were recovered. The fibrinogen and biofilm associated with the catheter samples was quantified following immunohistochemistry and FM 1-43FX staining, respectively, and imaging with a confocal microscope (LSM 700, Zeiss) (see Section 2.5.4). Representative confocal microscope images showed more fibrinogen and biofilm associated fluorescence on silicone devices when compared with Camstent catheters (Figure 5.10). The images merging the fibrinogen and biofilm associated fluorescence reveal sections on the catheters of overlapping fluorescence suggesting binding of bacterial to fibrinogen deposits, however they also show isolated fibrinogen and biofilm associated fluorescence sections, on both types of catheter. Quantifying the fibrinogen associated fluorescence showed a much higher amount of fibrinogen associated with silicone catheters (155.42 μg cm^{-2}) when compared with Camstent catheters (14.01 μg cm^{-2}) (Figure 5.11A). Biofilm biomass was also revealed to be lower on Camstent catheters (17.39 μg cm^{-2}) in comparison with silicone samples (317.98 μg cm^{-2}) (Figure 5.11B). Co-localization of fibrinogen and biofilm associated fluorescence on the catheter samples, measured in terms of Pearson correlation coefficient, showed considerable variability with Camstent catheters exhibiting a marginally higher average co-localization coefficient when compared with silicone devices (Figure 5.11C).

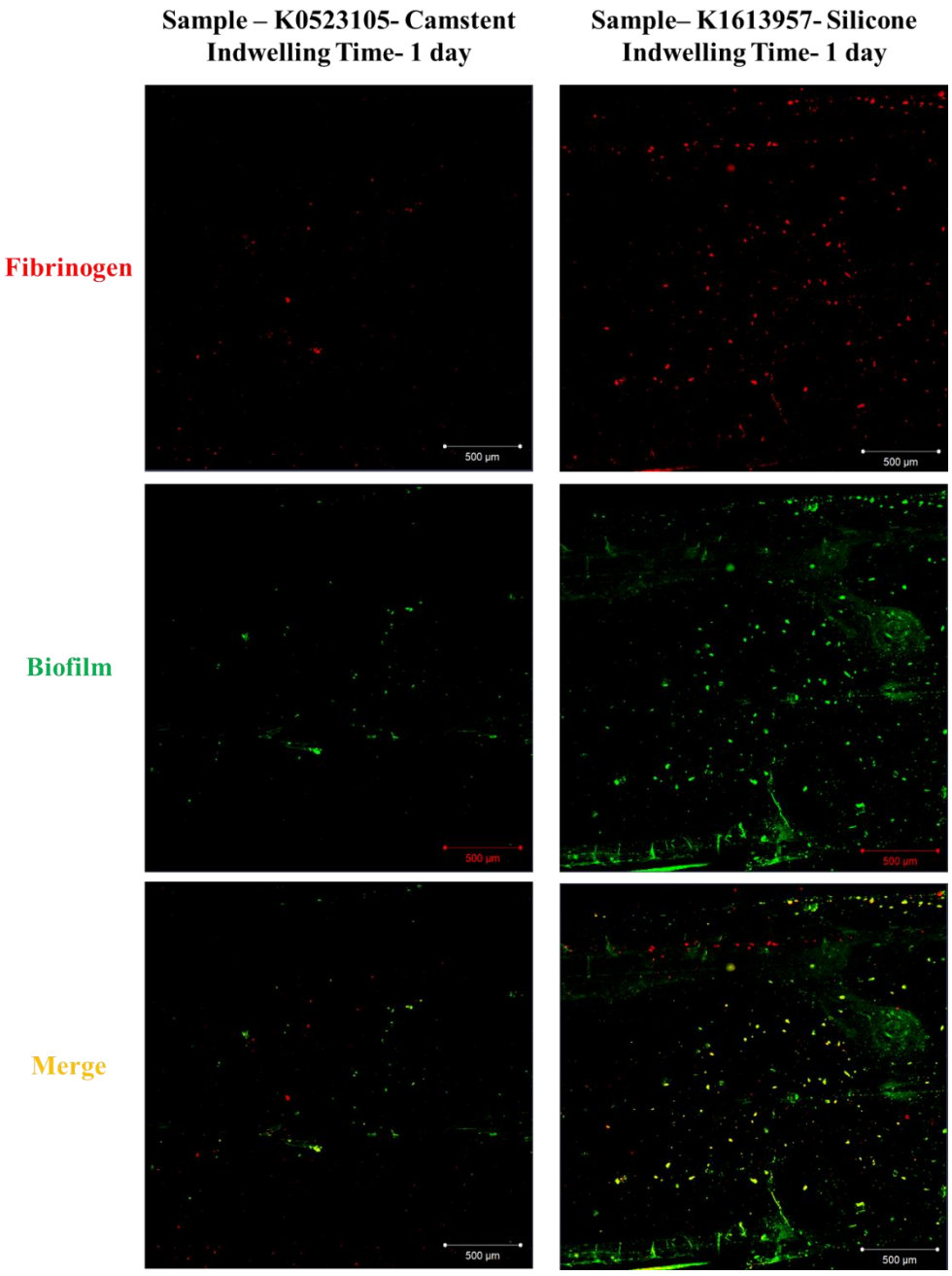

Figure 5.10: Fibrinogen and biofilm associated with Camstent and silicone clinical catheters

Representative confocal microscope images of fibrinogen (red), biofilm (green), and a merge (yellow) between the two channels, associated with Camstent and silicone catheters recovered from hospitalized patients. Fibrinogen was stained using primary (Fibrinogen alpha Polyclonal Antibody) and secondary antibodies (F(ab')2-Goat anti-Rabbit IgG (H+L) Secondary Antibody, Qdot 705) and biofilm was stained using FM 1-43FX dye (see Section 2.5.4). The images were generated using a confocal microscope (LSM 700, Zeiss).

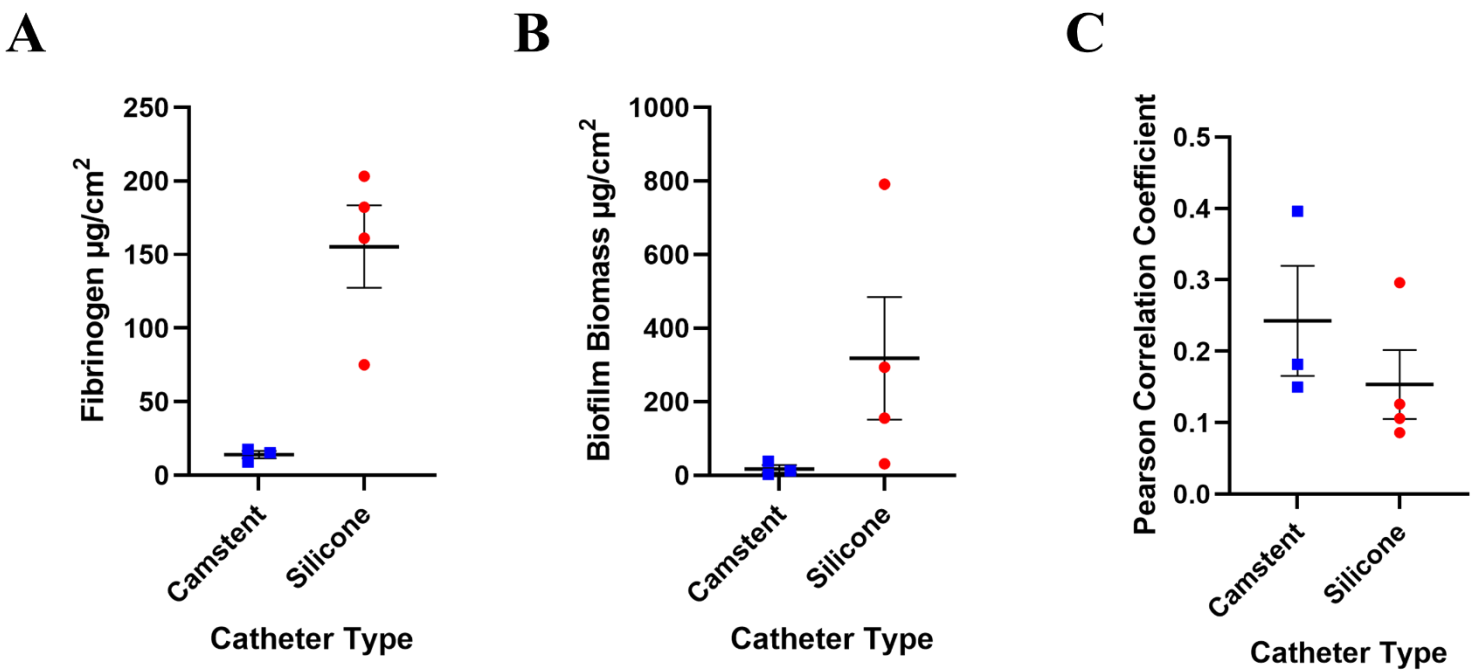

Figure 5.11: Fibrinogen and biofilm biomass associated with Camstent and silicone catheters recovered from hospitalized patients

(A) The fibrinogen associated with Camstent and silicone catheters quantified from confocal microscope images via comstat2/ImageJ following immunohistochemistry. (B) The biofilm biomass associated with Camstent and silicone catheters quantified from confocal microscopy images using comstat2/ImageJ following FM 1-43FX staining. (C) Pearson correlation coefficient measuring the colocalization if biofilm and fibrinogen on Camstent and silicone catheters, calculated from confocal microscope images using coloc2/Fiji. For details on methods of immunohistochemistry, FM 1-43 staining, and Pearson correlation coefficient calculations see section 2.5.4.

The plot exhibited within Figure 5.12 shows the correlation between the catheter associated fibrinogen and fibrinogen concentration within urine samples following catheterization with the respective catheters. Urinary fibrinogen concentration post-catheterization corresponding to both the Camstent (ranging between 2760.27 pg mL^{-1} and 5120.30 pg mL^{-1}) and silicone samples (ranging between 3377.77 and 6982.60 pg mL^{-1}) was comparable. However, the catheter associated fibrinogen corresponding to these urine samples was much higher for silicone devices (between 161.14 and 294.08 µg cm^{-2}), when compared with Camstent catheters (between 9.15 and 17.51 µg cm^{-2}). Camstent catheters therefore retain a lower amount of fibrinogen from urine when compared with silicone catheters.

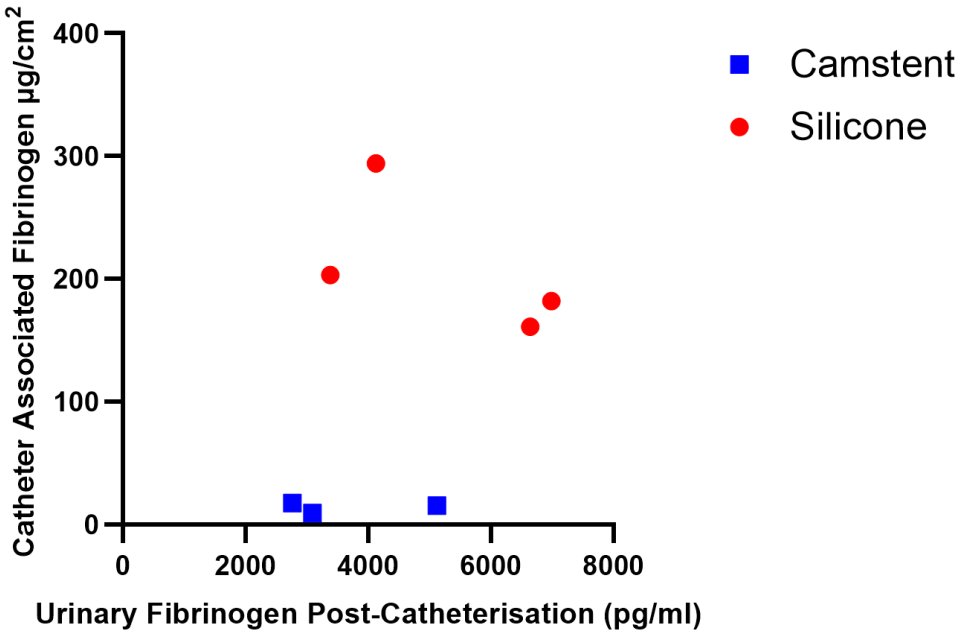

Figure 5.12: Correlating catheter associated fibrinogen with urinary fibrinogen post-catheterization

The figures shows the corelation between the fibrinogen associated with Camstent and silicone catheter samples, determined following immunohistochemistry and confocal microscopy (Section 2.5.4), and the fibrinogen concentration within the post-catheterization urine samples corresponding to the analysed catheters, quantified via a high sensitivity human fibrinogen ELISA kit (Abcam) (Section 2.5.3).

5.3 Discussion

The formation of biofilms and the accumulation of minerals on the surface IUCs is strongly associated with symptomatic CAUTI episodes in a variety of ways (see Chapter 1). The EGDPEA/DEGMA coating of Camstent catheters has been shown to reduce biofilm and mineral deposition on the medical devices in comparison to control silicone catheters not only during simulated *in vitro* infections, but also within a clinical environment, demonstrated by the first-in-man data presented within this chapter. The improved resistance of Camstent catheters to biofilm and mineral formation during catheterization of post-surgical patients indicates the potential of these coated devices to alleviate the impact of CAUTIs. This is also highlighted by the much lower biofilm and mineral accumulation on the sole Camstent catheter recovered from a patient diagnosed with a UTI, when compared to silicone samples sourced from patients also diagnosed with this type of infection. Additionally, the data provide a preliminary indication of the potential of the Camstent catheters to reduce the occurrence of CAUTI associated complications, with no blocked coated samples recovered from post-surgical patients, in comparison to the 3 blockage events documented to occur in patients with silicone catheters.

A smaller subset of clinical catheter samples, as well as pre- and post-catheterization urine samples were used to determine any differences in fibrinogen release within urine upon Camstent and silicone catheter insertion, as well as the accumulation of fibrinogen on the devices. The smaller change in fibrinogen concentration within urine following catheterization with Camstent catheters in comparison with silicone devices suggests less damage to the patient's mucosal lining and therefore a reduced immune response in the form of fibrinogen release (Flores-Mireles, Hreha and Hunstad, 2019). Additionally, a lower amount of fibrinogen was found to be attached to the lumens of Camstent catheters when compared with silicone devices, despite being exposed to urine with comparable fibrinogen concentrations, suggesting that the EGDPEA/DEGMA coating provides a less favourable surface for fibrinogen attachment. By reducing the amount of fibrinogen released following catheterization and fibrinogen binding to the luminal surface, Camstent catheters are less susceptible to the attachment of microorganisms carrying specific receptors for the host protein and capable causing CAUTIs such as *E. faecalis*, *S. aureus*, and *Candida albicans* among others (Sepúlveda *et al.*, 1998; Flores-Mireles *et al.*, 2014, 2016).

The EGDPEA/DEGMA Camstent coating provides an undesirable surface for biofilm formation, therefore any pathogenic bacteria attached to the medical device will likely only subsist as individual cells (Olson *et al.*, 2002). Biofilms would normally protect the bacteria against environmental pressures, however in their absence microorganisms become more susceptible stress factors such as antimicrobial treatments (Gebreyohannes *et al.*, 2019). By preventing biofilm formation on urinary catheters, the EGDPEA/DEGMA

coating would make any bacteria attached to the lumen more vulnerable and thus has the potential to improve the success rate of antibiotic therapies. The lower amount of biofilm formed on Camstent catheter devices also means a reduced potential to spread antibiotic resistance genes within the bacterial community, further improving the chances of success of any antimicrobial treatments administered to patients (Bowler, Murphy and Wolcott, 2020). The Camstent catheter coating also addresses the issues of antibiotic resistance associated with other CAUTI countermeasures, by not actively killing bacteria. The EGDPEA/DEGMA coated catheters therefore have the potential to reduce additional costs and nursing hours brought about by inefficient antimicrobial treatments, as well as prevent the incorporation of "last-resort" medicines such as carbapenems and polymyxins (Huttner *et al.*, 2012; Llor and Bjerrum, 2014; Prestinaci, Pezzotti and Pantosti, 2015; Dadgostar, 2019).

By preventing the formation of a catheter biofilm in the urinary tract, the EGDPEA/DEGMA coated Camstent catheters also reduce mineralization, as while planktonic urease producing microorganisms can still raise urinary pH, the absence of a biofilm community creating gradients in chemical concentrations near surfaces makes it more difficult to reach the supersaturation state (when ion activity product is greater than the ion activity product at equilibrium) necessary for the formation of minerals such as struvite (Schultz *et al.*, 2015). The reduction in mineral accumulation on Camstent catheters compared to silicone devices means that the EGDPEA/DEGMA coating provides improved resilience to encrustations, and thus has the potential to reduce the patient pain and discomfort commonly associated with this complication (Feneley, Hopley and Wells, 2015; Tay *et al.*, 2016).

There were several limitations to the clinical study carried out here including a focus on biofilms and mineralization rather than diagnosed CAUTIs, the lack of blinding of the samples analysed, and the relatively small sample size. It must be taken into consideration however that this was a pilot study attempting to generate preliminary data on the impact of the EGDPEA/DEGMA catheter coating on biofilm and mineralization within a clinical environment. While the lack of sample blinding during analysis was not ideal, all the data presented was the product of objective laboratory experimental procedures, minimizing the impact upon the outcome of the study. However, it would also be important to generate data on catheter devices which have been indwelling for longer periods of time than those examined within this study, as a current limitation of the data is related to the relatively few patients catheterized with an EGDPEA/DEGMA coated Camstent catheter for more than 30 days. This would help prove the long-term efficacy of the biomaterial coating in preventing biofilm formation on IUCs, which is where many of the other CAUTI prevention measures have fallen short due to the general tendency of the perineal flora to find a way to colonize the medical device's surface over time (Trautner and Darouiche, 2004). A large scale clinical trial in the future should aim to analyse long-term (>30 days) indwelling urinary catheters, collecting consistent clinical information which is relevant to the onset of CAUTIs and their associated complications, such as urine cultures pre- and post-catheterization, urinary pH, and note any pre-existing medical conditions such as cerebrovascular disease, pulmonary disease, renal disease, and sever liver disease which have been shown to significantly affect the chance of infection (Letica-Kriegel *et al.*, 2019).

5.4 Conclusions

- Biofilm accumulation on Camstent catheters recovered from post-surgical catheterized patients was significantly lower than the biofilm formed on silicone samples across all three clinical cohorts
- The mineral deposition on Camstent catheters was also significantly lower than the mineralization accumulated on silicone samples across the three clinical catheter cohorts
- There is a correlation between catheter indwelling time, biofilm and mineral accumulation within the catheter lumens
- Catheterization with Camstent catheters was shown to result in a smaller increase in urinary fibrinogen when compared with silicone catheters
- A lower amount of fibrinogen was found to be associated with the lumens of Camstent catheters in comparison with silicone devices following exposure to urine with comparable fibrinogen concentration

Chapter 6- Characterisation of biofilm formation and mineral accumulation on clinical catheter samples

6.1 Introduction

Complicated UTIs such as CAUTIs are most commonly polymicrobial, which has implications upon any biofilm formed on IUCs (Jacobsen *et al.*, 2008). Polymicrobial interactions can be synergistic, for example, the different species within the biofilm can exhibit metabolic cooperation. Synergistic interactions within polymicrobial biofilms confer a fitness advantage to the cooperating microbes. An example of such an advantage resulting from a synergistic interaction is the improved growth rate and anti-microbial resistance of dual-species biofilms formed by *Streptococcus mutans* and *Veillonella parvula* in comparison with single species biofilms of either microbe (Kara *et al.*, 2007). The advantage of co-existence for the two-species results from their metabolic compatibility, with the *St. mutans* strain utilizing carbohydrates to produce lactic acid, which is in turn catabolized by the *V. parvula* cells (Gibbons and Fitzgerald, 1969; Bradshaw *et al.*, 1994; Palmer, Diaz and Kolenbrander, 2006). Interactions within a polymicrobial biofilm can also be antagonistic, with the different microbial species competing for nutrients and space by various means, such as the production of growth-inhibitory agents like phenazines by *Ps. aeruginosa*, and bacteriocins such as colicin by *E. coli* (Price-Whelan, Dietrich and Newman, 2006; Gillor, Giladi and Riley, 2009; Elias and Banin, 2012).

The type of inter-species interactions which occur within a biofilm will commonly determine its characteristics, with microbial synergy producing a

range of metabolic niches within stratified biofilms, and antagonism resulting in domination by a single microbial species (Rao, Webb and Kjelleberg, 2005; Hibbing *et al.*, 2010). Synergistic polymicrobial biofilms offer ecological advantages over their single-species counterparts, with one example being the facilitation of transfer of anti-microbial resistance genes between the different species of microorganisms, this in turn makes infections associated with these diverse communities, such as CAUTIs, particularly difficult to eradicate (Roberts *et al.*, 1999; Azevedo *et al.*, 2017; Ch'ng *et al.*, 2019).

Polymicrobial biofilms within CAUTIs are often characterised by the presence of common urinary pathogens such as *E. coli, P. mirabilis*, and *K. pneumoniae*, co-existing on the same urinary catheters with uncommon microorganisms, which can be commensal or pathogenic such as *Delftia tsuruhatensis* and *Achromobacter xylosoxidans* (Frank *et al.*, 2009; Holá, Ruzicka and Horka, 2010; Xu *et al.*, 2012). While the established pathogens provide the crucial virulence factors necessary for the establishment of an infection such as surface adhesion organelles, biofilm forming capabilities, and urease production, the uncommon microorganisms contribute to the potency of the biofilms formed by the pathogens by enhancing their adhesion to surfaces, the organization of the microbial consortia, as well as the resistance of the bacteria within the biofilm to environmental cues (Lopes, Azevedo and Pereira, 2014; Azevedo *et al.*, 2016). *E. coli* is an example of a common urinary pathogen found to co-exist with uncommon bacteria such as *D. tsuruhatensis* and *A. xylosoxidans*, with synergistic interactions between the microorganisms resulting in an increased tolerance of their polymicrobial biofilm to a number of antibiotics commonly prescribed to treat CAUTIs (Azevedo *et al.*, 2016). Some

common inter-species interactions which can provide and improved resilience to antibiotic treatment to bacterial communities include: collective resistance, whereby community interactions increase the ability of the comprising bacteria to resist antibiotic action; collective tolerance, where cell state alteration within a community such as a reduction in the rate of metabolism can enable cells to delay cell death and thus overcome the temporary exposure to antibiotics; and exposure protection, in the case of which sensitive members of the microbial community are protected by reducing their exposure to the antibiotic (Vega and Gore, 2014; Meredith *et al.*, 2015; Bottery, Pitchford and Friman, 2020).

Mineralization of biofilms resulting from the presence of urease producing microorganisms plays an important role in the regulation of the structure and ecology of the microbial communities on IUCs, as well as inter-species interactions within these communities (Li, Lu, Hannah R Brady, *et al.*, 2016). Minerals precipitating from urine as a result of urease activity are incorporated within biofilms further enhancing their resilience to environmental pressures, making the presence of urease producing bacteria within polymicrobial communities particularly important (Li, Chopp, William A. Russin, *et al.*, 2016; Li, Lu, Hannah R Brady, *et al.*, 2016). *P. mirabilis* is one example of a potent urease producing urinary pathogen which has exhibited improved retention within polymicrobial biofilms as a result of biomineralization (Poore and Mobley, 2003; Konieczna *et al.*, 2013). Minerals produced by this bacterium, such as struvite, are highly porous, potentially facilitating the transport of nutrients and chemical signals throughout the multi-species communities of bacteria, as well as enhancing cell adhesion and biofilm

development by providing protection from antibiotics and host immune defence mechanisms (Prywer, Torzewska and Płociński, 2012).

The impact of mineralization upon urinary pathogen interactions has been clearly outlined in the past within mixed biofilms consisting of *P. mirabilis* and *Ps. aeruginosa*, where biomineralization improved the persistence of *P. mirabilis* cells and controlled its spatial distribution (Li, Lu, Hannah R. Brady, *et al.*, 2016). Mineral precipitation and incorporation within the biofilm thus favours the growth of potent urease producers such as *P. mirabilis* within polymicrobial communities, enabling them to become more abundant during long-term infections such as CAUTIs, and providing the opportunity to cause complications such as catheter encrustation and blockage (Armbruster and Mobley, 2012).

The urease producing bacterial species present within the biofilm formed on urinary catheter devices can be detrimental to the type of mineralization deposited within the catheter lumen. Struvite and apatite are among the most commonly identified types of mineral associated with urinary biofilms involving *P. mirabilis* and *Ps. aeruginosa* (Figure 6.1) (Broomfield *et al.*, 2009; Prywer and Torzewska, 2010; Prywer, Torzewska and Płociński, 2012; Flannigan *et al.*, 2018). Calcium carbonate is another type of mineralization commonly associated with bacterial metabolism during biofilm formation, produced by more than 200 different bacterial species (Figure 6.1) (Boquet, Boronat and Ramos-Cormenzana, 1973; Li *et al.*, 2015; Oppenheimer-Shaanan *et al.*, 2016). While struvite and apatite have distinct mineral morphologies, calcium carbonate can occur in a range of different forms including vaterite, aragonite, and calcite, depending on the environmental conditions during mineral

precipitation (Dhami, Reddy and Mukherjee, 2013; Mudgil *et al.*, 2018). The dolomite and aragonite forms of calcium carbonate mineralization have frequently been identified as components of urinary stones in catheterized patients (Gault *et al.*, 1993).

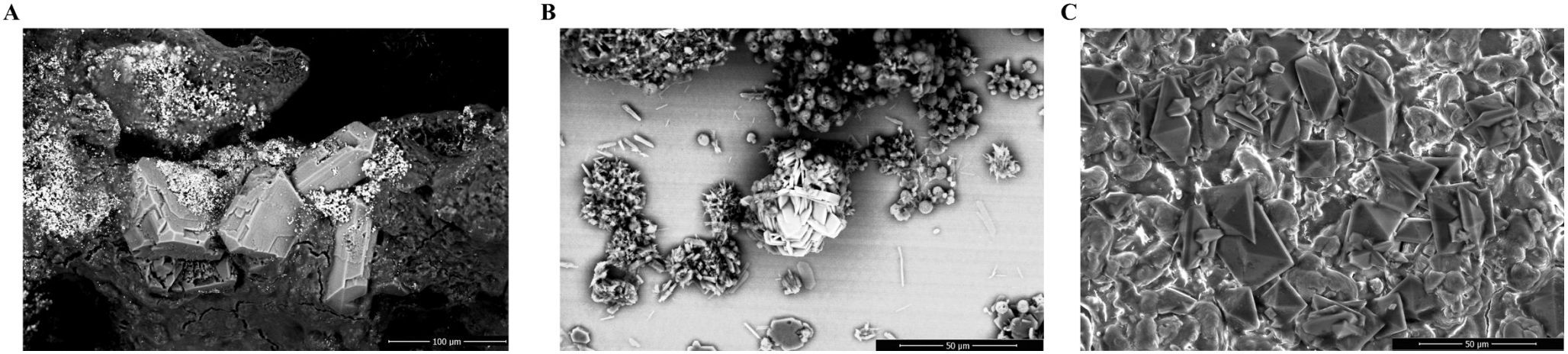

Figure 6.1: Different types of mineralization associated with the surfaces of clinical urinary catheter devices

Struvite and apatite (A), calcium carbonate (B), and calcium oxalate (C) minerals associated with the surfaces of clinical urinary catheters. Images were generated using an ESEM (FEI Quanta 650).

Mineralization of catheter devices has also been known to occur in the absence of biofilm formation. Patients with underlying conditions such as renal calculi, can have a higher urinary pH, which alongside dietary factors and endogenous patient metabolism can result in the precipitation of calcium oxalate onto the surface of urinary catheters (Berg and Tiselius, 1986; Grases *et al.*, 2001; Chai *et al.*, 2004; Frassetto, 2011; Ma *et al.*, 2017). The elemental composition of calcium oxalate consists of calcium, carbon, and oxygen, and the minerals exhibit a distinctive envelope shaped morphology (Figure 6.1) (Jacobsen, Åkesson and Shefterd, 1982; Koda, Watanabe and Iino, 2017). While this is the predominant type of mineral associated with the surface of urinary catheter devices in the absence of urinary tract infections, it has not been reported to cause encrustation or blockage as is the case for the common biofilm associated minerals such as struvite (Grases *et al.*, 2001).

The formation of crystalline biofilms is an important complication associated with CAUTIs, due to it being a crucial factor in the development of catheter encrustation leading to persistent infections and eventual device blockage. The EGDPEA/DEGMA coated Camstent catheter has demonstrated an improved resistance to biofilm formation and its associated mineralization in comparison to control silicone devices *in vitro* and within a clinical setting, as described in chapters 4 and 5. This chapter presents further characterisation of the biofilms, minerals, and bacterial populations, associated with Camstent and silicone catheter devices recovered from hospitalized patients. ESEM coupled with EDS analysis was conducted on selected clinical catheter samples, to determine the biofilm and mineral catheter associated morphologies and chemistry. SEM imaging was also performed to confirm the presence of

bacterial cells on the device surfaces. The bacterial populations associated with the catheters were identified by extracting genomic DNA and subjecting the samples 16S rRNA gene sequencing.

6.1.1 Hypothesis and aims

The lumens of silicone catheters were hypothesised to contain struvite, apatite, and calcium carbonate biofilm associated mineralization. Calcium oxalate was the predominant type of mineral hypothesised to be associated with Camstent catheters. Additionally, Camstent catheters were hypothesised to be colonized by different species of bacteria in comparison with silicone devices, as a result of the EGDPEA/DEGMA coating. The aim of this chapter was to differentiate between the types of minerals associated with Camstent and silicone clinical catheters, and to determine any differences in the bacterial species colonizing the two catheter types.

The objectives to address the aim of this work were to:

- Image biofilms and mineralization associated with Camstent and silicone clinical catheters using an ESEM and determine their elemental compositions using EDS analysis.
- Extract gDNA from Camstent and silicone clinical catheters and perform 16S rRNA gene sequencing, and compare the bacterial communities associated with the two catheter types.

6.2 Results

6.2.1 Biofilms and mineralization on catheters recovered from hospitalized patients

ESEM imaging and EDS analysis of the luminal surfaces of selected silicone and Camstent catheter samples recovered from catheterized patients, part of the clinical cohorts presented within chapter 5, revealed distinct differences in the morphology and elemental composition of the biofilms and mineralization present (Figure 6.2). Silicone samples 20 and 15 were both associated with biofilm structure of highly nitrogenous nature as exhibited by the EDS spectra associated with the images (Figure 6.2 A and B). The biofilms present on the surface of these samples however were associated with different types of mineralization, with silicone sample 20 presenting distinct struvite and apatite minerals, defined by the elemental composition made up of magnesium and phosphorus, and calcium and phosphorus, respectively (Figure 6.2A). Mineralization associated with the second silicone sample analysed here can be described as a form of calcium carbonate, defined by its high calcium content (Figure 6.2B). The Camstent catheter on the other hand presented a distinctively different morphology of mineralization on its surface when compared to the silicone catheters, coupled with a lack of nitrogenous biofilm structure which was observed on the uncoated samples (Figure 6.2C). The envelope shaped morphology and high content of calcium mean that the minerals associated with the Camstent catheter can be defined as calcium oxalate.

A

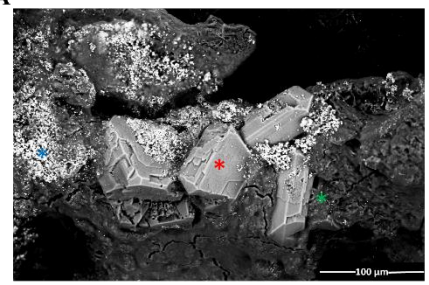

Clinical Catheter Sample 20- Silicone
Indwelling Time- 42 days

Symbol	Structure	Relative elemental composition (At %)			
		Nitrogen	Magnesium	Calcium	Phosphorus
*	Struvite	8.6	3.6	0.2	3.6
*	Biofilm	9.9	3.0	2	2.8
*	Apatite	4.7	0.2	5.9	3.8

B

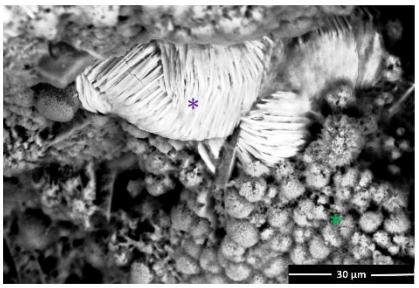

Clinical Catheter Sample 15- Silicone
Indwelling Time- 91 days

Symbol	Structure	Relative elemental composition (At %)			
		Nitrogen	Magnesium	Calcium	Phosphorus
*	Calcium Carbonate	0.1	0.1	6.8	0.1
*	Biofilm	24.8	0.1	0.4	0.2

C

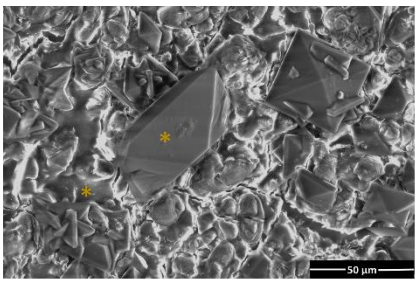

Clinical Catheter Sample 18- Camstent
Indwelling Time- 22 days

Symbol	Structure	Relative elemental composition (At %)			
		Nitrogen	Magnesium	Calcium	Phosphorus
*	Calcium Oxalate	0.0	0.0	9.3	0.1
*	Calcium Oxalate	0.0	0.0	7.6	0.1

Figure 6.2: ESEM imaging and EDS analysis of the luminal surfaces of silicone and Camstent clinical catheter samples

The morphologies of biofilm and minerals exhibited on silicone samples 20 (A) and 15 (B), and Camstent sample 18 (C) following ESEM imaging. These samples were selected for further characterisation from the clinical catheter cohorts present in chapter 5. Symbols associated with each of the images correspond to locations selected for EDS analysis spectrum generation. The spectra reveal the elemental composition of the analysed structures, with this data presented in the tables accompanying the ESEM images. Full EDS spectra can be found within Appendices Q, R, and S.

Imaging the lumens of clinical catheters by SEM, following a more extensive sample preparation procedure for improved contrast (see Section 2.6.1), revealed the presence of single bacterial cells on the surface of the silicone samples analysed (Figure 6.3). The luminal surfaces of silicone catheter samples 15 and 30 were colonized by coccoid shaped cells, within a mesh of EPS matrix and mineral (Figure 6.3A and C). The third silicone clinical catheter sample (20) analysed, presented a mixed population of rod and coccus bacterial cells associated with the catheter surface (Figure 6.3B). This data suggests differing bacterial populations present on the silicone catheter surfaces, which may offer an explanation for the differing biofilm and mineral morphologies observed during ESEM imaging and EDS analysis (Figure 6.2A and B). SEM imaging of the Camstent catheter sample chosen for analysis on the other hand did not show any easily distinguishable single-bacterial cells (Figure 6.4). This supports the data obtained from the ESEM/EDS analysis of the sample regarding the absence of a nitrogenous biofilm structure, as well as the definition of the calcium oxalate minerals which can precipitate in the absence of a CAUTI (Figure 6.2C).

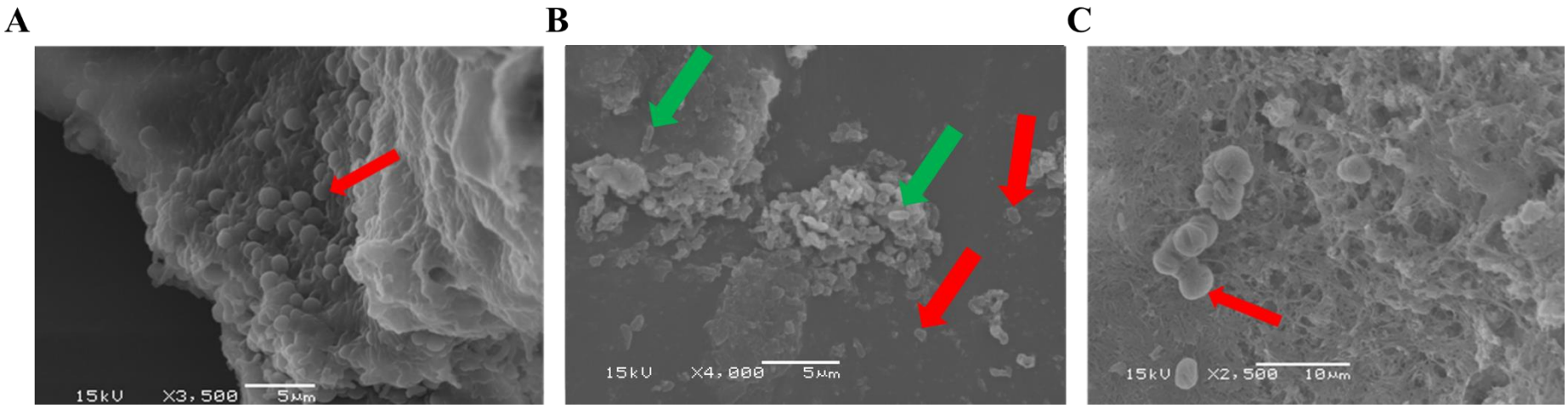

Figure 6.3: Single-cell SEM images of silicone catheter lumens

SEM images of silicone clinical catheter samples 15 (A), 20 (B), and 30 (C) exhibiting presence of single bacterial cells. Coccoid shaped cells are indicated by red arrows within sections (A), (B) and (C), while rod shaped single bacterial cells are depicted by the green arrows in section (B) of the figure. The images presented were generated using an (SEM FEI Quanta200 3D DualBeam). See section 2.6.1 for details on sample preparation procedure.

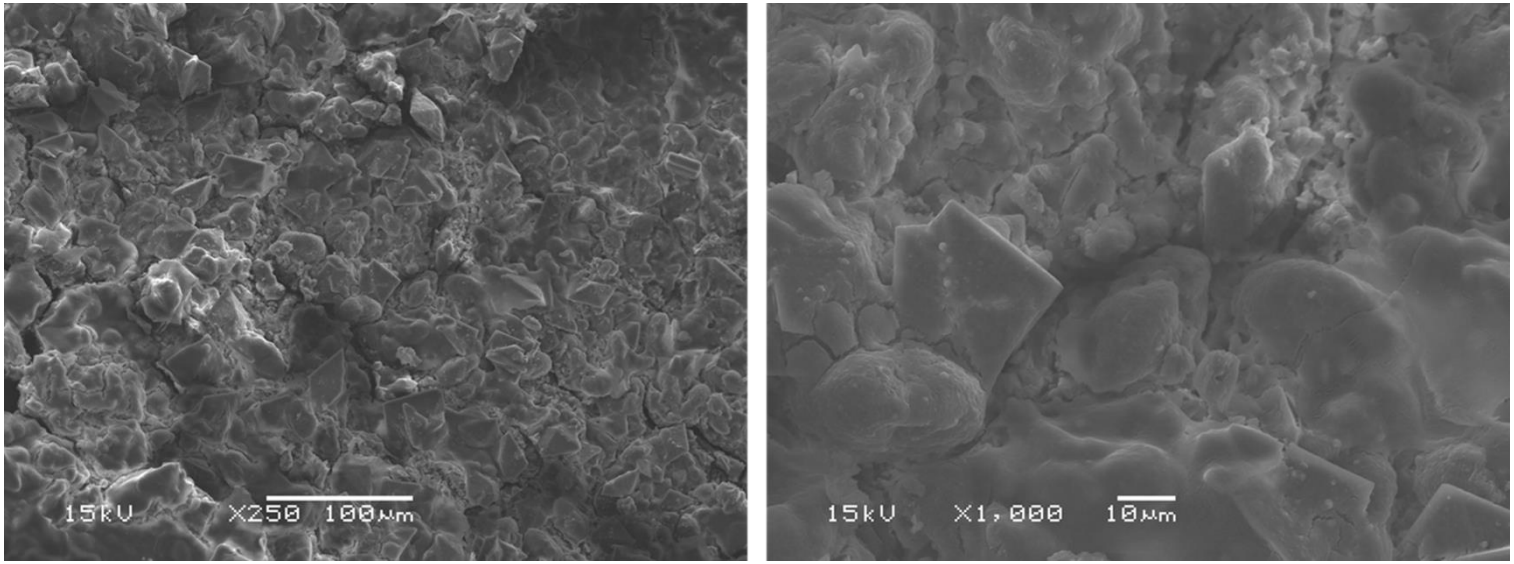

Figure 6.4: SEM images of Camstent catheter sample 18

SEM images of Camstent catheter sample 18, exhibiting a homogeneous mineral morphology and a lack of distinguished single bacterial cells. The images presented were generated using an (SEM FEI Quanta200 3D DualBeam). See section 2.6.1 for details on sample preparation procedure.

6.2.2 Calcium oxalate deposition on silicone and Camstent catheters recovered from hospitalized patients

To investigate further the deposition of calcium oxalate on Camstent catheters, the 10 samples with the greatest mineral content deposition as determined using confocal microscopy and image analysis were selected for quantification (Figure 6.5A). Linear regression analysis revealed a strong correlation (R^2- 0.715) between the amount of calcium oxalate associated with the Camstent samples, and that estimated via confocal imaging. As a means of comparison, the calcium oxalate concentration on the 10 silicone catheter samples with the greatest mineral content was also determined (Figure 6.5B). In contrast to the Camstent catheters, the silicone samples exhibited no significant correlation (R^2- 0.377) for calcium oxalate, determined using the two different methods. These findings are in agreement with observations from the ESEM/EDS analysis and SEM imaging conducted, with the minerals found on silicone samples being predominantly associated with the biofilm formed on the catheters and thus being defined as struvite, apatite, or calcium carbonate, rather than calcium oxalate. On the other hand, the Camstent catheters had little associated biofilm as shown by ESEM/EDS analysis and SEM imaging, instead showing calcium oxalate mineral morphology.

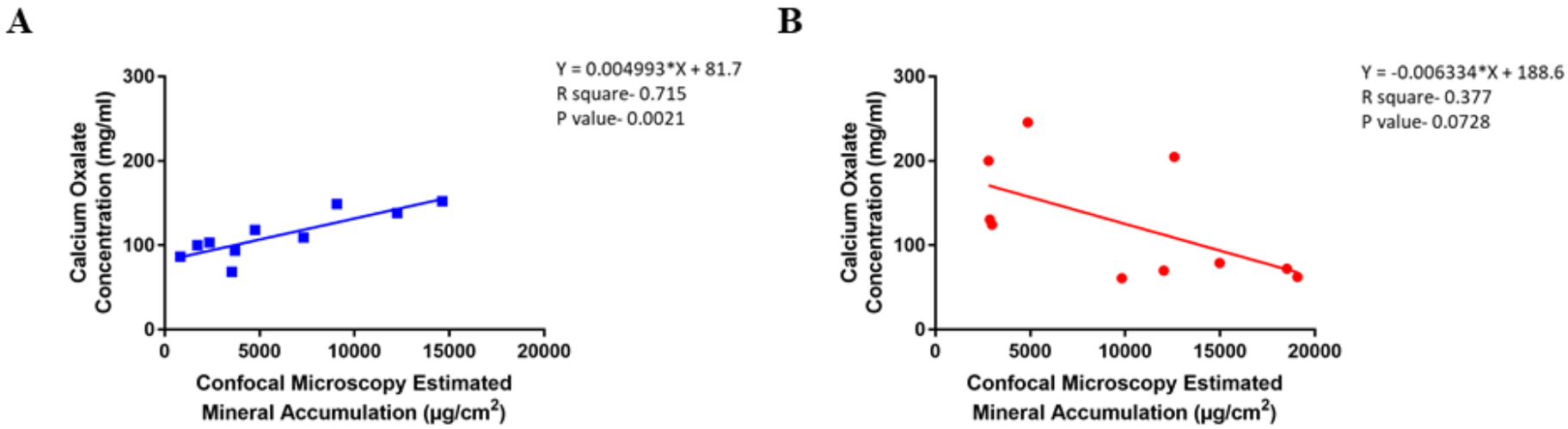

Figure 6.5: Calcium oxalate concentration vs. mineral accumulation on Camstent and silicone catheter samples

Linear regression analysis of the relationship between calcium oxalate concentration and confocal microscopy estimated mineral accumulation on 10 Camstent (A) and silicone (B) catheter samples from hospitalized patients. Methods used for calcium oxalate re-solubilization and quantification can be found in section 2.6.2.

6.2.3 Microbial communities on silicone and Camstent catheter samples recovered from hospitalized patients

16S gDNA extraction and 16S rRNA gene sequencing was conducted on 2 silicone and 3 Camstent clinical catheter samples. The extractions from the separate catheters were pooled together and split in triplicates for the purpose of evaluating the microbial communities present on the two different polymeric surfaces (see Section 2.6.3). The data revealed microbial communities of distinctly different composition on the two sample types in terms of the abundances of the most common phyla present (Figure 6.6). While both types of samples exhibited comparable abundances of firmicutes, silicone samples were found to be colonized by a much higher abundance of actinobacteria in comparison the Camstent catheters. The relative abundance of proteobacteria was found to be higher on Camstent catheters on the other hand. This data hints at a potential impact of the EGDPEA/DEGMA coating of Camstent catheters upon the type of microbes which are found on the surface of the devices, in comparison to silicone catheters.

The 16S rRNA data additionally revealed a higher number of observed microbial species on silicone in comparison to the Camstent coating (Figure 6.7A). These data suggest that a wider range of microbes are capable of colonizing the silicone surfaces. The 16S rRNA data analysis also enabled the determination of dissimilarity between the communities investigated in the form of weighted UniFrac distance. UniFrac is a measure of the distance between the communities chosen for comparison, calculated as a percentage of branch length that leads to descendants from only one of a pair of conditions tested. This measure differs from other dissimilarity measures such as Bray-Curtis, by

incorporating information on phylogenetic distances between the organisms observed during the analysis. Weighted UniFrac is a quantitative measure in that the relative abundance of the sequences is taken in to account when weighing the branch lengths (Lozupone *et al.*, 2007). The 16S rRNA gene sequencing data revealed a high dissimilarity coefficient, measured in weighted UniFrac distance, between the microbial communities colonizing the two polymer coatings, further supporting the proposed impact of the EGDPEA/DEGMA coating upon the communities of microorganisms colonizing the Camstent catheters (Figure 6.7B) (Lozupone *et al.*, 2007).

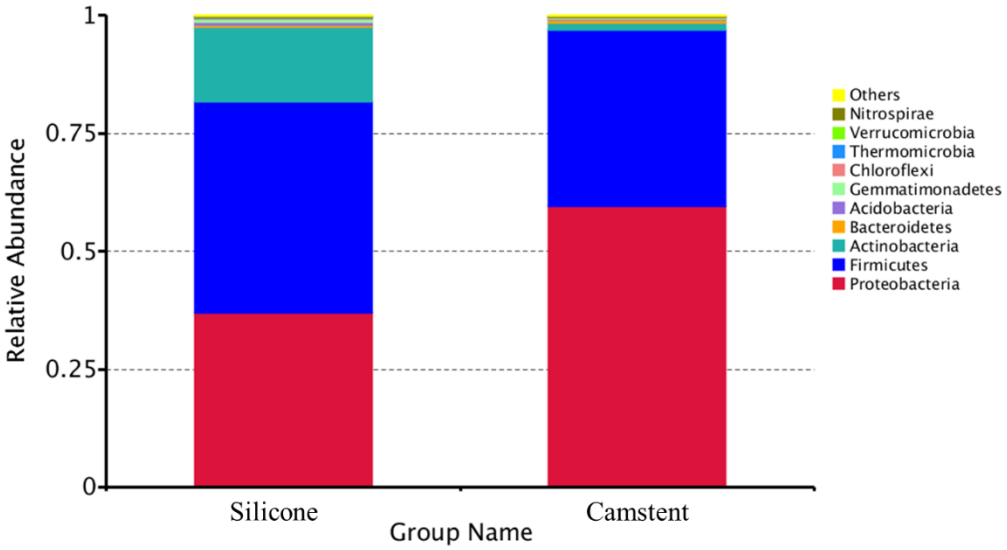

Figure 6.6: Relative abundance of the top 10 microbial phyla present on silicone and Camstent catheters from hospitalized patients

Genomic DNA extraction and 16S rRNA sequencing revealed the 10 most abundant microbial phyla on silicone and Camstent catheter devices recovered from hospitalized patients post-surgery. The data was generated from 2 silicone catheters (6 pooled gDNA extractions) and 3 Camstent catheters (9 pooled gDNA extractions).

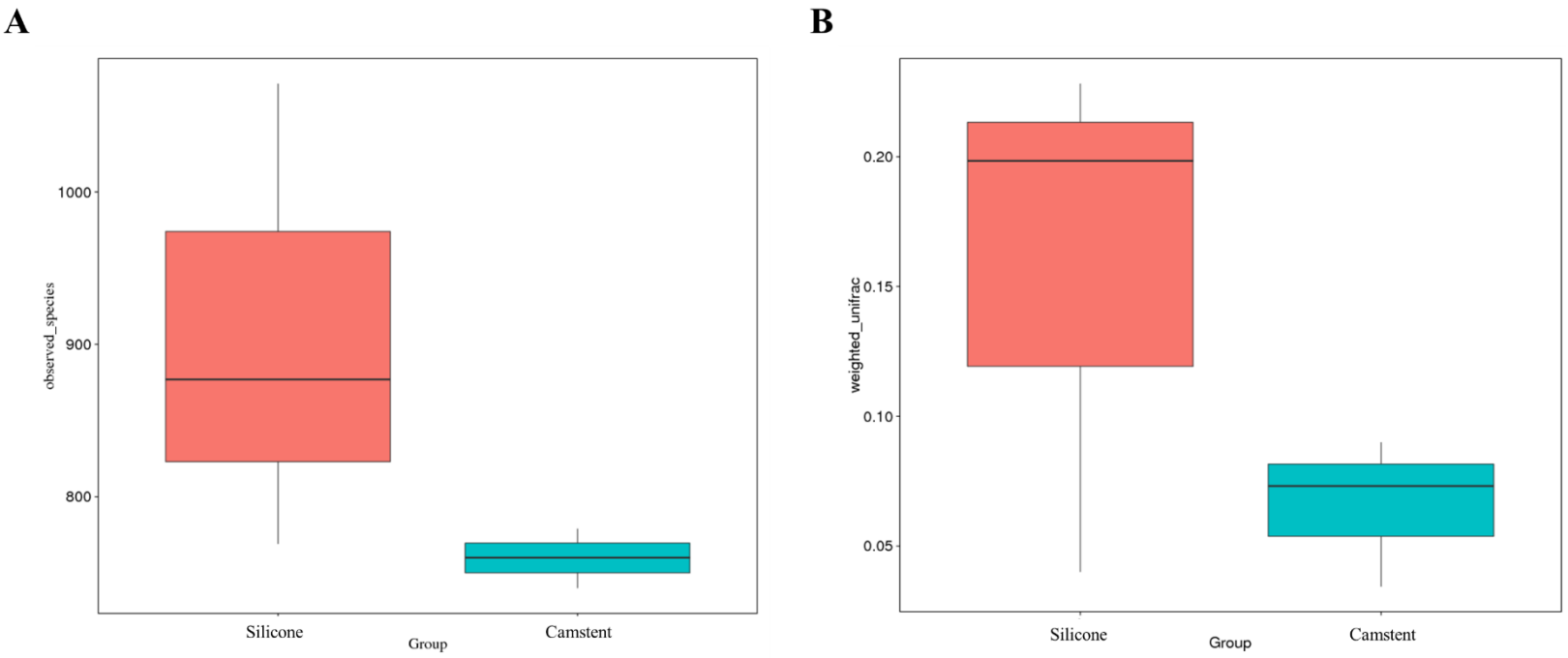

Figure 6.7: The number of observed microbial species and the microbial community dissimilarity coefficient between silicone and Camstent catheters

The alpha diversity plot (A) reveals the difference in microbial diversity, in terms of observed species, between silicone and Camstent clinical catheter samples. The beta diversity plot (B) describes the dissimilarity in microbial communities between the two catheter coatings, in the form of weighted UniFrac distance. Weighted UniFrac measures the distance between two communities by calculating the fraction of the branch length in a phylogenetic tree that leads to descendants in either, but not both, of the communities, where the branch lengths are weighted by the relative abundance of sequences within the samples (Lozupone *et al*., 2007).

6.3 Discussion

Since the EGDPEA/DEGMA coating provided resistance to biofilm formation *in vitro*, as well as reducing the amount of biofilm and mineral accumulation on patient samples, further characterisation of the Camstent coating was undertaken. Differences in the presence of bacterial cells, biofilm and mineral morphology, and chemistry in addition to bacterial communities' composition compared with silicone was observed. Data generated via ESEM imaging coupled with EDS analysis revealed distinctly different morphologies of biofilm and mineralization deposits on the two surfaces. Silicone surfaces were colonized by bacteria associated with struvite, apatite, and calcium carbonate mineralization resulting from the metabolism of the microorganisms, the single cells of which were exhibited through SEM imaging (Broomfield *et al.*, 2009; Prywer and Torzewska, 2010). The characteristic crystalline biofilms associated with silicone samples described here have been well documented in literature and associated with symptomatic CAUTI episodes as well as other significant patient health complications (Stickler, 2014; Feneley, Hopley and Wells, 2015).

The Camstent coating presented a contrasting picture to the one observed on silicone, with a distinct lack of single bacterial cells, nitrogenous biofilm, or minerals associated with biofilm formation. The only minerals observed within the lumens of the EGDPEA/DEGMA coated devices were instead identified as calcium oxalate which is associated with the endogenous patient metabolism (Chai *et al.*, 2004). As calcium oxalate deposition does not result in catheter blockage, the data presented here further supports initial findings of the reduced susceptibility of Camstent catheters to crystalline

biofilm formation, and therefore symptomatic CAUTI episodes. The potential impact of calcium oxalate deposition does however warrant further investigation as to the possibilities of bacterial growth on this type of mineral, as well as whether such crystals accumulate sufficiently to cause catheter blockage.

The comparison of the microbial communities associated with the two polymer surfaces analysed here, carried out via 16S rRNA gene sequencing, also revealed distinct differences in the type and abundance of colonizing microbes. These differences suggest that the EGDPEA/DEGMA coating impacts the colonization of the medical devices by commensals from the urinary tract. The lower number of observed microbial species associated with the coated Camstent catheters in comparison to the silicone samples was anticipated, as the anti-biofilm formation properties of the EGDPEA/DEGMA coating would make any bacteria initially attached to the surface more susceptible to environmental cues such as shear flow of urine or any antibiotics administered to the patient (Donlan and Costerton, 2002; Hook *et al.*, 2013) . This would in turn result in a reduced chance of retention of the bacteria on the surface of the catheter, and thus detection via the 16S rRNA gene sequencing method used here. The higher microbial diversity, in terms of the number of observed species, on silicone catheters suggests a higher chance of formation of a polymicrobial biofilm on these devices, and thus the possibility of development of antibiotic tolerance within the microbial communities formed (Xu *et al.*, 2012; Hall and Mah, 2017; Nabb *et al.*, 2019).

While the majority of the analytical methods employed focused on the luminal surfaces, the 16S gDNA extraction also included the outer surface.

Although the microbial communities within the lumen of the catheters were not exposed to the environment until they were sectioned under sterile laboratory conditions, the outer surface would have been handled by the medical/nursing staff responsible for removing the catheters from the patient. This may have resulted in the presence of additional microbial species which were not urinary tract associated.

16S rRNA gene sequencing for the determination of the microbiome associated with the two catheter types was selected for this experiment due to its simplicity and ability to provide an overview of the genera and relative abundance of bacteria present. For the purpose of clinical analysis and more specific investigation into the composition of the microbiome, alternative methods such as shotgun metagenomics can be applied (Allaband *et al.*, 2019). A large-scale study of the microbial communities associated with the silicone and Camstent coating would be required to reveal the basis behind the differences in bacterial communities presented. A focus on specific bacterial species present may also provide further insights into the impact of the EGDPEA/DEGMA coating upon the microbial consortia developing during urinary catheterization. While the 16S rRNA data presented here also revealed some species level information, including the presence of pathogen such as *P. mirabilis*, *Ps. aeruginosa*, and *E. coli*, it also remained inconclusive on the species of other bacteria identified such as certain *Staphylococci* in particular (data not shown). The relatively low level of confidence of this method with regards to species identification within the microbiome is the main reason why this part of the data was not presented within the piece of work. Future experiments should look to incorporate alternative approaches to 16S rRNA

gene sequencing, such as shotgun metagenomics, and complement them with extensive bacterial culturing, in an effort to provide a more comprehensive overview of the species associated with the two catheter surfaces investigated here.

6.4 Conclusions

- Camstent catheter lumens exhibited a distinct lack of nitrogenous biofilm content, which was observed within silicone samples.
- Silicone and Camstent surfaces presented distinct differences in mineralization morphology and elemental composition.
- The two types of catheter surface presented marked differences in microbial community composition
- A greater diversity of bacterial species was present on silicone compared with the Camstent coating

Chapter 7- General conclusions and future work

The principal aim of the first results chapter of this work was to generate a random *P. mirabilis* transposon mutant library, and select suitable swarming and urease negative mutants for further experimentation. While *flgI* and *ureR* mutants isolated from the transposon mutant library generated were incorporated in further experiments, all of the swarming and urease negative sequenced mutants carried the transposon insertion within the same 2 genes. The potential hot-spots identified within the transposon mutagenesis experiments conducted here thus raise a question regarding the applicability of the mini-Tn*5* vector for random mutant generation in *P. mirabilis*, when screening in experiments is conducted with a specific focus on selected virulence factors such as urease production and swarming. For this observation to be conclusive however, all of the 161 swarming negative mutant isolated within this study would be required to be sequenced.

While the study explored the impact of swarming and urease production upon the crystalline biofilm formation capabilities of *P. mirabilis*, the two virulence factors were only investigated separately. Future experiments exploring any link between swarming motility and urease production would also be of interest, due to multiple studies reporting differing levels of urease production within differentiated and un-differentiated *P. mirabilis* cells (Falkinham and Hoffman, 1984; Allison, Lai and Hughes, 1992; Jones *et al.*, 2004). Sequencing swarming negative mutants which were shown to be limited in urease production would be an important step to this potential future investigation (Figure 3.7). The presence of the *gfp* and *lux* genes within the mini-Tn*5* vector used for transposon mutant generation additionally enable the

mutants isolated to be used as reporters within future experiments. Generating data on the expression of *ureR* within isolated mutant during swarming on a solid medium containing urea, may shed further light on any link between this type of motility and urease production.

While the *ureR* gene and its product's function have been well established within *P. mirabilis*, strains of the bacterium mutated within *flgI* have yet to be explored (D'Orazio, Thomas and Collins, 1996; Poore and Mobley, 2003). Preliminary data on this type of mutant present within *in vitro* bladder model experiments here suggest and impact upon biofilm formation, which can be explored further via experiments generating data on its exopolysaccharide production in comparison to the wild-type *P. mirabilis* strain, through enzyme-linked lectinosorbent assays (Stankowska *et al.*, 2012; Czerwonka *et al.*, 2014; Moryl *et al.*, 2014). Prior to any future investigations incorporating the transposon mutants of interest generated here however, it would be imperative to conduct complementation experiments confirming the gene functions and mutation site within the strains.

The *in vitro* bladder model chapter within this work was used to successfully generate first biofilm and mineralization *in vitro* data on the complete novel EGDPEA/DEGMA co-polymer coated Camstent catheter. The chapter achieved its main objective of demonstrating the improved resilience of the coated catheter to *P. mirabilis* and *Ps. aeruginosa* biofilm formation and blockage in comparison with silicone catheters. Work within this chapter additionally further highlighted the importance of mineralization to blockage of urinary catheters, with *Ps. aeruginosa* and urease negative *P. mirabilis*, shown

to be incapable of blocking the medical devices over the 89 hour duration of the experiments.

Future adaptations to the model to increase the maximum experimental duration would enable the more accurate estimation of the susceptibility of Camstent catheters to blockage, as well as the importance of high potency urease production to this event. A set-back of the model set-up described here is the relatively low throughput, requiring a number of days for the generation of a single experimental replicate. Future adaptations of the model creating a heat jacket circuit, and incorporating multiple bladder chambers, would address this issue and extend the applicability of the model to a wider range of experiments. Additionally, exposure of catheters to infection relevant host-proteins such as fibrinogen and THP, prior to introduction within the *in vitro* bladder model, would bring the setup closer to accurately replicating the urinary tract environment (Raffi *et al.*, 2012; Flores-Mireles *et al.*, 2016). The bladder model setup presented here opens many avenues for future experimentation such as looking in to introduction of bacteria at different sites throughout the model, like the urethra or the catheter bag, thus exploring the susceptibility of the Camstent catheters to a wider range of infection routes, but also the importance of *P. mirabilis* virulence factors like swarming to successful biofilm establishment within these different scenarios (Daifuku and Stamm, 1984; Nickel, Grant and Costerton, 1985; Stamm, 1991; Tambyah, Halvorson and Maki, 1999; Warren, 2001).

Data on clinical samples from the first-in-man study presented within chapter 5 successfully demonstrated the effectiveness of the EGDPEA/DEGMA coating, in terms of reducing biofilm formation, mineral accumulation, and

fibrinogen deposition on catheter devices *in vivo*. The data highlights the potential of biomaterial coatings to address the issue of CAUTIs, and paves the way for larger future clinical studies specifically focusing on the incidence of these infections with Camstent catheters in comparison with silicone devices. A study incorporating a larger urine and catheter sample set investigating fibrinogen concentration change upon catheterisation and deposition on the device following removal would be necessary to confirm the difference between Camstent and silicone catheters with respect to the host-protein. Additionally, *in vitro* studies exploring the biofilm formation of bacteria carrying receptors for fibrinogen such as *S. aureus* and *E. faecalis*, upon Camstent and silicone catheters pre-exposed to the protein, would be instrumental to determining the mechanism behind the reduction in fibrinogen deposition and subsequent biofilm formation on the coated surfaces.

Characterisation of the catheter associated biofilms and mineralization conducted within chapter 6 provided further information on key differences between the performances of silicone and Camstent catheters *in vivo*. The chapter achieved its aim in exhibiting struvite, apatite, and calcium carbonate minerals associated with biofilms found on silicone catheters, in sharp contrast to the calcium oxalate mineralization found on Camstent catheters. While calcium oxalate did not seem to be associated with a biofilm on Camstent catheters, it is important to explore the potential implications of this type of mineralization upon the efficacy of the EGDPEA/DEGMA surface. As the layer of calcium oxalate minerals covers a large part of the Camstent catheter lumen, future experiments can look to investigate the possibility of biofilm formation on surfaces covered with this mineral. Additionally, it would be it would be of

interest to explore the levels of calcium oxalate precipitation necessary to block a catheter device completely within an *in vitro* bladder model, which can be achieved by employing an artificial urine medium containing oxalate and artificially raising the pH of the urine via the addition of urease thus instigating precipitation (Dayyoub *et al.*, 2017).

Observations from the 16S rRNA gene sequencing data on the differing microbial diversity and community compositions associated with Camstent and silicone catheters were in line with the secondary aim of Chapter 6. Exploring these differences at a species level, and over a larger set of samples, while potentially combining future investigations in to microbial communities with experiments involving the culturing of bacteria associated with the clinical devices, would provide more information on the specific impact of the EGDPEA/DEGMA coating (Thomas-White *et al.*, 2018).

References

Adlington, K. *et al.* (2016) 'Application of Targeted Molecular and Material Property Optimization to Bacterial Attachment-Resistant (Meth)acrylate Polymers', *Biomacromolecules*, 17(9), pp. 2830–2838. doi: 10.1021/acs.biomac.6b00615.

Agladze, K., Jackson, D. and Romeo, T. (2003) 'Periodicity of cell attachment patterns during *Escherichia coli* biofilm development', *Journal of Bacteriology*, 185(18), pp. 5632–5638. doi: 10.1128/JB.185.18.5632-5638.2003.

Al-Hazmi, H. (2015) 'Role of duration of catheterization and length of hospital stay on the rate of catheter-related hospital-acquired urinary tract infections', *Research and Reports in Urology*. Dove Medical Press Ltd., 7, pp. 41–47. doi: 10.2147/RRU.S75419.

Allaband, C. *et al.* (2019) 'Microbiome 101: Studying, Analyzing, and Interpreting Gut Microbiome Data for Clinicians', *Clinical gastroenterology and hepatology : the official clinical practice journal of the American Gastroenterological Association*. NIH Public Access, 17(2), p. 218. doi: 10.1016/J.CGH.2018.09.017.

Alling, B., Seeberg, S. and Svanborg, A. (1975) 'Effect of Consecutive Antibacterial Therapy on Bacteriuria in Hospitalized Geriatric Patients', *Scandinavian Journal of Infectious Diseases*, 7(3), pp. 201–207. doi: 10.3109/inf.1975.7.issue-3.09.

Allion, A., Baron, J. P. and Boulange-Petermann, L. (2006) 'Impact of surface energy and roughness on cell distribution and viability', *Biofouling*, 22(5), pp. 269–278. doi: 10.1080/08927010600902789.

Allison, C. *et al.* (1993) 'Cell differentiation of *Proteus mirabilis* is initiated by glutamine, a specific chemoattractant for swarming cells', *Molecular Microbiology*, 8(1), pp. 53–60. doi: 10.1111/j.1365-2958.1993.tb01202.x.

Allison, C. *et al.* (1994) 'The role of swarm cell differentiation and multicellular migration in the uropathogenicity of *Proteus mirabilis*', *Journal of Infectious Diseases*, 169(5), pp. 1155–1158. doi: 10.1093/infdis/169.5.1155.

Allison, C., Lai, H. -C and Hughes, C. (1992) 'Co-ordinate expression of virulence genes during swarm-cell differentiation and population migration of *Proteus mirabilis* ', *Molecular Microbiology*. John Wiley & Sons, Ltd, 6(12), pp. 1583–1591. doi: 10.1111/j.1365-2958.1992.tb00883.x.

Altschul, S. F. *et al.* (1990) 'Basic local alignment search tool', *Journal of Molecular Biology*. Academic Press, 215(3), pp. 403–410. doi: 10.1016/S0022-2836(05)80360-2.

Anbu, P. *et al.* (2016) 'Formations of calcium carbonate minerals by bacteria and its multiple applications', *SpringerPlus*. SpringerOpen, pp. 1–26. doi: 10.1186/s40064-016-1869-2.

Mac Aogáin, M., Rogers, T. R. and Crowley, B. (2016) 'Identification of emergent blaCMY-2-carrying *Proteus mirabilis* lineages by whole-genome

sequencing', *New Microbes and New Infections*. Elsevier Ltd, pp. 58–62. doi: 10.1016/j.nmni.2015.11.012.

Aparna, M. S. and Yadav, S. (2008) 'Biofilms: Microbes and disease', *Brazilian Journal of Infectious Diseases*. Contexto, pp. 526–530. doi: 10.1590/S1413-86702008000600016.

Apel, D. and Surette, M. G. (2008) 'Bringing order to a complex molecular machine: The assembly of the bacterial flagella', *Biochimica et Biophysica Acta - Biomembranes*. Elsevier, pp. 1851–1858. doi: 10.1016/j.bbamem.2007.07.005.

Aquilini, E. *et al.* (2010) 'Functional identification of the *Proteus mirabilis* core lipopolysaccharide biosynthesis genes', *Journal of Bacteriology*. American Society for Microbiology Journals, 192(17), pp. 4413–4424. doi: 10.1128/JB.00494-10.

Armbruster, C. E. *et al.* (2014) 'Increased incidence of urolithiasis and bacteremia during *Proteus mirabilis* and *Providencia stuartii* coinfection due to synergistic induction of urease activity.', *The Journal of infectious diseases*, 209(10), pp. 1524–32. doi: 10.1093/infdis/jit663.

Armbruster, C. E., Forsyth-DeOrnellas, V., *et al.* (2017) 'Genome-wide transposon mutagenesis of *Proteus mirabilis* : Essential genes, fitness factors for catheter-associated urinary tract infection, and the impact of polymicrobial infection on fitness requirements', *PLoS Pathogens*. Public Library of Science, 13(6). doi: 10.1371/journal.ppat.1006434.

Armbruster, C. E., Prenovost, K., *et al.* (2017) 'How Often Do Clinically Diagnosed Catheter-Associated Urinary Tract Infections in Nursing Homes Meet Standardized Criteria?', *Journal of the American Geriatrics Society*. Blackwell Publishing Inc., 65(2), pp. 395–401. doi: 10.1111/jgs.14533.

Armbruster, C. E., Smith, S. N., *et al.* (2017) 'The pathogenic potential of *Proteus mirabilis* is enhanced by other uropathogens during polymicrobial urinary tract infection', *Infection and Immunity*. American Society for Microbiology, 85(2). doi: 10.1128/IAI.00808-16.

Armbruster, C. E., Hodges, S. A. and Mobley, H. L. T. (2013) 'Initiation of swarming motility by Proteus mirabilis occurs in response to specific cues present in urine and requires excess L-glutamine', *Journal of Bacteriology*, 195(6), pp. 1305–1319. doi: 10.1128/JB.02136-12.

Armbruster, C. E. and Mobley, H. L. T. (2012) 'Merging mythology and morphology: The multifaceted lifestyle of *Proteus mirabilis*', *Nature Reviews Microbiology*. Nat Rev Microbiol, pp. 743–754. doi: 10.1038/nrmicro2890.

Armbruster, C. E., Mobley, H. L. T. and Pearson, M. M. (2018) 'Pathogenesis of *Proteus mirabilis* Infection', *EcoSal Plus*. American Society for Microbiology, 8(1). doi: 10.1128/ecosalplus.esp-0009-2017.

Assadi, F. (2018) 'Strategies for preventing catheter-associated urinary tract infections', *International Journal of Preventive Medicine*. Wolters Kluwer Medknow Publications. doi: 10.4103/ijpvm.IJPVM_299_17.

Van Asten, F. J. A. M. and Gaastra, W. (1999) 'Urea restrains swarming of

Proteus mirabilis', *Journal of Clinical Microbiology*. American Society for Microbiology, p. 1652. doi: 10.1128/jcm.37.5.1652-1652.1999.

Aubron, C. *et al.* (2012) 'Changes in urine composition after trauma facilitate bacterial growth', *BMC Infectious Diseases*. BioMed Central, 12(1), p. 330. doi: 10.1186/1471-2334-12-330.

Autret, N. *et al.* (2001) 'Identification of new genes involved in the virulence of *Listeria monocytogenes* by signature-tagged transposon mutagenesis', *Infection and Immunity*. American Society for Microbiology (ASM), 69(4), pp. 2054–2065. doi: 10.1128/IAI.69.4.2054-2065.2001.

Azevedo, A. S. *et al.* (2016) 'Impact of *Delftia tsuruhatensis* and *Achromobacter xylosoxidans* on *Escherichia coli* dual-species biofilms treated with antibiotic agents', *Biofouling*. Taylor and Francis Ltd., 32(3), pp. 227–241. doi: 10.1080/08927014.2015.1124096.

Azevedo, A. S. *et al.* (2017) 'An *in vitro* model of catheter-associated urinary tract infections to investigate the role of uncommon bacteria on the *Escherichia coli* microbial consortium', *Biochemical Engineering Journal*, 118, pp. 64–69. doi: 10.1016/j.bej.2016.11.013.

Babakhani, S. and Oloomi, M. (2018) 'Transposons: the agents of antibiotic resistance in bacteria', *Journal of Basic Microbiology*. Wiley-VCH Verlag, 58(11), pp. 905–917. doi: 10.1002/jobm.201800204.

Bachman, J. (2013) 'Site-directed mutagenesis', in *Methods in Enzymology*. Academic Press Inc., pp. 241–248. doi: 10.1016/B978-0-12-418687-3.00019-7.

Banerjee, I., Pangule, R. C. and Kane, R. S. (2011) 'Antifouling coatings: Recent developments in the design of surfaces that prevent fouling by proteins, bacteria, and marine organisms', *Advanced Materials*. Adv Mater, pp. 690–718. doi: 10.1002/adma.201001215.

Barbey, R. *et al.* (2009) 'Polymer brushes via surface-initiated controlled radical polymerization: synthesis, characterization, properties, and applications', *Chemical Reviews*, 109(11), pp. 5437–5527. doi: 10.1021/cr900045a.

Barford, J. M. T. *et al.* (2008) 'A model of catheter-associated urinary tract infection initiated by bacterial contamination of the catheter tip', *BJU International*. John Wiley & Sons, Ltd, 102(1), pp. 67–74. doi: 10.1111/j.1464-410X.2008.07465.x.

Barker, C. S. *et al.* (2017) 'An intrinsically disordered linker controlling the formation and the stability of the bacterial flagellar hook', *BMC Biology*. BioMed Central Ltd., 15(1), p. 97. doi: 10.1186/s12915-017-0438-7.

Barquist, L. *et al.* (2016) 'The TraDIS toolkit: Sequencing and analysis for dense transposon mutant libraries', *Bioinformatics*. Oxford University Press, 32(7), pp. 1109–1111. doi: 10.1093/bioinformatics/btw022.

Barratt, J. and Topham, P. (2007) 'Urine proteomics: The present and future of measuring urinary protein components in disease', *CMAJ*. Canadian Medical Association, pp. 361–368. doi: 10.1503/cmaj.061590.

Belas, R. (1996) '*Proteus mirabilis* swarmer cell differentiation and urinary tract

infection.', *Urinary tract infections: molecular pathogenesis and clinical management.*, pp. 271–293.

Belas, R., Erskine, D. and Flaherty, D. (1991) 'Transposon mutagenesis in *Proteus mirabilis*', *Journal of Bacteriology*, pp. 6289–6293. doi: 10.1128/jb.173.19.6289-6293.1991.

Belas, R., Goldman, M. and Ashliman, K. (1995) 'Genetic analysis of *Proteus mirabilis* mutants defective in swarmer cell elongation', *Journal of Bacteriology*. American Society for Microbiology, pp. 823–828. doi: 10.1128/jb.177.3.823-828.1995.

Belas, R., Schneider, R. and Melch, M. (1998) 'Characterization of *Proteus mirabilis* precocious swarming mutants: Identification of rsbA, encoding a regulator of swarming behavior', *Journal of Bacteriology*, 180(23), pp. 6126–6139.

Beloin, C., Roux, A. and Ghigo, J. M. (2008) '*Escherichia coli* biofilms', *Current Topics in Microbiology and Immunology*, pp. 249–289. doi: 10.1007/978-3-540-75418-3_12.

Bennett, P. M. (2008) 'Plasmid encoded antibiotic resistance: Acquisition and transfer of antibiotic resistance genes in bacteria', in *British Journal of Pharmacology*. Br J Pharmacol. doi: 10.1038/sj.bjp.0707607.

Berg, C. and Tiselius, H. G. (1986) 'The effect of pH on the risk of calcium oxalate crystallization in urine', *European Urology*. Eur Urol, 12(1), pp. 59–61. doi: 10.1159/000472578.

Berne, C. *et al.* (2015) 'Adhesins Involved in Attachment to Abiotic Surfaces by Gram-Negative Bacteria', *Microbiology Spectrum*. American Society for Microbiology, 3(4). doi: 10.1128/microbiolspec.mb-0018-2015.

Bhasin, A. *et al.* (2000) 'Characterization of a Tn5 pre-cleavage synaptic complex', *Journal of Molecular Biology*. Academic Press, 302(1), pp. 49–63. doi: 10.1006/jmbi.2000.4048.

Bhasin, A., Goryshin, I. Y. and Reznikoff, W. S. (1999) 'Hairpin formation in Tn5 transposition', *Journal of Biological Chemistry*. J Biol Chem, 274(52), pp. 37021–37029. doi: 10.1074/jbc.274.52.37021.

Bisht, K. and Ann Wakeman, C. (2019) 'Discovery and therapeutic targeting of differentiated biofilm subpopulations', *Frontiers in Microbiology*. Frontiers Media S.A. doi: 10.3389/fmicb.2019.01908.

Bjork, D. T., Pelletier, L. L. and Tight, R. R. (1984) 'Urinary tract infections with antibiotic resistant organisms in catheterized nursing home patients.', *Infection control : IC*, 5(4), pp. 173–6. doi: 10.1017/s0195941700059178.

Boer, J. L., Mulrooney, S. B. and Hausinger, R. P. (2014) 'Nickel-dependent metalloenzymes', *Archives of Biochemistry and Biophysics*, pp. 142–152. doi: 10.1016/j.abb.2013.09.002.

Bogino, P. C. *et al.* (2013) 'The role of bacterial biofilms and surface components in plant-bacterial associations', *International Journal of Molecular Sciences*, pp. 15838–15859. doi: 10.3390/ijms140815838.

Bokulich, N. A. *et al.* (2013) ‘Quality-filtering vastly improves diversity estimates from Illumina amplicon sequencing’, *Nature Methods*. Nature Publishing Group, 10(1), pp. 57–59. doi: 10.1038/nmeth.2276.

Boquet, E., Boronat, A. and Ramos-Cormenzana, A. (1973) ‘Production of calcite (Calcium carbonate) crystals by soil bacteria is a general phenomenon’, *Nature*, 246(5434), pp. 527–529. doi: 10.1038/246527a0.

Bose, J. L. (2016) ‘Chemical and UV mutagenesis’, in *Methods in Molecular Biology*. Humana Press Inc., pp. 111–115. doi: 10.1007/7651_2014_190.

Bottery, M. J., Pitchford, J. W. and Friman, V.-P. (2020) ‘Ecology and evolution of antimicrobial resistance in bacterial communities’, *The ISME Journal 2020 15:4*. Nature Publishing Group, 15(4), pp. 939–948. doi: 10.1038/s41396-020-00832-7.

Bottone, E. J. (2010) ‘*Bacillus cereus*, a volatile human pathogen’, *Clinical Microbiology Reviews*. American Society for Microbiology (ASM), pp. 382–398. doi: 10.1128/CMR.00073-09.

Bowler, P., Murphy, C. and Wolcott, R. (2020) ‘Biofilm exacerbates antibiotic resistance: Is this a current oversight in antimicrobial stewardship?’, *Antimicrobial Resistance and Infection Control*. BioMed Central Ltd, p. 162. doi: 10.1186/s13756-020-00830-6.

Bradshaw, D. J. *et al.* (1994) ‘Metabolic cooperation in oral microbial communities during growth on mucin’, *Microbiology*. Microbiology Society, 140(12), pp. 3407–3412. doi: 10.1099/13500872-140-12-3407.

Bratulic, S. and Badran, A. H. (2017) ‘Modern methods for laboratory diversification of biomolecules’, *Current Opinion in Chemical Biology*. Elsevier Ltd, pp. 50–60. doi: 10.1016/j.cbpa.2017.10.010.

Brodsky, I. E. *et al.* (2002) ‘mig-14 is a *Salmonella* gene that plays a role in bacterial resistance to antimicrobial peptides’, *Journal of Bacteriology*. American Society for Microbiology Journals, 184(12), pp. 3203–3213. doi: 10.1128/JB.184.12.3203-3213.2002.

Brooks, T. and Keevil, C. W. (1997) ‘A simple artificial urine for the growth of urinary pathogens’, *Letters in Applied Microbiology*. Blackwell Publishing Ltd, 24(3), pp. 203–206. doi: 10.1046/j.1472-765X.1997.00378.x.

Broomfield, R. J. *et al.* (2009) ‘Crystalline bacterial biofilm formation on urinary catheters by urease-producing urinary tract pathogens: A simple method of control’, *Journal of Medical Microbiology*, 58(10), pp. 1367–1375. doi: 10.1099/jmm.0.012419-0.

Burke, J. P., Larsen, R. A. and Stevens, L. E. (1986) ‘Nosocomial bacteriuria: estimating the potential for prevention by closed sterile urinary drainage.’, *Infection control : IC*, 7(2 Suppl), pp. 96–9. Available at: http://www.ncbi.nlm.nih.gov/pubmed/3633896 (Accessed: 3 September 2019).

Cameron, A. P. *et al.* (2010) ‘Bladder Management After Spinal Cord Injury in the United States 1972 to 2005’, *Journal of Urology*, 184(1), pp. 213–217. doi: 10.1016/j.juro.2010.03.008.

Camilli, A. and Bassler, B. L. (2006) 'Bacterial small-molecule signaling pathways', *Science*, pp. 1113–1116. doi: 10.1126/science.1121357.

Caporaso, J. G. *et al.* (2010) 'QIIME allows analysis of high-throughput community sequencing data', *Nature Methods*. Nat Methods, pp. 335–336. doi: 10.1038/nmeth.f.303.

Caporaso, J. G. *et al.* (2011) 'Global patterns of 16S rRNA diversity at a depth of millions of sequences per sample', *Proceedings of the National Academy of Sciences of the United States of America*. National Academy of Sciences, 108(SUPPL. 1), pp. 4516–4522. doi: 10.1073/pnas.1000080107.

Carr, H. A. (2000) 'A Short History of the Foley Catheter: From Handmade Instrument to Infection-Prevention Device', *Journal of Endourology*, 14(1), pp. 5–8. doi: 10.1089/end.2000.14.5.

Carter, E. L. *et al.* (2009) 'Interplay of metal ions and urease', *Metallomics*, pp. 207–221. doi: 10.1039/b903311d.

Carvalho, M. (2018) 'Urinary pH in calcium oxalate stone formers: does it matter?', *Jornal brasileiro de nefrologia : 'orgao oficial de Sociedades Brasileira e Latino-Americana de Nefrologia*. Sociedade Brasileira de Nefrologia, pp. 6–7. doi: 10.1590/1678-4685-JBN-2018-00010002.

Cebolla, A. and Arévalo-Rodríguez, M. (2010) 'Genetic Analysis of Gram-Negative Bacteria Using Mini Tn5 Transposons', in *Handbook of Hydrocarbon and Lipid Microbiology*. Springer Berlin Heidelberg, pp. 4243–4254. doi: 10.1007/978-3-540-77587-4_332.

Ch'ng, J. H. *et al.* (2019) 'Biofilm-associated infection by enterococci', *Nature Reviews Microbiology*. Nature Publishing Group, pp. 82–94. doi: 10.1038/s41579-018-0107-z.

Chai, W. *et al.* (2004) 'Oxalate absorption and endogenous oxalate synthesis from ascorbate in calcium oxalate stone formers and non-stone formers', *American Journal of Kidney Diseases*. Am J Kidney Dis, 44(6), pp. 1060–1069. doi: 10.1053/j.ajkd.2004.08.028.

Chao, Y. and Zhang, T. (2011) 'Optimization of fixation methods for observation of bacterial cell morphology and surface ultrastructures by atomic force microscopy', *Applied Microbiology and Biotechnology*. Springer, 92(2), pp. 381–392. doi: 10.1007/s00253-011-3551-5.

Chaudhuri, R. R. *et al.* (2013) 'Comprehensive Assignment of Roles for *Salmonella typhimurium* Genes in Intestinal Colonization of Food-Producing Animals', *PLoS Genetics*. PLoS Genet, 9(4). doi: 10.1371/journal.pgen.1003456.

Chen, C. Y. *et al.* (2012) '*Proteus mirabilis* urinary tract infection and bacteremia: Risk factors, clinical presentation, and outcomes', *Journal of Microbiology, Immunology and Infection*, 45(3), pp. 228–236. doi: 10.1016/j.jmii.2011.11.007.

Chen, T. *et al.* (2000) 'Identification and cloning of genes from *Porphyromonas gingivalis* after mutagenesis with a modified Tn4400 transposon from

Bacteroides fragilis', *Infection and Immunity*. American Society for Microbiology, 68(1), pp. 420–423. doi: 10.1128/IAI.68.1.420-423.2000.

Cheng, G. *et al.* (2007) 'Inhibition of bacterial adhesion and biofilm formation on zwitterionic surfaces.', *Biomaterials*. NIH Public Access, 28(29), pp. 4192–9. doi: 10.1016/j.biomaterials.2007.05.041.

Cheng, G. *et al.* (2009) 'Zwitterionic carboxybetaine polymer surfaces and their resistance to long-term biofilm formation', *Biomaterials*. Elsevier, 30(28), pp. 5234–5240. doi: 10.1016/j.biomaterials.2009.05.058.

Christensen, W. B. (1946) 'Urea Decomposition as a Means of Differentiating Proteus and Paracolon Cultures from Each Other and from *Salmonella* and *Shigella Types*', *Journal of bacteriology*, 52(4), pp. 461–466. doi: 10.1128/jb.52.4.461-466.1946.

Chuang-Smith, O. N. *et al.* (2010) 'Acceleration of *Enterococcus faecalis* biofilm formation by aggregation substance expression in an *Ex Vivo* model of cardiac valve colonization', *PLoS ONE*, 5(12), p. e15798. doi: 10.1371/journal.pone.0015798.

Cincarova, L. *et al.* (2016) 'Changes in the Expression of Biofilm-Associated Surface Proteins in *Staphylococcus aureus* Food-Environmental Isolates Subjected to Sublethal Concentrations of Disinfectants', *BioMed Research International*. Hindawi Limited, 2016. doi: 10.1155/2016/4034517.

Clarke, L. and Carbon, J. (1976) 'A colony bank containing synthetic CoI EI hybrid plasmids representative of the entire *E. coli* genome', *Cell*, 9(1), pp. 91–99. doi: 10.1016/0092-8674(76)90055-6.

Colin, M. *et al.* (2016) 'The exploitation of urease-producing bacteria in catheter-associated urinary tract infections using an infection-responsive biomaterial', *Frontiers in Bioengineering and Biotechnology*. Frontiers Media SA, 4. doi: 10.3389/conf.fbioe.2016.01.01524.

Colomer-Winter, C., Lemos, J. and Flores-Mireles, A. (2019) 'Biofilm Assays on Fibrinogen-coated Silicone Catheters and 96-well Polystyrene Plates', *BIO-PROTOCOL*. Bio-Protocol, LLC, 9(6). doi: 10.21769/bioprotoc.3196.

Cope, M. *et al.* (2009) 'Inappropriate Treatment of Catheter-Associated Asymptomatic Bacteriuria in a Tertiary Care Hospital', *Clinical Infectious Diseases*. Oxford University Press (OUP), 48(9), pp. 1182–1188. doi: 10.1086/597403.

Cortese, Y. J. *et al.* (2018) 'Review of catheter-associated urinary tract infections and in vitro urinary tract models', *Journal of Healthcare Engineering*. Hindawi Limited. doi: 10.1155/2018/2986742.

Costerton, J. W. *et al.* (1995) 'Microbial Biofilms - Annual Review of Microbiology, 49(1):711', *Annual review of microbiology*. Annual Reviews 4139 El Camino Way, P.O. Box 10139, Palo Alto, CA 94303-0139, USA, 49, pp. 711–45. doi: 10.1146/annurev.mi.49.100195.003431.

Costerton, J. W., Geesey, G. G. and Cheng, K. J. (1978) 'How bacteria stick.', *Scientific American*, 238(1), pp. 86–95. doi: 10.1038/scientificamerican0178-

86.

Cunningham, T. P., Montelaro, R. C. and Rushlow, K. E. (1993) 'Lentivirus envelope sequences and pro viral genomes are stabilized in *Escherichia coli* when cloned in low-copy-number plasmid vectors', *Gene*. Gene, 124(1), pp. 93–98. doi: 10.1016/0378-1119(93)90766-V.

Curcio, M. J. and Derbyshire, K. M. (2003) 'The outs and ins of transposition: From MU to kangaroo', *Nature Reviews Molecular Cell Biology*. Nat Rev Mol Cell Biol, pp. 865–877. doi: 10.1038/nrm1241.

Cusick, K. *et al.* (2012) 'Perturbation of FliL Interferes with *Proteus mirabilis* Swarmer Cell Gene Expression and Differentiation', *Journal of Bacteriology*. American Society for Microbiology (ASM), 194(2), p. 437. doi: 10.1128/JB.05998-11.

Czerwonka, G. *et al.* (2014) 'Morphological changes in *Proteus mirabilis* O18 biofilm under the influence of a urease inhibitor and a homoserine lactone derivative', *Archives of Microbiology*. Springer Verlag, 196(3), pp. 169–177. doi: 10.1007/s00203-014-0952-8.

D'Orazio, S. E. F. and Collins, C. M. (1993) 'The plasmid-encoded urease gene cluster of the family *Enterobacteriaceae* is positively regulated by UreR, a member of the AraC family of transcriptional activators', *Journal of Bacteriology*. J Bacteriol, 175(11), pp. 3459–3467. doi: 10.1128/jb.175.11.3459-3467.1993.

D'Orazio, S. E. F., Thomas, V. and Collins, C. M. (1996) 'Activation of transcription at divergent urea-dependent promoters by the urease gene regulator UreR', *Molecular Microbiology*, 21(3), pp. 643–655. doi: 10.1111/j.1365-2958.1996.tb02572.x.

Dadgostar, P. (2019) 'Antimicrobial resistance: implications and costs', *Infection and Drug Resistance*. Dove Medical Press Ltd., pp. 3903–3910. doi: 10.2147/IDR.S234610.

Daifuku, R. and Stamm, W. E. (1984) 'Association of rectal and urethral colonization with urinary tract infection in patients with indwelling catheters.', *JAMA*, 252(15), pp. 2028–30. Available at: http://www.ncbi.nlm.nih.gov/pubmed/6481909 (Accessed: 17 December 2019).

Datta, P. *et al.* (2014) 'Epidemiology of extended-spectrum β-lactamase, AmpC, and carbapenemase production in *Proteus mirabilis*', *Japanese Journal of Infectious Diseases*, 67(1), pp. 44–46. doi: 10.7883/yoken.67.44.

Dattelbaum, J. D. *et al.* (2003) 'UreR, the transcriptional activator of the *Proteus mirabilis* urease gene cluster, is required for urease activity and virulence in experimental urinary tract infections', *Infection and Immunity*. American Society for Microbiology Journals, 71(2), pp. 1026–1030. doi: 10.1128/IAI.71.2.1026-1030.2003.

Dayyoub, E. *et al.* (2017) 'Antibacterial and anti-encrustation biodegradable polymer coating for urinary catheter', *International Journal of Pharmaceutics*. Elsevier B.V., 531(1), pp. 205–214. doi: 10.1016/j.ijpharm.2017.08.072.

DeGroot-Kosolcharoen, J., Guse, R. and Jones, J. M. (1988) 'Evaluation of a urinary catheter with a preconnected closed drainage bag.', *Infection control and hospital epidemiology*, 9(2), pp. 72–6. Available at: http://www.ncbi.nlm.nih.gov/pubmed/3343502 (Accessed: 3 September 2019).

Delcaru, C. *et al.* (2016) 'Microbial biofilms in urinary tract infections and prostatitis: Etiology, pathogenicity, and combating strategies', *Pathogens*. MDPI AG. doi: 10.3390/pathogens5040065.

Dembek, M. *et al.* (2015) 'High-throughput analysis of gene essentiality and sporulation in *Clostridium difficile*', *mBio*. American Society for Microbiology, 6(2). doi: 10.1128/mBio.02383-14.

DeSantis, T. Z. *et al.* (2006) 'Greengenes, a chimera-checked 16S rRNA gene database and workbench compatible with ARB', *Applied and Environmental Microbiology*. Appl Environ Microbiol, 72(7), pp. 5069–5072. doi: 10.1128/AEM.03006-05.

Deshler, J. O. (1992) 'A simple method for randomly mutating cloned DNA fragments by using chemical mutagens and the polymerase chain reaction', *Genetic Analysis: Biomolecular Engineering*, 9(4), pp. 103–106. doi: 10.1016/1050-3862(92)90048-A.

Dhami, N. K., Reddy, M. S. and Mukherjee, M. S. (2013) 'Biomineralization of calcium carbonates and their engineered applications: A review', *Frontiers in Microbiology*. Frontiers Media S.A. doi: 10.3389/fmicb.2013.00314.

Diaz Blanco, C. *et al.* (2014) 'Building an antifouling zwitterionic coating on urinary catheters using an enzymatically triggered bottom-up approach', *ACS Applied Materials and Interfaces*. American Chemical Society, 6(14), pp. 11385–11393. doi: 10.1021/am501961b.

Djordjevic, M. L. *et al.* (2016) 'Urethral Stricture Disease: Challenges and Ongoing Controversies', *Advances in urology*. Adv Urol, 2016. doi: 10.1155/2016/1238369.

Donlan, R. M. (2002) 'Biofilms: Microbial life on surfaces', *Emerging Infectious Diseases*. Centers for Disease Control and Prevention (CDC), pp. 881–890. doi: 10.3201/eid0809.020063.

Donlan, R. M. and Costerton, J. W. (2002) 'Biofilms: Survival mechanisms of clinically relevant microorganisms', *Clinical Microbiology Reviews*, pp. 167–193. doi: 10.1128/CMR.15.2.167-193.2002.

Dufour, A., Furness, R. B. and Hughes, C. (1998) 'Novel genes that upregulate the *Proteus mirabilis* flhDC master operon controlling flagellar biogenesis and swarming', *Molecular Microbiology*, 29(3), pp. 741–751. doi: 10.1046/j.1365-2958.1998.00967.x.

Dumanski, A. J. *et al.* (1994) 'Unique ability of the *Proteus mirabilis* capsule to enhance mineral growth in infectious urinary calculi', *Infection and Immunity*. American Society for Microbiology, pp. 2998–3003. doi: 10.1128/iai.62.7.2998-3003.1994.

Dundas, A. A. *et al.* (2019) 'Validating a Predictive Structure–Property

Relationship by Discovery of Novel Polymers which Reduce Bacterial Biofilm Formation', *Advanced Materials*. Wiley-VCH Verlag, 31(49), p. 1903513. doi: 10.1002/adma.201903513.

Dzianach, P. A. *et al.* (2019) 'Challenges of biofilm control and utilization: Lessons from mathematical modelling', *Journal of the Royal Society Interface*. Royal Society Publishing. doi: 10.1098/rsif.2019.0042.

Eckert, S. E. *et al.* (2011) 'Retrospective application of transposon-directed insertion site sequencing to a library of signature-tagged mini-Tn5Km2 mutants of *Escherichia coli* O157:H7 screened in cattle', *Journal of Bacteriology*. J Bacteriol, 193(7), pp. 1771–1776. doi: 10.1128/JB.01292-10.

Edgar, R. C. (2004) 'MUSCLE: Multiple sequence alignment with high accuracy and high throughput', *Nucleic Acids Research*. Oxford Academic, 32(5), pp. 1792–1797. doi: 10.1093/nar/gkh340.

Edgar, R. C. *et al.* (2011) 'UCHIME improves sensitivity and speed of chimera detection', *Bioinformatics*. Oxford University Press, 27(16), pp. 2194–2200. doi: 10.1093/bioinformatics/btr381.

Edgar, R. C. (2013) 'UPARSE: Highly accurate OTU sequences from microbial amplicon reads', *Nature Methods*. Nature Publishing Group, 10(10), pp. 996–998. doi: 10.1038/nmeth.2604.

Elias, S. and Banin, E. (2012) 'Multi-species biofilms: Living with friendly neighbors', *FEMS Microbiology Reviews*. FEMS Microbiol Rev, pp. 990–1004. doi: 10.1111/j.1574-6976.2012.00325.x.

Estiu, G. and Merz, K. M. (2004) 'The hydrolysis of urea and the proficiency of urease', *Journal of the American Chemical Society*. American Chemical Society , 126(22), pp. 6932–6944. doi: 10.1021/ja049327g.

Falkinham, J. O. and Hoffman, P. S. (1984) 'Unique developmental characteristics of the swarm and short cells of *Proteus vulgaris* and *Proteus mirabilis*', *Journal of Bacteriology*. J Bacteriol, 158(3), pp. 1037–1040. doi: 10.1128/jb.158.3.1037-1040.1984.

Fels, U., Gevaert, K. and Van Damme, P. (2020) 'Bacterial Genetic Engineering by Means of Recombineering for Reverse Genetics', *Frontiers in Microbiology*. Frontiers Media S.A., p. 2161. doi: 10.3389/fmicb.2020.548410.

Feneley, R. C. L., Hopley, I. B. and Wells, P. N. T. (2015) 'Urinary catheters: History, current status, adverse events and research agenda', *Journal of Medical Engineering and Technology*. Taylor and Francis Ltd, 39(8), pp. 459–470. doi: 10.3109/03091902.2015.1085600.

Ferreiro, J. L. L. *et al.* (2017) '*Pseudomonas aeruginosa* urinary tract infections in hospitalized patients: Mortality and prognostic factors', *PLoS ONE*. Public Library of Science, 12(5). doi: 10.1371/journal.pone.0178178.

Finnegan, M. *et al.* (2010) 'Mode of action of hydrogen peroxide and other oxidizing agents: differences between liquid and gas forms', *Journal of Antimicrobial Chemotherapy*, 65(10), pp. 2108–2115. doi: 10.1093/jac/dkq308.

Fisher, H. *et al.* (2018) 'Continuous low-dose antibiotic prophylaxis for adults

with repeated urinary tract infections (AnTIC): a randomised, open-label trial', *The Lancet Infectious Diseases*. Lancet Publishing Group, 18(9), pp. 957–968. doi: 10.1016/S1473-3099(18)30279-2.

Flannigan, R. K. *et al.* (2018) 'Evaluating factors that dictate struvite stone composition: A multiinstitutional clinical experience from the EDGE Research Consortium', *Canadian Urological Association Journal*. Canadian Urological Association, 12(4), pp. 131–136. doi: 10.5489/cuaj.4804.

Flemming, H. C. and Wingender, J. (2010) 'The biofilm matrix', *Nature Reviews Microbiology*, pp. 623–633. doi: 10.1038/nrmicro2415.

Flores-Mireles, A., Hreha, T. N. and Hunstad, D. A. (2019) 'Pathophysiology, treatment, and prevention of catheter-associated urinary tract infection', *Topics in Spinal Cord Injury Rehabilitation*. Thomas Land Publishers Inc., 25(3), pp. 228–240. doi: 10.1310/sci2503-228.

Flores-Mireles, A. L. *et al.* (2014) 'EbpA vaccine antibodies block binding of *Enterococcus faecalis* to fibrinogen to prevent catheter-associated bladder infection in mice', *Science Translational Medicine*. American Association for the Advancement of Science, 6(254). doi: 10.1126/scitranslmed.3009384.

Flores-Mireles, A. L. *et al.* (2015) 'Urinary tract infections: Epidemiology, mechanisms of infection and treatment options', *Nature Reviews Microbiology*. Nature Publishing Group, pp. 269–284. doi: 10.1038/nrmicro3432.

Flores-Mireles, A. L. *et al.* (2016) 'Fibrinogen Release and Deposition on Urinary Catheters Placed during Urological Procedures', *Journal of Urology*. Elsevier Inc., 196(2), pp. 416–421. doi: 10.1016/j.juro.2016.01.100.

Francolini, I. *et al.* (2017) 'Antifouling and antimicrobial biomaterials: an overview', *APMIS*. Blackwell Munksgaard, pp. 392–417. doi: 10.1111/apm.12675.

Frank, D. N. *et al.* (2009) 'Culture-Independent Microbiological Analysis of Foley Urinary Catheter Biofilms', *PLoS ONE*. Edited by A. J. Ratner. Public Library of Science, 4(11), p. e7811. doi: 10.1371/journal.pone.0007811.

Franklin, T. J. and Snow, G. A. (2005) *Biochemistry and molecular biology of antimicrobial drug action*, *Biochemistry and Molecular Biology of Antimicrobial Drug Action*. Springer US. doi: 10.1007/0-387-27566-5.

Frassetto, L. (2011) *Treatment and Prevention of Kidney Stones: An Update*, *American Family Physician*. Available at: www.aafp.org/afp. (Accessed: 10 February 2021).

Freed, N. E. (2017) 'Creation of a dense transposon insertion library using bacterial conjugation in enterobacterial strains such as *Escherichia coli* or *Shigella flexneri*', *Journal of Visualized Experiments*. Journal of Visualized Experiments, 2017(127). doi: 10.3791/56216.

Fuchs, A. D. and Tiller, J. C. (2006) 'Contact-Active Antimicrobial Coatings Derived from Aqueous Suspensions', *Angewandte Chemie International Edition*, 45(40), pp. 6759–6762. doi: 10.1002/anie.200602738.

Fusco, A. *et al.* (2017) 'Biofilm formation and immunomodulatory activity of

Proteus mirabilis clinically isolated strains', *International Journal of Molecular Sciences*. MDPI AG, 18(2). doi: 10.3390/ijms18020414.

Gallagher, L. *et al.* (2007) 'Creating Recombination-Activated Genes and Sequence-Defined Mutant Libraries Using Transposons', *Methods in Enzymology*. Methods Enzymol, pp. 126–140. doi: 10.1016/S0076-6879(06)21012-7.

Gallagher, L. A. *et al.* (2013) 'Sequence-defined transposon mutant library of *Burkholderia thailandensis*', *mBio*. American Society for Microbiology, 4(6). doi: 10.1128/mBio.00604-13.

Gao, M. *et al.* (2016) 'A crucial role for spatial distribution in bacterial quorum sensing', *Scientific Reports*. Nature Publishing Group, 6. doi: 10.1038/srep34695.

Gaonkar, T. A., Caraos, L. and Modak, S. (2007) 'Efficacy of a Silicone Urinary Catheter Impregnated with Chlorhexidine and Triclosan Against Colonization With *Proteus mirabilis* and Other Uropathogens', *Infection Control & Hospital Epidemiology*, 28(05), pp. 596–598. doi: 10.1086/513449.

Gaonkar, T. A., Sampath, L. A. and Modak, S. M. (2003) 'Evaluation of the Antimicrobial Efficacy of Urinary Catheters Impregnated With Antiseptics in an In Vitro Urinary Tract Model', *Infection Control & Hospital Epidemiology*. Cambridge University Press (CUP), 24(7), pp. 506–513. doi: 10.1086/502241.

Gardner, A. *et al.* (2014) 'A point prevalence cross-sectional study of healthcare-associated urinary tract infections in six Australian hospitals', *BMJ Open*. BMJ Publishing Group, 4(7). doi: 10.1136/bmjopen-2014-005099.

Garibaldi, R. A. *et al.* (1974) 'Factors Predisposing to Bacteriuria during Indwelling Urethral Catheterization', *New England Journal of Medicine*, 291(5), pp. 215–219. doi: 10.1056/NEJM197408012910501.

Garrett, E. S., Perlegas, D. and Wozniak, D. J. (1999) 'Negative control of flagellum synthesis in *Pseudomonas aeruginosa* is modulated by the alternative sigma factor algT (algU)', *Journal of Bacteriology*. American Society for Microbiology, 181(23), pp. 7401–7404. doi: 10.1128/jb.181.23.7401-7404.1999.

Gault, M. H. *et al.* (1993) 'Calcium and calcium magnesium carbonate specimens submitted as urinary tract stones', *Journal of Urology*. J Urol, 149(2), pp. 244–249. doi: 10.1016/S0022-5347(17)36047-0.

Gebreyohannes, G. *et al.* (2019) 'Challenges of intervention, treatment, and antibiotic resistance of biofilm-forming microorganisms', *Heliyon*. Elsevier Ltd. doi: 10.1016/j.heliyon.2019.e02192.

Genevaux, P., Muller, S. and Bauda, P. (1996) 'A rapid screening procedure to identify mini-Tn10 insertion mutants of *Escherichia coli* K-12 with altered adhesion properties', *FEMS Microbiology Letters*. Oxford University Press (OUP), 142(1), pp. 27–30. doi: 10.1111/j.1574-6968.1996.tb08402.x.

Getliffe, K. A. (1994) 'The characteristics and management of patients with recurrent blockage of long-term urinary catheters', *Journal of Advanced*

Nursing, 20(1), pp. 140–149. doi: 10.1046/j.1365-2648.1994.20010140.x.

Ghanbari, A. *et al.* (2016) 'Inoculation density and nutrient level determine the formation of mushroom-shaped structures in *Pseudomonas aeruginosa* biofilms', *Scientific Reports*. Nature Publishing Group, 6, p. 32097. doi: 10.1038/srep32097.

Ghigo, J. M. (2001) 'Natural conjugative plasmids induce bacterial biofilm development', *Nature*, 412(6845), pp. 442–445. doi: 10.1038/35086581.

Giamarellos-Bourboulis, E. J. *et al.* (2006) 'Multidrug resistance to antimicrobials as a predominant factor influencing patient survival', *International Journal of Antimicrobial Agents*, 27(6), pp. 476–481. doi: 10.1016/j.ijantimicag.2005.12.013.

Giani, A. M. *et al.* (2020) 'Long walk to genomics: History and current approaches to genome sequencing and assembly', *Computational and Structural Biotechnology Journal*. Elsevier B.V., pp. 9–19. doi: 10.1016/j.csbj.2019.11.002.

Gibbons, R. J. and Fitzgerald, R. J. (1969) 'Dextran-induced agglutination of *Streptococcus mutans*, and its potential role in the formation of microbial dental plaques.', *Journal of bacteriology*. American Society for Microbiology (ASM), 98(2), pp. 341–6. Available at: http://www.ncbi.nlm.nih.gov/pubmed/5784196 (Accessed: 23 July 2020).

Gibbs, K. A., Urbanowski, M. L. and Greenberg, E. P. (2008) 'Genetic determinants of self identity and social recognition in bacteria', *Science*. NIH Public Access, 321(5886), pp. 256–259. doi: 10.1126/science.1160033.

Gillor, O., Giladi, I. and Riley, M. A. (2009) 'Persistence of colicinogenic *Escherichia coli* in the mouse gastrointestinal tract', *BMC Microbiology*. BMC Microbiol, 9. doi: 10.1186/1471-2180-9-165.

Girgis, H. S. *et al.* (2007) 'A comprehensive genetic characterization of bacterial motility', *PLoS Genetics*, 3(9), pp. 1644–1660. doi: 10.1371/journal.pgen.0030154.

Glahn, B. E. (1988) 'Influence of drainage conditions on mucosal bladder damage by indwelling catheters. I. Pressure study', *Scandinavian Journal of Urology and Nephrology*, 22(2), pp. 87–92. doi: 10.1080/00365599.1988.11690391.

Goble, N. M., Clarke, T. and Hammonds, J. C. (1989) 'Histological changes in the urinary bladder secondary to urethral catheterisation.', *British journal of urology*, 63(4), pp. 354–7. doi: 10.1111/j.1464-410x.1989.tb05216.x.

Godiska, R. *et al.* (2009) 'Linear plasmid vector for cloning of repetitive or unstable sequences in *Escherichia coli*', *Nucleic Acids Research*. Oxford University Press, 38(6), p. e88. doi: 10.1093/nar/gkp1181.

Gorbachinsky, I. *et al.* (2014) 'Altered perineal microbiome is associated with vulvovaginitis and urinary tract infection in preadolescent girls', *Therapeutic Advances in Urology*, 6(6), pp. 224–229. doi: 10.1177/1756287214542097.

Graeber, D. *et al.* (2019) 'Biofilm-specific uptake does not explain differences

in whole-stream DOC tracer uptake between a forest and an agricultural stream', *Biogeochemistry*. Springer International Publishing. doi: 10.1007/s10533-019-00573-6.

Grases, F. *et al.* (2001) 'Study on Concretions Developed around Urinary Catheters and Mechanisms of Renal Calculi Development', *Nephron*. Karger Publishers, 88(4), pp. 320–328. doi: 10.1159/000046015.

Greatbatch, W. and Holmes, C. F. (1991) 'History of Implantable Devices: Entrepreneurs, Bioengineers and the Medical Profession, in a Unique Collaboration, Build an Important New Industry', *IEEE Engineering in Medicine and Biology Magazine*. IEEE Eng Med Biol Mag, 10(3), pp. 38–41. doi: 10.1109/51.84185.

Green, B. *et al.* (2012) 'Insertion site preference of Mu, Tn5, and Tn7 transposons', *Mobile DNA*. BioMed Central, 3(1), p. 3. doi: 10.1186/1759-8753-3-3.

Griffith, D., Musher, D. and Itin, C. (1976) 'Urease. The primary cause of infection-induced urinary stones.', *Investigative urology*. Available at: https://europepmc.org/article/med/815197 (Accessed: 22 March 2021).

Guiton, P. S. *et al.* (2013) '*Enterococcus faecalis* overcomes foreign body-mediated inflammation to establish urinary tract infections', *Infection and Immunity*. American Society for Microbiology (ASM), 81(1), pp. 329–339. doi: 10.1128/IAI.00856-12.

Haas, B. J. *et al.* (2011) 'Chimeric 16S rRNA sequence formation and detection in Sanger and 454-pyrosequenced PCR amplicons', *Genome Research*. Genome Res, 21(3), pp. 494–504. doi: 10.1101/gr.112730.110.

Hadjifrangiskou, M. *et al.* (2012) 'Transposon mutagenesis identifies uropathogenic *Escherichia coli* biofilm factors', *Journal of Bacteriology*. American Society for Microbiology Journals, 194(22), pp. 6195–6205. doi: 10.1128/JB.01012-12.

Hall, C. W. and Mah, T. F. (2017) 'Molecular mechanisms of biofilm-based antibiotic resistance and tolerance in pathogenic bacteria', *FEMS Microbiology Reviews*. Oxford University Press, pp. 276–301. doi: 10.1093/femsre/fux010.

Hamamci, N. *et al.* (1998) *A quantitative study of genital skin ¯ora and urinary colonization in spinal cord injured patients*. Available at: http://www.stockton-press.co.uk/sc (Accessed: 21 January 2020).

Hamilton, A. L. *et al.* (2018) '*Proteus* spp. as putative gastrointestinal pathogens', *Clinical Microbiology Reviews*. American Society for Microbiology. doi: 10.1128/CMR.00085-17.

Harding, G. K. M. *et al.* (2002) 'Antimicrobial treatment in diabetic women with asymptomatic bacteriuria', *New England Journal of Medicine*. N Engl J Med, 347(20), pp. 1576–1583. doi: 10.1056/NEJMoa021042.

Harrison, J. J. *et al.* (2020) 'Elevated exopolysaccharide levels in *Pseudomonas aeruginosa* flagellar mutants have implications for biofilm growth and chronic infections', *PLoS Genetics*. Public Library of Science, 16(6), p. e1008848. doi:

10.1371/journal.pgen.1008848.

Harshey, R. M. (2012) ‘The Mu story: how a maverick phage moved the field forward’, *Mobile DNA*. Springer Nature, 3(1), p. 21. doi: 10.1186/1759-8753-3-21.

Hashmi, S. *et al.* (2003) ‘Urinary tract infection in surgical patients’, *American Journal of Surgery*. Elsevier Inc., pp. 53–56. doi: 10.1016/S0002-9610(03)00120-X.

Hauser, G. (1885) ‘Uber Faulnisbakterien und deren Beziehungen zur Septicamie. Ein Beitrag zur Morphologie der Spaltpilze’, *Vogel, Leipzig*.

Hedstrom, L. (2002) ‘Serine protease mechanism and specificity.’, *Chemical reviews*, 102(12), pp. 4501–24. Available at: http://www.ncbi.nlm.nih.gov/pubmed/12475199 (Accessed: 1 June 2019).

Hensel, M. and Holden, D. W. (1996) ‘Molecular genetic approaches for the study of virulence in both pathogenic bacteria and fungi’, *Microbiology*. Microbiology Society, pp. 1049–1058. doi: 10.1099/13500872-142-5-1049.

Heydorn, A. *et al.* (2000) ‘Quantification of biofilm structures by the novel computer program COMSTAT’, *Microbiology*. Society for General Microbiology, 146(10), pp. 2395–2407. doi: 10.1099/00221287-146-10-2395.

Hibbing, M. E. *et al.* (2010) ‘Bacterial competition: Surviving and thriving in the microbial jungle’, *Nature Reviews Microbiology*. Nat Rev Microbiol, pp. 15–25. doi: 10.1038/nrmicro2259.

Hickman, J. W. and Harwood, C. S. (2008) ‘Identification of FleQ from *Pseudomonas aeruginosa* as a c-di-GMP-responsive transcription factor’, *Molecular Microbiology*. Blackwell Publishing Ltd, 69(2), pp. 376–389. doi: 10.1111/j.1365-2958.2008.06281.x.

Himpsl, S. D. *et al.* (2008) ‘Identification of virulence determinants in uropathogenic *Proteus mirabilis* using signature-tagged mutagenesis’, *Journal of Medical Microbiology*, 57(9), pp. 1068–1078. doi: 10.1099/jmm.0.2008/002071-0.

Hiraku, Y. *et al.* (2004) ‘Mechanism of carcinogenesis induced by a veterinary antimicrobial drug, nitrofurazone, via oxidative DNA damage and cell proliferation’, *Cancer Letters*. Cancer Lett, 215(2), pp. 141–150. doi: 10.1016/j.canlet.2004.05.016.

Hizukuri, Y. *et al.* (2006) ‘Role of the intramolecular disulfide bond in FlgI, the flagellar P-ring component of *Escherichia coli*’, *Journal of Bacteriology*. J Bacteriol, 188(12), pp. 4190–4197. doi: 10.1128/JB.01896-05.

Hizukuri, Y. *et al.* (2008) ‘Systematic Cys mutagenesis of FlgI, the flagellar P-ring component of *Escherichia coli*’, *Microbiology*. Microbiology Society, 154(3), pp. 810–817. doi: 10.1099/mic.0.2007/013854-0.

Hoffman, S. B. (2001) ‘Mechanisms of Antibiotic Resistance’, *Compendium on Continuing Education for the Practicing Veterinarian*, 23(5), pp. 464–472. doi: 10.1128/microbiolspec.vmbf-0016-2015.

Hola, V., Peroutkova, T. and Ruzicka, F. (2012) 'Virulence factors in *Proteus* bacteria from biofilm communities of catheter-associated urinary tract infections', *FEMS Immunology & Medical Microbiology*, 65(2), pp. 343–349. doi: 10.1111/j.1574-695X.2012.00976.x.

Holá, V., Ruzicka, F. and Horka, M. (2010) 'Microbial diversity in biofilm infections of the urinary tract with the use of sonication techniques: Table 1', *FEMS Immunology & Medical Microbiology*. Blackwell Publishing Ltd, 59(3), pp. 525–528. doi: 10.1111/j.1574-695X.2010.00703.x.

Holland, A. and Fish, D. (2012) 'Benefits of the Insertion Tip and Closed-System Sleeve for Intermittent Catheterization', *C. R. Bard Inc., Murray Hill, NJ, USA,* (http://m.bardmedical.com/media/135500/touchless_whitepaper.pdf, 2012).

Hollenbeak, C. S. and Schilling, A. L. (2018) 'The attributable cost of catheter-associated urinary tract infections in the United States: A systematic review', *American Journal of Infection Control*. Mosby Inc., 46(7), pp. 751–757. doi: 10.1016/j.ajic.2018.01.015.

Holling, N. *et al.* (2014) 'Elucidating the genetic basis of crystalline biofilm formation in *Proteus mirabilis*', *Infection and Immunity*. American Society for Microbiology, 82(4), pp. 1616–1626. doi: 10.1128/IAI.01652-13.

Hook, A. L. *et al.* (2012) 'Combinatorial discovery of polymers resistant to bacterial attachment', *Nature Biotechnology*, 30(9), pp. 868–875. doi: 10.1038/nbt.2316.

Hook, A. L. *et al.* (2013) 'Discovery of Novel Materials with Broad Resistance to Bacterial Attachment Using Combinatorial Polymer Microarrays', *Advanced Materials*, 25(18), pp. 2542–2547. doi: 10.1002/adma.201204936.

Hooton, T. M. *et al.* (2010) 'Diagnosis, prevention, and treatment of catheter-associated urinary tract infection in adults: 2009 international clinical practice guidelines from the Infectious Diseases Society of America', *Clinical Infectious Diseases*. Clin Infect Dis, pp. 625–663. doi: 10.1086/650482.

Horwitz, D. *et al.* (2015) 'Decreased microbiota diversity associated with urinary tract infection in a trial of bacterial interference', *Journal of Infection*. W.B. Saunders Ltd, 71(3), pp. 358–367. doi: 10.1016/j.jinf.2015.05.014.

Hoyle, B. D., Alcantara, J. and Costerton, J. W. (1992) '*Pseudomonas aeruginosa* biofilm as a diffusion barrier to piperacillin', *Antimicrobial Agents and Chemotherapy*. American Society for Microbiology (ASM), pp. 2054–2056. doi: 10.1128/AAC.36.9.2054.

Hsiao, C. Y. *et al.* (2015) 'Risk Factors for Development of Septic Shock in Patients with Urinary Tract Infection', *BioMed Research International*. Hindawi Publishing Corporation, 2015. doi: 10.1155/2015/717094.

Hu, R. *et al.* (2020) 'Biological Characteristics and Genetic Analysis of a Highly Pathogenic *Proteus mirabilis* Strain Isolated From Dogs in China', *Frontiers in Veterinary Science*. Frontiers Media S.A., 7, p. 589. doi: 10.3389/fvets.2020.00589.

Hustinx, W. N. *et al.* (1991) 'Impact of concurrent antimicrobial therapy on catheter-associated urinary tract infection.', *The Journal of hospital infection*, 18(1), pp. 45–56. doi: 10.1016/0195-6701(91)90092-m.

Huttner, B. *et al.* (2012) 'Drugs of last resort? the use of polymyxins and tigecycline at us veterans affairs medical centers, 2005-2010', *PLoS ONE*. Public Library of Science, 7(5). doi: 10.1371/journal.pone.0036649.

Imelfort, M. *et al.* (2009) 'Genome sequencing approaches and successes', *Methods in Molecular Biology*. Humana Press, 513, pp. 345–358. doi: 10.1007/978-1-59745-427-8_18.

Island, M. D. and Mobley, H. L. T. (1995) '*Proteus mirabilis* urease: Operon fusion and linker insertion analysis of ure gene organization, regulation, and function', *Journal of Bacteriology*. American Society for Microbiology, 177(19), pp. 5653–5660. doi: 10.1128/jb.177.19.5653-5660.1995.

Ivics, Z. and Izsvák, Z. (2010) 'The expanding universe of transposon technologies for gene and cell engineering', *Mobile DNA*. BioMed Central, pp. 1–15. doi: 10.1186/1759-8753-1-25.

Jacobs, M. A. *et al.* (2003) 'Comprehensive transposon mutant library of *Pseudomonas aeruginosa*', *Proceedings of the National Academy of Sciences of the United States of America*. National Academy of Sciences, 100(SUPPL. 2), pp. 14339–14344. doi: 10.1073/pnas.2036282100.

Jacobsen, D., Åkesson, I. and Shefterd, E. (1982) 'Urinary calcium oxalate monohydrate crystals in ethylene glycol poisoning', *Scandinavian Journal of Clinical and Laboratory Investigation*. Informa Healthcare, pp. 231–234. doi: 10.1080/00365518209168078.

Jacobsen, S. M. *et al.* (2008) 'Complicated catheter-associated urinary tract infections due to *Escherichia coli* and *Proteus mirabilis*', *Clinical Microbiology Reviews*, pp. 26–59. doi: 10.1128/CMR.00019-07.

Jacobsen, S. M. and Shirtliff, M. E. (2011) '*Proteus mirabilis* biofilms and catheter-associated urinary tract infections'. doi: 10.4161/viru.2.5.17783.

Jacoby, G. A. (2009) 'AmpC B-Lactamases', *Clinical Microbiology Reviews*, pp. 161–182. doi: 10.1128/CMR.00036-08.

Jansen, A. M. *et al.* (2004) 'Mannose-resistant *Proteus*-like fimbriae are produced by most *Proteus mirabilis* strains infecting the urinary tract, dictate the in vivo localization of bacteria, and contribute to biofilm formation', *Infection and Immunity*, 72(12), pp. 7294–7305. doi: 10.1128/IAI.72.12.7294-7305.2004.

Johnson, J. R. (1991) 'Virulence factors in *Escherichia coli* urinary tract infection', *Clinical Microbiology Reviews*. American Society for Microbiology, 4(1), pp. 80–128. doi: 10.1128/CMR.4.1.80.

Johnson, J. R., Kuskowski, M. A. and Wilt, T. J. (2006) 'Systematic review: Antimicrobial urinary catheters to prevent catheter-associated urinary tract infection in hospitalized patients', *Annals of Internal Medicine*. American College of Physicians, pp. 116–126. doi: 10.7326/0003-4819-144-2-

200601170-00009.

Jones, B. D. and Mobley, H. L. T. (1988) '*Proteus mirabilis* urease: Genetic organization, regulation, and expression of structural genes', *Journal of Bacteriology*. American Society for Microbiology Journals, 170(8), pp. 3342–3349. doi: 10.1128/jb.170.8.3342-3349.1988.

Jones, B. D. and Mobley, H. L. T. (1989) '*Proteus mirabilis* urease: Nucleotide sequence determination and comparison with jack bean urease', *Journal of Bacteriology*. J Bacteriol, 171(12), pp. 6414–6422. doi: 10.1128/jb.171.12.6414-6422.1989.

Jones, B. V. *et al.* (2004) 'Ultrastructure of *Proteus mirabilis* swarmer cell rafts and role of swarming in catheter-associated urinary tract infection', *Infection and Immunity*, 72(7), pp. 3941–3950. doi: 10.1128/IAI.72.7.3941-3950.2004.

Jones, B. V. *et al.* (2005) 'Role of swarming in the formation of crystalline *Proteus mirabilis* biofilms on urinary catheters', *Journal of Medical Microbiology*, 54(9), pp. 807–813. doi: 10.1099/jmm.0.46123-0.

Jones, C. J. *et al.* (1990) 'Stoichiometric analysis of the flagellar hook-(basal-body) complex of *Salmonella typhimurium*', *Journal of Molecular Biology*. Academic Press, 212(2), pp. 377–387. doi: 10.1016/0022-2836(90)90132-6.

Jordan, R. P. C. and Nicolle, L. E. (2014) 'Preventing Infection Associated with Urethral Catheter Biofilms', *Biofilms in Infection Prevention and Control*. Academic Press, pp. 287–309. doi: 10.1016/B978-0-12-397043-5.00016-5.

Joung, Y. H. (2013) 'Development of implantable medical devices: From an engineering perspective', *International Neurourology Journal*. Korean Continence Society, 17(3), pp. 98–106. doi: 10.5213/inj.2013.17.3.98.

Kadonaga, J. T. and Knowles, J. R. (1985) 'A simple and efficient method for chemical mutagenesis of DNA', *Nucleic Acids Research*. Oxford University Press, 13(5), pp. 1733–1745. doi: 10.1093/nar/13.5.1733.

Kadurugamuwa, J. L. *et al.* (2005) 'Noninvasive biophotonic imaging for monitoring of catheter-associated urinary tract infections and therapy in mice', *Infection and Immunity*. Infect Immun, 73(7), pp. 3878–3887. doi: 10.1128/IAI.73.7.3878-3887.2005.

Kara, D. *et al.* (2007) 'Microstructural differences between single-species and dual-species biofilms of *Streptococcus mutans* and *Veillonella parvula*, before and after exposure to chlorhexidine', *FEMS Microbiology Letters*. John Wiley & Sons, Ltd, 271(1), pp. 90–97. doi: 10.1111/j.1574-6968.2007.00701.x.

Kazan, Z. *et al.* (2006) 'Effective prevention of microbial biofilm formation on medical devices by low-energy surface acoustic waves', *Antimicrobial Agents and Chemotherapy*. American Society for Microbiology Journals, 50(12), pp. 4144–4152. doi: 10.1128/AAC.00418-06.

Kearns, D. B. (2010) 'A field guide to bacterial swarming motility', *Nature Reviews Microbiology*, pp. 634–644. doi: 10.1038/nrmicro2405.

Kerchove, A. J. de and Elimelech, M. (2008) 'Bacterial Swimming Motility Enhances Cell Deposition and Surface Coverage', *Environmental Science &*

Technology, 42(12), pp. 4371–4377. doi: 10.1021/es703028u.

Kerfeld, C. A. and Scott, K. M. (2011) 'Using BLAST to Teach "E-value-tionary" Concepts', *PLoS Biology*. Edited by C. A. Kerfeld. Public Library of Science, 9(2), p. e1001014. doi: 10.1371/journal.pbio.1001014.

Khatoon, Z. *et al.* (2018) 'Bacterial biofilm formation on implantable devices and approaches to its treatment and prevention', *Heliyon*. Elsevier Ltd. doi: 10.1016/j.heliyon.2018.e01067.

Khmel, I. A. and Metlitskaya, A. Z. (2006) 'Quorum sensing regulation of gene expression: A promising target for drugs against bacterial pathogenicity', *Molecular Biology*, pp. 169–182. doi: 10.1134/S0026893306020014.

Kiljunen, S. *et al.* (2014) 'Generation of comprehensive transposon insertion mutant library for the model archaeon, *Haloferax volcanii*, and its use for gene discovery', *BMC Biology*. BioMed Central Ltd., 12(1). doi: 10.1186/s12915-014-0103-3.

Kilonzo, M. *et al.* (2014) 'Cost effectiveness of antimicrobial catheters for adults requiring short-term catheterisation in hospital', *European Urology*. Elsevier, 66(4), pp. 615–618. doi: 10.1016/j.eururo.2014.05.035.

Klausen, M., Heydorn, A., *et al.* (2003) 'Biofilm formation by *Pseudomonas aeruginosa* wild type, flagella and type IV pili mutants', *Molecular Microbiology*, 48(6), pp. 1511–1524. doi: 10.1046/j.1365-2958.2003.03525.x.

Klausen, M., Aaes-Jørgensen, A., *et al.* (2003) 'Involvement of bacterial migration in the development of complex multicellular structures in *Pseudomonas aeruginosa* biofilms', *Molecular Microbiology*, 50(1), pp. 61–68. doi: 10.1046/j.1365-2958.2003.03677.x.

Kline, K. A. and Lewis, A. L. (2016) 'Gram-Positive Uropathogens, Polymicrobial Urinary Tract Infection, and the Emerging Microbiota of the Urinary Tract', *Microbiology Spectrum*. American Society for Microbiology, 4(2). doi: 10.1128/microbiolspec.uti-0012-2012.

Koda, R., Watanabe, H. and Iino, N. (2017) 'Calcium oxalate monohydrate crystals in ethylene glycol poisoning', *Clinical and Experimental Nephrology*. Springer Tokyo, 21(4), pp. 741–742. doi: 10.1007/s10157-016-1332-2.

Kohler-Ockmore, J. (1996) 'Long-term catheterization of the bladder: Prevalence and morbidity', *British Journal of Urology*. Blackwell Publishing Ltd., 77(3), pp. 347–351. doi: 10.1046/j.1464-410X.1996.09074.x.

Konieczna, I. *et al.* (2013) 'Bacterial Urease and its Role in Long-Lasting Human Diseases', *Current Protein and Peptide Science*. Bentham Science Publishers Ltd., 13(8), pp. 789–806. doi: 10.2174/138920312804871094.

Kostakioti, M., Hadjifrangiskou, M. and Hultgren, S. J. (2013) 'Bacterial biofilms: Development, dispersal, and therapeutic strategies in the dawn of the postantibiotic era', *Cold Spring Harbor Perspectives in Medicine*, 3(4). doi: 10.1101/cshperspect.a010306.

Kostriken, R., Morita, C. and Heffron, F. (1981) 'Transposon Tn3 encodes a site-specific recombination system: Identification of essential sequences, genes,

and actual site of recombination', *Proceedings of the National Academy of Sciences of the United States of America*. Proc Natl Acad Sci U S A, 78(7 I), pp. 4041–4045. doi: 10.1073/pnas.78.7.4041.

Köves, B., Magyar, A. and Tenke, P. (2017) 'Spectrum and antibiotic resistance of catheter-associated urinary tract infections.', *GMS infectious diseases*, 5, p. Doc06. doi: 10.3205/id000032.

Kristich, C. J. *et al.* (2008) 'Development and use of an efficient system for random mariner transposon mutagenesis to identify novel genetic determinants of biofilm formation in the core *Enterococcus faecalis* genome', *Applied and Environmental Microbiology*. Appl Environ Microbiol, 74(11), pp. 3377–3386. doi: 10.1128/AEM.02665-07.

Kucheria, R. *et al.* (2005) 'Urinary tract infections: New insights into a common problem', *Postgraduate Medical Journal*. Postgrad Med J, pp. 83–86. doi: 10.1136/pgmj.2004.023036.

Kulasekara, H. D. (2014) 'Transposon mutagenesis', *Methods in Molecular Biology*. Humana Press Inc., 1149, pp. 501–519. doi: 10.1007/978-1-4939-0473-0_39.

Kumar, R. and Münstedt, H. (2005) 'Silver ion release from antimicrobial polyamide/silver composites', *Biomaterials*, 26(14), pp. 2081–2088. doi: 10.1016/j.biomaterials.2004.05.030.

Kumar, S. and Muchmore, A. (1990) 'Tamm-Horsfall protein - uromodulin (1950-1990)', *Kidney International*, pp. 1395–1401. doi: 10.1038/ki.1990.128.

Kunin, C. M. (2006) 'Urinary-catheter-associated infections in the elderly', *International Journal of Antimicrobial Agents*, 28, pp. 78–81. doi: 10.1016/j.ijantimicag.2006.05.013.

Kunin, C. M., Chin, Q. F. and Chambers, S. (1987) 'Indwelling urinary catheters in the elderly. Relation of "catheter life" to formation of encrustations in patients with and without blocked catheters', *The American Journal of Medicine*, 82(3), pp. 405–411. doi: 10.1016/0002-9343(87)90438-4.

Kunin, C. N. M. (1989) 'Blockage of urinary catheters: Role of microorganisms and constituents of the urine on formation of encrustations', *Journal of Clinical Epidemiology*, 42(9), pp. 835–842. doi: 10.1016/0895-4356(89)90096-6.

Kunln, C. M. *et al.* (1992) 'The association between the use of urinary catheters and morbidity and mortality among elderly patients in nursing homes', *American Journal of Epidemiology*. Oxford University Press, 135(3), pp. 291–301. doi: 10.1093/oxfordjournals.aje.a116283.

Labrou, N. (2010) 'Random Mutagenesis Methods for In Vitro Directed Enzyme Evolution', *Current Protein & Peptide Science*. Bentham Science Publishers Ltd., 11(1), pp. 91–100. doi: 10.2174/138920310790274617.

Lahaye, É. *et al.* (2014) 'A multi-scale approach of the mechanisms underlying exopolysaccharide auto-organization in the *Proteus mirabilis* extracellular matrix', *Analyst*. The Royal Society of Chemistry, 139(19), pp. 4879–4886. doi: 10.1039/c4an00618f.

Langridge, G. C. *et al.* (2009) 'Simultaneous assay of every *Salmonella typhi* gene using one million transposon mutants', *Genome Research*. Genome Res, 19(12), pp. 2308–2316. doi: 10.1101/gr.097097.109.

Lapides, J. *et al.* (1972) 'Clean, intermittent self-catheterization in the treatment of urinary tract disease.', *The Journal of urology*. J Urol, 107(3), pp. 458–461. doi: 10.1016/S0022-5347(17)61055-3.

Lasic, D. D. and Papahadjopoulos, D. (1998) *Medical applications of liposomes*. Elsevier. Available at: https://books.google.co.uk/books?hl=en&lr=&id=UO0tuUW7cCwC&oi=fnd&pg=PP1&ots=D0ZzYu9s50&sig=q_hnEzeBsxyt-x_yb16uGx8Wip4&redir_esc=y#v=onepage&q&f=false (Accessed: 23 May 2019).

Lebeaux, D. *et al.* (2013) 'From in vitro to in vivo models of bacterial biofilm-related infections', *Pathogens*. MDPI AG, pp. 288–356. doi: 10.3390/pathogens2020288.

Lee, C. A. and Grossman, A. D. (2007) 'Identification of the origin of transfer (oriT) and DNA relaxase required for conjugation of the integrative and conjugative element ICEBs1 of *Bacillus subtilis*', *Journal of Bacteriology*. American Society for Microbiology Journals, 189(20), pp. 7254–7261. doi: 10.1128/JB.00932-07.

Lehman, S. M. and Donlan, R. M. (2015) 'Bacteriophage-mediated control of a two-species biofilm formed by microorganisms causing catheter-associated urinary tract infections in an in vitro urinary catheter model', *Antimicrobial Agents and Chemotherapy*. American Society for Microbiology, 59(2), pp. 1127–1137. doi: 10.1128/AAC.03786-14.

Lemire, J. A., Harrison, J. J. and Turner, R. J. (2013) 'Antimicrobial activity of metals: Mechanisms, molecular targets and applications', *Nature Reviews Microbiology*, pp. 371–384. doi: 10.1038/nrmicro3028.

Letica-Kriegel, A. S. *et al.* (2019) 'Identifying the risk factors for catheter-associated urinary tract infections: A large cross-sectional study of six hospitals', *BMJ Open*. BMJ Publishing Group, 9(2). doi: 10.1136/bmjopen-2018-022137.

Levy, A., Schwartz, S. and Ast, G. (2009) 'Large-scale discovery of insertion hotspots and preferential integration sites of human transposed elements', *Nucleic Acids Research*. Oxford University Press, 38(5), pp. 1515–1530. doi: 10.1093/nar/gkp1134.

Lewenza, S. *et al.* (2005) 'Construction of a mini-Tn5-luxCDABE mutant library in *Pseudomonas aeruginosa* PAO1: A tool for identifying differentially regulated genes', *Genome Research*. Cold Spring Harbor Laboratory Press, 15(4), pp. 583–589. doi: 10.1101/gr.3513905.

Li, L. *et al.* (2005) 'Protein adsorption on oligo(ethylene glycol)-terminated alkanethiolate self-assembled monolayers: The molecular basis for nonfouling behavior', *Journal of Physical Chemistry B*, 109(7), pp. 2934–2941. doi: 10.1021/jp0473321.

Li, X. *et al.* (2015) ‘Spatial patterns of carbonate biomineralization in biofilms’, *Applied and Environmental Microbiology*. American Society for Microbiology, 81(21), pp. 7403–7410. doi: 10.1128/AEM.01585-15.

Li, X., Lu, N., Brady, Hannah R, *et al.* (2016) ‘Biomineralization strongly modulates the formation of *Proteus mirabilis* and *Pseudomonas aeruginosa* dual-species biofilms’, *FEMS Microbiology Ecology*, 92(12), p. fiw189. doi: 10.1093/femsec/fiw189.

Li, X., Lu, N., Brady, Hannah R., *et al.* (2016) ‘Biomineralization strongly modulates the formation of *Proteus mirabilis* and *Pseudomonas aeruginosa* dual-species biofilms’, *FEMS Microbiology Ecology*. Oxford University Press (OUP), 92(12), p. fiw189. doi: 10.1093/femsec/fiw189.

Li, X., Chopp, D. L., Russin, William A., *et al.* (2016) ‘In situ biomineralization and particle deposition distinctively mediate biofilm susceptibility to chlorine’, *Applied and Environmental Microbiology*. American Society for Microbiology, 82(10), pp. 2886–2892. doi: 10.1128/AEM.03954-15.

Li, Y. H. and Tian, X. (2012) ‘Quorum sensing and bacterial social interactions in biofilms’, *Sensors*. Multidisciplinary Digital Publishing Institute (MDPI), pp. 2519–2538. doi: 10.3390/s120302519.

Liang, X. *et al.* (2012) ‘A method for multi-site-directed mutagenesis based on homologous recombination’, *Analytical Biochemistry*. Academic Press Inc., 427(1), pp. 99–101. doi: 10.1016/j.ab.2012.05.002.

Liu, L. *et al.* (2018) ‘Development of a novel indwelling catheter for urethral surgery’, *Medicine (United States)*. Lippincott Williams and Wilkins, 97(35). doi: 10.1097/MD.0000000000012030.

Llamas, I. *et al.* (2000) ‘Transposon mutagenesis in *Halomonas eurihalina*’, *Research in Microbiology*, 151(1), pp. 13–18. doi: 10.1016/S0923-2508(00)00132-7.

Llor, C. and Bjerrum, L. (2014) ‘Antimicrobial resistance: Risk associated with antibiotic overuse and initiatives to reduce the problem’, *Therapeutic Advances in Drug Safety*. Ther Adv Drug Saf, pp. 229–241. doi: 10.1177/2042098614554919.

Locke, J. R., Hill, D. E. and Walzer, Y. (1985) ‘Incidence of squamous cell carcinoma in patients with long-term catheter drainage.’, *The Journal of urology*, 133(6), pp. 1034–5. doi: 10.1016/s0022-5347(17)49366-9.

Lodge, J. K., Weston-Hafer, K. and Berg, D. E. (1988) *Transposon Tn5 Target Specificity: Preference for Insertion at G/C Pairs*.

Long, S. S. (2018) ‘Urinary Tract Infections: Molecular Pathogenesis and Clinical Management, second edition’, *Clinical Infectious Diseases*, 66(2), pp. 320–320. doi: 10.1093/cid/cix649.

Lopes, S. P., Azevedo, N. F. and Pereira, M. O. (2014) ‘Emergent Bacteria in Cystic Fibrosis: In Vitro Biofilm Formation and Resilience under Variable Oxygen Conditions’, *BioMed Research International*. doi: 10.1155/2014/678301.

López, D., Vlamakis, H. and Kolter, R. (2010) 'Biofilms.', *Cold Spring Harbor perspectives in biology*. doi: 10.1101/cshperspect.a000398.

De Lorenzo, V. *et al.* (1990) *Mini-Tn5 Transposon Derivatives for Insertion Mutagenesis, Promoter Probing, and Chromosomal Insertion of Cloned DNA in Gram-Negative Eubacteria*, *Journal of Bacteriology*.

Lorite, G. S. *et al.* (2011) 'The role of conditioning film formation and surface chemical changes on *Xylella fastidiosa* adhesion and biofilm evolution', *Journal of Colloid And Interface Science*, 359, pp. 289–295. doi: 10.1016/j.jcis.2011.03.066.

Lowe, G. D. O., Rumley, A. and Mackie, I. J. (2004) 'Plasma fibrinogen', *Annals of Clinical Biochemistry*, pp. 430–440. doi: 10.1258/0004563042466884.

Lozupone, C. A. *et al.* (2007) 'Quantitative and qualitative β diversity measures lead to different insights into factors that structure microbial communities', *Applied and Environmental Microbiology*. American Society for Microbiology (ASM), pp. 1576–1585. doi: 10.1128/AEM.01996-06.

Lyell, N. L. *et al.* (2008) 'Effective mutagenesis of *Vibrio fischeri* by using hyperactive mini-Tn5 derivatives', *Applied and Environmental Microbiology*. American Society for Microbiology, 74(22), pp. 7059–7063. doi: 10.1128/AEM.01330-08.

Lyte, M. and Ernst, S. (1992) 'Catecholamine induced growth of gram negative bacteria', *Life Sciences*. Life Sci, 50(3), pp. 203–212. doi: 10.1016/0024-3205(92)90273-R.

Ma, R. hong *et al.* (2017) 'The systematic classification of urinary stones combine-using FTIR and SEM-EDAX', *International Journal of Surgery*. Elsevier Ltd, 41, pp. 150–161. doi: 10.1016/j.ijsu.2017.03.080.

Mach, K. E. *et al.* (2009) 'Multiplex Pathogen Identification for Polymicrobial Urinary Tract Infections Using Biosensor Technology: A Prospective Clinical Study', *Journal of Urology*, 182(6), pp. 2735–2741. doi: 10.1016/j.juro.2009.08.028.

Macleod, S. M. and Stickler, D. J. (2007) 'Species interactions in mixed-community crystalline biofilms on urinary catheters', *Journal of Medical Microbiology*. Microbiology Society, 56(11), pp. 1549–1557. doi: 10.1099/jmm.0.47395-0.

Macnab, R. M. (2003) 'How Bacteria Assemble Flagella', *Annual Review of Microbiology*. Annual Reviews, 57(1), pp. 77–100. doi: 10.1146/annurev.micro.57.030502.090832.

MacVane, S. H. (2017) 'Antimicrobial Resistance in the Intensive Care Unit: A Focus on Gram-Negative Bacterial Infections.', *Journal of intensive care medicine*, 32(1), pp. 25–37. doi: 10.1177/0885066615619895.

Maddamsetti, R. and Lenski, R. E. (2018) 'Analysis of bacterial genomes from an evolution experiment with horizontal gene transfer shows that recombination can sometimes overwhelm selection', *PLOS Genetics*. Edited by I. Matic. Public

Library of Science, 14(1), p. e1007199. doi: 10.1371/journal.pgen.1007199.

Magill, S. S. *et al.* (2014) 'Multistate Point-Prevalence Survey of Health Care–Associated Infections', *The New England journal of medicine*. NIH Public Access, 370(13), p. 1198. doi: 10.1056/NEJMOA1306801.

Magliano, E. *et al.* (2012) 'Gender and age-dependent etiology of community-acquired urinary tract infections', *The Scientific World Journal*, 2012. doi: 10.1100/2012/349597.

Magoc, T. and Salzberg, S. L. (2011) 'FLASH: fast length adjustment of short reads to improve genome assemblies', *Bioinformatics*. Oxford Academic, 27(21), pp. 2957–2963. doi: 10.1093/bioinformatics/btr507.

Maierl, M. *et al.* (2015) 'In vitro Dynamic Model of a Catheterized Bladder and Biofilm Assay.', *Bio-protocol*, 5(2). doi: 10.21769/BioProtoc.1381.

Malagón, F. and Aguilera, A. (1998) 'Genetic stability and DNA rearrangements associated with a 2 x 1.1-Kb perfect palindrome in *Escherichia coli*', *Molecular and General Genetics*. Mol Gen Genet, 259(6), pp. 639–644. doi: 10.1007/s004380050858.

Manders, E. M. M. *et al.* (1992) 'Dynamics of three-dimensional replication patterns during the S-phase, analysed by double labelling of DNA and confocal microscopy', *Journal of Cell Science*, 103(3), pp. 857–862. Available at: https://europepmc.org/article/med/1478975 (Accessed: 27 March 2021).

Mann, E. E. and Wozniak, D. J. (2012) '*Pseudomonas* biofilm matrix composition and niche biology', *FEMS Microbiology Reviews*, pp. 893–916. doi: 10.1111/j.1574-6976.2011.00322.x.

Manoil, C. (2000) 'Tagging exported proteins using *Escherichia coli* alkaline phosphatase gene fusions', *Methods in Enzymology*. Academic Press Inc., 326, pp. 35–47. doi: 10.1016/s0076-6879(00)26045-x.

Martínez-García, E. *et al.* (2014) 'New transposon tools tailored for metabolic engineering of Gram-negative microbial cell factories', *Frontiers in Bioengineering and Biotechnology*. Frontiers Media S.A., 2(OCT), p. 46. doi: 10.3389/fbioe.2014.00046.

Martínez, L. C. and Vadyvaloo, V. (2014) 'Mechanisms of post-transcriptional gene regulation in bacterial biofilms', *Frontiers in Cellular and Infection Microbiology*. Frontiers Research Foundation. doi: 10.3389/fcimb.2014.00038.

Mastrigt, R. *et al.* (2009) 'Development and application of the condom catheter method for non-invasive measurement of bladder pressure', in *Indian Journal of Urology*. Wolters Kluwer -- Medknow Publications, pp. 99–104. doi: 10.4103/0970-1591.45546.

Mathur, S. *et al.* (2006a) 'Factors affecting crystal precipitation from urine in individuals with long-term urinary catheters colonized with urease-positive bacterial species', *Urological Research*. Urol Res, 34(3), pp. 173–177. doi: 10.1007/s00240-006-0036-6.

Mathur, S. *et al.* (2006b) 'Prospective study of individuals with long-term urinary catheters colonized with Proteus species', *BJU International*. BJU Int,

97(1), pp. 121–128. doi: 10.1111/j.1464-410X.2006.05868.x.

Mattick, J. S. (2002) ‘Type IV Pili and Twitching Motility’, *Annual Review of Microbiology*. Annual Reviews, 56(1), pp. 289–314. doi: 10.1146/annurev.micro.56.012302.160938.

McLean, R. and Brown, E. (2020) ‘Potential Influences of Bacterial Cell Surfaces and Nano-Sized Cell Fragments on Struvite Biomineralization’, *Crystals*. MDPI AG, 10(8), p. 706. doi: 10.3390/cryst10080706.

Meddings, J. *et al.* (2010) ‘Systematic Review and Meta-Analysis: Reminder Systems to Reduce Catheter-Associated Urinary Tract Infections and Urinary Catheter Use in Hospitalized Patients’, *Clinical Infectious Diseases*. Oxford University Press (OUP), 51(5), pp. 550–560. doi: 10.1086/655133.

Meredith, H. R. *et al.* (2015) ‘Collective antibiotic tolerance: mechanisms, dynamics and intervention’, *Nature chemical biology*. Nat Chem Biol, 11(3), pp. 182–188. doi: 10.1038/NCHEMBIO.1754.

Mika, F. and Hengge, R. (2013) ‘Small regulatory RNAs in the control of motility and biofilm formation in *E. Coli* and *Salmonella*’, *International Journal of Molecular Sciences*, pp. 4560–4579. doi: 10.3390/ijms14034560.

Miles, A. A., Misra, S. S. and Irwin, J. O. (1938) ‘The estimation of the bactericidal power of the blood’, *Journal of Hygiene*. Cambridge University Press, 38(6), pp. 732–749. doi: 10.1017/S002217240001158X.

Miller, M. B. and Bassler, B. L. (2001) ‘Quorum Sensing in Bacteria’, *Annual Review of Microbiology*. Annual Reviews, 55(1), pp. 165–199. doi: 10.1146/annurev.micro.55.1.165.

Milo, S. *et al.* (2016) ‘An in-situ infection detection sensor coating for urinary catheters’, *Biosensors and Bioelectronics*. Elsevier Ltd, 81, pp. 166–172. doi: 10.1016/j.bios.2016.02.059.

Milo, S. *et al.* (2017) ‘Prevention of encrustation and blockage of urinary catheters by: *Proteus mirabilis* via pH-triggered release of bacteriophage’, *Journal of Materials Chemistry B*. Royal Society of Chemistry, 5(27), pp. 5403–5411. doi: 10.1039/c7tb01302g.

Milo, S. *et al.* (2021) ‘A small-molecular inhibitor against *Proteus mirabilis* urease to treat catheter-associated urinary tract infections’, *Scientific Reports*. Springer Science and Business Media LLC, 11(1), p. 3726. doi: 10.1038/s41598-021-83257-2.

Mittal, R. *et al.* (2009) ‘Urinary tract infections caused by *Pseudomonas aeruginosa*: A minireview’, *Journal of Infection and Public Health*, 2(3), pp. 101–111. doi: 10.1016/j.jiph.2009.08.003.

Mobley, H. L. *et al.* (1987) ‘Expression of type 1 fimbriae may be required for persistence of *Escherichia coli* in the catheterized urinary tract.’, *Journal of clinical microbiology*, 25(12), pp. 2253–7. Available at: http://www.ncbi.nlm.nih.gov/pubmed/2892855 (Accessed: 20 December 2019).

Mobley, H. L. T., Island, M. D. and Hausinger, R. P. (1995) *Molecular Biology of Microbial Ureases, MICROBIOLOGICAL REVIEWS*.

Mobley, H. L. T. and Warren, J. W. (1987) 'Urease-positive bacteriuria and obstruction of long-term urinary catheters', *Journal of Clinical Microbiology*, 25(11), pp. 2216–2217.

Monds, R. D. and O'Toole, G. A. (2009) 'The developmental model of microbial biofilms: ten years of a paradigm up for review', *Trends in Microbiology*, pp. 73–87. doi: 10.1016/j.tim.2008.11.001.

Morgenstein, R. M., Szostek, B. and Rather, P. N. (2010) 'Regulation of gene expression during swarmer cell differentiation in *Proteus mirabilis*', *FEMS Microbiology Reviews*, pp. 753–763. doi: 10.1111/j.1574-6976.2010.00229.x.

Morimoto, Y. V. and Minamino, T. (2014) 'Structure and function of the bi-directional bacterial flagellar motor', *Biomolecules*. MDPI AG, pp. 217–234. doi: 10.3390/biom4010217.

Morris, N. S. and Stickler, D. J. (1998) 'Encrustation of indwelling urethral catheters by *Proteus mirabilis* biofilms growing in human urine', *Journal of Hospital Infection*. W.B. Saunders Ltd, 39(3), pp. 227–234. doi: 10.1016/S0195-6701(98)90262-6.

Morris, Nicola Sian and Stickler, D. J. (1998) 'The effect of urease inhibitors on the encrustation of urethral catheters', *Urological Research*, 26(4), pp. 275–279. doi: 10.1007/s002400050057.

Moryl, M. *et al.* (2014) 'Effect of nutrient and stress factors on polysaccharides synthesis in *Proteus mirabilis* biofilm', *Acta Biochimica Polonica*, 61(1), pp. 133–9. Available at: www.actabp.pl (Accessed: 24 March 2021).

Mosesson, M. W. (2005) 'Fibrinogen and fibrin structure and functions', *Journal of Thrombosis and Haemostasis*, 3(8), pp. 1894–1904. doi: 10.1111/j.1538-7836.2005.01365.x.

Mudgil, D. *et al.* (2018) 'Biomineralization Potential of *Bacillus subtilis*, *Rummeliibacillus stabekisii* and *Staphylococcus epidermidis* Strains In Vitro Isolated from Speleothems, Khasi Hill Caves, Meghalaya, India', *Geomicrobiology Journal*. Taylor and Francis Inc., 35(8), pp. 675–694. doi: 10.1080/01490451.2018.1450461.

Muyzer, G., De Waal, E. C. and Uitterlinden, A. G. (1993) 'Profiling of complex microbial populations by denaturing gradient gel electrophoresis analysis of polymerase chain reaction-amplified genes coding for 16S rRNA', *Applied and Environmental Microbiology*. American Society for Microbiology (ASM), 59(3), pp. 695–700. doi: 10.1128/aem.59.3.695-700.1993.

Nabb, D. L. *et al.* (2019) 'Polymicrobial Interactions Induce Multidrug Tolerance in *Staphylococcus aureus* Through Energy Depletion', *Frontiers in Microbiology*. Frontiers Media S.A., 10, p. 2803. doi: 10.3389/fmicb.2019.02803.

Nadell, C. D. *et al.* (2008) 'The Evolution of Quorum Sensing in Bacterial Biofilms', *PLoS Biology*. Edited by N. A. Moran, 6(1), p. e14. doi: 10.1371/journal.pbio.0060014.

Nallapareddy, S. R. *et al.* (2006) 'Endocarditis and biofilm-associated pili of

Enterococcus faecalis', *Journal of Clinical Investigation*, 116(10), pp. 2799–2807. doi: 10.1172/JCI29021.

Naorem, S. S. *et al.* (2018) 'Efficient transposon mutagenesis mediated by an IPTG-controlled conditional suicide plasmid', *BMC Microbiology*. BioMed Central Ltd., 18(1), p. 158. doi: 10.1186/s12866-018-1319-0.

Nazareno, E. S., Acharya, B. and Dumenyo, C. K. (2020) 'A mini-Tn5-derived transposon with reportable and selectable markers enables rapid generation and screening of insertional mutants in Gram-negative bacteria', *Letters in Applied Microbiology*. Blackwell Publishing Ltd, p. lam.13423. doi: 10.1111/lam.13423.

Nicholson, E. B. *et al.* (1993) '*Proteus mirabilis* urease: Transcriptional regulation by UreR', *Journal of Bacteriology*. J Bacteriol, 175(2), pp. 465–473. doi: 10.1128/jb.175.2.465-473.1993.

Nickel, C. J. *et al.* (1994) 'Bacterial biofilms: Influence on the pathogenesis, diagnosis and treatment of urinary tract infections', *Journal of Antimicrobial Chemotherapy*, 33, pp. 31–41. doi: 10.1093/jac/33.suppl_A.31.

Nickel, J. C., Grant, S. K. and Costerton, J. W. (1985) 'Catheter-associated bacterium. An experimental study', *Urology*, 26(4), pp. 369–375. doi: 10.1016/0090-4295(85)90185-2.

Nicolle, L. E. (2005) 'Catheter-related urinary tract infection', *Drugs and Aging*, pp. 627–639. doi: 10.2165/00002512-200522080-00001.

Nicolle, L. E. (2012) 'Urinary Catheter-Associated Infections', *Infectious Disease Clinics of North America*, pp. 13–27. doi: 10.1016/j.idc.2011.09.009.

Nicolle, L. E. (2014) 'Catheter associated urinary tract infections', *Antimicrobial Resistance and Infection Control*. BioMed Central Ltd. doi: 10.1186/2047-2994-3-23.

Niël-Weise, B. S. and Van Den Broek, P. J. (2009) 'Urinary catheter policies for long-term bladder drainage', *Cochrane Database of Systematic Reviews*. John Wiley and Sons Ltd. doi: 10.1002/14651858.CD004201.pub2.

Nzakizwanayo, J. *et al.* (2019) 'An In Vitro Bladder Model for Studying Catheter-Associated Urinary Tract Infection and Associated Analysis of Biofilms', in *Methods in Molecular Biology*. Humana Press Inc., pp. 139–158. doi: 10.1007/978-1-4939-9601-8_14.

O'May, C. and Tufenkji, N. (2011) 'The swarming motility of *Pseudomonas aeruginosa* is blocked by cranberry proanthocyanidins and other tannin-containing materials', *Applied and Environmental Microbiology*. American Society for Microbiology (ASM), 77(9), pp. 3061–3067. doi: 10.1128/AEM.02677-10.

Oki, K. *et al.* (2010) 'The Role of Urease Activity on Biofilm Formation by *Staphylococcus* sp. T-02 Isolated from the Toilet Bowl', *Biosci. Biotechnol. Biochem*, 74(3), pp. 583–589. doi: 10.1271/bbb.90796.

Olson, M. E. *et al.* (2002) 'Biofilm bacteria: Formation and comparative susceptibility to antibiotics', *Canadian Journal of Veterinary Research*.

Canadian Veterinary Medical Association, 66(2), pp. 86–92.

Oppenheimer-Shaanan, Y. *et al.* (2016) 'Spatio-Temporal assembly of functional mineral scaffolds within microbial biofilms', *npj Biofilms and Microbiomes*. Nature Publishing Group, 2(1), pp. 1–10. doi: 10.1038/npjbiofilms.2015.31.

Ouslander, J. G., Greengold, B. and Chen, S. (1987) 'External Catheter Use and Urinary Tract Infections Among Incontinent Male Nursing Home Patients', *Journal of the American Geriatrics Society*. J Am Geriatr Soc, 35(12), pp. 1063–1070. doi: 10.1111/j.1532-5415.1987.tb04922.x.

Overhage, J. *et al.* (2005) 'Expression of the psl operon in *Pseudomonas aeruginosa* PAO1 biofilms: PslA performs an essential function in biofilm formation', *Applied and Environmental Microbiology*, 71(8), pp. 4407–4413. doi: 10.1128/AEM.71.8.4407-4413.2005.

Overhage, J. *et al.* (2007) 'Identification of genes involved in swarming motility using a *Pseudomonas aeruginosa* PAO1 mini-Tn5-lux mutant library', *Journal of Bacteriology*. American Society for Microbiology Journals, 189(5), pp. 2164–2169. doi: 10.1128/JB.01623-06.

Pak, C. Y. C. (1998) 'Kidney stones', *Lancet*. Lancet Publishing Group, pp. 1797–1801. doi: 10.1016/S0140-6736(98)01295-1.

Pak, J. *et al.* (2001) 'Tamm-Horsfall Protein Binds to Type 1 Fimbriated *Escherichia coli* and Prevents *E. coli* from Binding to Uroplakin Ia and Ib Receptors', *Journal of Biological Chemistry*, 276(13), pp. 9924–9930. doi: 10.1074/jbc.M008610200.

Palmer, J., Flint, S. and Brooks, J. (2007) 'Bacterial cell attachment, the beginning of a biofilm', *Journal of Industrial Microbiology and Biotechnology*, 34(9), pp. 577–588. doi: 10.1007/s10295-007-0234-4.

Palmer, R. J., Diaz, P. I. and Kolenbrander, P. E. (2006) 'Rapid succession within the *Veillonella* population of a developing human oral biofilm in situ', *Journal of Bacteriology*. J Bacteriol, 188(11), pp. 4117–4124. doi: 10.1128/JB.01958-05.

Papenfort, K. and Bassler, B. (2016) 'Quorum-Sensing Signal-Response Systems in Gram-Negative Bacteria', *Nature reviews. Microbiology*. NIH Public Access, 14(9), p. 576. doi: 10.1038/NRMICRO.2016.89.

Parsek, M. R. and Singh, P. K. (2003) 'Bacterial Biofilms: An Emerging Link to Disease Pathogenesis', *Annual Review of Microbiology*. Annual Reviews, 57(1), pp. 677–701. doi: 10.1146/annurev.micro.57.030502.090720.

Parsons, C. L. (1986) 'Pathogenesis of urinary tract infections. Bacterial adherence, bladder defense mechanisms.', *The Urologic clinics of North America*, 13(4), pp. 563–8. Available at: http://www.ncbi.nlm.nih.gov/pubmed/2877517 (Accessed: 20 December 2019).

Pearson, J. P., Van Delden, C. and Iglewski, B. H. (1999) 'Active efflux and diffusion are involved in transport of *Pseudomonas aeruginosa* cell-to-cell signals.', *Journal of bacteriology*, 181(4), pp. 1203–10. Available at:

http://www.ncbi.nlm.nih.gov/pubmed/9973347 (Accessed: 1 June 2019).

Pearson, M. M. *et al.* (2008) 'Complete genome sequence of uropathogenic *Proteus mirabilis*, a master of both adherence and motility', *Journal of Bacteriology*. J Bacteriol, 190(11), pp. 4027–4037. doi: 10.1128/JB.01981-07.

Pearson, M. M. *et al.* (2010) 'Transcriptome of swarming *Proteus mirabilis*', *Infection and Immunity*, 78(6), pp. 2834–2845. doi: 10.1128/IAI.01222-09.

Pearson, M. M. *et al.* (2011) 'Transcriptome of *Proteus mirabilis* in the murine urinary tract: Virulence and nitrogen assimilation gene expression', *Infection and Immunity*, 79(7), pp. 2619–2631. doi: 10.1128/IAI.05152-11.

Peng, D. *et al.* (2018a) 'Epidemiology of pathogens and antimicrobial resistanceof catheter-associated urinary tract infections in intensivecare units: A systematic review and meta-analysis', *American Journal of Infection Control*, 46(12), pp. e81–e90. doi: 10.1016/j.ajic.2018.07.012.

Peng, D. *et al.* (2018b) 'Epidemiology of pathogens and antimicrobial resistanceof catheter-associated urinary tract infections in intensivecare units: A systematic review and meta-analysis', *American Journal of Infection Control*. Mosby Inc., 46(12), pp. e81–e90. doi: 10.1016/j.ajic.2018.07.012.

Pertsemlidis, A. and Fondon, J. W. (2001) 'Having a BLAST with bioinformatics (and avoiding BLAST phemy)', *Genome Biology*. BioMed Central, p. reviews2002.1. doi: 10.1186/gb-2001-2-10-reviews2002.

Peter Kingshott, *,† *et al.* (2003) 'Covalent Attachment of Poly(ethylene glycol) to Surfaces, Critical for Reducing Bacterial Adhesion'. American Chemical Society . doi: 10.1021/LA034032M.

Peters, P. *et al.* (2011) 'The purple urine bag syndrome: A visually striking side effect of a highly alkaline urinary tract infection', *Journal of the Canadian Urological Association*, 5(4), pp. 233–234. doi: 10.5489/cuaj.10177.

Petrova, O. E. and Sauer, K. (2012) 'Sticky situations: Key components that control bacterial surface attachment', *Journal of Bacteriology*, pp. 2413–2425. doi: 10.1128/JB.00003-12.

Peychl, L. and Zalud, R. (2008) '[Changes in the urinary bladder caused by short-term permanent catheter insertion].', *Casopis lekaru ceskych*, 147(6), pp. 325–9. Available at: http://www.ncbi.nlm.nih.gov/pubmed/18724530 (Accessed: 20 December 2019).

Pickard, Robert *et al.* (2012a) 'Antimicrobial catheters for reduction of symptomatic urinary tract infection in adults requiring short-term catheterisation in hospital: A multicentre randomised controlled trial', *The Lancet*, 380(9857), pp. 1927–1935. doi: 10.1016/S0140-6736(12)61380-4.

Pickard, Robert *et al.* (2012b) 'Antimicrobial catheters for reduction of symptomatic urinary tract infection in adults requiring short-term catheterisation in hospital: A multicentre randomised controlled trial', *The Lancet*. Elsevier B.V., 380(9857), pp. 1927–1935. doi: 10.1016/S0140-6736(12)61380-4.

Pickard, R. *et al.* (2012) 'Types of urethral catheter for reducing symptomatic urinary tract infections in hospitalised adults requiring short-term

catheterisation: Multicentre randomised controlled trial and economic evaluation of antimicrobial- and antisepticimpregnated urethral catheters (the CATHETER trial)', *Health Technology Assessment*. NIHR Journals Library, 16(47). doi: 10.3310/hta16470.

Platt, R. *et al.* (1982) 'Mortality Associated with Nosocomial Urinary-Tract Infection', *New England Journal of Medicine*, 307(11), pp. 637–642. doi: 10.1056/NEJM198209093071101.

Platt, R. *et al.* (1983) 'Reduction of Mortality Associated with Nosocomial Urinary-Tract Infection', *The Lancet*, 321(8330), pp. 893–897. doi: 10.1016/S0140-6736(83)91327-2.

Pobigaylo, N. *et al.* (2006) 'Construction of a large signature-tagged mini-Tn5 transposon library and its application to mutagenesis of *Sinorhizobium meliloti*', *Applied and Environmental Microbiology*, 72(6), pp. 4329–4337. doi: 10.1128/AEM.03072-05.

Poore, C. A. *et al.* (2001) 'Identification of the domains of UreR, an AraC-like transcriptional regulator of the urease gene cluster in *Proteus mirabilis*', *Journal of Bacteriology*. American Society for Microbiology (ASM), 183(15), pp. 4526–4535. doi: 10.1128/JB.183.15.4526-4535.2001.

Poore, C. A. and Mobley, H. L. T. (2003) 'Differential regulation of the *Proteus mirabilis* urease gene cluster by UreR and H-NS', *Microbiology*. Society for General Microbiology, 149(12), pp. 3383–3394. doi: 10.1099/mic.0.26624-0.

Prestinaci, F., Pezzotti, P. and Pantosti, A. (2015) 'Antimicrobial resistance: A global multifaceted phenomenon', *Pathogens and Global Health*. Maney Publishing, pp. 309–318. doi: 10.1179/2047773215Y.0000000030.

Price-Whelan, A., Dietrich, L. E. P. and Newman, D. K. (2006) 'Rethinking "secondary" metabolism: Physiological roles for phenazine antibiotics', *Nature Chemical Biology*. Nature Publishing Group, pp. 71–78. doi: 10.1038/nchembio764.

Prywer, J., Sadowski, R. R. and Torzewska, A. (2015) 'Aggregation of Struvite, Carbonate Apatite, and *Proteus mirabilis* as a Key Factor of Infectious Urinary Stone Formation', *Crystal Growth & Design*, 15(3), pp. 1446–1451. doi: 10.1021/cg5018032.

Prywer, J. and Torzewska, A. (2010) 'Biomineralization of struvite crystals by *Proteus mirabilis* from artificial urine and their mesoscopic structure', in *Crystal Research and Technology*. John Wiley & Sons, Ltd, pp. 1283–1289. doi: 10.1002/crat.201000344.

Prywer, J., Torzewska, A. and Płociński, T. (2012) 'Unique surface and internal structure of struvite crystals formed by *Proteus mirabilis*', *Urological Research*. Springer Verlag, 40(6), pp. 699–707. doi: 10.1007/s00240-012-0501-3.

Pugach, J. L. *et al.* (1999) 'Antibiotic hydrogel coated Foley catheters for prevention of urinary tract infection in a rabbit model.', *The Journal of urology*, 162(3 Pt 1), pp. 883–7. Available at: http://www.ncbi.nlm.nih.gov/pubmed/10458402 (Accessed: 1 June 2019).

Puttamreddy, S., Cornick, N. A. and Minion, F. C. (2010) 'Genome-wide transposon mutagenesis reveals a role for pO157 genes in biofilm development in *Escherichia coli* O157:H7 EDL933', *Infection and Immunity*. American Society for Microbiology (ASM), 78(6), pp. 2377–2384. doi: 10.1128/IAI.00156-10.

Raffi, H. S. *et al.* (2012) 'Tamm-Horsfall protein facilitates catheter associated urinary tract infection', *BMC Research Notes*, 5. doi: 10.1186/1756-0500-5-532.

Rajendran, N. *et al.* (1994) 'Transposon Tn5 mutagenesis of *Pseudomonas fluorescens* to isolate mutants deficient in antibacterial activity', *FEMS Microbiology Letters*, 115(2–3), pp. 191–196. doi: 10.1111/j.1574-6968.1994.tb06636.x.

Rakowski, S. A. and Filutowicz, M. (2013) 'Plasmid R6K replication control', *Plasmid*. NIH Public Access, pp. 231–242. doi: 10.1016/j.plasmid.2013.02.003.

Rampoldi, L. *et al.* (2011) 'The rediscovery of uromodulin (Tamm-Horsfall protein): From tubulointerstitial nephropathy to chronic kidney disease', *Kidney International*. Nature Publishing Group, pp. 338–347. doi: 10.1038/ki.2011.134.

Ramsay, J. W. *et al.* (1989) 'Biofilms, bacteria and bladder catheters. A clinical study.', *British journal of urology*, 64(4), pp. 395–8. doi: 10.1111/j.1464-410x.1989.tb06050.x.

Rao, D., Webb, J. S. and Kjelleberg, S. (2005) 'Competitive interactions in mixed-species biofilms containing the marine bacterium *Pseudoalteromonas tunicata*', *Applied and Environmental Microbiology*. American Society for Microbiology, 71(4), pp. 1729–1736. doi: 10.1128/AEM.71.4.1729-1736.2005.

Rather, P. N. (2019) 'Methods for Transposon Mutagenesis in *Proteus mirabilis*', in *Methods in Molecular Biology*. Humana Press Inc., pp. 81–85. doi: 10.1007/978-1-4939-9570-7_8.

Ratnakar, P. V. A. L. *et al.* (1996) 'The replication initiator protein is of the plasmid R6K specifically interacts with the host-encoded helicase DnaB (initiation of replication/protein-protein interaction)', *Biochemistry*, 93, pp. 5522–5526.

Raz, R., Colodner, R. and Kunin, C. M. (2005) 'Who Are You--*Staphylococcus saprophyticus*?', *Clinical Infectious Diseases*. Oxford Academic, 40(6), pp. 896–898. doi: 10.1086/428353.

Regev-Shoshani, G. *et al.* (2011) 'Comparative efficacy of commercially available and emerging antimicrobial urinary catheters against bacteriuria caused by *E. coli* in vitro', *Urology*. Elsevier Inc., 78(2), pp. 334–339. doi: 10.1016/j.urology.2011.02.063.

Reznikoff, W. S. *et al.* (1999) 'Tn5: A molecular window on transposition', *Biochemical and Biophysical Research Communications*. Academic Press Inc., 266(3), pp. 729–734. doi: 10.1006/bbrc.1999.1891.

Reznikoff, W. S. (2003) 'Tn5 as a model for understanding dna transposition', *Molecular Microbiology*. Mol Microbiol, pp. 1199–1206. doi: 10.1046/j.1365-2958.2003.03382.x.

Riley, D. K. *et al.* (1995) ‘A large randomized clinical trial of a silver-impregnated urinary catheter: Lack of efficacy and staphylococcal superinfection’, *The American Journal of Medicine*. Am J Med, 98(4), pp. 349–356. doi: 10.1016/S0002-9343(99)80313-1.

Roberts, A. P. *et al.* (1999) ‘ Transfer of a conjugative transposon, Tn 5397 in a model oral biofilm ’, *FEMS Microbiology Letters*. Oxford University Press (OUP), 177(1), pp. 63–66. doi: 10.1111/j.1574-6968.1999.tb13714.x.

Rodriguez-Navarro, C. *et al.* (2012) ‘Influence of substrate mineralogy on bacterial mineralization of calcium carbonate: Implications for stone conservation’, *Applied and Environmental Microbiology*, 78(11), pp. 4017–4029. doi: 10.1128/AEM.07044-11.

Rogers, J. *et al.* (1996) ‘Examination of biofilm formation and risk of infection associated with the use of urinary catheters with leg bags’, *Journal of Hospital Infection*. W.B. Saunders Ltd, 32(2), pp. 105–115. doi: 10.1016/S0195-6701(96)90052-3.

Rollefson, J. B., Levar, C. E. and Bond, D. R. (2009) ‘Identification of genes involved in biofilm formation and respiration via mini-Himar transposon mutagenesis of *Geobacter sulfurreducens*’, *Journal of Bacteriology*. American Society for Microbiology Journals, 191(13), pp. 4207–4217. doi: 10.1128/JB.00057-09.

Rose, R. *et al.* (1977) ‘Morbidity/mortality and economics of hospital-acquired blood stream infections: a controlled study.’, *Southern medical journal*, 70(11), pp. 1267–9. doi: 10.1097/00007611-197711000-00005.

Rosenblatt, J. *et al.* (2017) ‘Foley Catheter with Peri-Urethral Antimicrobial Irrigation for the Prevention of Catheter Associated Urinary Tract Infections – Assessment in an In Vitro Model’, *Open Forum Infectious Diseases*. Oxford University Press (OUP), 4(suppl_1), pp. S481–S481. doi: 10.1093/ofid/ofx163.1235.

Rózalski, A., Sidorczyk, Z. and Kotełko, K. (1997) ‘Potential virulence factors of *Proteus* bacilli.’, *Microbiology and molecular biology reviews : MMBR*. American Society for Microbiology, 61(1), pp. 65–89. doi: 10.1128/.61.1.65-89.1997.

Rutherford, S. T. and Bassler, B. L. (2012) ‘Bacterial quorum sensing: Its role in virulence and possibilities for its control’, *Cold Spring Harbor Perspectives in Medicine*. Cold Spring Harbor Laboratory Press. doi: 10.1101/cshperspect.a012427.

Saak, C. C. and Gibbs, K. A. (2016) ‘The self-identity protein IdsD is communicated between cells in swarming *Proteus mirabilis* colonies’, *Journal of Bacteriology*. American Society for Microbiology, 198(24), pp. 3278–3286. doi: 10.1128/JB.00402-16.

Sabbuba, N., Hughes, G. and Stickler, D. J. (2002) ‘The migration of *Proteus mirabilis* and other urinary tract pathogens over Foley catheters’, *BJU International*, 89(1), pp. 55–60. doi: 10.1046/j.1464-4096.2001.01721.x.

Saeb, A. T. M. *et al.* (2017) ‘Genome sequencing and analysis of the first

spontaneous Nanosilver resistant bacterium *Proteus mirabilis* strain SCDR1', *Antimicrobial Resistance and Infection Control*. BioMed Central Ltd., 6(1), p. 119. doi: 10.1186/s13756-017-0277-x.

Saint, S. *et al.* (1998) 'The efficacy of silver alloy-coated urinary catheters in preventing urinary tract infection: A meta-analysis', *American Journal of Medicine*. Am J Med, pp. 236–241. doi: 10.1016/S0002-9343(98)00240-X.

Saint, S. *et al.* (2000) 'Are physicians aware of which of their patients have indwelling urinary catheters?', *American Journal of Medicine*. Elsevier Inc., 109(6), pp. 476–480. doi: 10.1016/S0002-9343(00)00531-3.

Sakata, N. *et al.* (2019) 'Transposon mutagenesis reveals *Pseudomonas cannabina pv. alisalensis* optimizes its virulence factors for pathogenicity on different hosts', *PeerJ*. PeerJ Inc., 2019(9). doi: 10.7717/peerj.7698.

Salvarci, A., Koroglu, M. and Gurpinar, T. (2015) 'Evaluation of antimicrobial activities of minocycline and rifampin-impregnated silicone surfaces in an in vitro urinary system model.', *JPMA. The Journal of the Pakistan Medical Association*, 65(2), pp. 115–9. Available at: http://www.ncbi.nlm.nih.gov/pubmed/25842542 (Accessed: 24 January 2020).

Sauer, K. *et al.* (2002) '*Pseudomonas aeruginosa* displays multiple phenotypes during development as a biofilm', *Journal of Bacteriology*, 184(4), pp. 1140–1154. doi: 10.1128/jb.184.4.1140-1154.2002.

Sauer, K. *et al.* (2004) 'Characterization of nutrient-induced dispersion in *Pseudomonas aeruginosa* PAO1 biofilm', *Journal of Bacteriology*, 186(21), pp. 7312–7326. doi: 10.1128/JB.186.21.7312-7326.2004.

Schaffer, J. N. *et al.* (2016) '*Proteus mirabilis* fimbriae- and urease-dependent clusters assemble in an extracellular niche to initiate bladder stone formation', *Proceedings of the National Academy of Sciences of the United States of America*. National Academy of Sciences, 113(16), pp. 4494–4499. doi: 10.1073/pnas.1601720113.

Schaffer, J. N. and Pearson, M. M. (2015) '*Proteus mirabilis* and Urinary Tract Infections', *Microbiology Spectrum*. American Society for Microbiology, 3(5). doi: 10.1128/microbiolspec.uti-0017-2013.

Schierholz, J. M. *et al.* (1998) 'Efficacy of silver-coated medical devices', *Journal of Hospital Infection*. W.B. Saunders Ltd, pp. 257–262. doi: 10.1016/S0195-6701(98)90301-2.

Schindelin, J. *et al.* (2012) 'Fiji: An open-source platform for biological-image analysis', *Nature Methods*. Nature Publishing Group, pp. 676–682. doi: 10.1038/nmeth.2019.

Schultz, L. N. *et al.* (2015) 'Struvite stone formation by ureolytic biofilm infections', in *The Role of Bacteria in Urology*. Springer International Publishing, pp. 41–49. doi: 10.1007/978-3-319-17732-8_5.

Sepúlveda, P. *et al.* (1998) '*Candida albicans* fibrinogen binding mannoprotein: expression in clinical strains and immunogenicity in patients with candidiasis.', *International microbiology : the official journal of the Spanish Society for*

Microbiology, 1(3), pp. 209–16. Available at: http://www.ncbi.nlm.nih.gov/pubmed/10943362 (Accessed: 20 December 2019).

Serafini-Cessi, F., Malagolini, N. and Cavallone, D. (2003) 'Tamm-Horsfall glycoprotein: Biology and clinical relevance', *American Journal of Kidney Diseases*. W.B. Saunders, 42(4), pp. 658–676. doi: 10.1016/S0272-6386(03)00829-1.

Shbeeb, A. *et al.* (2014) 'Lock-Out valve to decrease catheter-associated urinary tract infections', *Advances in Urology*. doi: 10.1155/2014/765756.

Shortle, D. and Nathans, D. (1978) 'Local mutagenesis: A method for generating viral mutants with base substitutions in preselected regions of the viral genome', *Proceedings of the National Academy of Sciences of the United States of America*. National Academy of Sciences, 75(5), pp. 2170–2174. doi: 10.1073/pnas.75.5.2170.

Shu, M. *et al.* (2003) 'Role of Urease Enzymes in Stability of a 10-Species Oral Biofilm Consortium Cultivated in a Constant-Depth Film Fermenter', *Infection and Immunity*, 71(12), pp. 7188–7192. doi: 10.1128/IAI.71.12.7188-7192.2003.

Siddiq, D. M. and Darouiche, R. O. (2012) 'New strategies to prevent catheter-associated urinary tract infections', *Nature Reviews Urology*, pp. 305–314. doi: 10.1038/nrurol.2012.68.

Siguier, P., Gourbeyre, E. and Chandler, M. (2014) 'Bacterial insertion sequences: Their genomic impact and diversity', *FEMS Microbiology Reviews*. Blackwell Publishing Ltd, 38(5), pp. 865–891. doi: 10.1111/1574-6976.12067.

Singh, S. *et al.* (2017) 'Understanding the Mechanism of Bacterial Biofilms Resistance to Antimicrobial Agents', *The Open Microbiology Journal*. Bentham Science Publishers Ltd., 11(1), pp. 53–62. doi: 10.2174/1874285801711010053.

Singha, P., Locklin, J. and Handa, H. (2017) 'A Review of the Recent Advances in Antimicrobial Coatings for Urinary Catheters', *Acta biomaterialia*. NIH Public Access, 50, p. 20. doi: 10.1016/J.ACTBIO.2016.11.070.

Smith, G. A. and Enquist, L. W. (1999) 'Construction and Transposon Mutagenesis in *Escherichia coli* of a Full-Length Infectious Clone of Pseudorabies Virus, an Alphaherpesvirus', *Journal of Virology*. American Society for Microbiology, 73(8), pp. 6405–6414. doi: 10.1128/jvi.73.8.6405-6414.1999.

Smits, T. H. M. (2019) 'The importance of genome sequence quality to microbial comparative genomics', *BMC Genomics*. BioMed Central Ltd., 20(1), p. 662. doi: 10.1186/s12864-019-6014-5.

Smoger, S. H., Felice, T. L. and Kloecker, G. H. (2000) 'Urinary incontinence among male veterans receiving care in primary care clinics', *Annals of Internal Medicine*. American College of Physicians, 132(7), pp. 547–551. doi: 10.7326/0003-4819-132-7-200004040-00006.

Soto, S. M. (2013) 'Role of efflux pumps in the antibiotic resistance of bacteria embedded in a biofilm', *Virulence*. Taylor and Francis Inc., 4(3), pp. 223–229.

doi: 10.4161/viru.23724.

Sriwanthana, B., Island, M. D. and Mobley, H. L. T. (1993) 'Sequence of the *Proteus mirabilis* urease accessory gene ureG', *Gene*. Gene, 129(1), pp. 103–106. doi: 10.1016/0378-1119(93)90703-6.

Stamm, W. E. (1991) 'Catheter-associated urinary tract infections: Epidemiology, pathogenesis, and prevention', *The American Journal of Medicine*. Am J Med, 91(3 SUPPL. 2). doi: 10.1016/0002-9343(91)90345-X.

Stankowska, D. *et al.* (2012) 'Influence of quorum sensing signal molecules on biofilm formation in *Proteus mirabilis* O18', *Folia Microbiologica*. Springer, 57(1), pp. 53–60. doi: 10.1007/s12223-011-0091-4.

Sternberg, C. and Tolker-Nielsen, T. (2006) 'Growing and Analyzing Biofilms in Flow Cells', in *Current Protocols in Microbiology*. John Wiley & Sons, Inc. doi: 10.1002/9780471729259.mc01b02s00.

Stewart, P. S. and Costerton, J. W. (2001) 'Antibiotic resistance of bacteria in biofilms', *Lancet*. Elsevier Limited, pp. 135–138. doi: 10.1016/S0140-6736(01)05321-1.

Stickler, D. *et al.* (1998) 'Studies on the formation of crystalline bacterial biofilms on urethral catheters', *European Journal of Clinical Microbiology & Infectious Diseases*. Springer Nature America, Inc, 17(9), pp. 649–652. doi: 10.1007/bf01708349.

Stickler, D. *et al.* (2003) 'Why are Foley catheters so vulnerable to encrustation and blockage by crystalline bacterial biofilm?', *Urological Research*, 31(5), pp. 306–311. doi: 10.1007/s00240-003-0340-3.

Stickler, D. and Hughes, G. (1999) *Ability of Proteus mirabilis to Swarm over Urethral Catheters, Eur J Clin Microbiol Infect Dis*. Springer-Verlag.

Stickler, D. J. *et al.* (2006) 'A clinical assessment of the performance of a sensor to detect crystalline biofilm formation on indwelling bladder catheters', *BJU International*, 98(6), pp. 1244–1249. doi: 10.1111/j.1464-410X.2006.06562.x.

Stickler, D. J. (2008) 'Bacterial biofilms in patients with indwelling urinary catheters', *Nature Clinical Practice Urology*, pp. 598–608. doi: 10.1038/ncpuro1231.

Stickler, D. J. (2014) 'Clinical complications of urinary catheters caused by crystalline biofilms: something needs to be done', *Journal of Internal Medicine*, 276(2), pp. 120–129. doi: 10.1111/joim.12220.

Stickler, D. J. and Feneley, R. C. L. (2010) 'The encrustation and blockage of long-term indwelling bladder catheters: A way forward in prevention and control', *Spinal Cord*, pp. 784–790. doi: 10.1038/sc.2010.32.

Stickler, D. J. and Mclean, R. J. C. (1995) *Biomaterials Associated Infections: The Scale of the Problem, Cells and Materials*. Available at: http://digitalcommons.usu.edu/cellsandmaterialshttp://digitalcommons.usu.edu/cellsandmaterials/vol5/iss2/6 (Accessed: 2 September 2019).

Stickler, D. J., Morris, N. S. and Williams, T. J. (1996) 'An assessment of the

ability of a silver-releasing device to prevent bacterial contamination of urethral catheter drainage systems', *British Journal of Urology*, 78(4), pp. 579–588. doi: 10.1046/j.1464-410x.1996.16915.x.

Stickler, D. J., Morris, N. S. and Winters, C. (1999) 'Simple physical model to study formation and physiology of biofilms on urethral catheters.', *Methods in enzymology*, 310, pp. 494–501. doi: 10.1016/s0076-6879(99)10037-5.

Stickler, D. J. and Zimakoff, J. (1994) 'Complications of urinary tract infections associated with devices used for long-term bladder management', *Journal of Hospital Infection*, pp. 177–194. doi: 10.1016/0195-6701(94)90101-5.

Stock, I. (2003) 'Natural antibiotic susceptibility of *Proteus* spp., with special reference to *P. mirabilis* and *P. penneri* strains', *Journal of Chemotherapy*. E.S.I.F.T. srl, 15(1), pp. 12–26. doi: 10.1179/joc.2003.15.1.12.

Takahashi, S. *et al.* (2014) 'Development of a prokaryotic universal primer for simultaneous analysis of Bacteria and Archaea using next-generation sequencing', *PLoS ONE*. Public Library of Science, 9(8), p. 105592. doi: 10.1371/journal.pone.0105592.

Tambutté, E. *et al.* (2011) 'Calcein labelling and electrophysiology: Insights on coral tissue permeability and calcification', *Proceedings of the Royal Society B: Biological Sciences*. Royal Society, 279(1726), pp. 19–27. doi: 10.1098/rspb.2011.0733.

Tambyah, P. A., Halvorson, K. T. and Maki, D. G. (1999) 'A prospective study of pathogenesis of catheter-associated urinary tract infections', *Mayo Clinic Proceedings*. Elsevier Ltd, 74(2), pp. 131–136. doi: 10.4065/74.2.131.

Tambyah, P. A. and Maki, D. G. (2000) 'Catheter-associated urinary tract infection is rarely symptomatic: A prospective study of 1497 catheterized patients', *Archives of Internal Medicine*, 160(5), pp. 678–682. doi: 10.1001/archinte.160.5.678.

Tang, X., Lu, B. F. and Pan, S. Q. (1999) 'A bifunctional transposon mini-Tn 5gfp-km which can be used to select for promoter fusions and report gene expression levels in *Agrobacterium tumefaciens*', *FEMS Microbiology Letters*. Oxford University Press (OUP), 179(1), pp. 37–42. doi: 10.1111/j.1574-6968.1999.tb08704.x.

Tansirichaiya, S., Mullany, P. and Roberts, A. P. (2016) 'PCR-based detection of composite transposons and translocatable units from oral metagenomic DNA', *FEMS Microbiology Letters*. Oxford University Press, p. 195. doi: 10.1093/femsle/fnw195.

Tavichakorntrakool, R. *et al.* (2012) 'Extensive characterizations of bacteria isolated from catheterized urine and stone matrices in patients with nephrolithiasis', *Nephrology Dialysis Transplantation*, 27(11), pp. 4125–4130. doi: 10.1093/ndt/gfs057.

Tay, L. J. *et al.* (2016) 'Impact of the lack of community urinary catheter care services on the Emergency Department', *BJU International*. Blackwell Publishing Ltd, 118(2), pp. 327–334. doi: 10.1111/bju.13430.

Tenovuo, J. (2002) ‘Clinical applications of antimicrobial host proteins lactoperoxidase, lysozyme and lactoferrin in xerostomia: efficacy and safety.’, *Oral diseases*, 8(1), pp. 23–9. Available at: http://www.ncbi.nlm.nih.gov/pubmed/11936452 (Accessed: 23 May 2019).

Terlizzi, M. E., Gribaudo, G. and Maffei, M. E. (2017) ‘UroPathogenic *Escherichia coli* (UPEC) infections: Virulence factors, bladder responses, antibiotic, and non-antibiotic antimicrobial strategies’, *Frontiers in Microbiology*. Frontiers Media S.A. doi: 10.3389/fmicb.2017.01566.

Tettelin, H. *et al.* (2008) ‘Comparative genomics: the bacterial pan-genome’, *Current Opinion in Microbiology*. Elsevier Current Trends, pp. 472–477. doi: 10.1016/j.mib.2008.09.006.

Thoendel, M. *et al.* (2011) ‘Peptide signaling in the *Staphylococci*’, *Chemical Reviews*. Chem Rev, 111(1), pp. 117–151. doi: 10.1021/cr100370n.

Thomas-White, K. *et al.* (2018) ‘Culturing of female bladder bacteria reveals an interconnected urogenital microbiota’, *Nature Communications*. Nature Publishing Group, 9(1), pp. 1–7. doi: 10.1038/s41467-018-03968-5.

Thomas, V. J. and Collins, C. M. (1999) ‘Identification of UreR binding sites in the *Enterobacteriaceae* plasmid-encoded and *Proteus mirabilis* urease gene operons’, *Molecular Microbiology*. Blackwell Publishing Ltd., 31(5), pp. 1417–1428. doi: 10.1046/j.1365-2958.1999.01283.x.

Thompson, R. B. and Stamey, T. A. (1973) ‘Bacteriology of infected stones’, *Urology*, 2(6), pp. 627–633. doi: 10.1016/0090-4295(73)90323-3.

Thornton, G. F. and Andriole, V. T. (1970) ‘Bacteriuria during indwelling catheter drainage. II. Effect of a closed sterile drainage system.’, *JAMA*, 214(2), pp. 339–42. Available at: http://www.ncbi.nlm.nih.gov/pubmed/4918243 (Accessed: 3 September 2019).

Tien, B. Y. Q. *et al.* (2017) ‘*Enterococcus faecalis* promotes innate immune suppression and polymicrobial catheterassociated urinary tract infection’, *Infection and Immunity*. American Society for Microbiology, 85(12). doi: 10.1128/IAI.00378-17.

Timofeeva, L. and Kleshcheva, N. (2011) ‘Antimicrobial polymers: Mechanism of action, factors of activity, and applications’, *Applied Microbiology and Biotechnology*. Springer, pp. 475–492. doi: 10.1007/s00253-010-2920-9.

Tipping, M. J. and Gibbs, K. A. (2019) ‘Peer pressure from a *Proteus mirabilis* self-recognition system controls participation in cooperative swarm motility’, *PLOS Pathogens*. Edited by M. R. Parsek, 15(7), p. e1007885. doi: 10.1371/journal.ppat.1007885.

Torzewska, A. and Rozalski, A. (2014) ‘Inhibition of crystallization caused by *Proteus mirabilis* during the development of infectious urolithiasis by various phenolic substances’, *Microbiological Research*. Urban und Fischer Verlag Jena, 169(7–8), pp. 579–584. doi: 10.1016/j.micres.2013.09.020.

Toutain, C. M. *et al.* (2007) ‘Roles for flagellar stators in biofilm formation by *Pseudomonas aeruginosa*’, *Research in Microbiology*, 158(5), pp. 471–477.

doi: 10.1016/j.resmic.2007.04.001.

Trautner, B. W. (2010) ‘Management of catheter-associated urinary tract infection’, *Current Opinion in Infectious Diseases*, pp. 76–82. doi: 10.1097/QCO.0b013e328334dda8.

Trautner, B. W. and Darouiche, R. O. (2004) ‘Role of biofilm in catheter-associated urinary tract infection’, *American Journal of Infection Control*. Mosby Inc., pp. 177–183. doi: 10.1016/j.ajic.2003.08.005.

Tuson, H. H. and Weibel, D. B. (2013) ‘Bacteria-surface interactions’, *Soft Matter*. Royal Society of Chemistry, pp. 4368–4380. doi: 10.1039/c3sm27705d.

Vaezeslami, S., Sterling, R. and Reznikoff, W. S. (2007) ‘Site-directed mutagenesis studies of Tn5 transposase residues involved in synaptic complex formation’, *Journal of Bacteriology*. American Society for Microbiology Journals, 189(20), pp. 7436–7441. doi: 10.1128/JB.00524-07.

Vandecandelaere, I. *et al.* (2017) ‘Metabolic activity, urease production, antibiotic resistance and virulence in dual species biofilms of *Staphylococcus epidermidis* and *Staphylococcus aureus*’. doi: 10.1371/journal.pone.0172700.

Vega, N. M. and Gore, J. (2014) ‘Collective antibiotic resistance: mechanisms and implications’, *Current opinion in microbiology*. Curr Opin Microbiol, 21, pp. 28–34. doi: 10.1016/J.MIB.2014.09.003.

Vyas, H. K. N. *et al.* (2019) ‘Current Understanding of Group A *Streptococcal* Biofilms’, *Current Drug Targets*. Bentham Science Publishers Ltd., 20(9), pp. 982–993. doi: 10.2174/1389450120666190405095712.

Walker, J. N. *et al.* (2017) ‘Catheterization alters bladder ecology to potentiate *Staphylococcus aureus* infection of the urinary tract’, *Proceedings of the National Academy of Sciences of the United States of America*. National Academy of Sciences, 114(41), pp. E8721–E8730. doi: 10.1073/pnas.1707572114.

Wang, J.-T. *et al.* (2014) ‘Antimicrobial susceptibilities of *Proteus mirabilis*: a longitudinal nationwide study from the Taiwan surveillance of antimicrobial resistance (TSAR) program’, *BMC Infectious Diseases*, 14(1), p. 486. doi: 10.1186/1471-2334-14-486.

Wang, Q. *et al.* (2007) ‘Naïve Bayesian classifier for rapid assignment of rRNA sequences into the new bacterial taxonomy’, *Applied and Environmental Microbiology*. American Society for Microbiology, 73(16), pp. 5261–5267. doi: 10.1128/AEM.00062-07.

Warren, John W., Tenney, J. H., *et al.* (1982) ‘A prospective microbiologic study of bacteriuria in patients with chronic indwelling urethral catheters’, *Journal of Infectious Diseases*, 146(6), pp. 719–723. doi: 10.1093/infdis/146.6.719.

Warren, J W *et al.* (1982) ‘Cephalexin for susceptible bacteriuria in afebrile, long-term catheterized patients.’, *JAMA*, 248(4), pp. 454–8. Available at: http://www.ncbi.nlm.nih.gov/pubmed/7045440 (Accessed: 18 December 2019).

Warren, John W., Anthony, W. C., *et al.* (1982) ‘Cephalexin for Susceptible

Bacteriuria in Afebrile, Long-term Catheterized Patients', *JAMA: The Journal of the American Medical Association*, 248(4), pp. 454–458. doi: 10.1001/jama.1982.03330040042029.

Warren, J. W. (2001) 'Catheter-associated urinary tract infections', in *International Journal of Antimicrobial Agents*, pp. 299–303. doi: 10.1016/S0924-8579(00)00359-9.

Warren, J. W., Muncie, H. L. and Hall-Craggs, M. (1988) 'Acute pyelonephritis associated with bacteriuria during long-term catheterization: A prospective clinicopathological study', *Journal of Infectious Diseases*, 158(6), pp. 1341–1346. doi: 10.1093/infdis/158.6.1341.

Wasfi, R. *et al.* (2020) 'Proteus mirabilis Biofilm: Development and Therapeutic Strategies', *Frontiers in Cellular and Infection Microbiology*. Frontiers Media S.A., p. 414. doi: 10.3389/fcimb.2020.00414.

Watanakunakorn, C. and Perni, S. C. (1994) '*Proteus mirabilis* bacteremia: A review of 176 cases during 1980-1992', *Scandinavian Journal of Infectious Diseases*. Informa Healthcare, 26(4), pp. 361–367. doi: 10.3109/00365549409008605.

Wattam, A. R. *et al.* (2016) 'Improvements to PATRIC, the all-bacterial Bioinformatics Database and Analysis Resource Center', *Nucleic Acids Research*, 45, pp. 535–542. doi: 10.1093/nar/gkw1017.

Webb, R. J., Lawson, A. L. and Neal, D. E. (1990) 'Clean Intermittent Self-catheterisation in 172 Adults', *British Journal of Urology*. Br J Urol, 65(1), pp. 20–23. doi: 10.1111/j.1464-410X.1990.tb14653.x.

Weerdenburg, E. M. *et al.* (2015) 'Genome-wide transposon mutagenesis indicates that *Mycobacterium marinum* customizes its virulence mechanisms for survival and replication in different hosts', *Infection and Immunity*. American Society for Microbiology, 83(5), pp. 1778–1788. doi: 10.1128/IAI.03050-14.

Weitz, H. J. *et al.* (2001) ' Construction of a modified mini-Tn 5 lux CDABE transposon for the development of bacterial biosensors for ecotoxicity testing ', *FEMS Microbiology Letters*. Oxford University Press (OUP), 197(2), pp. 159–165. doi: 10.1111/j.1574-6968.2001.tb10598.x.

Wenren, L. M. *et al.* (2013) 'Two independent pathways for self-recognition in *Proteus mirabilis* are linked by type VI-dependent export', *mBio*. American Society for Microbiology, 4(4). doi: 10.1128/mBio.00374-13.

Wilks, S. A., Fader, M. J. and Keevil, C. W. (2015) 'Novel insights into the *Proteus mirabilis* crystalline biofilm using real-time imaging', *PLoS ONE*. Public Library of Science, 10(10). doi: 10.1371/journal.pone.0141711.

Williams, F. D. and Schwarzhoff, R. H. (1978) 'Nature of the Swarming Phenomenon in *Proteus*', *Annual Review of Microbiology*. Annual Reviews, 32(1), pp. 101–138. doi: 10.1146/annurev.mi.32.100178.000533.

Williams, P. and Cámara, M. (2009) 'Quorum sensing and environmental adaptation in *Pseudomonas aeruginosa*: a tale of regulatory networks and multifunctional signal molecules', *Current Opinion in Microbiology*. Curr Opin

Microbiol, pp. 182–191. doi: 10.1016/j.mib.2009.01.005.

Winson, M. K. *et al.* (1998) 'Engineering the luxCDABE genes from *Photorhabdus luminescens* to provide a bioluminescent reporter for constitutive and promoter probe plasmids and mini-Tn 5 constructs', *FEMS Microbiology Letters*. Oxford University Press (OUP), 163(2), pp. 193–202. doi: 10.1111/j.1574-6968.1998.tb13045.x.

Woodworth, B. A. *et al.* (2008) 'An in vitro model of *Pseudomonas aeruginosa* biofilms on viable airway epithelial cell monolayers', *American Journal of Rhinology*, 22(3), pp. 235–238. doi: 10.2500/ajr.2008.22.3178.

Wright, M.-O. *et al.* (2011) 'Reporting Catheter-Associated Urinary Tract Infections: Denominator Matters', *Infection Control & Hospital Epidemiology*. Cambridge University Press (CUP), 32(7), pp. 635–640. doi: 10.1086/660765.

Xia, Y. *et al.* (2019) 'A modified SDS-based DNA extraction method from raw soybean', *Bioscience Reports*. Portland Press Ltd, 39(2), p. 20182271. doi: 10.1042/BSR20182271.

Xu, J. zhong and Zhang, W. guo (2016) 'Strategies used for genetically modifying bacterial genome: site-directed mutagenesis, gene inactivation, and gene over-expression', *Journal of Zhejiang University: Science B*. Zhejiang University Press, pp. 83–99. doi: 10.1631/jzus.B1500187.

Xu, Y. *et al.* (2012) 'Culture-dependent and -independent investigations of microbial diversity on urinary catheters', *Journal of Clinical Microbiology*, 50(12), pp. 3901–3908. doi: 10.1128/JCM.01237-12.

Yin, W. *et al.* (2019) 'Biofilms: The microbial "protective clothing" in extreme environments', *International Journal of Molecular Sciences*. MDPI AG, 20(14). doi: 10.3390/ijms20143423.

Zarb, P. *et al.* (2012) 'The European Centre for Disease Prevention and Control (ECDC) pilot point prevalence survey of healthcare-associated infections and antimicrobial use', *Eurosurveillance*. European Centre for Disease Prevention and Control, 17(46), p. 20316. doi: 10.2807/ese.17.46.20316-en.

Zhang, S. *et al.* (2020) 'Superhydrophobic Coatings for Urinary Catheters to Delay Bacterial Biofilm Formation and Catheter-Associated Urinary Tract Infection', *ACS Applied Bio Materials*. American Chemical Society, 3(1), pp. 282–291. doi: 10.1021/acsabm.9b00814.

Zhou, C. *et al.* (2019) 'Urease is an essential component of the acid response network of *Staphylococcus aureus* and is required for a persistent murine kidney infection', *PLoS Pathogens*. Public Library of Science, 15(1). doi: 10.1371/journal.ppat.1007538.

Appendices

Appendix A- Overview ESEM images of biofilms and mineralization associated with silicone catheters recovered from the *in vitro* bladder model following single- and dual-species experiments with *Ps. aeruginosa* and *P. mirabilis*

Ps. aeruginosa **PAO1-UW (*mTurquoise*)- Silicone**

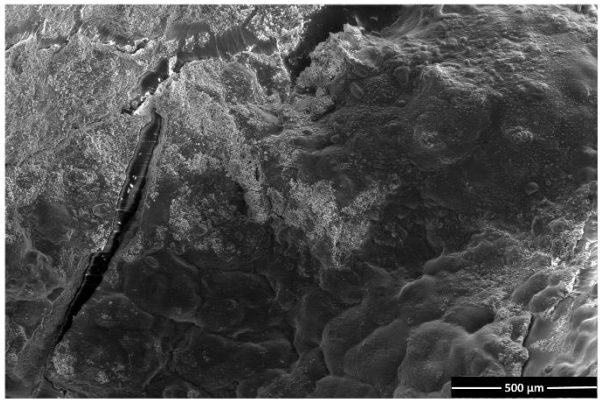

P. mirabilis **WT (*dsRed*)- Silicone**

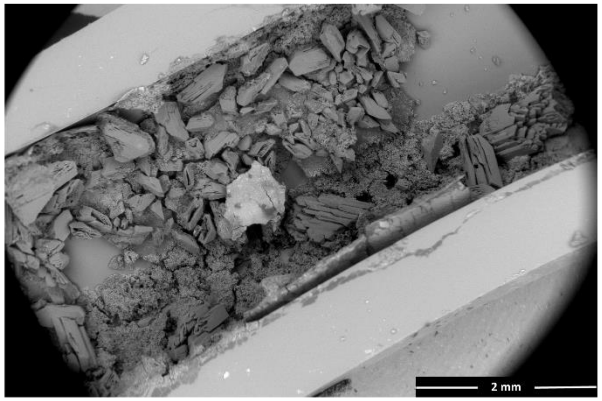

Ps. aeruginosa **PAO1-UW (*mTurquoise*) and *P. mirabilis* WT *(dsRed)*- Silicone**

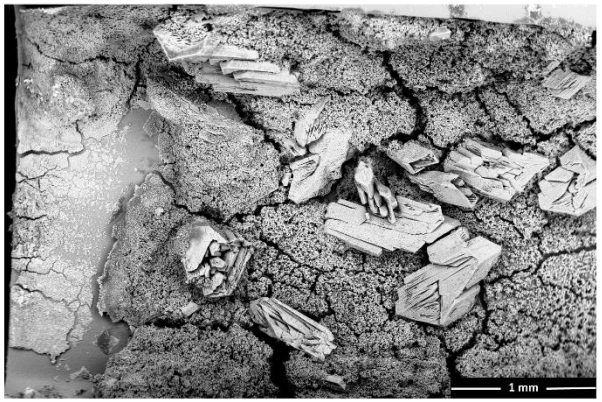

ESEM overview images of the morphology of biofilms and mineralization associated with silicone catheters recovered from the *in vitro* bladder model following single- and dual-species experiments with *Ps. aeruginosa* and *P. mirabilis*

The ESEM images reveal the biofilms and mineralization associated with 1 cm silicone catheter sections recovered from the *in vitro* bladder model following experiments with *P. aeruginosa* PAO1-UW(*mTurquoise*) and *P. mirabilis* WT (*dsRed*) in single- and dual-species inoculations. The samples were vapour fixed with 4 % (v/v) formaldehyde and imaged using ESEM (FEI Quanta 650).

Appendix B- Overview ESEM images of biofilms and mineralization associated with Camstent catheters recovered from the *in vitro* bladder model following single- and dual-species experiments with *Ps. aeruginosa* and *P. mirabilis*

***Ps. aeruginosa* PAO1-UW (*mTurquoise*)- Camstent**

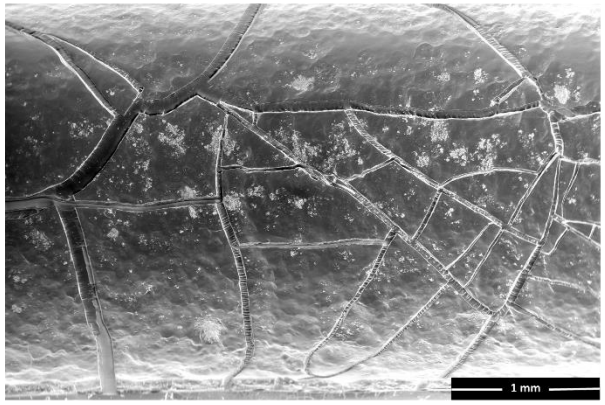

***P. mirabilis* WT (*dsRed*)- Camstent**

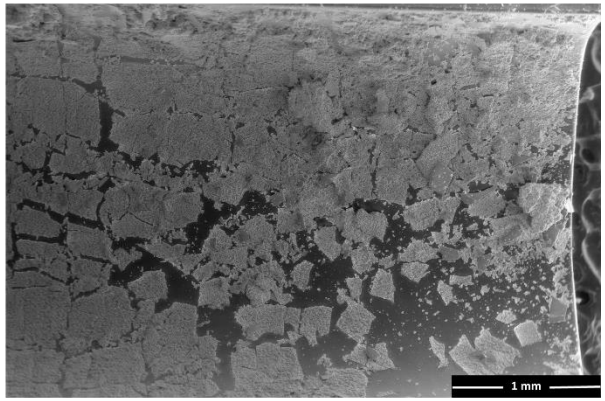

***Ps. aeruginosa* PAO1-UW (*mTurquoise*) and *P. mirabilis* WT (*dsRed*)- Camstent**

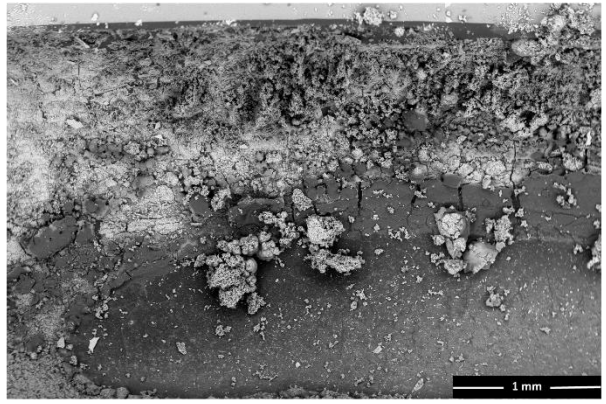

ESEM overview images of the morphology of biofilms and mineralization associated with Camstent catheters recovered from the *in vitro* bladder model following single- and dual-species experiments with *Ps. aeruginosa* and *P. mirabilis*

The ESEM images reveal the biofilms and mineralization associated with 1 cm Camstent catheter sections recovered from the *in vitro* bladder model following experiments with *P. aeruginosa* PAO1-UW(*mTurquoise*) and *P. mirabilis* WT (*dsRed*) in single- and dual-species inoculations. The samples were vapour fixed with 4 % (v/v) formaldehyde and imaged using ESEM (FEI Quanta 650).

Appendix C: Raw EDS spectra of biofilm and mineralization associated with silicone catheters recovered from the *in vitro* bladder model following single-species experiments with *Ps. aeruginosa* and *P. mirabilis*

***Ps. aeruginosa* PAO1-UW (*mTurquoise*)**

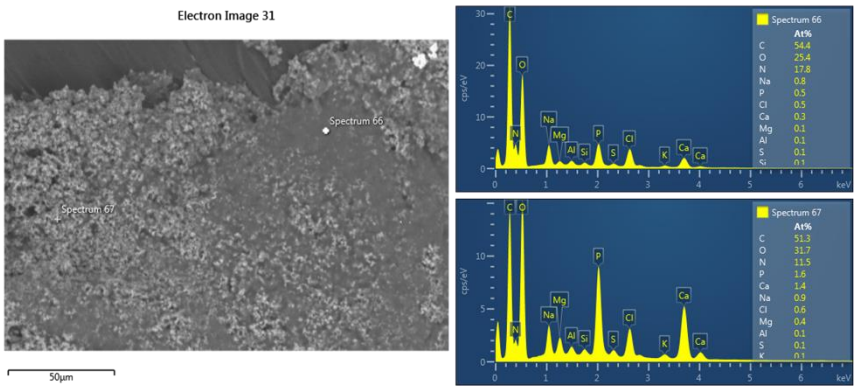

***P. mirabilis* WT (*dsRed*)**

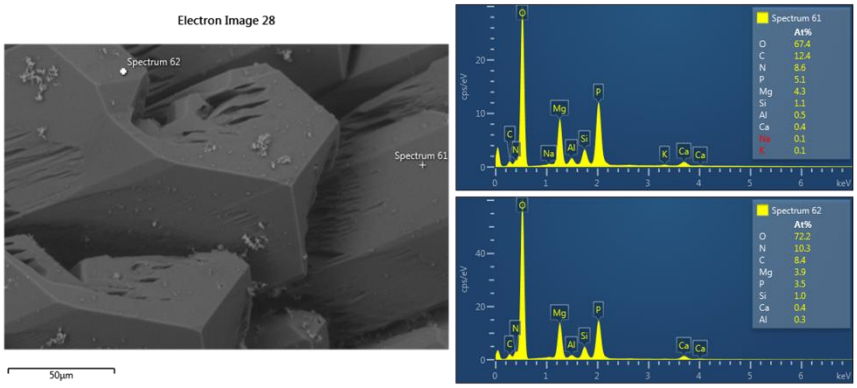

Raw EDS analysis spectra of biofilms and mineralization associated with silicone catheters following single-species *in vitro* bladder model experiments with *Ps. aeruginosa* and *P. mirabilis*

Raw EDS analysis spectra exhibiting the elemental peaks associated with the ESEM images of the sites selected for analysis. The data presented within the figure was obtained from silicone catheters recovered from the *in vitro* bladder model following single-species inoculations with *Ps. aeruginosa* PAO1-UW (*mTurquoise*) and *P. mirabilis* WT (*dsRed*).

Appendix D: Raw EDS spectra of biofilm and mineralization associated with a silicone catheter recovered from the *in vitro* bladder model following a dual-species experiment with *Ps. aeruginosa* and *P. mirabilis*

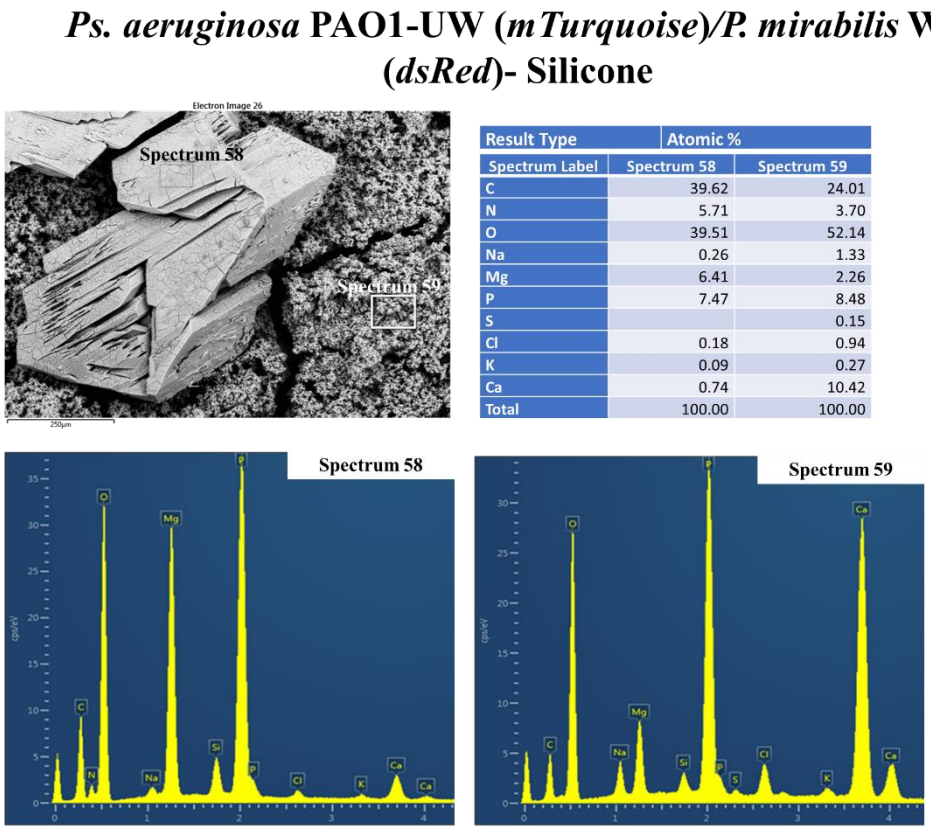

Raw EDS analysis spectra of biofilm and mineralization associated with a silicone catheter following a dual-species *in vitro* bladder model experiment with *Ps. aeruginosa* and *P. mirabilis*

Raw EDS analysis spectra exhibiting the elemental peaks associated with the ESEM images of the sites selected for analysis. The data presented within the figure was obtained from a silicone catheter recovered from the *in vitro* bladder model following a dual-species inoculation with *Ps. aeruginosa* PAO1-UW (*mTurquoise*) and *P. mirabilis* WT (*dsRed*).

Appendix E: Raw EDS spectra of biofilm and mineralization associated with a Camstent catheter recovered from the *in vitro* bladder model following a single-species experiment with *Ps. aeruginosa*

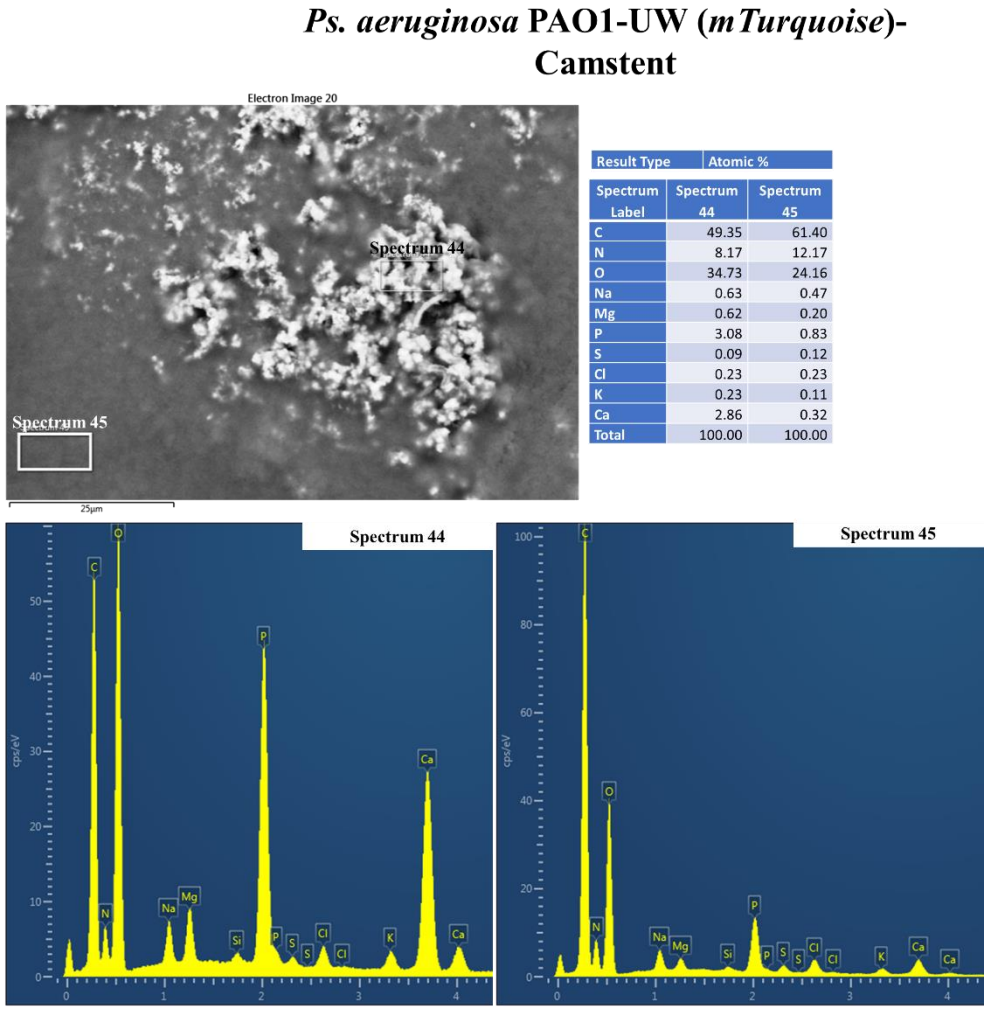

Raw EDS analysis spectra of biofilm and mineralization associated with a Camstent catheter following *in vitro* bladder model experiments with *Ps. aeruginosa*

Raw EDS analysis spectra exhibiting the elemental peaks associated with the ESEM images of the sites selected for analysis. The data presented within the figure was obtained from a Camstent catheter recovered from the *in vitro* bladder model following an inoculation with *Ps. aeruginosa* PAO1-UW (*mTurquoise*).

Appendix F: Raw EDS spectra of biofilm and mineralization associated with a Camstent catheter recovered from the *in vitro* bladder model following a single-species experiment with *P. mirabilis*

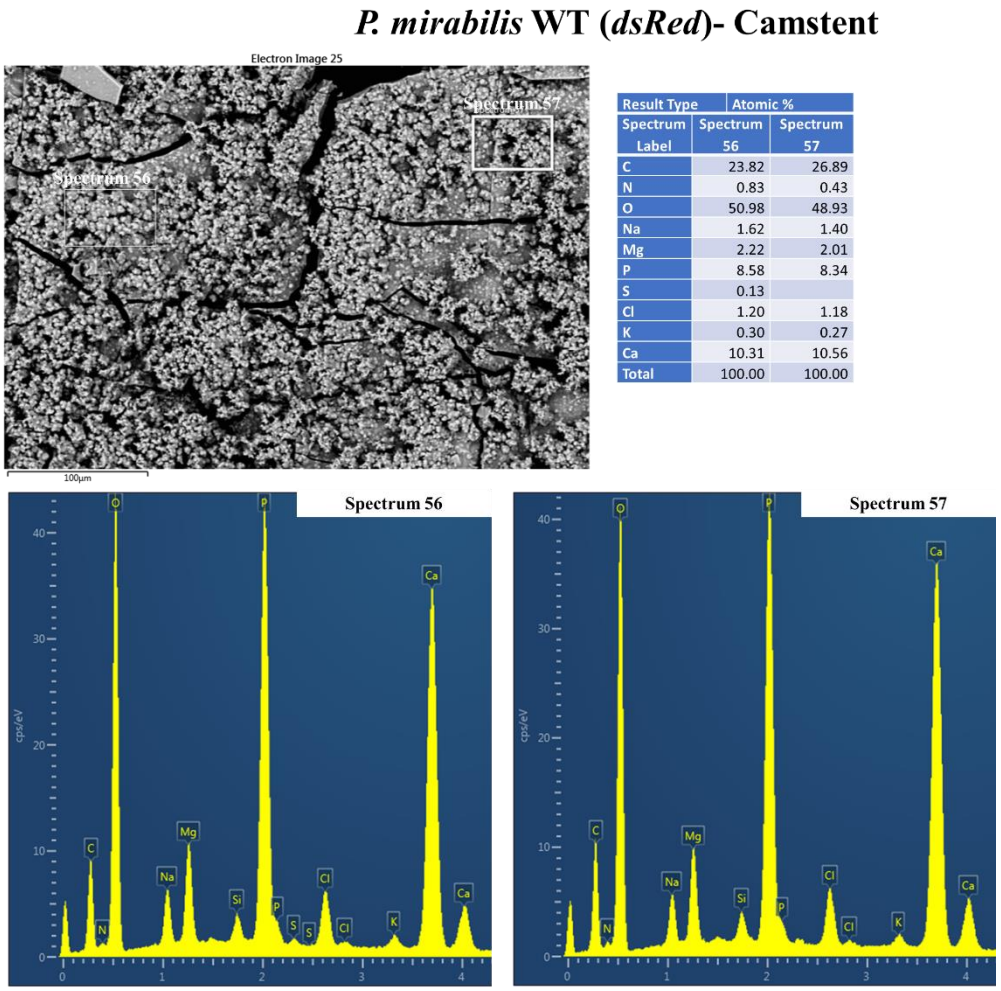

Result Type	Atomic %	
Spectrum Label	Spectrum 56	Spectrum 57
C	23.82	26.89
N	0.83	0.43
O	50.98	48.93
Na	1.62	1.40
Mg	2.22	2.01
P	8.58	8.34
S	0.13	
Cl	1.20	1.18
K	0.30	0.27
Ca	10.31	10.56
Total	100.00	100.00

Raw EDS analysis spectra of biofilm and mineralization associated with a Camstent catheter following *in vitro* bladder model experiments with *P. mirabilis*

Raw EDS analysis spectra exhibiting the elemental peaks associated with the ESEM images of the sites selected for analysis. The data presented within the figure was obtained from a Camstent catheter recovered from the *in vitro* bladder model following an inoculation with *P. mirabilis* WT (*dsRed*).

Appendix G: Raw EDS spectra of biofilm and mineralization associated with a Camstent catheter recovered from the *in vitro* bladder model following a dual-species experiment with *P. mirabilis* and *Ps. aeruginosa*

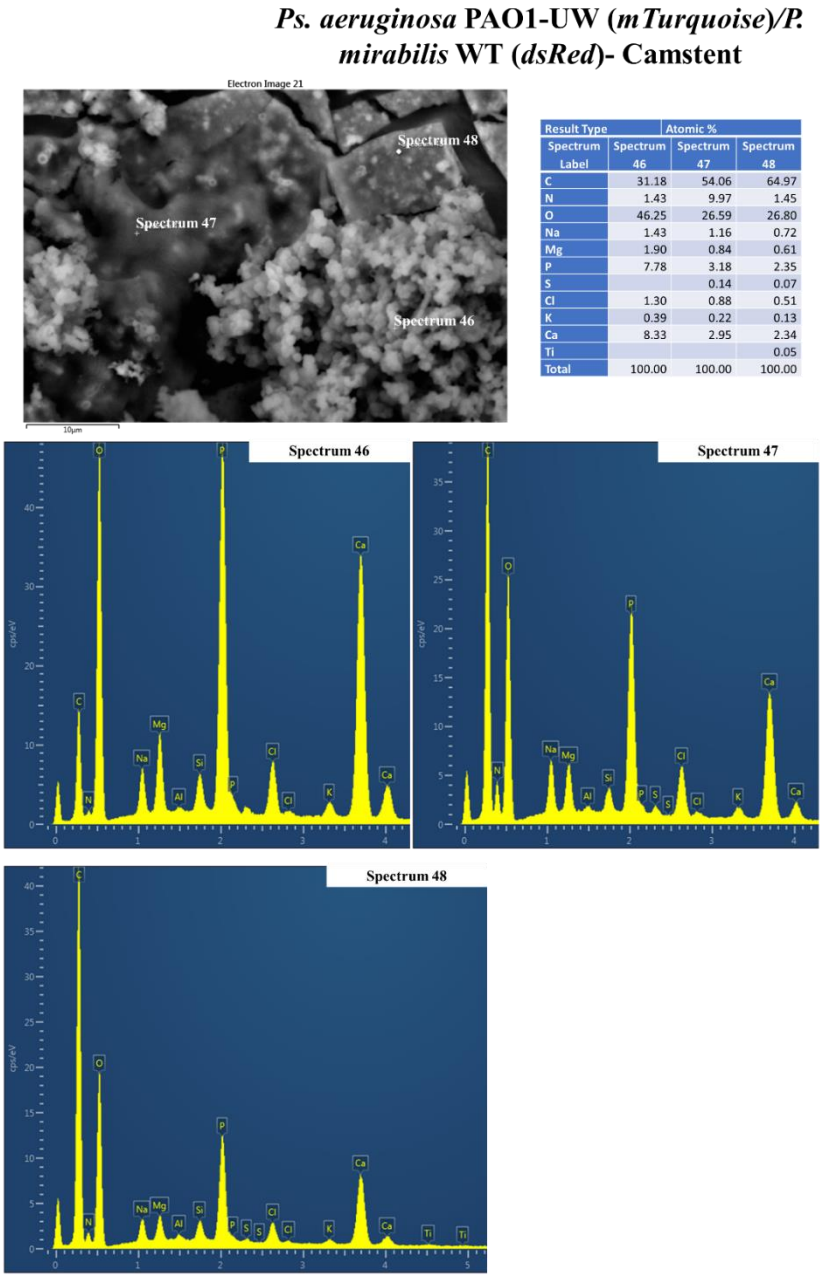

Result Type	Atomic %		
Spectrum Label	Spectrum 46	Spectrum 47	Spectrum 48
C	31.18	54.06	64.97
N	1.43	9.97	1.45
O	46.25	26.59	26.80
Na	1.43	1.16	0.72
Mg	1.90	0.84	0.61
P	7.78	3.18	2.35
S		0.14	0.07
Cl	1.30	0.88	0.51
K	0.39	0.22	0.13
Ca	8.33	2.95	2.34
Ti			0.05
Total	100.00	100.00	100.00

Raw EDS analysis spectra of biofilm and mineralization associated with a Camstent catheter following a dual-species *in vitro* bladder model experiment with *Ps. aeruginosa* and *P. mirabilis*

Raw EDS analysis spectra exhibiting the elemental peaks associated with the ESEM images of the sites selected for analysis. The data presented within the figure was obtained from a Camstent catheter recovered from the *in vitro* bladder model following a dual-species inoculation with *Ps. aeruginosa* PAO1-UW (*mTurquoise*) and *P. mirabilis* WT (*dsRed*).

Appendix H- Overview ESEM images of biofilms and mineralization associated with silicone catheters recovered from the *in vitro* bladder model following experiments with *P. mirabilis* WT, and the *flgI* and *ureR* mutants

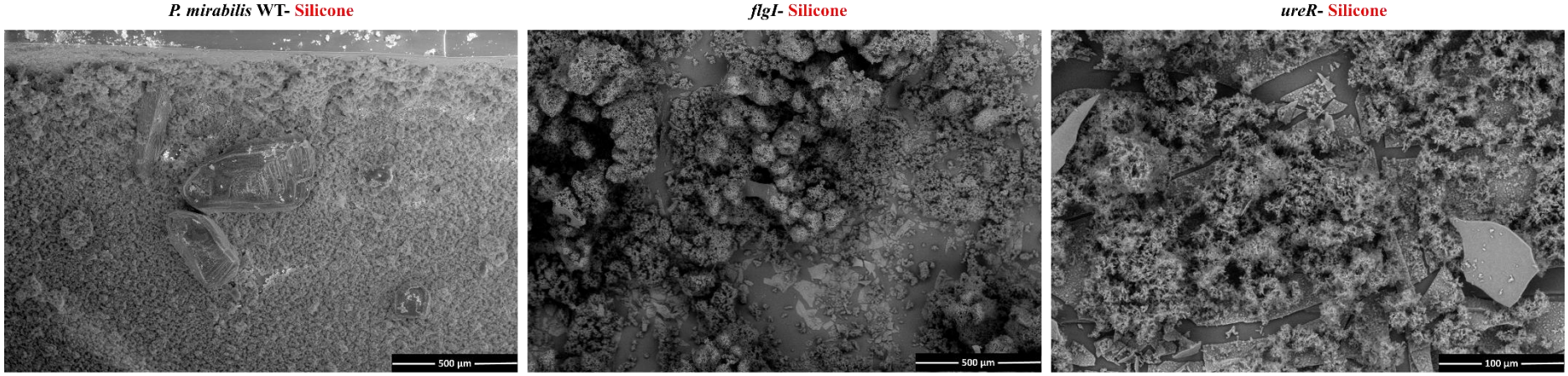

ESEM overview images of the morphology of biofilms and mineralization associated with silicone catheters recovered from the *in vitro* bladder model following experiments with *P. mirabilis* WT, and the *flgI* and *ureR* mutants

The ESEM images reveal the biofilms and mineralization associated with 1 cm silicone catheter sections recovered from the *in vitro* bladder model following experiments with *P. mirabilis* WT, and the *flgI* and *ureR* mutants. The samples were vapour fixed with 4 % (v/v) formaldehyde and imaged using ESEM (FEI Quanta 650).

Appendix I: Raw EDS spectra of biofilm and mineralization associated with a silicone catheter recovered from the *in vitro* bladder model following an experiment with *P. mirabilis* WT

***P. mirabilis* WT- Silicone**

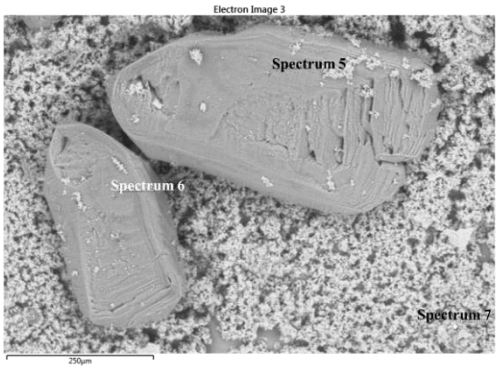

Result Type	Atomic %		
Spectrum Label	Spectrum 5	Spectrum 6	Spectrum 7
C	10.34	13.24	28.37
N	6.76	5.91	
O	66.77	62.06	51.41
Na			0.17
Mg	6.55	6.53	1.56
Al	0.24	0.29	0.27
Si	1.06	1.24	1.97
P	7.04	8.75	7.25
K	0.10	0.13	0.15
Ca	1.15	1.84	8.69
Fe			0.16
Total	100.00	100.00	100.00

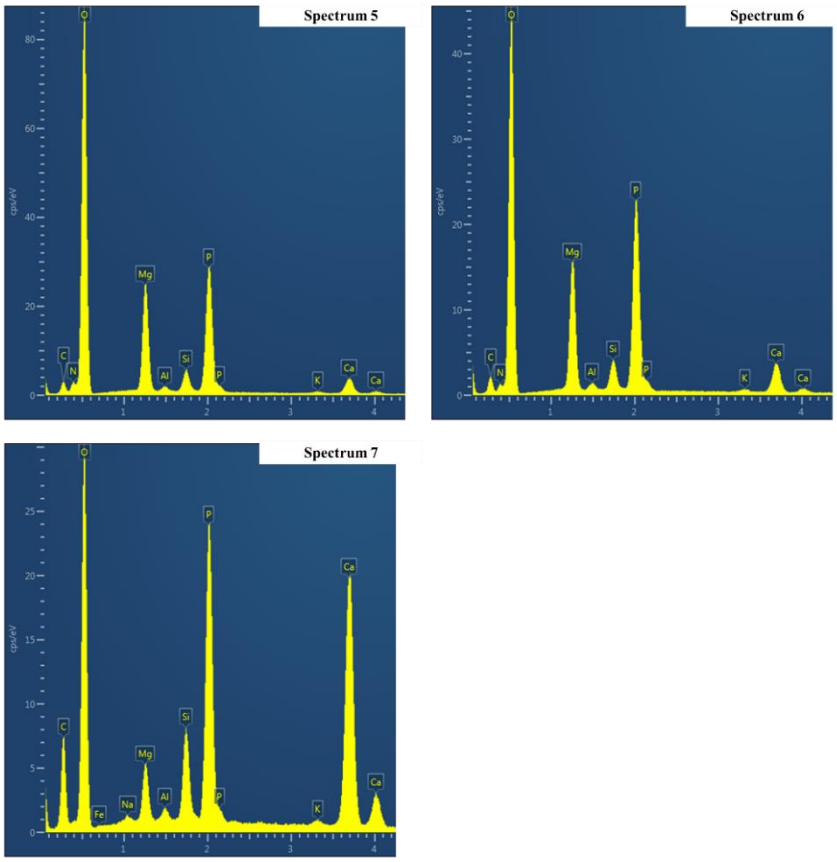

Raw EDS analysis spectra of biofilm and mineralization associated with a silicone catheter following an *in vitro* bladder model experiment with *P. mirabilis*

Raw EDS analysis spectra exhibiting the elemental peaks associated with the ESEM images of the sites selected for analysis. The data presented within the figure was obtained from a silicone catheter recovered from the *in vitro* bladder model following an inoculation with *P. mirabilis* WT.

Appendix J: Raw EDS spectra of biofilm and mineralization associated with a silicone catheter recovered from the *in vitro* bladder model following an experiment with the *flgI* mutant

***flgI*- Silicone**

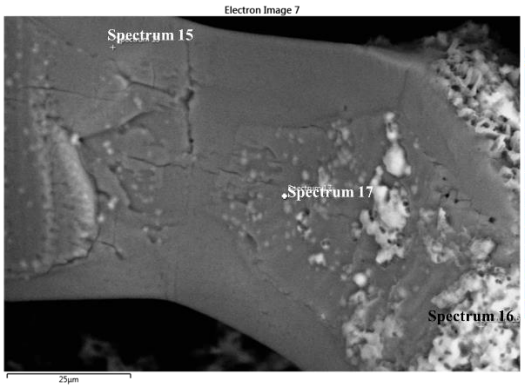

Result Type	Atomic %		
Spectrum Label	Spectrum 15	Spectrum 16	Spectrum 17
C	28.28	19.35	27.02
N	4.64		3.09
O	49.76	48.88	50.70
Na	0.37	0.48	0.41
Mg	6.33	1.44	1.34
Si	6.02	2.96	5.72
P	5.61	10.98	5.41
Cl	0.12	0.47	0.14
K	0.24	0.19	0.15
Ca	1.35	15.10	7.09
Fe		0.13	
Total	100.00	100.00	100.00

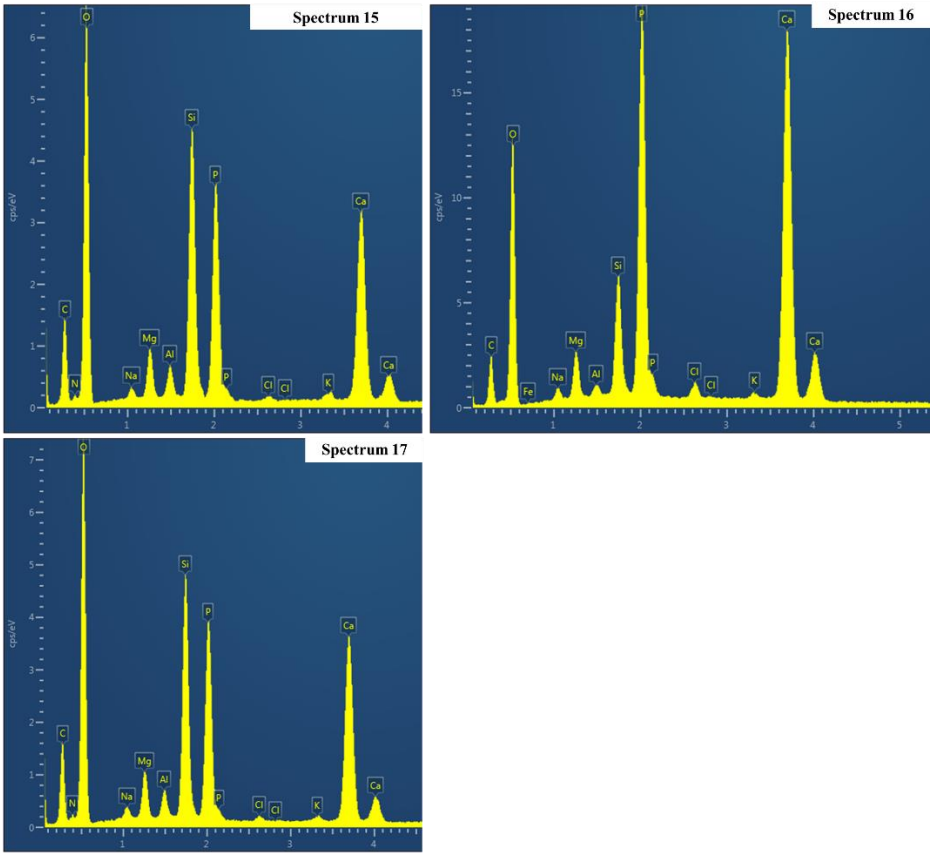

Raw EDS analysis spectra of biofilm and mineralization associated with a silicone catheter following an *in vitro* bladder model experiment with the *P. mirabilis flgI* mutant

Raw EDS analysis spectra exhibiting the elemental peaks associated with the ESEM images of the sites selected for analysis. The data presented within the figure was obtained from a silicone catheter recovered from the *in vitro* bladder model following an inoculation with the *P. mirabilis flgI* mutant.

Appendix K: Raw EDS spectra of biofilm and mineralization associated with silicone catheter devices recovered from the *in vitro* bladder model following experiments with the *flgI* mutant

***ureR*- Silicone**

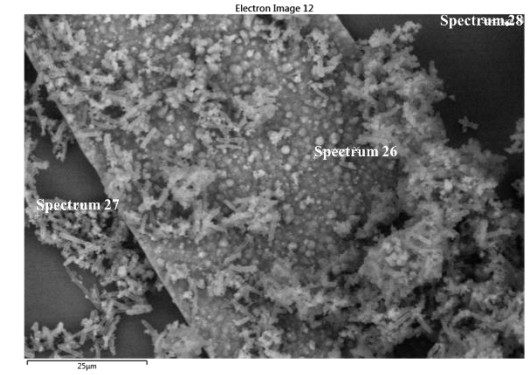

Result Type	Atomic %		
Spectrum Label	Spectrum 26	Spectrum 27	Spectrum 28
C	24.81	29.67	29.69
N		0.33	1.14
O	49.37	51.05	42.59
Na	0.47	0.41	0.33
Mg	1.28	0.97	0.80
Si	6.08	8.10	15.38
P	7.59	4.32	4.52
Cl	0.31	0.19	0.22
K	0.14	0.08	0.09
Ca	9.94	4.88	5.22
Total	100.00	100.00	100.00

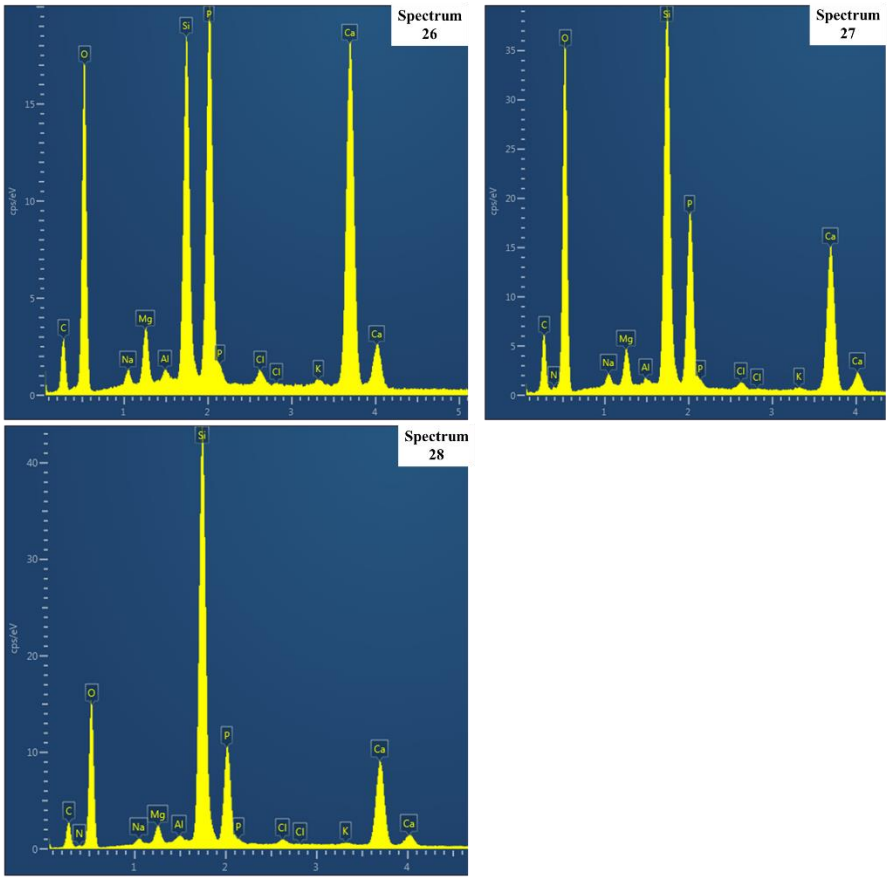

Raw EDS analysis spectra of biofilm and mineralization associated with a silicone catheter following an *in vitro* bladder model experiment with the *P. mirabilis ureR* mutant

Raw EDS analysis spectra exhibiting the elemental peaks associated with the ESEM images of the sites selected for analysis. The data presented within the figure was obtained from a silicone catheter recovered from the *in vitro* bladder model following an inoculation with the *P. mirabilis ureR* mutant.

A pilot study to characterise the effectiveness of a bacteriophobic coating in preventing biofilm accumulation on urinary catheters

Final Version 2.0
14th August 2020

Short title:	**Preventing biofilm on urinary catheters**
Acronym:	
Trial Registration:	
IRAS Project ID:	232293
Trial Sponsor:	University of Nottingham
Sponsor reference:	18057
Funding Source:	*Catheters and catheter transport bags gifted by Camstent. / analysis costs will be met by University of Nottingham, Professor Paul William's laboratory in collaboration with Camstent.*

TRIAL / STUDY PERSONNEL AND CONTACT DETAILS

Sponsor:
Contact name

University of Nottingham
Ms Angela Shone
Research and Innovation
University of Nottingham
East Atrium
Jubilee Conference Centre
Triumph Road
Nottingham
NG8 1DH
Email: sponsor@nottingham.ac.uk

Chief investigator:

David Humes
Associated Professor of Surgery
Phone: 01158231153
Email: david.humes@nottingham.ac.uk

Co-investigators:

Professor Paul Williams
Centre for Biomolecular Sciences
University of Nottingham
NG7 2RD.
Paul.williams@nottingham.ac.uk

Mr. David Hampton (Camstent)

Mr. Alfie Adiamah (Research Fellow University of Nottingham)

Trial / Study Statistician:

Mr David Humes

Phone: 01158231153
Email david.humes@nottingham.ac.uk

Trial / Study Coordinating Centre: NDDC BRU Nottingham, E Floor West Block, Nottingham, NG7 2UH

SYNOPSIS

Title	A pilot study to characterise the effectiveness of a bacteriophobic coating in preventing biofilm accumulation on urinary catheters
Acronym	
Short title	Preventing biofilm on urinary catheters
Chief Investigator	David Humes
Objectives	To assess if a bacteriophobic coating prevents biofilm and host protein accumulation on urinary catheters and inflammatory protein release in urine following catheterization
Trial Configuration	Sequential patients requiring a catheter for colorectal surgery
Setting	Secondary care
Sample size estimate	This is a pilot study to assess if it is feasible to quantify biofilm and host protein accumulation on the coated and non-coated catheters to provide pilot data for a further randomised control trail. No information is available for a power calculation.
Number of participants	50 40 Patients: (20 will receive standard catheter and 20 will receive the coated catheter.) 10 Patients: 5 will receive standard catheter and 5 will receive the coated catheter. In addition, these patients will also provide a pre-catheterisation urine sample (40ml) and a 40ml post-catheterisation urine sample.
Eligibility criteria	• Any patient receiving a urinary catheter as part of their planned surgical procedure for colorectal surgery. • Males and Females Aged 18-85yrs • Able to give Informed Consent
Description of interventions	First 40 patients undergoing colorectal procedures and requiring a urinary catheter as part of their routine care at the QMC will be eligible for the study. Sequential patients will have either a coated or non-coated catheter inserted in the following order; the first 10 receive standard catheter, next 10 pts receive the coated catheter, next 10 receive standard and final 10 receive coated. Following 10 patients: First 5 patients will receive standard catheter with following 5 to receive the coated catheter
Duration of study	Up to 24 months from start of recruitment

Randomisation and blinding	This is not a randomised study as we need to establish if a large enough difference in biofilm accumulation can be measured reliably on the catheters. This information will be used to design and power a subsequent randomised controlled trial.
Outcome measures	The primary outcome is the percentage of catheter surface colonised by biofilm, calculated as (light / (light + dark) x 100% in measurement of stained samples using fluorescence microscopy.
Statistical methods	Not powered to statistical significance: Calculation of mean difference in biofilm coverage between coated and uncoated catheters; scattergram of trajectories of biofilm accumulation in coated and uncoated catheters (X-axis time, y-axis % accumulation)

ABBREVIATIONS

AE	Adverse Event
CI	Chief Investigator overall
CRF	Case Report Form
DMC	Data Monitoring Committee
GCP	Good Clinical Practice
ICF	Informed Consent Form
NHS	National Health Service
PI	Principal Investigator at a local centre
PIS	Participant Information Sheet
REC	Research Ethics Committee
R&D	Research and Development department
SAE	Serious Adverse Event

TABLE OF CONTENTS

SYNOPSIS **297**

ABBREVIATIONS **299**

TRIAL / STUDY BACKGROUND INFORMATION AND RATIONALE **302**

TRIAL / STUDY OBJECTIVES AND PURPOSE **304**

PURPOSE 304
PRIMARY OBJECTIVE 304
SECONDARY OBJECTIVES 304

DETAILS OF PRODUCT(S) **304**

Description 305
Manufacture 305
Packaging and labelling 306
Storage, dispensing and return 306
Placebo 307
Known Side Effects 307

TRIAL / STUDY DESIGN **307**

TRIAL / STUDY CONFIGURATION 307
Primary endpoint 307
Secondary endpoint 307
Safety endpoints 308
Stopping rules and discontinuation 308
TRIAL/STUDY MANAGEMENT 308
DURATION OF THE TRIAL / STUDY AND PARTICIPANT INVOLVEMENT 308
End of the Trial 308
SELECTION AND WITHDRAWAL OF PARTICIPANTS 308
Recruitment 309
Eligibility criteria: 309
Inclusion criteria 309
Exclusion criteria 309
Expected duration of participant participation 310
Removal of participants from therapy or assessments/Participant Withdrawal 310
Informed consent 310

TRIAL / STUDY TREATMENT AND REGIMEN **311**

Compliance 311
Criteria for terminating trial 311
TRANSPORT AND STORAGE OF THE TISSUES 312
LABORATORY ANALYSES 312

STATISTICS **313**

Methods 313
Sample size and justification 314

Assessment of efficacy 314
Assessment of safety 314
Procedures for missing, unused and spurious data 314
Definition of populations analysed 314

ADVERSE EVENTS 314

Definitions 314
Causality 316
Reporting of adverse events 316
TRIAL TREATMENT / INTERVENTION RELATED SAES 316
Participant removal from the study due to adverse events 317

ETHICAL AND REGULATORY ASPECTS 317

ETHICS COMMITTEE AND REGULATORY APPROVALS 317
INFORMED CONSENT AND PARTICIPANT INFORMATION 318
RECORDS 318
Case Report Forms 318
Sample Labelling 319
Source documents 319
Direct access to source data / documents 319
DATA PROTECTION 319

QUALITY ASSURANCE & AUDIT 320

INSURANCE AND INDEMNITY 320
TRIAL CONDUCT 320
TRIAL DATA 320
RECORD RETENTION AND ARCHIVING 321
DISCONTINUATION OF THE TRIAL BY THE SPONSOR 321
STATEMENT OF CONFIDENTIALITY 321

PUBLICATION AND DISSEMINATION POLICY 322

USER AND PUBLIC INVOLVEMENT 322

STUDY FINANCES 322

Funding source 322
Participant stipends and payments 322

SIGNATURE PAGES 323

REFERENCES 324

TRIAL / STUDY BACKGROUND INFORMATION AND RATIONALE

Hospital Acquired Infections (HAI) cause significant problems that affect patient outcomes and hospital costs in the NHS, and globally. A recent report by the UK House of Commons (Reducing HAI in Hospitals in England, 2009) suggested that as little as a 10% reduction in the incidence of HAI could save the NHS over £100m each year and free up over one million bed-days. Efforts have been made to address the problem through better staff training and minimising the duration of device use, but these have had little impact on infection rates[3-4].

Forty percent of all HAIs are associated with the use of urinary catheters[2, 5, 6]; standard of care is a flexible tube inserted through the urethra to drain the bladder[7]. Twenty-five percent of the 16 million patients treated each year in NHS hospitals are catheterised, totalling four million uses each year, yet these devices have a 3% per day infection rate and each infected patient costs an additional £2,000 and needs another 6 days hospitalisation[8, 9, 12, 13].

Many acquired infections are caused by bacteria colonising the surface of consumable medical devices such as tubes, shunts, and catheters[1]. For the example of Urinary Tract Infections (UTI's), the mechanism is a biofilm which is produced as an extracellular matrix produced by micro-organisms adhering to the surface of the catheter. As a result, cell debris and non-adherent organisms from the urinary tract attaches to the wall of the catheter. The bacteria further produce toxins and other irritants that inflame and injure adjacent tissues, creating pain and discomfort. The ultimate outcome is partial blockage of the catheter, impairing drainage of the bladder.

Current preventative strategies attempt to kill the bacteria by coating device surfaces with antibiotic drugs or silver toxins to create a hostile environment. Recent studies have demonstrated that these coatings are not effective in reducing infection rates because they can also encourage antibiotic-resistant bacteria to flourish, leading to serious bladder infections that can spread disease through at-risk populations. The time taken to treat a urinary tract infection (UTI) results in a bed being occupied for days longer than required, adding overall cost and inefficiency to patient treatment.[10-11]. Alternative approaches are urgently needed[14-16].

Recent research findings, reported in Nature Biotechnology, have suggested that a family of inert coating materials may render surfaces inhospitable to urinary tract bacteria; effectively a "non-stick" coating, that discourages free-swimming bacteria from attaching to surfaces, preventing formation of biofilms that lead to infections. Laboratory tests in Nottingham, replicated elsewhere, have demonstrated a 90% or greater reduction in the colonisation of surfaces treated with monomer 4 diethylene glycol methyl ether methacrylate (M4D). Additionally, since the 'bacteria-phobic' surface does not lyse the bacteria organisms, it does not lead to the release of cell-associated toxins

Working with Nottingham University, Camstent have developed this finding into a proprietary coating for clinical use with urinary catheters[17-20] The patented 'M4D coating' is applied to inner and outer surfaces using a 'dip/dry' process before sterilisation, creating a safe, inert, and long-lasting finish. The coating reduces friction of the catheter surface, enhancing patient comfort on insertion and withdrawal. It also incorporates the materials which virtually preclude biofilm formation. The coating doesn't elute antibacterial agents or toxins, avoiding the build-up of dead bacteria on the device surface and retaining effectiveness throughout extended use (NB. Effectiveness is not lost because of leaching away of an active antimicrobial agent). Finally, the absence of anti-bacterial moieties means that the healthy microbial flora is not disturbed.

Together, the advantage of the M4D coating is that it does not select for bacterial antimicrobial resistance, the cost of treating infections is avoided, the catheters remain fully patent, and the risk of spreading resistant pathogens in a ward or care home setting is minimised. The product may achieve an overall reduction in patient care cost and enhanced outcomes for both the patient and the hospital. (CE mark approval for the Camstent coated product has been received).

Urethral catherization is linked to the induction of an inflammatory host response that results in the release of host proteins such as fibrinogen into the urine (Flores-Mirales et al, 2016). Fibrinogen deposits on silicone catheters and promotes bacterial biofilm formation by Gram positive bacteria such as staphylococci and enterococci that express fibrinogen receptors (Flores-Mirales et al, 2016). Fibrinogen deposition on urinary catheters also enhances MRSA persistence in the urinary tract and can lead to more invasive infections (Walker et al 2017).

An important advantage of the CAMSTENT type-coatings is that they should reduce protein deposition:

As part of this study we will collect pre- and post- catheterization urine for analysis from up to 10 patients (with either silicone or Camstent catheters; 5 each) Each of these 10 patients will provide a 40ml urine sample prior to having their catheter fitted and provide a 40ml urine sample once the catheter has been removed. Urine samples will be used to determine:

(a) Host protein content including fibrinogen and uromodulin (Tamm-Horsfall)
(b) *In vitro* silicone and Camstent catheter urine pre-conditioning to evaluate whether pre-conditioning promotes biofilm formation to a greater extent in post- compared with pre-catherization urine
(c) The presence/absence of host proteins on silicone and Camstent catheters post patient removal.

The data obtained will help support the mechanism by which CAMSTENT coatings prevent biofilm formation; catheter associated urinary tract infection, (CAUTI); this is because they do not support host protein deposition post catheterization and hence drive biofilm formation by fibrinogen receptor expressing urinary pathogens. The results obtained will also indicate, whether or not Camstent catheters induce a host inflammatory response as shown for silicone urinary catheters.

TRIAL / STUDY OBJECTIVES AND PURPOSE

PURPOSE

The purpose of the study is to provide pilot information on the characteristics of the biofilm formed on the coated catheter compared to a standard catheter. The two objectives are;

1) to evaluate the catheter's on-label performance in customary clinical use.

2) to quantify biofilm formation on the catheter surface, and to compare it with biofilm formation on the hospitals current uncoated catheters.

PRIMARY OBJECTIVE

An analytic characterisation of catheters after routine patient use, will yield estimates of the difference in biofilm density between coated and non-coated catheters.

SECONDARY OBJECTIVES

(i) Secondary outcomes will be logging of events, including catheter blockage or presumed catheter associated urinary tract infection.
(ii) We will also look at ease of insertion and removal of the catheter since it creates a very smooth and slippery surface using the NHS staff standard clinical feedback form.

DETAILS OF PRODUCT(S)

The Camstent Coated Foley Catheter is an all-silicone two-way Foley-type urinary catheter, to which a proprietary polymeric coating has been applied. It is intended for the drainage of urine via the urethra for patients requiring urinary catheterisation.

The coating enhances lubricity, significantly reducing insertion force.

The base, uncoated, all-silicone urinary catheter has a long, safe history of on-market use from other legal manufacturers. The coating itself is a simple co-polymer of acrylate and methacrylate monomers which is barely visible to the naked eye. The Camstent Coated Foley Catheter is a single use, gamma-sterilised, Class IIa device, for up to 30 days' use.

The catheter has a full CE mark and has been in prior patient use at UCL Westmoreland.

Description

Product Code	Description
CSF12F10	Coated all-silicone Foley catheter, 250mm (female), 12Fr, 5-10cm^3 balloon, with X-ray opaque line
CSF12S10	Coated all-silicone Foley catheter, 420mm (standard), 12Fr, 5-10cm^3 balloon, with X-ray opaque line
CSF14S10	Coated all-silicone Foley catheter, 420mm (standard), 14Fr, 5-10cm^3 balloon, with X-ray opaque line
CSF16S10	Coated all-silicone Foley catheter, 420mm (standard), 16Fr, 5-10cm3 balloon, with X-ray opaque line
CSF18S10	Coated all-silicone Foley catheter, 420mm (standard), 18Fr, 5-10cm3 balloon, with X-ray opaque line
CSF20S10	Coated all-silicone Foley catheter, 420mm (standard), 20Fr, 5-10cm3 balloon, with X-ray opaque line

Manufacture

Legal Manufacturer is Camstent Ltd, and the product Is CE marked in the UK for sale to hospitals.

Registered Address

Camstent Limited
St. Johns Innovation Centre
Cowley Road
Cambridge CB4 0WS
United Kingdom

Company Site - Operations

Camstent Ltd.
The Exchange
Colworth Science Park
Sharnbrook
Bedford MK44 1LQ
United Kingdom

Packaging and labelling

The product is packaged and labelled by

Riverside Medical Packaging Company Limited
Newmarket Drive
Derby
DE24 8SW
United Kingdom
Tel: +44 (0) 1332 755622
www.riversidemedical.co.uk

Sterilisation is performed by:
Swann Morton Limited
Owlerton Green
Sheffield S6 2BJ
United Kingdom
Tel: +44 (0)114 234 4231
http://www.swann-morton.com/

The Legal Manufacturer is Camstent Ltd, which delivers sterile product in quantities of 10 individual packages per carton.

The package label is:

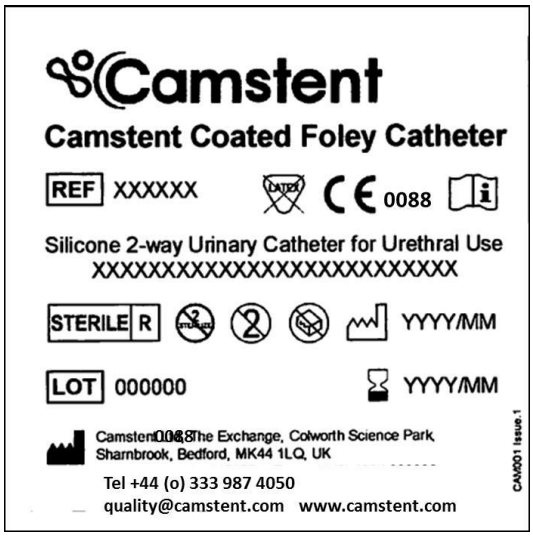

Storage, dispensing and return

The coated catheters will be stored in theatre 14 at QMC. Size 12 and 14 catheters will be used as is standard practice. Catheters will be removed on the ward according to local policies for removal and sealed in standard shipping bags, which will be refrigerated on the ward prior to transfer to the lab at the University of Nottingham.

Placebo

The current Bard standard sealed catheter will be used as the uncoated comparison catheter.

Known Side Effects

The main side effect of urinary catheterisation is trauma to the urinary tract or subsequent infection. The coated catheter is more flexible than a standard catheter and should minimise trauma. It is hoped the coated catheter should reduce the occurrence of catheter associated infections.

Reference source: These are the standard side effects of catheters.

TRIAL / STUDY DESIGN

TRIAL / STUDY CONFIGURATION

This is a single centre non-randomised pilot study.

Primary endpoint

The primary outcome is the percentage of catheter surface colonised by biofilm, calculated as (light / (light + dark) x 100% in measurement of stained samples using fluorescence microscopy.

Secondary endpoint

Secondary outcomes will be logging of events, including catheter blockage or presumed catheter associated urinary tract infection.

Safety endpoints

We do not anticipate any increase in adverse events. The normal risks associated with urinary catheterisation will not be increased by this study.

Stopping rules and discontinuation

The trial will be stopped if we note any increase in adverse events such as catheter associated infection or trauma associated with the new catheter; however, given it is already in use in the UK this is unlikely.

TRIAL/STUDY MANAGEMENT

This is a small pilot study of patients and will be overseen by the Chief Investigator.

The Chief Investigator has overall responsibility for the study and shall oversee all study management.

The data custodian will be the Chief Investigator.

DURATION OF THE TRIAL / STUDY AND PARTICIPANT INVOLVEMENT

Study Duration: Patients will be consented to the study on the day of surgery by one of the study team at QMC. The catheters will be removed as per standard clinical care by the Ward nurses at QMC. They will then be stored on the ward prior to collection and taken to the University of Nottingham labs.

Participant Duration: The patients will be enrolled in the trial whilst they have their catheter. (Up to 14 days).

End of the Trial

The end of the trial will be the last post-catheter urine sample collected from the last patient.

SELECTION AND WITHDRAWAL OF PARTICIPANTS

Recruitment

Participants will be recruited from surgical clinics. The initial approach will be from a member of the patient's usual care team (which may include the investigator), who will explain the study briefly and give the patient a copy of the Participant Information Sheet to read. Potential participants will have at least 24hrs to decide whether they wish to take part or not. If they decide that they would like to take part, they can inform one of the ward nurses who will inform the Investigator team.

The investigator or their nominee, e.g. from the research team or a member of the participant's usual care team, will inform the participant or their nominated representative (other individual or other body with appropriate jurisdiction), of all aspects pertaining to participation in the study.

If needed, the usual hospital interpreter and translator services will be available to assist with discussion of the trial, the participant information sheets, and consent forms, and / but the consent forms and information sheets will / will not be available printed in other languages.

It will be explained to the potential participant that entry into the trial is entirely voluntary and that their treatment and care will not be affected by their decision. It will also be explained that they can withdraw at any time but attempts will be made to avoid this occurrence. In the event of their withdrawal it will be explained that their data collected so far cannot be erased and we will seek consent to use the data in the final analyses where appropriate. Final consent will be taken on the morning of surgery by a member of the study team.

N.B. Data should not be erased as it should be possible to recreate a participant's participation up to their point of withdrawal. Also once data has been entered onto the UoN secure network, data cannot be erased as UoN backups cannot be tampered with. This is covered on clause 2 of the consent form and the withdrawal section of the participant information sheet template.

Eligibility criteria:

Inclusion criteria

1. All patients undergoing colorectal resection routinely requiring a urinary catheter as part of their standard post-operative care.
2. Patients aged 18-85 years will be eligible for the study.
3. Able to give informed consent.

Exclusion criteria

1. Patients that have or recently (within 3 weeks) had a urinary catheter, or those with signs of current urinary tract infection.
2. Pregnant patients.
3. Patients with a potentially immunocompromised condition (steroids, HIV)
4. Patients who are unable to give informed consent

Expected duration of participant participation

Study participants will be participating in the study for up to 14 days whilst the catheter is inserted.

Removal of participants from therapy or assessments/Participant Withdrawal

Participants may be withdrawn from the trial either at their own request or at the discretion of the Investigator. The participants will be made aware should they choose to withdraw that this will not affect their future care. Participants will be informed via the information sheet and consent form that should they withdraw the data collected to date cannot be erased and may still be used in the final analysis. We will destroy any identifiable samples (catheters) but we will need to use the data collected up to their withdrawal.

Participants who withdraw prior to receiving the catheter will be replaced but those withdrawn after receiving the catheter will not be replaced. Participants that require further antibiotics after initial dose given as part of the standard wound infection bundle, or those that are administered antibiotics following an infection whilst the trial urinary catheter is in situ will be withdrawn.

Informed consent

All participants will provide written informed consent. The Informed Consent Form will be signed and dated by the participant before they enter the trial. The Investigator will explain the details of the trial and provide a Participant Information Sheet, ensuring that the participant has sufficient time to consider participating or not. The Investigator will answer any questions that the participant has concerning study participation.

Informed consent will be collected from each participant before they undergo any interventions (including physical examination and history taking) related to the study. One copy of this will be kept by the participant, one will be kept by the Investigator, and a third will be retained in the patient's hospital records.

Should there be any subsequent amendment to the final protocol, which might affect a participant's participation in the trial, continuing consent will be obtained using an amended Consent form which will be signed by the participant.

Consent will be taken on the morning of the patient's surgery. They will have received information regarding the study prior to this in clinic.

TRIAL / STUDY TREATMENT AND REGIMEN

As part of the routine monitoring of patients following colorectal surgical resection a patient will have a urinary catheter placed. In this study half of the participants will have the standard catheter inserted used in the Nottingham Colorectal Service and the other half will have a M4D coated catheter provided by Camstent. The catheter will be inserted in the sequence of 20 standard and 20 coated for the first 40 participants; the following 10 will be allocated as; 5 standard followed by 5 coated. These final 10 participants will also provide two 40ml urine samples; one pre-catheterisation and one post-catheterisation - (sample will be collected 3-4 days after insertion).

The catheter will remain until the standard clinical decision to remove it is made. At this point the catheter will be removed by a nurse in the standard way and placed in a sealed BioBag (Air-Sea) and placed in the ward fridge. It will then be collected by the study team and transported to the University of Nottingham Laboratory. Data will be collected on the age, sex, any use of additional antibiotics We will access participants medical notes for information where relevant to this research study; to include checking for any antibiotic use and viewing the results of any urine tests taken prior to surgery and any additional ones taken as part of standard care along with any co-existing medical complaints of the patient along with the duration the catheter has been used for. As per normal standard of care, clinical staff will complete a clinical feedback form which collates information such as ease of insertion and removal of the catheter.

Compliance

The drug card of the participants will be reviewed to ensure no additional antibiotics have been given. We will also access the results of any urinalysis performed as routine care prior to and after surgery which will be used to confirm the presence of a catheter associated urinary tract infection.

Criteria for terminating trial

It is not anticipated that the trial will be stopped early as it is a pilot study to provide data for further studies of the catheter.

TRANSPORT AND STORAGE OF THE TISSUES

Samples (catheters and urine pots) will be stored in a linked anonymised format and labelled using a combination of study reference, unique study identifier and cross referenced with location code numbers to permit accurate linkage to study data and the consent form.
Bagged catheters will be refrigerated and transferred from the Ward to the lab following removal of the catheter on the day of removal or if at night the following day. Urine samples will be transferred from the ward to the lab on the day of collection or refrigerated and sent the following day.

The master database will be held by Mr David Humes in a password encrypted file on a University of Nottingham server.

The analysis of samples will take place at the University of Nottingham within the Department of Microbiology.

Samples will be refrigerated and transferred from the Ward to the lab following removal of the catheter on the day of removal or if at night the following day.

LABORATORY ANALYSES

All catheters will be sent to a laboratory for surface examination rather than immediately disposed of as medical waste. Harvested catheters will be bagged in an airtight plastic bag and tagged with a record identifier. A record identifier will be used to establish catheter traceability and duration, and will not compromise patient anonymity. The catheter will be kept refrigerated and transported to the analysis laboratory at Nottingham University within two days.

At the Nottingham Laboratory, the catheters will be subjected to qualitative and quantitative analysis to determine the percentage of biofilm coverage on the surface. This will initially be achieved using staining followed by microscopic visual examination of the catheter surface, and images taken of any surface encrustation.

For Fluorescence Microscopy, the procedure will be:

1. Cut the catheter into segments then wash three times in ~15 of PBS with gentle agitation.
2. Transfer the washed catheter segments into the wells of a sterile 24 well plate and stain with SYTO17 Red Fluorescent Nucleic Acid Stain.
3. For detection of host protein deposition on catheter segments, fibrinogen and uromodulin will be detected on the surface of the sectioned catheters by immunofluorescence using a fibrinogen specific primary rabbit antibody followed by a goat anti-rabbit QDot700 far-red fluorescent secondary antibody.

4. Segments will be imaged using a laser scanning confocal microscope using a 10 X objective lens over a 1024 µm x 1024 µm area.
5. A z-section will be imaged (each section is 4µm apart with 36 images taken over 140µm) such that the entire curved surface is imaged. The coverage data will then be taken from a maximum intensity z-projection.
6. Data analysis will be carried out in ImageJ using the maximum intensity z-projection images.
7. Images will be converted to 8-bit greyscale images, a threshold applied to select the data correctly and the biofilm coverage measured.
8. The percentage of coverage for each sample will be computed as (Light) / (Light + Dark) * 100%.

Urine sample analysis:

To quantify urinary host proteins, their deposition and the bacterial response, urine collected pre- and post-catheterization will be subject to the following procedures:

1. The concentration of host proteins in pre- and post- catheterization urine will be determined using ELISA microplate immunofluorescence assays employing primary commercial antibodies specific for host proteins including fibrinogen and uromodulin and detected using far-red fluorescent secondary antibodies as outlined above.
2. Since bio mineralization on the patient catheters can interfere with the detection of surface associated host proteins and bacteria, pre- and post-catheterization urine will be used to condition fresh silicone and coated catheter segments by incubation for 16 h at 4^{o}C. The urine conditioned samples will either be (a) subjected to the same host protein fluorescence antibody imaging microscopy procedure described above for catheters removed from patients and (b) incubated with green-fluorescent labelled bacteria e.g. *Staphylococcus aureus*. Bacterial binding to host proteins deposited on the surface will be imaged using confocal fluorescence microscopy and quantified via image analysis as described above.

Urine samples will be disposed of after analysis.

STATISTICS

Methods

Aggregate descriptive statistics will be calculated (mean accumulation, variance), and biofilm coverage will be plotted against the duration of catheterisation as a scattergram (x-axis: Time, y-axis: % Accumulation). The study is not powered to permit statistical analysis.

Prior laboratory experiments predict that the difference in biofilm coverage could exceed 80 % (animal work). If larger differences are seen in harvested catheters, then a Total Cell Count Assay, in which the biofilm is sonicated free of the surface and then assessed through serial dilution, may be substituted for Fluorescence Microscopy.

Sample size and justification

This is a pilot study primarily to assess if it is possible to determine the amount and difference in biofilm formation on standard compared to coated catheters, so no formal power calculation could be undertaken.

A t-test for difference of means will be calculated as an indicative measure but is not conclusive as a pilot study is not powered to significance.

Assessment of efficacy

The percentage of coverage (% accumulation) for each sample will be computed as (Light) / (Light + Dark) * 100%.

Assessment of safety

The catheter has a full CE mark and has been in prior patient use at UCL Westmoreland. We do not anticipate any safety issues with the catheter.

Procedures for missing, unused and spurious data

No variables will be used in the analysis from participants, so we do not anticipate any need to account for missing data.

Definition of populations analysed

Safety set: All participants who receive a catheter.
Full Analysis set: All participants, who received a catheter.
Per protocol set: All participants in the Full Analysis set who are deemed to have no major protocol violations that could interfere with the objectives of the study.

ADVERSE EVENTS

Definitions

An adverse event is any unfavourable and unintended sign, symptom, syndrome or illness that develops or worsens during the period of observation in the study.
An AE does include a / an:

1. Exacerbation of a pre-existing illness.

2. Increase in frequency or intensity of a pre-existing episodic event or condition.

3. Condition detected or diagnosed after medicinal product administration even though it may have been present prior to the start of the study.

4. Continuous persistent disease or symptoms present at baseline that worsen following the start of the study.

An AE does not include a / an:

1. Development of catheter related urinary tract infection

2. Pre-existing disease or conditions present or detected at the start of the study that did not worsen.

3. Situations where an untoward medical occurrence has not occurred (e.g., hospitalisations for cosmetic elective surgery, social and / or convenience admissions).

4. Disease or disorder being studied, or sign or symptom associated with the disease or disorder unless more severe than expected for the participant's condition.

5. Overdose of concurrent medication without any signs or symptoms.

A Serious Adverse Event (SAE) is any adverse event occurring following study mandated procedures, having received the treatment or intervention that results in any of the following outcomes:

1. Death

2. A life-threatening adverse event

3. Inpatient hospitalisation or prolongation of existing hospitalisation

4. A disability / incapacity

5. A congenital anomaly in the offspring of a participant

Important medical events that may not result in death, be life-threatening, or require hospitalisation may be considered a serious adverse event when, based upon appropriate medical judgment, they may jeopardize the patient or participant and may require medical or surgical intervention to prevent one of the outcomes listed in this definition

All adverse events will be assessed for seriousness, expectedness and causality:

A distinction is drawn between serious and severe AEs. Severity is a measure of intensity whereas seriousness is defined using the criteria above. Hence, a severe AE need not necessarily be serious.

Causality

Not related or improbable: a clinical event including laboratory test abnormality with temporal relationship to trial treatment / intervention administration which makes a causal relationship incompatible or for which other treatments, chemicals or disease provide a plausible explanation**.** This will be counted as “unrelated” for notification purposes.

Possible: a clinical event, including laboratory test abnormality, with temporal relationship to trial treatment / intervention administration which makes a causal relationship a reasonable possibility, but which could also be explained by other interventions, chemicals or concurrent disease. This will be counted as “related” for notification purposes.

Probable: a clinical event, including laboratory test abnormality, with temporal relationship to trial treatment / intervention administration which makes a causal relationship a reasonable possibility, and is unlikely to be due to other interventions, chemicals or concurrent disease. This will be counted as “related” for notification purposes.

Definite: a clinical event, including laboratory test abnormality, with temporal relationship to trial treatment / intervention administration which makes a causal relationship a reasonable possibility, and which can definitely not be attributed to other causes. This will be counted as “related” for notification purposes.

With regard to the criteria above, medical and scientific judgment shall be used in deciding whether prompt reporting is appropriate in that situation.

Reporting of adverse events

Participants will be asked to contact the study site immediately in the event of any serious adverse event. All adverse events will be recorded and closely monitored until resolution, stabilisation, or until it has been shown that the study treatment / intervention is not the cause. The Chief Investigator shall be informed immediately of any serious adverse events and shall determine seriousness and causality in conjunction with any treating medical practitioners.

All treatment related serious adverse events will be recorded and reported to the REC as part of the annual reports. Unexpected serious adverse events will be reported within the timeframes to the REC as stated below. The Chief Investigator shall be responsible for all adverse event reporting.

Trial Treatment / Intervention Related SAEs

A serious adverse event that is unexpected in its severity and seriousness *and* deemed directly related to or suspected to be related to the trial treatment or intervention shall be reported to the ethics committee that gave a favourable opinion as stated below.

The event shall be reported immediately of knowledge of its occurrence to the Chief Investigator.

The Chief Investigator will:

- Assess the event for seriousness, expectedness and relatedness to the trial treatment or intervention.
- Take appropriate medical action, which may include halting the trial and inform the Sponsor of such action.
- If the event is deemed related to the trial treatment or intervention shall inform the REC using the reporting form found on the HRA web page within 7 days of knowledge of the event.
- Shall, within a further eight days send any follow-up information and reports to the REC.
- Make any amendments as required to the study protocol and inform the REC as required

Participant removal from the study due to adverse events

Any participant who experiences an adverse event may be withdrawn from the study at the discretion of the Investigator.

ETHICAL AND REGULATORY ASPECTS

ETHICS COMMITTEE AND REGULATORY APPROVALS

The trial will not be initiated before the protocol, informed consent forms and participant information sheets have received approval / favourable opinion from the Research Ethics Committee (REC), the respective National Health Service (NHS) or other healthcare provider's Research & Development (R&D) department, and the Health Research Authority (HRA) if required. Should a protocol amendment be made that requires REC approval, the changes in the protocol will not be instituted until the amendment and revised informed consent forms and participant information sheets (if appropriate) have been reviewed and received approval / favourable opinion from the REC and R&D departments. A protocol amendment intended to eliminate an apparent immediate hazard to participants may be implemented immediately providing that the REC are notified as soon as possible and an approval is requested. Minor protocol amendments only for logistical or administrative changes may be submitted to the HRA only and implemented according to the timelines advised.

The trial will be conducted in accordance with the ethical principles that have their origin in the Declaration of Helsinki, 1996; the principles of Good Clinical

Practice, and the UK Department of Health Policy Framework for Health and Social Care, 2017.

INFORMED CONSENT AND PARTICIPANT INFORMATION

The process for obtaining participant informed consent will be in accordance with the REC guidance, and Good Clinical Practice (GCP) and any other regulatory requirements that might be introduced. The investigator or their nominee and the participant shall both sign and date the Informed Consent Form before the person can participate in the study.

The participant will receive a copy of the signed and dated forms and the original will be retained in the Trial Master File. A second copy will be filed in the participant's medical notes and a signed and dated note made in the notes that informed consent was obtained for the trial.

The decision regarding participation in the study is entirely voluntary. The investigator or their nominee shall emphasize to them that consent regarding study participation may be withdrawn at any time without penalty or affecting the quality or quantity of their future medical care, or loss of benefits to which the participant is otherwise entitled. No trial-specific interventions will be done before informed consent has been obtained.

The investigator will inform the participant of any relevant information that becomes available during the course of the study, and will discuss with them, whether they wish to continue with the study. If applicable, they will be asked to sign revised consent forms.

If the Informed Consent Form is amended during the study, the investigator shall follow all applicable regulatory requirements pertaining to approval of the amended Informed Consent Form by the REC and use of the amended form (including for ongoing participants).

RECORDS

Case Report Forms

Each participant will be assigned a trial identity code number, allocated at randomisation if appropriate, for use on CRFs other trial documents and the electronic database. The documents and database will also use their initials (of first and last names separated by a hyphen or a middle name initial when available) and date of birth (dd/mm/yy).

CRFs will be treated as confidential documents and held securely in accordance with regulations. The investigator will make a separate confidential record of the participant's name, date of birth, local hospital number or NHS

number, and Participant Trial Number (the Trial Recruitment Log), to permit identification of all participants enrolled in the trial, in accordance with regulatory requirements and for follow-up as required
CRFs shall be restricted to those personnel approved by the Chief or local Principal Investigator and recorded on the 'Trial Delegation Log.'

All paper forms shall be filled in using black ballpoint pen. Errors shall be lined out but not obliterated by using correction fluid and the correction inserted, initialled and dated.
The Chief or local Principal Investigator shall sign a declaration ensuring accuracy of data recorded in the CRF.

Sample Labelling

Each participant will be assigned a trial identity code number for use on the samples, consent forms and other study documents and the electronic database. The documents and database will also use their initials (of first and last names separated by a hyphen or a middle name initial when available) and date of birth (dd/mm/yy). Samples will also be labelled with the duration of use.

Source documents

Source documents shall be filed at the investigator's site and may include but are not limited to, consent forms, current medical records, laboratory results and records. A CRF may also completely serve as its own source data. Only trial staff as listed on the Delegation Log shall have access to trial documentation other than the regulatory requirements listed below.

Direct access to source data / documents

The CRF and all source documents, including progress notes and copies of laboratory and medical test results shall made be available at all times for review by the Chief Investigator, Sponsor's designee and inspection by relevant regulatory authorities (e.g. DH, Human Tissue Authority).

DATA PROTECTION

All trial staff and investigators will endeavour to protect the rights of the trial's participants to privacy and informed consent, and will adhere to the Data Protection Act, 2018. The CRF will only collect the minimum required information for the purposes of the trial. CRFs will be held securely, in a locked room, or locked cupboard or cabinet. Access to the information will be limited to the trial staff and investigators and relevant regulatory authorities (see above). Computer held data including the trial database will be held securely

and password protected. All data will be stored on a secure dedicated web server. Access will be restricted by user identifiers and passwords (encrypted using a one-way encryption method).
Information about the trial in the participant's medical records / hospital notes will be treated confidentially in the same way as all other confidential medical information.

Electronic data will be backed up every 24 hours to both local and remote media in encrypted format.

QUALITY ASSURANCE & AUDIT

INSURANCE AND INDEMNITY

Insurance and indemnity for trial participants and trial staff is covered within the NHS Indemnity Arrangements for clinical negligence claims in the NHS, issued under cover of HSG (96)48. There are no special compensation arrangements, but trial participants may have recourse through the NHS complaints procedures.

The University of Nottingham as research Sponsor indemnifies its staff, research participants and research protocols with both public liability insurance and clinical trials insurance. These policies include provision for indemnity in the event of a successful litigious claim for proven non-negligent harm.

TRIAL CONDUCT

Trial conduct may be subject to systems audit of the Trial Master File for inclusion of essential documents; permissions to conduct the trial; Trial Delegation Log; CVs of trial staff and training received; local document control procedures; consent procedures and recruitment logs; adherence to procedures defined in the protocol (e.g. inclusion / exclusion criteria, correct randomisation, timeliness of visits); adverse event recording and reporting; accountability of trial materials and equipment calibration logs.

The Trial Coordinator/Academic Supervisor, or where required, a nominated designee of the Sponsor, shall carry out site systems audit at least yearly.

TRIAL DATA

Monitoring of trial data shall include confirmation of informed consent; source data verification; data storage and data transfer procedures; local quality control checks and procedures, back-up and disaster recovery of any local databases and validation of data manipulation. The Trial Coordinator/Academic

Supervisor, or where required, a nominated designee of the Sponsor, shall carry out monitoring of trial data as an ongoing activity.

Entries on CRFs will be verified by inspection against the source data. A sample of CRFs (10% or as per the study risk assessment) will be checked on a regular basis for verification of all entries made. In addition, the subsequent capture of the data on the trial database will be checked. Where corrections are required, these will carry a full audit trail and justification.

Trial data and evidence of monitoring and systems audits will be made available for inspection by REC as required.

RECORD RETENTION AND ARCHIVING

In compliance with the ICH/GCP guidelines, regulations and in accordance with the University of Nottingham Research Code of Conduct and Research Ethics, the Chief or local Principal Investigator will maintain all records and documents regarding the conduct of the study. These will be retained for at least 7 years or for longer if required. If the responsible investigator is no longer able to maintain the study records, a second person will be nominated to take over this responsibility.

The Trial Master File and trial documents held by the Chief Investigator on behalf of the Sponsor shall be finally archived at secure archive facilities at the University of Nottingham. This archive shall include all trial databases and associated meta-data encryption codes.

DISCONTINUATION OF THE TRIAL BY THE SPONSOR

The Sponsor reserves the right to discontinue this trial at any time for failure to meet expected enrolment goals, for safety or any other administrative reasons. The Sponsor shall take advice from the Trial Steering Committee and Data Monitoring Committee as appropriate in making this decision.

STATEMENT OF CONFIDENTIALITY

Individual participant medical information obtained as a result of this study are considered confidential and disclosure to third parties is prohibited with the exceptions noted above.
Participant confidentiality will be further ensured by utilising identification code numbers to correspond to treatment data in the computer files.

Such medical information may be given to the participant's medical team and all appropriate medical personnel responsible for the participant's welfare.

If information is disclosed during the study that could pose a risk of harm to the participant or others, the researcher will discuss this with the CI and where appropriate report accordingly.

Data generated as a result of this trial will be available for inspection on request by the participating physicians, the University of Nottingham representatives, the REC, local R&D Departments and the regulatory authorities.

PUBLICATION AND DISSEMINATION POLICY

The data will be submitted for presentation at National and International meetings along with potential submission for publication.

USER AND PUBLIC INVOLVEMENT

The study is a pilot study we have consulted with the NDDC BRC PPI co-ordinator who has advised on a package of PPI measures that could be considered if a full trial is developed.

STUDY FINANCES

Funding source

There is no external funding for the study. The catheters have been provided by Camstent. and the laboratory costs are to be covered by Professor Williams's team at The University of Nottingham, in collaboration with Camstent who will make a financial contribution to cover some of the laboratory work.

Participant stipends and payments

Participants will not be paid to participate in the trial. Travel expenses will be offered for any hospital visits in excess of usual care.

SIGNATURE PAGES

Signatories to Protocol:

Chief Investigator: (name) _____

Signature: _____

Date: _____

Co- investigator: (name) _____

Signature: _____

Date: _____

Trial Statistician: (name) _____

Signature: _____

Date: _____

REFERENCES

References:

1) Stickler, David J. "Bacterial biofilms in patients with indwelling urinary catheters." *Nature Reviews. Urology* 5.11 (2008): 598.
2) Trautner, Barbara W. "Management of catheter-associated urinary tract infection (CAUTI)." *Current opinion in infectious diseases* 23.1 (2010): 76.
3) Siddiq, Danish M., and Rabih O. Darouiche. "New strategies to prevent catheter-associated urinary tract infections." *Nature Reviews Urology* 9.6 (2012): 305-314.
4) Barber, Amelia E., et al. "Urinary tract infections: current and emerging management strategies." *Clinical infectious diseases* 57.5 (2013): 719-724.
5) Lo, Evelyn, et al. "Strategies to prevent catheter-associated urinary tract infections in acute care hospitals: 2014 update." *Infection Control & Hospital Epidemiology* 35.5 (2014): 464-479.
6) Nicolle, Lindsay E. "Catheter associated urinary tract infections." *Antimicrobial resistance and infection control* 3.1 (2014): 23.
7) Lam, Thomas BL, et al. "Types of indwelling urethral catheters for short-term catheterisation in hospitalised adults." *The Cochrane Library* (2014).
8) Stone, Patricia. Economic burden of healthcare-associated infections: An American perspective." *Expert Rev. Phrmacoeconomics Outcomes Res.* 9(5) (2009): 417-422.
9) Scott, R. Douglas. "The direct medical costs of healthcare-associated infections in US hospitals and the benefits of prevention." (2009).
10) Pickard, Robert, et al. "Antimicrobial catheters for reduction of symptomatic urinary tract infection in adults requiring short-term catheterisation in hospital: a multicentre randomised controlled trial." *The lancet* 380.9857 (2012): 1927-1935.
11) Makuta, G., M. Chrysafis, and T. Lam. "Measuring the efficacy of antimicrobial catheters." *Nursing times* 109.44 (2012): 16-18.
12) Kennedy, Edward H., M. Todd Greene, and Sanjay Saint. "Estimating hospital costs of catheter-associated urinary tract infection." *Journal of hospital medicine* 8.9 (2013): 519-522. Kennedy, Edward H., M. Todd Greene, and Sanjay Saint. "Estimating hospital costs of catheter-associated urinary tract infection." *Journal of hospital medicine* 8.9 (2013): 519-522.
13) Kilonzo, Mary, et al. "Cost effectiveness of antimicrobial catheters for adults requiring short-term catheterisation in hospital." *European urology* 66.4 (2014): 615-618.
14) MHasan, Jafar, Russell J. Crawford, and Elena P. Ivanova. "Antibacterial surfaces: the quest for a new generation of biomaterials." *Trends in biotechnology* 31.5 (2013): 295-304.
15) Salwiczek, Mario, et al. "Emerging rules for effective antimicrobial coatings." *Trends in biotechnology* 32.2 (2014): 82-90.
16) Mandakhalikar, Kedar Diwakar, Rongyuan Ray Chua, and Paul Anantharajah Tambyah. "New Technologies for Prevention of Catheter Associated Urinary Tract Infection." *Current Treatment Options in Infectious Diseases* 8.1 (2016): 24-41.
17) Hook, Andrew L., et al. "Combinatorial discovery of polymers resistant to bacterial attachment." *Nature biotechnology* 30.9 (2012): 868-875.
18) Hasan, Jafar, Russell J. Crawford, and Elena P. Ivanova. "Antibacterial surfaces: the quest for a new generation of biomaterials." *Trends in biotechnology* 31.5 (2013): 295-304.
19) Magennis, E. P., et al. "Engineering serendipity: High-throughput discovery of materials that resist bacterial attachment." *Acta biomaterialia* 34 (2016): 84-92.
20) Adlington, Kevin, et al. "Application of Targeted Molecular and Material Property Optimization to Bacterial Attachment-Resistant (Meth) acrylate Polymers." *Biomacromolecules* 17.9 (2016): 2830-2838.
21) Flores-Mireles AL, et al. (2016) "Fibrinogen release and deposition of urinary catheters placed during urological procedures." *J Urol* 196:416-421.

22) Walker et al. (2017) “Catheterization alters bladder ecology to potentiate Staphylococcus aureus infection of the urinary tract.” *Proc Nat Acad USA* 114:E8721-E8730

Appendix M: Participant information sheet for the "Preventing biofilm formation on urinary catheters" study

Local Letterhead to be added

Participant Information Sheet
(PD001-170 **Final Version 2.0 14 August 2020)**
IRAS Project ID: **232293**

Short Title of Study: Preventing biofilm on urinary catheters

Name of Chief Investigator: Dr David Humes
Local Researcher(s): Prof. Paul Williams, Dr David Hampton

We would like to invite you to take part in our research study. Before you decide we would like you to understand, why the research is being done and what it would involve for you. One of our team will go through the information sheet with you and answer any questions you have. Talk to others about the study if you wish. Ask us if there is anything that is not clear.

What is the Background and Purpose of the study?

The study aims to measure the amount of bacterial biofilm accumulation on the surface of your urinary catheter after use.

Biofilm is a sticky coating produced by bacteria which forms and then attracts more bacteria and debris from the bladder; this may lead to a catheter eventually become blocked. One consequence might be that bacteria may move back into the bladder and cause infection. It is believed that a form of bacteria (bacterial biofilms) that grow on the surface of urinary catheters could cause urinary tract infections (UTIs).
We are testing whether a coated Foley catheter gathers less bacteria compared to a standard non-coated Foley hospital catheter; we will also test urine samples for proteins that may also play a part in bacterial biofilm formation.

The coated catheter we will be using has been thoroughly tested by independent laboratories. Tests have shown it to resist bacteria. This data has been reviewed by an organisation (UK Notified Body) whose role it is to decide that appropriate testing has taken place and that the product is safe for use. The coated catheter has been granted a CE mark approval for hospital use.

We will also look at ease of insertion and removal of the catheter since it creates a very smooth and slippery surface using the NHS staff standard clinical feedback form.

If the results of this pilot study show that the coated catheter has less biofilm (than the non-coated catheter) and therefore will reduce the likelihood of developing an infection then we would like to use these results to plan a larger scale clinical trial.
The standard-issue uncoated Foley catheter and the coated Foley Catheter are both CE mark approved for routine hospital use in draining urine from the bladder. The coated catheter is produced by dip-coating a standard commercial catheter already used by the NHS.

What is a Foley Catheter?

Catheters are used to drain urine from the bladder; there are two types of catheter. A straight catheter is a hollow rubber tube inserted through the urethral opening into the bladder to empty urine (drain the bladder) once and are not reused.
A Foley Catheter; sometimes called an Indwelling catheter, is a thin, hollow flexible tube inserted through the urethral opening into the bladder and is used to drain the bladder over a longer period of time i.e. over a day(s) or weeks, it is held in place by a small water-filled balloon which is inflated in the bladder to keep the catheter from falling out while you go about your normal activities. Urine will automatically drain out of the bladder into the bag, which is attached to the catheter.

Why have I been invited?

You are invited to take part in this study because you are likely to be catheterised as part of your routine hospital care, prescribed treatment by your doctor/clinician.
We are inviting 40 participants like you, to take part.

Do I have to take part?

No, it is entirely up to you if you decide to take part or not. If you do decide to take part, you will be given this information sheet to keep and be asked to sign a consent form first.
If you decide to take part, you are still free to withdraw at any time and without giving a reason. This would not affect your legal rights.

What will happen to me if I take part?

If you decide to take part, your doctor/treating physician will still treat you as they normally would; so the duration of time you have a catheter, the method of insertion/withdrawal and your aftercare will not change by taking part. We are comparing the standard NHS non-coated Foley catheter with the same NHS catheter with a coating designed to inhibit biofilm formation. We plan for half the patients taking part in this study to receive the standard non-coated catheter and half will receive the coated catheter.
Instead of disposing of the catheter as medical waste as soon it is removed; it will be refrigerated and transported to the Microbiology laboratory, University of Nottingham to be tested for any microbial growth. As soon as the analysis is completed, the catheter will be disposed of in the usual way. We have already collected catheters from 40 patients and are looking to recruit an additional 10 patients. As part of this additional 10; as well as us collecting your catheter for the research; we would like to obtain two 40ml urine samples from you, one before you have your catheter fitted and another once you have had your catheter in for 3-4 days. (40mls equates to approximately 2.5 tablespoons).
We will be required to access your medical notes for information where relevant to this research study; such as checking for any antibiotic use and the results of any urine tests you have prior to your surgery and any additional ones taken as part of your standard care.

Expenses and payments

Participants will not be paid to participate in the study. There will be no change to your standard care routine.

What are the possible disadvantages and risks of taking part?

We do not anticipate any disadvantages for taking part in the study.

What are the possible benefits of taking part?

We cannot promise the study will help you but the information we get from this study may help us identify whether the coating on the coated catheter prevents bacteria from attaching to it. Bacterial attachment has been associated with infection.

It is hoped that the data from this study will be used to develop a larger study; and this larger study will be designed to measure its impact on infection.

If we obtain the results we hope for, the benefit will be the reduction in the likelihood/frequency of infection and discomfort for future patients, as well as helping to reduce the cost of hospitalisation.

What happens when the research study stops?

Once the study is completed and the results analysed, the findings may be presented at medical conferences or submitted for publication in a suitable medical journal. Participants will not be identified in any report, publication or presentations about the study. The results of the study may also be used to plan further research.

What if there is a problem?

If you have a concern about any aspect of this study, you should ask to speak to the researchers who will do their best to answer your questions. The researchers' contact details are given at the end of this information sheet. If you remain unhappy and wish to complain formally, you can do this through the NHS Complaints Procedure. Details can be obtained by contacting the Patients Advise and Liaison Service (PALS) on 0800 183 0204, pals@nuh.nhs.uk or write to: NHS NUH Trust, c/o PALS, Freepost, NEA 14614, Nottingham. NG7 1BR.

Will my taking part in the study be kept confidential?

We will follow ethical and legal practice and all information about you will be handled in confidence.

If you join the study, we will use information collected from you and your medical records during the course of the research. This information will be kept **strictly confidential**, stored in a secure and locked office, and on a password-protected database at the University of Nottingham. Under UK Data Protection laws the University is the Data Controller (legally responsible for the data security) and the Chief Investigator of this study (named above) is the Data Custodian (manages access to the data). This means we are responsible for looking after your information and using it properly. Your rights to access, change or move your information are limited, as we need to manage your information in specific ways to comply with certain laws and for the research to be reliable and accurate. To safeguard your rights we will use the minimum personally – identifiable information possible.

You can find out more about how we use your information and to read our privacy notice at:

https://www.nottingham.ac.uk/utilities/privacy.aspx.

The data collected for the study will be looked at and stored by authorised persons from the University of Nottingham who are organising the research. They may also be looked at by authorised people from regulatory organisations to check that the study is being carried out correctly. All will have a duty of confidentiality to you as a research participant and we will do our best to meet this duty.
Where possible information about you which leaves the hospital will have your name and address removed and a unique code will be used so that you cannot be recognised from it, however sometimes we need to ensure that we can recognise you to link the research data with your medical records so in these instances we will need to know your name and date of birth.

Your contact information will be kept by the University of Nottingham for up to 12months after the end of the study so that we are able to contact you about the findings of the study and possible follow-up studies (unless you advise us that you do not wish to be contacted). This information will be kept separately from the research data collected and only those who need to will have access to it. All other data (research data) will be kept securely for 7 years. After this time, your data will be disposed of securely. During this time, all precautions will be taken by all those involved to maintain your confidentiality, only members of the research team given permission by the data custodian will have access to your personal data.
In accordance with the University of Nottingham's, the Government's and our funders' policies we may share our research data with researchers in other Universities and organisations, including those in other countries, for research in health and social care. Sharing research data is important to allow peer scrutiny, re-use (and therefore avoiding duplication of research) and to understand the bigger picture in particular areas of research. Data sharing in this way is usually anonymised (so that you could not be identified) but if we need to share identifiable information, we will seek your consent for this and ensure it is secure. You will be made aware then if the data is to be shared with countries whose data protection laws differ to those of the UK and how we will protect your confidentiality. Your treating physician will be informed of your participation in this study.

What will happen if I don't want to carry on with the study?

Your participation is voluntary and you are free to withdraw at any time, without giving any reason, and without your legal rights being affected. If you withdraw we will no longer collect any information about you or from you but we will keep the information about you that we have already obtained as we are not allowed to tamper with study records and this information may have already been used in some analyses and may still be used in the final study analyses. Any identifiable samples (catheters) will be destroyed.
To safeguard your rights, we will use the minimum personally identifiable information possible.

Involvement of the General Practitioner/Family doctor (GP)

We will inform your treating physician of your participation in this study.

What will happen to any samples I give?

Once your catheter has been removed, it will be refrigerated and transported to the Microbiology Laboratories at University of Nottingham to be analysed for any bacterial growth. As soon as the analyses is completed, all catheters will be disposed of as normal clinical waste. Urine samples will collected, refrigerated and transported to the Microbiology lab for analysis.

Once analysis is complete, all urine samples will be disposed of as per normal clinical waste.

What will happen to the results of the research study?

Once the study is completed and the results analysed, the findings may be presented at medical conferences or submitted for publication in a suitable medical journal. Participants will not be identified in any report, publication or presentation about the study. The results of the study may also be used to plan further research.

Who is organising and funding the research?

This research is being organised by the University of Nottingham.
Camstent will donate the coated Foley Catheters and make a financial contribution to cover some of the laboratory work.

Who has reviewed the study?

All research in healthcare is looked at by independent group of people, called a Research Ethics Committee, to protect your interests. This study has been reviewed and given favourable opinion by **[East Midlands – Nottingham 2]** Research Ethics Committee.

Further information and contact details

Dr David Humes (Chief Investigator) NIHR Nottingham Digestive Diseases Biomedical Research Centre (NDDBRC) E Floor, West Block, Queen's Medical Centre, NOTTINGHAM, NG7 2UH. Tel. 0115 746 5124		Scientific Support: Dr David Hampton Email: dave.hampton@camstent.com Telephone: 07860 559492
Email: David.Humes@nottingham.ac.uk		
Telephone: Lauren Cowie (NHS PA) Tel: 0115 9249924 ext. 64525		

Appendix N: Consent form: Preventing biofilm on urinary catheters

(Form to be printed on local headed paper)

CONSENT FORM
(Final version 2.0 14th August 2020)

Short Title: Preventing biofilm on urinary catheters

IRAS Project ID: 232293

Name of Researcher:

Name of Participant: **Please initial box**

1. I confirm that I have read and understand the information sheet version number **2.0** __dated **14/08/2020** for the above study and have had the opportunity to ask questions. ☐
2. I understand that my participation is voluntary and that I am free to withdraw at any time, without giving any reason, and without my medical care or legal rights being affected. I understand that should I withdraw then the information collected so far cannot be erased and that this information may still be used in the project analysis. ☐
3. I understand that relevant sections of my medical notes and data collected in the study may be looked at by authorised individuals from the University of Nottingham, the research group and regulatory authorities where it is relevant to my taking part in this study. I give permission for these individuals to have access to these records and to collect, store, analyse and publish information obtained from my participation in this study. I understand that my personal details will be kept confidential. ☐
4. I agree to provide urine samples for analysis in this study. ☐
5. I understand and agree that my catheter will be taken for microbiological analysis. ☐
6. I agree to my treating physician being informed of my participation in this study. ☐
7. I agree to take part in the above study. ☐

Name of Participant	Date	Signature

Name of Person taking consent	Date	Signature

3 copies: 1 for participant, 1 for the project notes and 1 for the medical notes

Appendix O: Biofilm and mineral quantification per section of Camstent and silicone clinical catheter samples

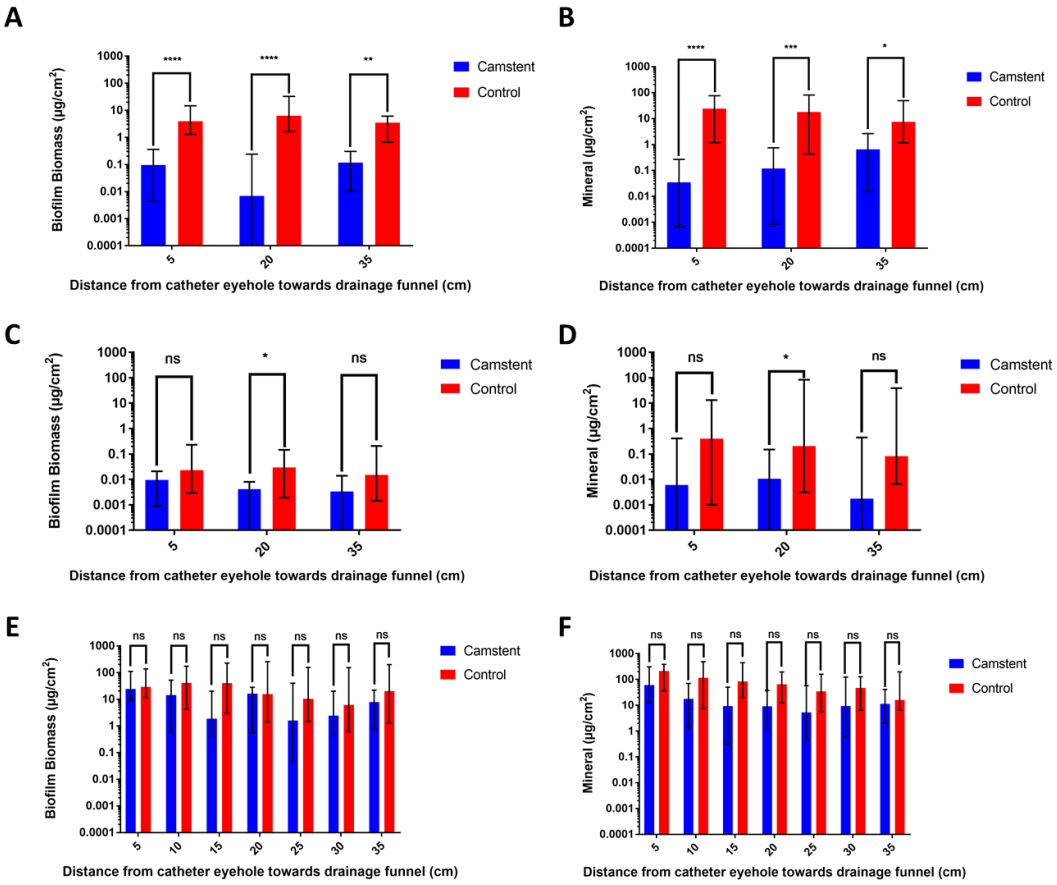

Biofilm and mineral quantification per section of Camstent and silicone clinical catheter samples

The median confocal microscopy estimated biofilm and mineral accumulated on sections of clinical catheter samples analysed within cohorts 1 (A and B), 2 (C and D), and 3 (E and F). The data was used to generate mineral and biofilm biomass values per catheter sample within section 5.3.2. The data has been normalized by dividing biofilm and mineral values for each catheter sample by the square root of their respective indwelling time. Error bars represent the 95% confidence intervals of the median values. (not significant (ns) ≥ 0.05, *$p \leq 0.05$, **$p \leq 0.01$, ***$p \leq 0.001$, ****$p \leq 0.0001$)

Appendix P: Standard curve used for quantification of urinary fibrinogen

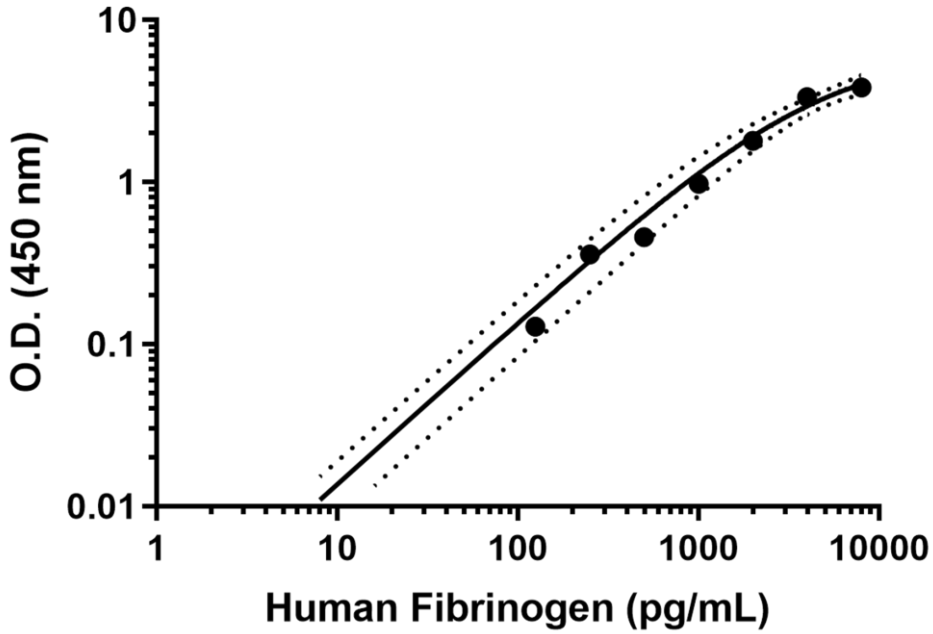

Human fibrinogen standard curve

The standard curve (hyperbola) was generated by reconstituting human fibrinogen in Sample Diluent NS, preparing a stock solution at a concentration of 100000 pg mL^{-1}. A serial dilution was performed in Sample Diluent NS to prepare concentrations for the standard curve of 8000, 4000, 2000, 1000, 500, 250, 125, and 0 pg mL^{-1} (blank control). The samples were processed following the manufacturer's instructions, and quantified by reading the OD at 450 nm using a TECAN (Infinite, M200Pro).

Appendix Q: Raw EDS spectra of biofilm and mineralization associated with silicone clinical catheter sample 20

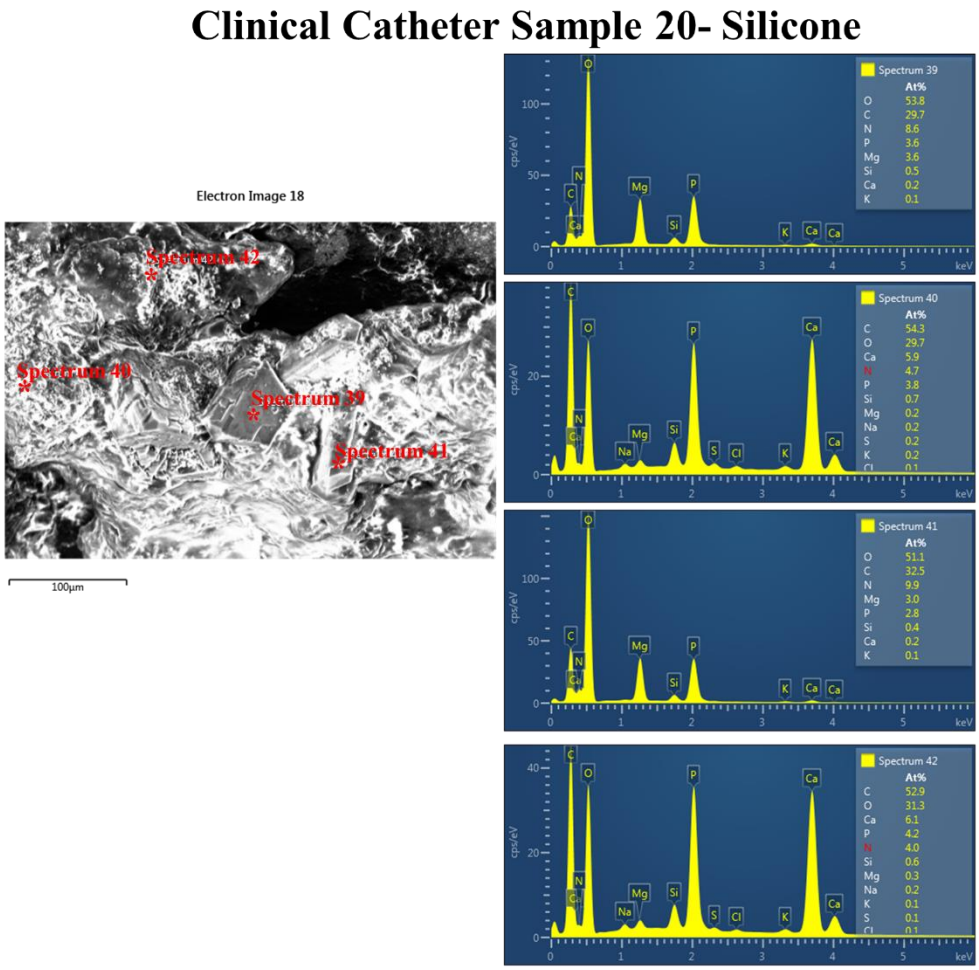

Raw EDS analysis spectra of biofilm and mineralization associated with silicone clinical catheter sample 20

Raw EDS analysis spectra exhibiting the elemental peaks associated with the ESEM images of the sites selected for analysis. The data presented within the figure was obtained from silicone clinical catheter sample 20, recovered from a hospitalized patient following 42 days of indwelling time.

Appendix R: Raw EDS spectra of biofilm and mineralization associated with silicone clinical catheter sample 15

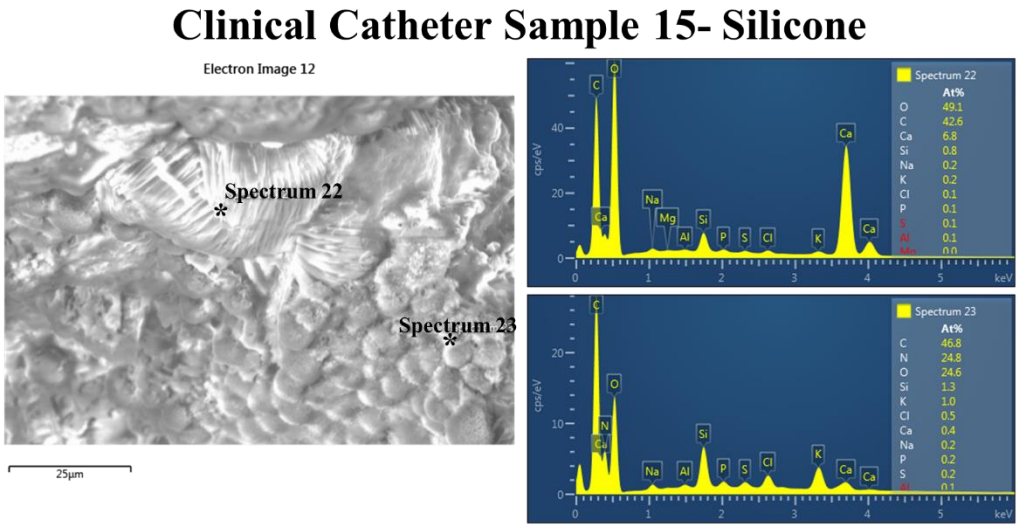

Raw EDS analysis spectra of biofilm and mineralization associated with silicone clinical catheter sample 15

Raw EDS analysis spectra exhibiting the elemental peaks associated with the ESEM images of the sites selected for analysis. The data presented within the figure was obtained from silicone clinical catheter sample 15, recovered from a hospitalized patient following 91 days of indwelling time.

Appendix S: Raw EDS spectra of biofilm and mineralization associated with Camstent clinical catheter sample 18

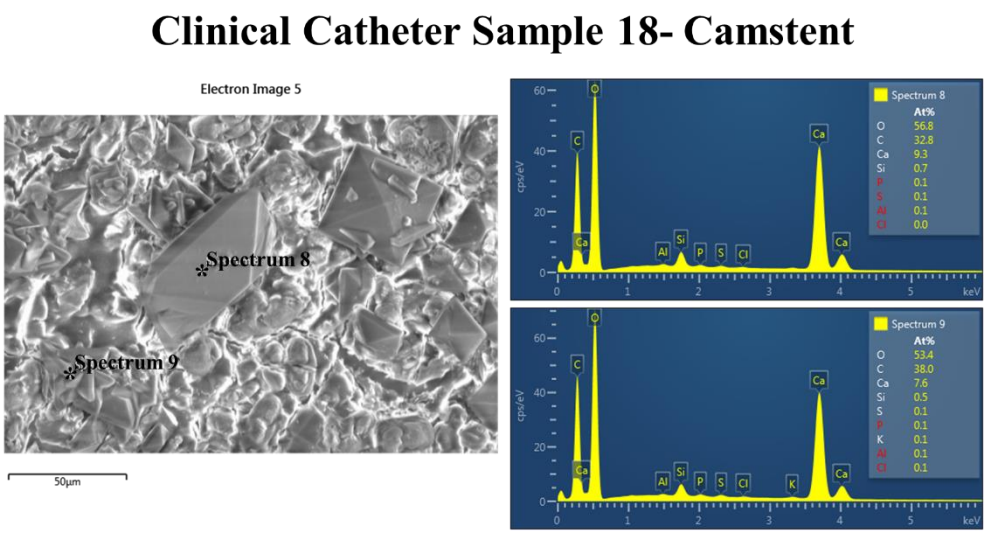

Raw EDS analysis spectra of biofilm and mineralization associated with Camstent clinical catheter sample 18

Raw EDS analysis spectra exhibiting the elemental peaks associated with the ESEM images of the sites selected for analysis. The data presented within the figure was obtained from Camstent clinical catheter sample 18, recovered from a hospitalized patient following 22 days of indwelling time.